Chair of Mathematics and Statistics

Doctoral Thesis

Geometry and topology of self-affine tiles and Rauzy fractals

Shuqin Zhang

April 2019

This thesis was written within the framework of the

Program "Discrete Mathematics"

supported by the Austrian Science Fund
(FWF grant W1230)

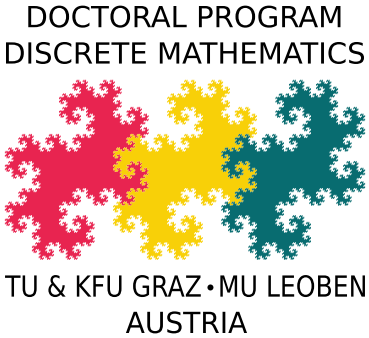

www.math.tugraz.at/discrete

Betreuer:
Ao.Univ.-Prof. Dipl.-Ing. Dr.techn. Jörg Thuswaldner

Lehrstuhl für Mathematik und Statistik
Department Mathematik und Informationstechnologie
Montanuniversität Leoben

AFFIDAVIT

I declare on oath that I wrote this thesis independently, did not use other than the specified sources and aids, and did not otherwise use any unauthorized aids.

I declare that I have read, understood, and complied with the guidelines of the senate of the Montanuniversität Leoben for "Good Scientific Practice".

Furthermore, I declare that the electronic and printed version of the submitted thesis are identical, both, formally and with regard to content.

Date 11.04.2019

Signature Author
Shuqin, Zhang
Matriculation Number: 01535624

Acknowledgements

This thesis is dedicated to the most important and beloved people in my life.
My advisor and his family: I am really lucky to have Prof. Jörg Thuswaldner being my advisor. I thank him to give me the chance to study in Leoben and constantly supported from the time I contacting him. At very beginning, his wife Christiane and he helped me to settle down and provided me with necessities. Every year they invite me to join the Christmas activities. I really enjoy the time with his kids. All these help me a lot to enjoy the life in a foreign country. In my PhD study, he is a great guider. He always shows a keen interest in any problems I asked him and gives me positive answers. And he is full of patience. He is surely a Doktorvater.
My mentor: Benoit Loridant was the second person that I knew in Leoben. Before moving to Leoben, he already helped me to find an apartment and helped to book hotel for my husband and me. He is a joyful person that you want to talk. His smile always infects all of us. I thank him for a lot of effective discussions when we had the first joint paper. And also thank him for his efforts to give an interesting lecture on Algebraic Topology.
Prof. Rao Hui: I studied in Wuhan from 2010-2015 with Prof. Rao. Frankly speaking, it was his effort that made me to become who I am today. He is the one who taught me how to think and solve a problem in a mathematical way. I really enjoyed the time when we discuss mathematics and that was my most valuable memories in Wuhan. During the PhD study here, I also visited Prof. Rao several times, I really thank his group and him for the warm hospitality.
Prof. Akiyama Shigeki: He is the most interesting mathematician I had ever met. He always has many many impressive ideas and statements. He is the one who can easily discover the merits of others. When I talked with him, I felt comfortable and being encouraged. I am very much obliged by his hospitality when I spent two and half months in Japan. And I really thank his student Ito Hiroaki for his kindly help which allowed me to spend a really 'hot' but wonderful summer in Japan.
Prof. Pethö Attila: I attended a short semester (spring, 2017) lecture of him. At that moment we went to TU Graz and came back to Leoben together every week. I still remember that he was still full of passion after the whole afternoon lecture. I guess he is always excited when he is talking about mathematics. I really thank him to teach me how to use the coffee machine during the ester break in our department. And he also inspired me to work harder on mathematics.
Leoben group: It is an internationally small group (Arnold, Andrea, Benoit, Christiaan, Debora, Jörg, Jonas, Mario, Manuela, Myriam, Yasushi (he left for UK this Spring), and Prof. Kirschenhofer). I love the people in the department of math. They are my family in Leoben. I can't imagine the life here without them. I enjoyed all the activities we attended together, eating, hiking and so on. Every day we go for lunch together in Mensa. The most important part comes the coffee break and we share our daily experience at this time. I am looking forward for every work day because of the coffee break.
My family: first for my parents they gave me life and raised me up adult. They contributed all they have to my study. My grandpa, he was the one who gave me the name, the one that made me feel being cared when I was young, and the one who

taught me how it is important to be an honest individual. He always talked with me about something interesting which is not related anything about my study. My sister and brother: It is great to have them. They are the most precious gifts I had ever got from my parents. My husband: I really thank him for his understanding and support of my personal career. I thank him for coming together with me to Leoben for the first time. Actually it was the first trip that we travelled abroad. We were worried and excited. But finally we arrived Leoben safely. I know it is not easy for him to stay in China alone, and I always feel I owe him a lot and I can't give him any help when he needs. He told me that we are young and should work harder to have a better future. I am grateful for having such an excellent husband. My best friend: what is the friend? In my sense, I think that it is the one who is just as weird as you. But they can always bring you back from the brink. I am lucky to have such best ones (Wu Fan, Zhang Man, Huang Liangyi, Hou Aidong) in my life. They appeared in different period of my study journey. They totally understand my short and unpredictable temper, keep company with me and support me. My appreciation is beyond words.

I am also very thankful that the great Doctoral Program funded by the Austrian Science Fund (FWF) gave me the opportunity to study in three Universities (MU, TU Graz and KFU) and supported me to travel worldwide for conferences and research stays and met lots of people who share the same interest.

Contents

Introduction

This thesis is focused on the topological problems related to self-affine tiles, crystallographic tiles and the construction of space-filling curves (SFCs) for self-affine tiles and Rauzy fractals. In what follows, we will introduce these topics. We start with the topological properties of self-affine tiles.

Subject 1: Self-affine tiles. (cf. Chapter 1)

Let $\{f_1, f_2, \ldots, f_n\}$ be a family of contractions on $\mathbb{R}^m$. Hutchinson [**37**] proved that there exists a unique nonempty compact set K satisfying

$$K = f_1(K) \cup f_2(K) \cup \cdots \cup f_n(K).$$

We call K the *invariant set* of the *iterated function system* (IFS for short) $\{f_1, \ldots, f_n\}$. We are interested in special cases of invariant sets. In particular, we will consider IFS whose functions f_i are affine and have the same linear part.

To be more precise recall first that a matrix is expanding if all its eigenvalues are strictly greater than 1 in modulus. Let M be a $m \times m$ real expanding matrix and suppose that $|\det(M)| = n$ ($\det(M)$ is the determinant of M) for some integer $n > 1$. Let $\mathcal{D} = \{d_1, \ldots, d_n\} \subset \mathbb{R}^m$ be a finite set of vectors which we will call a *digit set*. Then by the above-mentioned result of Hutchinson there is a nonempty compact set $T = T(M, \mathcal{D})$ satisfying

$$MT = \bigcup_{i=1}^{n} (T + d_i). \tag{0.1}$$

This set equation we can simply write as $MT = T + \mathcal{D}$. If T has positive Lebesgue measure we call it a *self-affine tile* (see Lagarias and Wang [**51, 52, 53**]). Especially, if the expanding matrix M is a similarity, *i.e.*, $M = \lambda Q$ where $\lambda > 1$ and Q is an orthogonal matrix, then a self-affine tile degenerates to a self-similar tile. (See for instance [**9, 31, 45, 65, 70**]). If $\mathcal{D} \subset \mathbb{Z}^m$ and $T + \mathbb{Z}^m = \mathbb{R}^m$ with $(T + a)$ and $(T + a')$ are disjoint in the sense that the Lebesgue measure of the intersection is zero for any $a, a' \in \mathbb{Z}^m$ with $a \neq a'$, we call T a self-affine $\mathbb{Z}^m$-tile.

Self-affine tiles have been extensively studied in many papers and play a role in many differemt contexts, for instance in the theory of radix expansions ([**71, 66, 43, 39, 21**]), in dynamics ([**85, 17, 46, 73, 89**]), in wavelets ([**32, 31, 90, 97**], and in physics ([**16**]). The fractal structure of their boundary also attracts the attention of many mathematicians ([**94, 27, 3**]). As objects giving interesting tilings of $\mathbb{R}^m$, self-affine tiles also have been investigated by [**9, 11, 25, 33, 44, 92**]. An and Lau [**5**] worked on giving a characterization of digit sets of the planar self-affine sets. One direction that we are particularly interested in and to which the thesis is devoted, is

the topology of self-affine tiles. Starting with the fundamental work of Hata [**34**] on topological properties of invariant set of IFS the study of the topological properties of self-affine tiles attracted many mathematicians. For instance, Kirat and Lau [**47**] and Akiyama and Gjini [**1**] studied the connectedness property of tiles, Bandt and Wang [**12**] and Lau and Leung [**55**] gave criteria for a planar self-affine tile to be homeomorphic to a disk, the planar connected self-affine tiles with disconnected interior were treated by Ngai and Tang [**70**]. Most of the previous topological results of self-affine tiles are devoted to the 2-dimensional case. The study of topological properties of 3-dimensional self-affine tiles just came to the fore a few years ago, for instance in Bandt [**10**] (he studies the 3-dimensional twin dragons), Conner and Thuswaldner [**20**] (they give criteria for a 3-dimensional self-affine tile to be homeomorphic to a 3-ball), and Deng *et al.* [**26**] (they present a certain class of 3-dimensional self-affine tiles which is homeomorphic to a 3-ball).

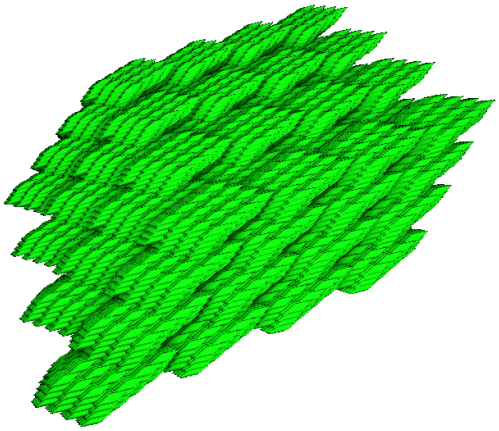

FIGURE 1. An example of 3-dimensional self-affine tile.

A powerful tool in the study of topological properties is the *neighbor graph*: it gives a precise description of the boundary of a given self-affine tile in terms of a graph. This graph induces a graph directed iterated function system (GIFS) describing the boundary ∂T. To find the neighbors of the $\mathbb{Z}^m$-tile, an algorithm was set up in [**81**]. For any given tile, we can work out the neighbor graph with the algorithm. But it is always difficult to deal with infinite classes of tiles.

In this thesis we study topological properties of 3-dimensional self-affine tiles with collinear digit set. We say that $\mathcal{D} \subset \mathbb{Z}^m$ is a *collinear digit set* for the integral expanding matrix M if there is a vector $v \in \mathbb{Z}^m \setminus \{0\}$ such that

$$\mathcal{D} = \{0, v, 2v, \ldots, (|\det M| - 1)v\}. \tag{0.2}$$

If $\mathcal{D}$ has this form we call a self-affine tile $T = T(M, \mathcal{D})$ a *self-affine tile with collinear digit set* (see [**55**]). Figure 1 contains an example of a three dimensional self-affine tile with collinear digit set. It turns out that each self-affine tile with collinear digits set in $\mathbb{R}^3$ can be brought a normal for in the following way. For any integers A, B, C with $1 \leq A \leq B < C$, we consider a self-affine tile T' in $\mathbb{R}^3$ induced by an expanding integer 3×3 matrix with characteristic polynomial $x^3 + Ax^2 + Bx + C$ and collinear digit set (0.2). Akiyama and Loridant [**3**] observed that T' can be transformed to

so-called *ABC-tile* by the discussion in (1.11) in Section 1.2.2. Hence, to study the topological property of T' it suffices to study a related ABC-tile.

ABC-tiles are defined as follows. A self-affine tile T given by $MT = T + \mathcal{D}$ with

$$M = \begin{pmatrix} 0 & 0 & -C \\ 1 & 0 & -B \\ 0 & 1 & -A \end{pmatrix} \quad \text{and} \quad \mathcal{D} = \left\{ \begin{pmatrix} 0 \\ 0 \\ 0 \end{pmatrix}, \begin{pmatrix} 1 \\ 0 \\ 0 \end{pmatrix}, \ldots, \begin{pmatrix} C-1 \\ 0 \\ 0 \end{pmatrix} \right\},$$

where $A, B, C \in \mathbb{Z}$ satisfy $1 \leq A \leq B < C$, is called *ABC-tile*.

We will show in Lemma 1.12 that an ABC-tile is a $\mathbb{Z}^3$-tile. And we also find that the algorithm in [**81**] can work on the whole family of ABC-tiles. Then we obtain that the ABC-tiles have 14-neighbors under certain conditions of A, B, C, see Proposition 1.16 in Section 1.2.4 (for the general result see Theorem 1.4). Moreover, we also give a complete characterization of the directed graphs of multiple intersections in Section 1.2.5 (see Lemma 1.26).

Roughly speaking, a tile has nice topological behavior if it has few neighbors. For the two dimensional self-affine tiles this has been investigated by Bandt and Wang [**12**] which proved that the planar self-affine tiles with 6 neighbors often are homeomorphic to a closed disk (accordingly, a tiling of $\mathbb{R}^2$ by unit squares in *general position* has 6 neighbors). Similarly, the 14 neighbors phenomena of T means that T has the same number of neighbors as each tile in a lattice tiling of $\mathbb{R}^3$ by unit cubes *in general position* (meaning that the cubes in this tiling are not aligned whenever possible). We prove that the boundary of such a tile T is homeomorphic to a 2-sphere whenever its set of neighbors contains 14 elements. Moreover, we give a characterization of 3-, 4-, 5-fold intersection of such kind of $\mathbb{Z}^3$-tiles (see Theorem 1.1). In our proofs we use results of R. H. Bing on the topological characterization of m-spheres for $m \leq 3$, although in his paper Bing does not mention self-affine sets, his characterization is very well suited for self-affine structures. We even think that Bing's result has the potential to be applied in many topological questions around self-affine sets and attractors of iterated function systems in the sense of Hutchinson [**37**]. Our approach can be turned into an algorithm that allows to check if a given 3-dimensional self-affine tile with 14 neighbors has spherical boundary and even has the potential to be generalized to higher dimensions.

Chapter 1 relies on the following submitted paper.

- Jörg Thuswaldner and **Shu-Qin Zhang**, On self-affine tiles whose boundary is a sphere, 2018, submitted. (See [**93**].)

Subject 2: Cystallographic replication tiles. (cf. Chapter 2)

Let us start with the definition of a *tiling* of $\mathbb{R}^m$ by isometries. Assume T is a non-empty compact set such that the closure of its interior T° is equal to T. If there exists a class Γ of isometries in $\mathbb{R}^m$ such that

$$\mathbb{R}^m = \bigcup_{\gamma \in \Gamma} \gamma(T) \text{ with } \gamma(T^\circ) \cap \gamma'(T^\circ) = \emptyset \text{ for } \gamma \neq \gamma' \in \Gamma, \tag{0.3}$$

then we call $\{\gamma(T);\ \gamma \in \Gamma\}$ a *tiling* of $\mathbb{R}^m$ with a single tile T. The special case as we considered in previous Subject 1 is that Γ is isomorphic to $\mathbb{Z}^m$, *i.e.*, $\mathbb{R}^m = T + \mathbb{Z}^m$. In this case the collection $\{\gamma(T); \gamma \in \Gamma\}$ is a lattice tiling of $\mathbb{R}^m$. Here we are interested in a more general case where Γ is a *crystallographic group* which is a discrete cocompact subgroup of the group $\mathrm{Isom}(\mathbb{R}^m)$ of isometries in $\mathbb{R}^m$. In this situation we call $\{\gamma(T);\ \gamma \in \Gamma\}$ a *crystallographic tiling* of $\mathbb{R}^m$.

A *crystallographic replication tile* (*crystile* for short) with respect to a crystallographic group $\Gamma \subset \mathrm{Isom}(\mathbb{R}^m)$ is a nonempty compact set $T \subset \mathbb{R}^m$ such that $\{\gamma(T);\ \gamma \in \Gamma\}$ is a crystallographic tiling of $\mathbb{R}^m$ and T satisfies the following property.

- *Self-affine property*: There is an expanding affine mapping $g : \mathbb{R}^m \to \mathbb{R}^m$ such that $g \circ \Gamma \circ g^{-1} \subset \Gamma$, and a finite collection $\mathcal{D} \subset \Gamma$ called *digit set* such that

$$g(T) = \bigcup_{\delta \in \mathcal{D}} \delta(T). \tag{0.4}$$

A crystile T means that the associated digit set $\mathcal{D}$ must be a complete set of right coset representatives of the subgroup $g \circ \Gamma \circ g^{-1}$. On the other side, Gelbrich [**30**] proves that there is a subset $\Gamma' \subset \Gamma$ called *tiling set* such that the family $\{\gamma(T); \gamma \in \Gamma'\}$ is a tiling of $\mathbb{R}^m$ when $T \subset \mathbb{R}^m$ is a nonempty compact set satisfying (0.4) and $\mathcal{D}$ is a complete set of right coset representatives of the subgroup $g \circ \Gamma \circ g^{-1}$. However, unlike the lattice case (see [**53**]) it is not clear if the tiling set Γ' is always a subgroup of the crystallographic group Γ. Fortunately, the *crystallographic number systems* which were created by Loridant [**59**] in similar way to the canonical number systems from the lattice case (see [**42**]) gives a way to construct classes of crystiles whose tiling set is the whole group Γ. An infinite class of examples given in [**59**] reads as follows.

$p2$-crystallographic replication tiles. Let T be a crystile in $\mathbb{R}^2$. We call T a *$p2$-crystallographic replication tile* ($p2$-cystile) if T tiles the plane by the $p2$-group which is a group of isometries of $\mathbb{R}^2$ isomorphic to the subgroup of $\mathrm{Isom}(\mathbb{R}^2)$ generated by the translations a, b and the π-rotation c where $a(x, y) = (x+1, y),\ b(x, y) = (x, y+1),\ c(x, y) = (-x, -y)$.

In this thesis (Chapter 2), we will study a special class of $p2$-cystiles. For $A, B \in \mathbb{Z}$ satisfying $|A| \leq B \geq 2$, let the expanding mapping g and the digit set $\mathcal{D}$ be defined by

$$g(x, y) = \begin{pmatrix} 0 & -B \\ 1 & -A \end{pmatrix} \begin{pmatrix} x \\ y \end{pmatrix} + \begin{pmatrix} \frac{B-1}{2} \\ 0 \end{pmatrix}, \quad \mathcal{D} = \{id, a, a^2, \ldots, a^{B-2}, c\}. \tag{0.5}$$

Then T determined by equation (0.4) with the above mapping g and digit set $\mathcal{D}$ defines a crystile whose tiling set is the whole group $p2$. For $A \geq -1$, the crystallographic number system property gives the tiling property by [**59**], and we will deduce it for all values of A by Proposition 2.6. However, the more interesting part for us is about of the topological properties of the above tiles. For the lattice tiling, there is a large literature (see the previous introduction for self-affine tiles). Especially, we are interested in when the above $p2$-tiles are homeomorphic to a closed disk which we call *disk-likeness*. Loridant [**59**] shows that the union of T and $-T$ is

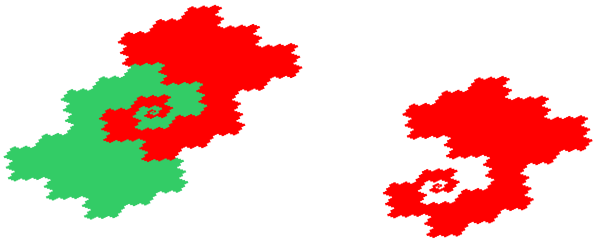

(a) The lattice tile T^ℓ (b) The crystallographic tile T

FIGURE 2. Lattice tile and Crystile for $A = 1, B = 3$.

a translation of the self-affine lattice tile T^ℓ defined by the following equation. (See Figure 2.)

$$\begin{pmatrix} 0 & -B \\ 1 & -A \end{pmatrix} T^\ell = T^\ell \cup \left(T^\ell + \begin{pmatrix} 1 \\ 0 \end{pmatrix} \right) \cup \cdots \cup \left(T^\ell + \begin{pmatrix} B-1 \\ 0 \end{pmatrix} \right). \tag{0.6}$$

Then we can obtain topological information on T by comparing it T^l. Moreover,

(a) The lattice tile T^ℓ (b) The crystallographic tile T

FIGURE 3. Lattice tile and Crystile for $A = 2, B = 3$.

Leung and Lau [**55**] prove that T^ℓ is disk-like if and only if $2|A| < B + 3$. However, it was noticed in [**59**] that it can happen that T^ℓ is disk-like while T is not disk-like (see Figure 3).

It is always necessary to study the neighbor graph when we study the topological properties of a tile. The structure of the boundary of the tile can be descried in detail by a GIFS. Scheicher and Thuswaldner [**80**] introduce an algorithm to give the neighbor graph for any given tile T, while it is usually difficult to deal with infinite classes of tiles. However, Akiyama and Thuswaldner computed the neighbor graph for the class of planar self-affine lattice tiles (0.6) associated with canonical number systems and used it to characterize the disk-like tiles among this class [**4**]. Loridant *et al.* ([**61, 62**]) extend this method on neighbor graph to crystiles. Then we will establish exactly for which parameters A, B this phenomenon occurs. For $2|A| - B < 3$, the associated lattice tile T^ℓ is disk-like and a result of

Akiyama and Thuswaldner [**4**] allow us to estimate the set of neighbors of T by the relation of T and T^ℓ. Finding out the disk-like tiles for parameters satisfying $2|A| - B < 3$ will then rely on the construction of the associated neighbor graphs for the whole class (see Section 2.3 and Section 2.4 for more details). For $2|A| - B \geq 3$, a purely topological argument will enable us to prove that the associated tiles are not disk-like (see Section 2.7). Our results easily generalize to a broader class of crystallographic replication tiles, closely related to the class of self-affine tiles with consecutive collinear digit set as studied by Leung and Lau in [**55**] (see the discussion in Section 2.2.2). Therefore, we are able to show the classification Theorem 2.1. And in fact, the theorem give all possible cases for $B \geq 2$.

Chapter 2 relies on the following publication.

- B. Loridant and **Shu-Qin Zhang**, Topology of a class of $p2$-crystallographic replication tiles, *Indag. Math. (N.S.)*, 28 (2017), pp.805-823. (See [**63**].)

Subject 3: Space-filling curves for self-affine sets. (cf. Chapter 3.)

Space-filling curves have fascinated mathematicians for over a century after the monumental construction of Peano in 1890 [**72**]. Here we mention the book of Sagan [**79**] for a general reference to the early works on space-filling curves (SFCs). All the known constructions of SFCs depend on certain 'substitution rules', for instance, the L-system method by Lindenmayer [**58**] and the recurrent set method by Dekking [**24**] provide exact meaning of 'substitution rule' and build a bridge from substitution rules to SFCs, but they do not tell how to construct substitution rules. Recently, Rao and Zhang [**76**], Dai, Rao and Zhang [**22**], Rao and Zhang [**77**] introduce a systematic method to construct space-filling curves for connected self-similar sets. In their work, they specify the meaning of SFC:

A space-filling curve is an almost one to one, measure preserving and Hölder continuous mapping from the unit interval $[0, 1]$ *to a compact set with positive Hausdorff measure.*

There are several significant parts contained in the series of papers [**76**][**22**][**77**]. The first one is that we introduce the new concept *linear graph-directed IFS* and show that there exists SFC for the invariant sets of the linear GIFS with certain conditions. Then, we introduce the definition of a skeleton of a self-similar set which plays a key role in the whole theory. Using the skeleton, an *edge-to-trail substitution* can be constructed and hence a linear structure followed the substitution will be induced. Actually the self-similar set will be presented as a disjoint union of the invariant sets of a linear GIFS.

Following this method for self-similar sets, we have a brief look at self-affine sets. For one side, we can extend some of the definitions we did for self-similar sets, for example the skeleton, the ordered GIFS, and the linear GIFS, to the self-affine sets induced by contractions instead of similitudes. For the other side, the self-affine sets have more complex structure than self-similar sets due to the different contraction ratios in different directions. There are almost no systematic works on the space-filling curves of self-affine sets except some examples provided by Dekking [**24**], Sirvent's study under some special conditions [**86, 87**], boundary parametrizations

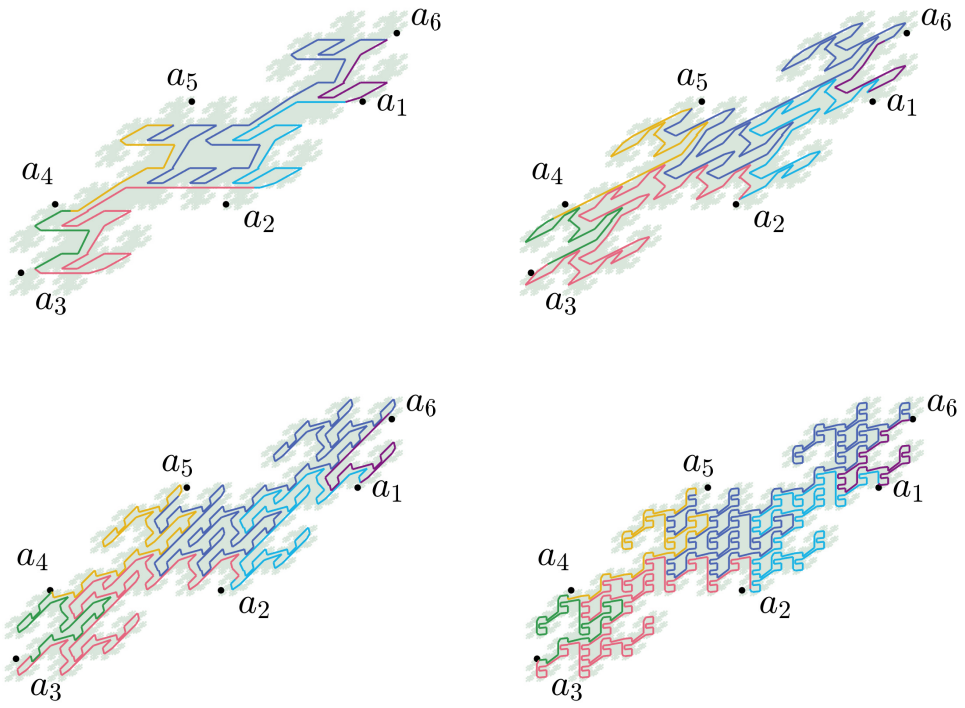

FIGURE 4. The approximating curves of AB- tile with $A = 2, B = 2$.

of self-affine tiles by Akiyama and Loridant [**2, 3**], and boundary parametrizations of a class of cubic Rauzy fractals by Loridant [**60**]. The purpose of the Chapter 3 is to carry out first systematic studies in this direction. First, we generalize the result of [**76**] to the invariant sets of a linear *single-matrix GIFS* (see Section 3.1.1) which is Theorem 3.5 (see Section 3.1.3 for the statement of it and Section 3.2.3.2 for the proof). Then we will extend the definition of skeleton to the graph-directed iterated function system as well as the construction of edge-to-trail substitution. In terms of these, we can continue to study of the space-filling curves of self-affine sets and Rauzy fractals. In Sections 3.4, 3.5, 3.6, we will show the constructions by different examples, such as McMullen sets, self-affine lattice tiles given by equation (0.6) (see Figure 4) and the classical Rauzy fractal (see Figure 5). On the whole chapter we show more about the constructions of SFCs for exact examples other than the theoretical part.

Chapter 3 is related to the following manuscript and publications.

- **Shu-Qin Zhang**, Optimal parametrizations of a class of self-affine sets, 2019, in preparing. (See [**98**].)
- Hui Rao and **Shu-Qin Zhang**, Space-filling curves of self-similar sets (I): iterated function systems with ordered structures, *Nonlinearity*, 29(2016), pp. 2112-2132. (See [**76**].)

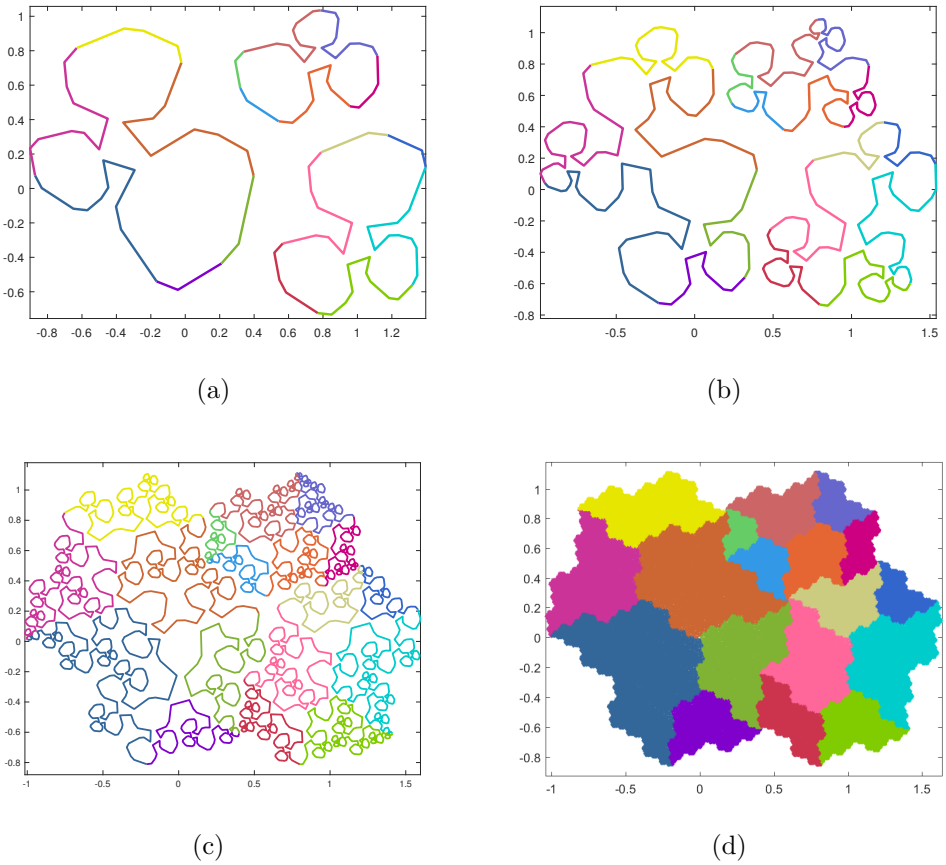

(a) (b)

(c) (d)

FIGURE 5. The approximating curves of the classical Rauzy fractal in Chapter 3.6.1.

- Xin-rong Dai, Hui Rao and **Shu-Qin Zhang**, Space-filling curves of self-similar sets (II): Edge-to-trail substitution rule, *Nonlinearity*, 32(2019), pp. 1772-1809. (See [**22**].)

CHAPTER 1

On self-affine tiles whose boundary is a sphere

This chapter contains the manuscript [**93**] with the same title. It is joint work with Jörg Thuswaldner. This manuscript is currently submitted.

1.1. Introduction

Let $m \in \mathbb{N}$ and suppose that M is an $m \times m$ integer matrix which is *expanding*, *i.e.*, each of its eigenvalues is greater than 1 in modulus. Let $\mathcal{D} \subset \mathbb{Z}^m$ be a set of cardinality $|\det M|$ which is called *digit set*. By a result of Hutchinson [**37**], there exists a unique nonempty compact subset $T = T(M, \mathcal{D})$ of $\mathbb{R}^m$ such that

$$MT = T + \mathcal{D}. \tag{1.1}$$

If T has positive Lebesgue measure we call it a *self-affine tile*. Images of two 3-dimensional self-affine tiles with typical "fractal" boundary are shown in Figure 6

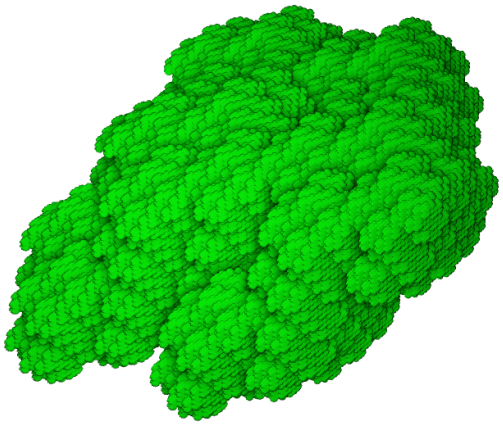

FIGURE 6. An example of 3-dimensional self-affine tile.

(all images of 3-dimensional tiles in this paper are created using IFStile [**69**]). Initiated by the work of Thurston [**92**] and Kenyon [**44**] self-affine tiles have been studied extensively in the literature. A systematic theory of self-affine tiles including the lattice tilings they often induce has been established in the 1990ies by Gröchenig and Haas [**31**] as well as Lagarias and Wang [**51, 52, 53**]. Since then, self-affine tiles have been investigated in many contexts. One field of interest, the one to which the present paper is devoted, is the topology of self-affine tiles. Based on the pioneering work of Hata [**34**] on topological properties of attractors of iterated function systems many authors explored the topology of self-affine tiles. For instance, Kirat and Lau [**47**] and Akiyama and Gjini [**1**] dealt with connectivity of tiles. Later, finer topological properties of 2-dimensional self-affine tiles came into the focus of

research. Bandt and Wang [**12**] gave criteria for a self-affine tile to be homeomorphic to a disk (see also Lau and Leung [**55**]), Ngai and Tang [**70**] dealt with planar connected self-affine tiles with disconnected interior, and Akiyama and Loridant [**3**] provided parametrizations of the boundary of planar tiles.

Only a few years ago first results on topological properties of 3-dimensional self-affine tiles came to the fore. Bandt [**10**] studied the combinatorial topology of 3-dimensional twin dragons. Very recently, Conner and Thuswaldner [**20**] gave criteria for a 3-dimensional self-affine tile to be homeomorphic to a 3-ball by using upper semi-continuous decompositions and a criterion of Cannon [**19**] on tame embeddings of 2-spheres. Deng *et al.* [**26**] showed that a certain class of 3-dimensional self-affine tiles is homeomorphic to a 3-ball.

Let M be an expanding $m \times m$ integer matrix. We say that $\mathcal{D}$ is a *collinear digit set* for M if there is a vector $v \in \mathbb{Z}^m \setminus \{0\}$ such that

$$\mathcal{D} = \{0, v, 2v, \dots, (|\det M| - 1)v\}. \tag{1.2}$$

If $\mathcal{D}$ has this form we call a self-affine tile $T = T(M, \mathcal{D})$ a *self-affine tile with collinear digit set* (such tiles have been studied by many authors in recent years, see for instance Lau and Leung [**55**]). In the present paper we establish a general characterization of 3-dimensional self-affine tiles with collinear digit set whose boundary is homeomorphic to a 2-sphere. In its proof we use a result of Bing [**15**] that provides a topological characterization of m-spheres for $m \leq 3$ (although in his paper Bing does not mention self-affine sets, his characterization is very well suited for self-affine structures). Our methods can also be turned into an algorithm that allows to decide if a given 3-dimensional self-affine tile (with given arbitrary digit set) has a boundary that is homeomorphic to a 2-sphere (see Remark 1.53).

Before we state our main results we introduce some notation. Let $T = T(M, \mathcal{D})$ be a self-affine tile in $\mathbb{R}^m$ with collinear digit set and define the set of *neighbours* of T by

$$\mathcal{S} = \{\alpha \in \mathbb{Z}[M, \mathcal{D}] \setminus \{0\};\ T \cap (T + \alpha) \neq \emptyset\}, \tag{1.3}$$

where

$$\mathbb{Z}[M, \mathcal{D}] = \mathbb{Z}[\mathcal{D}, M\mathcal{D}, \dots, M^{m-1}\mathcal{D}] \subset \mathbb{Z}^m$$

is the smallest M-invariant lattice containing $\mathcal{D}$. This definition is motivated by the fact that the collection $\{T + \alpha;\ \alpha \in \mathbb{Z}[M, \mathcal{D}]\}$ often tiles the space $\mathbb{R}^m$ with overlaps of Lebesgue measure 0 (see *e.g.* Lagarias and Wang [**53**]). The translated tiles $T + \alpha$ with $\alpha \in \mathcal{S}$ are then those tiles of this tiling which touch the "central tile" T. It is clear that $\mathcal{S}$ is a finite set since T is compact by definition. Set

$$\boldsymbol{B}_\alpha = T \cap (T + \alpha) \qquad (\alpha \in \mathbb{Z}[M, \mathcal{D}] \setminus \{0\}). \tag{1.4}$$

More generally, for $\ell \geq 1$ and a subset $\boldsymbol{\alpha} = \{\alpha_1, \dots, \alpha_\ell\} \subset \mathbb{Z}[M, \mathcal{D}] \setminus \{0\}$ we define the $(\ell + 1)$-*fold intersections* by

$$\boldsymbol{B}_{\boldsymbol{\alpha}} = \boldsymbol{B}_{\alpha_1, \dots, \alpha_\ell} = T \cap (T + \alpha_1) \cap \dots \cap (T + \alpha_\ell) \qquad (\boldsymbol{\alpha} \subset \mathbb{Z}[M, \mathcal{D}] \setminus \{0\}).$$

Compactness of T again yields that there exist only finitely many sets $\boldsymbol{\alpha} \subset \mathbb{Z}[M, \mathcal{D}]$ with $\boldsymbol{B}_{\boldsymbol{\alpha}} \neq \emptyset$.

THEOREM 1.1. *Let $T = T(M, \mathcal{D})$ be a 3-dimensional self-affine tile with collinear digit set and assume that the characteristic polynomial $x^3 + Ax^2 + Bx + C$ of M satisfies $1 \le A \le B < C$. Then $\{T + \alpha;\, \alpha \in \mathbb{Z}[M, \mathcal{D}]\}$ tiles the space $\mathbb{R}^3$ with overlaps of Lebesgue measure 0. If T has 14 neighbors then the following assertions hold.*

(1) *The boundary ∂T is homeomorphic to a 2-sphere.*
(2) *If $\alpha \in \mathbb{Z}[M, \mathcal{D}] \setminus \{0\}$, the 2-fold intersection $\boldsymbol{B}_\alpha$ is homeomorphic to a closed disk for each $\alpha \in \mathcal{S}$ and empty otherwise.*
(3) *If $\boldsymbol{\alpha} \subset \mathbb{Z}[M, \mathcal{D}] \setminus \{0\}$ contains two elements, the 3-fold intersection $\boldsymbol{B}_{\boldsymbol{\alpha}}$ is either homeomorphic to an arc or empty. The 36 sets $\boldsymbol{\alpha}$ with $\boldsymbol{B}_{\boldsymbol{\alpha}} \neq \emptyset$ can be given explicitly.*
(4) *If $\boldsymbol{\alpha} \subset \mathbb{Z}[M, \mathcal{D}] \setminus \{0\}$ contains three elements, the 4-fold intersection $\boldsymbol{B}_{\boldsymbol{\alpha}}$ is either a single point or empty. The 24 sets $\boldsymbol{\alpha}$ with $\boldsymbol{B}_{\boldsymbol{\alpha}} \neq \emptyset$ can be given explicitly.*
(5) *If $\boldsymbol{\alpha} \subset \mathbb{Z}[M, \mathcal{D}] \setminus \{0\}$ contains $\ell \ge 4$ elements, the $(\ell + 1)$-fold intersection $\boldsymbol{B}_{\boldsymbol{\alpha}}$ is always empty.*

REMARK 1.2. Note that Theorem 1.1 (1) and (2) imply that for $\alpha \in \mathcal{S}$ the boundary $\partial_{\partial T} \boldsymbol{B}_\alpha$ is a simple closed curve. Here and in the sequel we denote by ∂_X the boundary taken w.r.t. the subspace topology on $X \subset \mathbb{R}^3$.

REMARK 1.3. We posed the restriction $1 \le A \le B < C$ on the coefficients of the characteristic polynomial of M because it makes the combinatorial preparations in Section 1.2 a lot easier. Using the characterization of contracting (and, hence, also of expanding) polynomials going back to Schur [**83**] it should be possible to treat the remaining expanding characteristic polynomials and, hence, arbitrary expanding 3×3 matrices. This will lead to several different cases of neighbor graphs, however, the topological methods of Section 1.3 should go through without modification.

We see from the statement of Theorem 1.1 that the number of neighbors plays an important role for the topological behavior of ∂T and the sets of intersections. The fact that T has 14 neighbors means that T has the same number of neighbors as each tile in a lattice tiling of $\mathbb{R}^3$ by unit cubes *in general position* (meaning that the cubes in this tiling are not aligned whenever possible). Sloppily speaking, if a tile has few neighbors then it tends to behave topologically nice. For the case of 2-dimensional self-affine tiles this has been explored by Bandt and Wang [**12**]. In particular, they proved that in two dimensions, self-affine tiles with 6 neighbors often are homeomorphic to a closed disk (accordingly, a tiling of $\mathbb{R}^2$ by unit squares in general position has 6 neighbors).

Theorem 1.1 raises the question when 3-dimensional self-affine tiles with collinear digit set have 14 neighbors. This question is answered as follows.

THEOREM 1.4. *Let $T = T(M, \mathcal{D})$ be a 3-dimensional self-affine tile with collinear digit set and assume that the characteristic polynomial $x^3 + Ax^2 + Bx + C$ of M satisfies $1 \le A \le B < C$.*

Then T has 14 neighbors if and only if A, B, C satisfy one of the following conditions.

(1) *$1 \le A < B < C$, $B \ge 2A - 1$, and $C \ge 2(B - A) + 2$;*

(2) $1 \le A < B < C$, $B < 2A - 1$, *and* $C \ge A + B - 2$.

The paper is organized as follows. In Section 1.2 we prove Theorem 1.4. The main ingredient of this proof are certain graphs that contain information on the neighbors of T. These graphs also can be used to define so-called *graph-directed iterated function systems* in the sense of Mauldin and Williams [**67**] whose attractor is the collection $\{\boldsymbol{B}_\alpha;\, \alpha \in \mathcal{S}\}$. We will also establish graphs that describe the nonempty ℓ-fold intersections $\boldsymbol{B}_{\boldsymbol{\alpha}}$. All these results will be needed in Section 1.3, the core part of the present paper, where we will combine them with Bing's results from [**15**] and other topological results including dimension theory to establish Theorem 1.1. In Section 1.4 we discuss perspectives for further research.

1.2. Intersections and neighbors

In this section we set up graphs that describe the intersections of a self-affine tile with its neighbors. The basic definitions are given in Section 1.2.1. In Section 1.2.2 we show that there exists a normal form for self-affine tiles with collinear digit set that we can use in all what follows. Sections 1.2.3 and 1.2.4 deal with the calculation of the so-called contact and neighbor graph for the class of tiles we are interested in. In particular, in Proposition 1.16 the proof of Theorem 1.4 is finished. Finally, Section 1.2.5 deals with ℓ-fold intersections of tiles.

1.2.1. Graphs related to the boundary of a tile. We start with collecting some basic properties of self-affine tiles that will be used in Definition 1.5, where particular self-affine tiles, so-called $\mathbb{Z}^m$-tiles, will be defined. These $\mathbb{Z}^m$-tiles are important for us and allow the definition of certain graphs that are related to the intersections $\boldsymbol{B}_\alpha$ defined in (1.4).

Let M be an expanding $m \times m$ integer matrix and $\mathcal{D} \subset \mathbb{Z}^m$. It is shown in Bandt [**9**] that the fact that $\mathcal{D} \subset \mathbb{Z}^m$ is a complete set of coset representatives of $\mathbb{Z}^m/M\mathbb{Z}^m$ implies that $T = T(M, \mathcal{D})$ has positive Lebesgue measure and, hence, is a self-affine tile. If $T = T(M, \mathcal{D})$ is a self-affine tile, according to Lagarias and Wang [**51**, Lemma 2.1] we may assume w.l.o.g. that the digit set $\mathcal{D}$ is *primitive for* M in the sense that $\mathbb{Z}[M, \mathcal{D}] = \mathbb{Z}^m$. Moreover, Lagarias and Wang [**53**] proved that for a self-affine tile with primitive digit set the collection $\{T+\alpha;\, \alpha \in \mathbb{Z}^m\}$ often tiles the space $\mathbb{R}^m$, *i.e.*, $T + \mathbb{Z}^m = \mathbb{R}^m$ with (μ_m denotes the m-dimensional Lebesgue measure)

$$\mu_m((T + \alpha_1) \cap (T + \alpha_2)) = 0 \qquad (\alpha_1, \alpha_2 \in \mathbb{Z}^m \text{ distinct}). \tag{1.5}$$

Motivated by these results we follow Bandt and Wang [**12**] and give the following definition.

Definition 1.5. Let M be an expanding $m \times m$ integer matrix and assume that $\mathcal{D} \subset \mathbb{Z}^m$ is a complete set of coset representatives of $\mathbb{Z}^m/M\mathbb{Z}^m$ which is primitive for M. If the self-affine tile $T = T(M, \mathcal{D})$ tiles $\mathbb{R}^m$ w.r.t. the lattice $\mathbb{Z}^m$ we call T a *$\mathbb{Z}^m$-tile*.

If M and $\mathcal{D}$ are given in a way that $T = T(M, \mathcal{D})$ is a $\mathbb{Z}^m$-tile we obviously have

$$\partial T = \bigcup_{\alpha \in \mathcal{S}} \boldsymbol{B}_\alpha. \tag{1.6}$$

Here $\mathcal{S}$ and $\boldsymbol{B}_\alpha$ are defined as in (1.3) and (1.4), respectively; note that $\mathbb{Z}[M,\mathcal{D}] = \mathbb{Z}^m$ in these definitions because the $\mathbb{Z}^m$-tile T has primitive digit set. One of our main concerns in this section will be the description of the boundary of a $\mathbb{Z}^m$-tile T by studying the sets $\boldsymbol{B}_\alpha$ with $\alpha \in \mathcal{S}$. By the definition of $\boldsymbol{B}_\alpha$ in (1.4) and the defining set equation for T in (1.1) we get

$$\begin{aligned} \boldsymbol{B}_\alpha &= T \cap (T+\alpha) \\ &= M^{-1}(T+\mathcal{D}) \cap M^{-1}(T+\mathcal{D}+M\alpha) \\ &= M^{-1} \bigcup_{d,d'\in\mathcal{D}} (\boldsymbol{B}_{M\alpha+d'-d} + d). \end{aligned} \tag{1.7}$$

This subdivision of $\boldsymbol{B}_\alpha$ has been noted for instance by Strichartz and Wang [**91**] and Wang [**96**].

The graphs that we will be interested in will match the pattern of the following definition.

Definition 1.6 (*cf.* [**81**, Definition 3.2]). Let M be an expanding integer matrix and let $\mathcal{D}$ be a complete set of coset representatives of $\mathbb{Z}^m/M\mathbb{Z}^m$. For a subset $\Gamma \subset \mathbb{Z}^m$ we define a labeled directed graph $G(\Gamma)$ as follows. The states of $G(\Gamma)$ are the elements of Γ, and there is a labeled edge

$$\alpha \xrightarrow{d|d'} \alpha' \quad \text{if and only if } M\alpha + d' - d = \alpha' \text{ with } \alpha,\alpha' \in \Gamma \text{ and } d,d' \in \mathcal{D}. \tag{1.8}$$

In this case α is called a *predecessor* of α' and α' is called a *successor* of α.

In (1.8) the vector d' is determined by α, α', d. Thus we sometimes just write $\alpha \xrightarrow{d} \alpha'$ instead of $\alpha \xrightarrow{d|d'} \alpha'$. We will write $\alpha \in G(\Gamma)$ to indicate that α is a vertex of $G(\Gamma)$ and $\alpha \xrightarrow{d} \alpha' \in G(\Gamma)$ to indicate that $\alpha \xrightarrow{d} \alpha'$ is an edge of $G(\Gamma)$. For walks we will use an analogous notation.

The graph $G(\mathbb{Z}^m)$ is the largest graph related to the pair $(M,\mathcal{D})$. All graphs we consider later will be subgraphs of $G(\mathbb{Z}^m)$. The following symmetry property follows from Definition 1.6.

Lemma 1.7. *Let $\Gamma \subset \mathbb{Z}^m$ be given. If $\alpha,\alpha',-\alpha,-\alpha' \in \Gamma$ then*

$$\alpha \xrightarrow{d|d'} \alpha' \in G(\Gamma) \quad \Longleftrightarrow \quad -\alpha \xrightarrow{d'|d} -\alpha' \in G(\Gamma).$$

We will now set up two important subgraphs of $G(\mathbb{Z}^m)$ that will be related to the boundary of a $\mathbb{Z}^m$-tile $T = T(M,\mathcal{D})$. The first graph we are interested in is the *neighbor graph* $G(\mathcal{S})$, where $\mathcal{S}$ is the set of neighbors of T defined in (1.3) (recall again that $\mathbb{Z}[M,\mathcal{D}] = \mathbb{Z}^m$ by primitivity of $\mathcal{D}$ for M). From (1.7) we see that $\{\boldsymbol{B}_\alpha;\ \alpha \in \mathcal{S}\}$ is the attractor of a graph-directed iterated function system (in the sense of Mauldin and Williams [**67**]) directed by the graph $G(\mathcal{S})$, that is, the nonempty compact sets $\boldsymbol{B}_\alpha$, $\alpha \in \mathcal{S}$, are uniquely determined by the set equations

$$\boldsymbol{B}_\alpha = \bigcup_{\substack{d\in\mathcal{D},\alpha'\in\mathcal{S} \\ \alpha\xrightarrow{d}\alpha'\in G(\mathcal{S})}} M^{-1}(\boldsymbol{B}_{\alpha'} + d) \qquad (\alpha \in \mathcal{S}). \tag{1.9}$$

The union in (1.9) is extended over all d,α' such that $\alpha \xrightarrow{d} \alpha'$ is an edge in the graph $G(\mathcal{S})$. Thus by (1.6) the boundary is determined by the graph $G(\mathcal{S})$. This

fact was used implicitly in Wang [**96**] in order to establish a formula for the Hausdorff dimension of the boundary of a $\mathbb{Z}^m$-tile T.

The second graph is the *contact graph* $G(\mathcal{R})$. This graph can be easily constructed and also determines the boundary of T. Scheicher and Thuswaldner [**81**] proved that (save for stranding vertices and the vertex 0) $G(\mathcal{R})$ is a subgraph of $G(\mathcal{S})$ and showed that $G(\mathcal{S})$ can be algorithmically constructed from $G(\mathcal{R})$. Also in the present paper $G(\mathcal{R})$ is used in order to construct $G(\mathcal{S})$. We introduce some notation. Let $\{e_1, e_2, \ldots, e_m\}$ be a basis of the lattice $\mathbb{Z}^m$, set $R_0 = \{0, \pm e_1, \ldots, \pm e_m\}$ and define R_n inductively by

$$R_n := \{k \in \mathbb{Z}^m;\ (Mk + \mathcal{D}) \cap (\ell + \mathcal{D}) \neq \emptyset \text{ for } \ell \in R_{n-1}\} \cup R_{n-1}. \tag{1.10}$$

We know from Gröchenig and Haas [**31**, Section 4] (see also Duvall *et al.* [**27**]) that R_n stabilizes after finitely many steps, that is $R_{n-1} = R_n$ holds for n large enough. Therefore, $\mathcal{R} = \bigcup_{n\geq 0} R_n$ is a finite set. By Definition 1.6 we get a finite directed graph with set of states $\mathcal{R}$, and call it the *contact graph* $G(\mathcal{R})$. We say that $\mathcal{R}$ is the set of *contact neighbors* of the $\mathbb{Z}^m$-tile. As for the set of neighbors $\mathcal{S}$, also the set $\mathcal{R}$ can be used to define the boundary of T. Indeed, we have

$$\partial T = \bigcup_{\alpha\in\mathcal{R}} \boldsymbol{B}_\alpha$$

(see *e.g.* [**81**]). In [**31**, Section 4] as well as in [**81**] it is explained why the elements of $\mathcal{R}$ are called "contact neighbors". The elements of $\mathcal{R}$ turn out to be neighbors in a tiling of certain approximations T_n of the self-affine tile T, which also form tilings w.r.t. the lattice $\mathbb{Z}^m$ for each $n \geq 0$. However, we will not need this interpretation in the sequel.

Note that in the graph $G(\mathcal{S})$ there cannot occur any *stranding* vertices, *i.e.*, vertices that have no successor. Indeed, if $\alpha \in \mathcal{S}$ would be a stranding vertex this would entail that for this α the right hand side of the set equation (1.9) would be empty. However, this yields $\boldsymbol{B}_\alpha = T \cap (T + \alpha) = \emptyset$, a contradiction to $\alpha \in \mathcal{S}$.

On the contrary, depending on the chosen basis $\{e_1, \ldots, e_m\}$ it may well happen that the graph $G(\mathcal{R})$ contains stranding vertices. Since these vertices are of no use for our purposes, we want to get rid of them. Thus we give the following definition.

Definition 1.8. Let G be a directed graph. By $\mathrm{Red}(G)$ we denote the largest subgraph of G that has no stranding vertex, *i.e.*, $\mathrm{Red}(G)$ emerges from G by successively removing all stranding vertices.

The following product allows to construct the graph $G(\mathcal{S})$, and *a fortiori* the set $\mathcal{S}$, from $\mathcal{R}$.

Definition 1.9 (*cf.* [**81**, Definition 3.5]). Let G_1 and G_1' be subgraphs of $G(\mathbb{Z}^m)$. The product graph $G_2 := G_1 \otimes G_1'$ is defined in the following way. Let r_1, s_1 be vertices of G_1 and r_1', s_1' be vertices of G_1'. Furthermore, let $\ell_1, \ell_1', \ell_2 \in \mathcal{D}$.

- r_2 is a vertex of G_2 if $r_2 = r_1 + r_1'$.
- There exists an edge $r_2 \xrightarrow{\ell_1|\ell_2} s_2$ in G_2 if there exist the edges

$$r_1 \xrightarrow{\ell_1|\ell_1'} s_1 \in G_1 \text{ and } r_1' \xrightarrow{\ell_1'|\ell_2} s_1' \in G_1'$$

with $r_1 + r'_1 = r_2$ and $s_1 + s'_1 = s_2$ or there exist the edges

$$r_1 \xrightarrow{\ell'_1|\ell_2} s_1 \in G_1 \text{ and } r'_1 \xrightarrow{\ell_1|\ell'_1} s'_1 \in G'_1$$

with $r_1 + r'_1 = r_2$ and $s_1 + s'_1 = s_2$.

Scheicher and Thuswaldner [**81**] proved that $G(\mathcal{S})$ can be determined by the following algorithm.

ALGORITHM 1.10 (*cf.* [**81**, Algorithm 3.6]). *The following algorithm computes* $G(\mathcal{S})$ *starting from* $G(\mathcal{R})$.

$p := 1$
$A[1] := \mathrm{Red}(G(\mathcal{R}))$
`repeat`
  $p := p + 1$
  $A[p] := \mathrm{Red}(A[p-1] \otimes A[1])$
`until` $A[p] = A[p-1]$
$G(\mathcal{S}) := A[p] \setminus \{0\}$

Since $0 \in \mathcal{R}$ the sequence of graphs $A[p]$ produced by this algorithm is nested, *i.e.*, $A[1] \subset A[2] \subset \cdots$.

It is immediate from the definition of $\mathcal{R}$ and $\mathcal{S}$ that

$$\alpha \in \mathcal{R} \Longleftrightarrow -\alpha \in \mathcal{R} \qquad \text{and} \qquad \alpha \in \mathcal{S} \Longleftrightarrow -\alpha \in \mathcal{S}.$$

Thus the graphs $G(\mathcal{R})$ and $G(\mathcal{S})$ both enjoy the symmetry property stated in Lemma 1.7 for all vertices. This fact will be often used in the sequel.

1.2.2. A normal form for self-affine tiles with collinear digit set. Let M' be an expanding 3×3 integer matrix with characteristic polynomial x^3+Ax^2+Bx+C and $\mathcal{D}' \subset \mathbb{Z}^3$ a collinear digit set as in (1.2) for some $v \in \mathbb{Z}^3$. Assume that $T' = T'(M', \mathcal{D}')$ has positive Lebesgue measure. Then T' is a self-affine tile with collinear digit set. Akiyama and Loridant [**2**] observed that T' can be transformed in a normal form as follows.

Note first that $\{v, M'v, M'^2v\}$ has to be a basis of $\mathbb{R}^3$ because otherwise T' would have zero Lebesgue measure. Denote by E the matrix of the change of bases from the standard basis $\{e_1, e_2, e_3\}$ of $\mathbb{R}^3$ to the basis $\{v, M'v, M'^2v\}$. Then set

(1.11)

$$M = E^{-1}M'E = \begin{pmatrix} 0 & 0 & -C \\ 1 & 0 & -B \\ 0 & 1 & -A \end{pmatrix} \text{ and } \mathcal{D} = E^{-1}\mathcal{D}' = \left\{ \begin{pmatrix} 0 \\ 0 \\ 0 \end{pmatrix}, \begin{pmatrix} 1 \\ 0 \\ 0 \end{pmatrix}, \ldots, \begin{pmatrix} C-1 \\ 0 \\ 0 \end{pmatrix} \right\}.$$

Define T by $MT = T + \mathcal{D}$. Then we have $T = E^{-1}T'$ and, because E is invertible, this implies that T is a self-affine tile. The linear mapping induced by E^{-1} maps $\mathbb{Z}[M', \mathcal{D}']$ to $\mathbb{Z}^3$. Moreover, $\partial T = E^{-1}\partial T'$ and for $\{\alpha_1, \ldots, \alpha_\ell\} \subset \mathbb{Z}[M', \mathcal{D}']$ we have

$$E^{-1}(T' \cap (T' + \alpha_1) \cap \cdots \cap (T' + \alpha_\ell)) = T \cap (T + E^{-1}\alpha_1) \cap \cdots \cap (T + E^{-1}\alpha_\ell).$$

Thus it is sufficient to prove Theorem 1.1 and Theorem 1.4 for self-affine tiles of the form $T = T(M, \mathcal{D})$ and in all what follows we may focus on the following class of $\mathbb{Z}^3$-tiles.

DEFINITION 1.11. A self-affine tile T given by $MT = T + \mathcal{D}$ with M and $\mathcal{D}$ as in (1.11), where $A, B, C \in \mathbb{Z}$ satisfy $1 \le A \le B < C$, is called *ABC-tile*.

The tiles in Figure 6 and Figure 1 are approximations of ABC-tiles for the choice $(A, B, C) = (1, 1, 2)$ and $(A, B, C) = (1, 2, 4)$, respectively. The ABC-tile corresponding to $(A, B, C) = (2, 3, 5)$ is approximated in Figure 7.

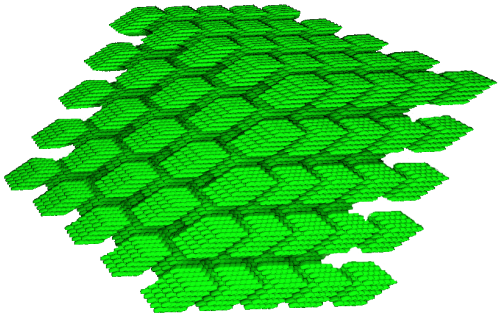

FIGURE 7. The ABC-tile for the choice $(A, B, C) = (2, 3, 5)$.

Everything we did in Section 1.2.1 was done for $\mathbb{Z}^m$-tiles. To apply these results to ABC-tiles we need the following lemma.

LEMMA 1.12. *Each ABC-tile is a $\mathbb{Z}^3$-tile.*[1]

PROOF. Each ABC-tile T is defined as $T = T(M, \mathcal{D})$ with M and $\mathcal{D}$ as in (1.11) with $1 \le A \le B < C$. It is straightforward to check that $\mathcal{D}$ is a complete set of coset representatives of $\mathbb{Z}^3/M\mathbb{Z}^3$ and that it is a primitive digit set for M. Thus it remains to show that $\{T + \alpha;\ \alpha \in \mathbb{Z}^3\}$ tiles $\mathbb{R}^3$. Let

$$\Delta(M, \mathcal{D}) = \bigcup_{\ell \ge 0} ((\mathcal{D} - \mathcal{D}) + M(\mathcal{D} - \mathcal{D}) + \cdots + M^\ell(\mathcal{D} - \mathcal{D})).$$

We claim that $\Delta(M, \mathcal{D}) = \mathbb{Z}^3$. Obviously, $\Delta(M, \mathcal{D}) \subset \mathbb{Z}^3$. We have to prove the reverse inclusion. Since $1 \le A \le B < C$, Barat *et al.* [**13**, Theorem 3.3] implies that $x^3 + Ax^2 + Bx + C$ is the basis of a so-called *canonical number system*. In view of Barat *et al.* [**13**, Definition 3.2 and the paragraph above it] this is equivalent to the fact that $(M, \mathcal{D})$ is a *matrix numeration system*. However, by definition this means that each $z \in \mathbb{Z}^3$ can be represented in the form $z = d_0 + Md_1 + \cdots + M^\ell d_\ell$ with some $\ell \ge 0$ and $d_0, \ldots, d_\ell \in \mathcal{D}$. Thus $\mathbb{Z}^3 \subset \Delta(M, \mathcal{D})$ and the claim is proved.

The result now follows from [**52**, Theorem 1.2 (ii)]. □

In view of the transformation in (1.11) this lemma proves the tiling assertion in Theorem 1.1.

1.2.3. The contact graph. Let T be an ABC-tile which is a $\mathbb{Z}^3$-tile by Lemma 1.12 and recall the definition of R_n from (1.10). We know from Section 1.2.1 that R_n stabilizes after finitely many steps to the set of contact neighbors $\mathcal{R}$ of the ABC-tile T. In the following lemma we characterize this set.

[1]Another way to prove this would be via the general result [**53**, Theorem 6.2]. This would also require several new notations. So we decided to do it this way.

LEMMA 1.13. *Let T be an ABC-tile and let $R_0 = \{0, \pm e_1, \pm e_2, \pm e_3\}$ with $\{e_1, e_2, e_3\}$ being the standard basis of $\mathbb{R}^3$. Then $R_4 = R_3$,* i.e.*, the set of contact neighbors $\mathcal{R}$ is equal to R_3. In particular, set*

$$R^* = \{(B, A, 1)^t, (B-1, A, 1)^t, (B-A, A-1, 1)^t, (B-A+1, A-1, 1)^t, (A, 1, 0)^t, (A-1, 1, 0)^t\}.$$

Then the following assertions hold.

(1) *If $1 \le A < B < C$, then $\mathcal{R} = R_0 \cup R^* \cup (-R^*)$.*
(2) *If $1 \le A = B < C$, then $\mathcal{R} = (R_0 \cup R^* \cup (-R^*)) \setminus \{(1, A-1, 1)^t, -(1, A-1, 1)^t\}$.*

PROOF. We know that $R_0 \subset R_1 \subset R_2 \subset R_3 \subset R_4 \subset \cdots \subset \mathcal{R}$ by definition. From (1.10) it follows that $s \in R_n$ if and only if $s \in \mathbb{Z}^3$ and $Ms + d' - d \in R_{n-1}$ for some $d, d' \in \mathcal{D}$. Thus to calculate R_n it suffices to find all possible predecessors of elements of R_{n-1} in $G(\mathbb{Z}^3)$. Since for $s = (p, q, r)^t \in \mathbb{Z}^3$ we have $Ms = (-Cr,\ p - Br,\ q - Ar)^t$, and $\mathcal{D} - \mathcal{D} = \{(x, 0, 0)^t;\ 1 - C \le x \le C - 1\}$ the vector s is a pedecessor of a given vector s' if and only if

$$s' \in Ms + \mathcal{D} - \mathcal{D} = \{(x - Cr, p - Br, q - Ar)^t;\ 1 - C \le x \le C - 1\}. \tag{1.12}$$

We now start our construction with the calculation of R_1. The first coordinate of the elements of R_0 varies between -1 and 1. Let $s = (p, q, r)^t$ be the predecessor of an element $s' \in R_0$ in $G(\mathbb{Z}^3)$. By (1.12) the first coordinate of $s' = (x - Cr, p - Br, q - Ar)^t$ satisfies $-1 \le x - Cr \le 1$ with $1 - C \le x \le C - 1$ which implies that $r \in \{0, \pm 1\}$. We now inspect each of these cases.

- For $r = 0$, we have $Ms = (0, p, q)^t$. As we need $s' = Ms + d' - d \in R_0$ for some $d, d' \in \mathcal{D}$, the possible choices of (p, q) are $(0, 0), \pm(1, 0), \pm(0, 1)$. Hence $(0, 0, 0)^t, \pm(1, 0, 0)^t, \pm(0, 1, 0)^t$ are elements of R_1 (since all of them are already contained in R_0 this does not contribute a new element to R_1).
- For $r = 1$, we have $Ms = (-C, p - B, q - A)^t$. Since the first coordinate of $Ms + \mathcal{D} - \mathcal{D}$ can be at most -1, the only choice of $s' \in Ms + \mathcal{D} - \mathcal{D}$ being an element of R_0 is that $Ms + d' - d = (-1, 0, 0)^t$ which corresponds to the digits $d = (0, 0, 0)^t, d' = (C - 1, 0, 0)^t$. This is possible only for $p - B = 0, q - A = 0$. Thus $s = (B, A, 1)^t$ is a new element of R_1.
- For $r = -1$ we get from the symmetry stated in Lemma 1.7 that $s = -(B, A, 1)^t$ is an element of R_1.

Denote $s_1 = (B, A, 1)^t$, then we have $R_1 = R_0 \cup \{s_1, -s_1\}$.

To calculate R_2 from R_1 let $s = (p, q, r)^t$ be the predecessor of an element $s' \in R_1$ in $G(\mathbb{Z}^3)$. Again we consider the first coordinate of $s' \in Ms + \mathcal{D} - \mathcal{D}$. By (1.12) this first coordinate is of the form $x - Cr$ with $1 - C \le x \le C - 1$. But since $s' \in R_1$ its first coordinate also satisfies $-C < -B \le x - Cr \le B < C$. Combining these two inequalities yields $-2C + 1 < -Cr < 2C - 1$ which forces $-1 \le r \le 1$. Hence, again we have to deal with three cases.

- For $r = 0$, comparing with the discussion leading to R_1, the new elements $\pm s_1 \in R_1$ admit the two new choices $(p, q) = \pm(A, 1)$. Hence, $\pm(A, 1, 0)^t \in R_2$.

- For $r = 1$, we have $Ms = (-C, p - B, q - A)^t$. Since the first coordinate of $s' \in Ms + \mathcal{D} - \mathcal{D}$ will be at most -1. The only possible values for s' are $(-1, 0, 0)^t$ and $(-B, -A, -1)^t$. This forces $(p - B, q - A) = (0, 0)$ or $(p-B, q-A) = (-A, -1)$. Hence, we get the new element $s = (B-A, A-1, 1)^t \in R_2$.
- For $r = -1$, Lemma 1.7 yields $s = -(B - A, A - 1, 1)^t \in R_2$.

Set $s_2 = (A, 1, 0)^t$ and $s_3 = (B - A, A - 1, 1)^t$, then $R_2 = R_1 \cup \{\pm s_2, \pm s_3\}$. In particular, if $B = A = 1$, then $s_3 = (0, 0, 1)$ being already an element of R_0.

The next step is to calculate R_3 from R_2. Let $s = (p, q, r)^t$ be the predecessor of an element $s' \in R_2$ in $G(\mathbb{Z}^3)$. Since the largest first coordinate of an element of R_2 is less than C in modulus the same reasoning as in the last paragraph yields $-1 \leq r \leq 1$ and we have to deal with three cases again.

- For $r = 0$ we get that an element $s' \in Ms+\mathcal{D}-\mathcal{D}$ is of the form $s' = (x, p, q)^t$ with $1 - C \leq x \leq C - 1$. We added $\pm s_2, \pm s_3$ to R_2 so these elements can contribute new predecessors. Since the pairs of second and third coordinates of $\pm s_2$ already occur in elements of R_1, $\pm s_2$ contribute no new options for (p, q). However, $\pm s_3$ gives the choices $\pm(p, q) = \pm(A - 1, 1)$ which yields to $s = \pm(A - 1,\ 1,\ 0)^t$, two new elements of R_3 if $A \geq 2$.
- For $r = 1$ we get that an element of $s' \in Ms + \mathcal{D} - \mathcal{D}$ is of the form $s' = (x-C,\ p-B,\ q-A)^t$ with $1-C \leq x \leq C-1$, and, hence, the maximal value of the first coordinate of such an element is -1. So if s is a predecessor of an element of R_2, the possible new values of $(x - C,\ p - B,\ q - A)^t$ are $-s_2 = -(A,\ 1,\ 0)^t$ and $-s_3 = -(B - A,\ A - 1,\ 1)^t$. For $-s_3$ to be possible we need the additional condition that $B > A$ (which is the same as $A \neq B$), because otherwise $B - A = 0$ which is not allowed since the first coordinate $x - C$ can be at most -1. Thus $(p - B, q - A) = -(1, 0)$ and $(p-B,\ q-A) = -(A-1, 1)$ (if $A \neq B$) can occur. Thus $(p, q) = (B-1, A)$ or $(p, q) = (B-A+1, A-1)$, hence, $(B-1, A, 1)^t$ and $(B-A+1, A-1, 1)^t$ (if $A \neq B$) are new elements of R_3.
- For $r = -1$, Lemma 1.7 yields that $-(B - A + 1, A - 1, 1)^t$ (if $A \neq B$) and $-(B - 1, A, 1)^t$ are new elements of R_3.

Set $s_4 = (A - 1, 1, 0)^t$, $s_5 = (B - 1, A, 1)^t$, and $s_6 = (B - A + 1, A - 1, 1)^t$, then $R_3 = R_2 \cup \{\pm s_4, \pm s_5, \pm s_6\}$, where s_6 only occurs for $A \neq B$.

We claim that $R_4 = R_3$ by the following facts. Indeed, if $s = (p, q, r)^t$ is the predecessor of an element $s' \in R_3$ in $G(\mathbb{Z}^3)$ then r should satisfy $-1 \leq r \leq 1$ by the same reasoning as in the previous paragraphs. Moreover, the pairs of the second and the third coordinates of the elements of R_3 are the same as in R_2. Thus we conclude that there will be no new elements in R_4. □

The reduced graph $\mathrm{Red}(G(\mathcal{R}))$ is now obtained by deleting the stranding vertices of $G(\mathcal{R})$.

Corollary 1.14.

(1) *For $1 < A < B$ the vertex set of $\mathrm{Red}(G(\mathcal{R}))$ has the 15 elements*

$$\{(0,0,0)^t, \pm(1,0,0)^t, \pm(B,A,1)^t, \pm(B-1,A,1)^t, \pm(B-A,A-1,1)^t,$$
$$\pm(B-A+1,A-1,1)^t, \pm(A,1,0)^t, (A-1,1,0)^t\}.$$

(2) *For* $1 = A < B$*, the vertex set of* $\mathrm{Red}(G(\mathcal{R}))$ *has the* 15 *elements*
$$\{(0,0,0)^t, \pm(1,0,0)^t, \pm(B,1,1)^t, \pm(B-1,1,1)^t, \pm(B-1,0,1)^t, \pm(B,0,1)^t, \pm(1,1,0)^t, \pm(0,1,0)^t\}.$$

(3) *For* $1 < A = B$ *the vertex set of* $\mathrm{Red}(G(\mathcal{R}))$ *has the* 13 *elements*
$$\{(0,0,0)^t, \pm(1,0,0)^t, (A-1,1,0)^t, \pm(0,A-1,1)^t, \pm(A-1,A,1)^t, \pm(A,1,0)^t, \pm(A,A,1)^t\}.$$

(4) *For* $1 = A = B$*, the vertex set of* $\mathrm{Red}(G(\mathcal{R}))$ *has the* 13 *elements*
$$\{(0,0,0)^t, \pm(1,0,0)^t, \pm(0,1,0)^t, \pm(0,0,1)^t, \pm(1,1,0)^t, \pm(0,1,1)^t, \pm(1,1,1)^t\}.$$

Table 1 shows half of the edges of $G(\mathcal{R})$ *(plus the edges leading away from* $(0,0,0)^t$*). The remaining edges can easily be constructed by Lemma 1.7. In particular, since* $\mathcal{R} = -\mathcal{R}$ *we have* $\alpha \xrightarrow{d|d'} \alpha' \in G(\mathcal{R})$ *if and only if* $-\alpha \xrightarrow{d'|d} -\alpha' \in G(\mathcal{R})$*.*

Proof. By the definition, we should delete the vertices which are stranding from $G(\mathcal{R})$. Table 1 shows the graph $G(\mathcal{R})$ in detail. From this table one easily obtains the statements of the corollary. □

Figure 8 shows the reduced graph $\mathrm{Red}(G(R) \setminus \{(0,0,0)^t\})$ under the condition $1 < A < B < C$.

Remark 1.15. By [**81**, Lemma 4.4], we know that we can always choose the basis $\{e_1, e_2, e_3\}$ in a way that $\mathrm{Red}(G(\mathcal{R})) = G(\mathcal{R})$, that means every state of $\mathcal{R}$ is a starting state of an infinite walk. In our situation, we could have chosen for instance $\{e_1, e_2, e_3\} = \{(1,0,0)^t, (B,A,1)^t, (A,1,0)^t\}$.

The fact that $0 \in \mathcal{R}$ is a natural consequence of the way this set is constructed. However, it will often be more convenient for us to work with $\mathcal{R} \setminus \{0\}$ and $\mathrm{Red}(G(\mathcal{R} \setminus \{0\})) = \mathrm{Red}(G(\mathcal{R})) \setminus \{0\}$ instead of $\mathcal{R}$ and $\mathrm{Red}(G(\mathcal{R}))$, respectively (like for instance in Figure 8).

1.2.4. The neighbor graph. In Section 1.2.3 we constructed the contact graph $G(\mathcal{R})$ of an ABC-tile and its reduced version $\mathrm{Red}(G(\mathcal{R}))$. For the sake of easier notation we will always assume that $G(\mathcal{R}) = \mathrm{Red}(G(\mathcal{R}))$ for ABC-tiles. According to Remark 1.15 this assumption does not mean any loss of generality and can always be achieved by choosing the starting set R_0 appropriately. According to Corollary 1.14 we know the reduced contact graph $\mathrm{Red}(G(\mathcal{R}))$ explicitly. We now turn to the construction of the neighbor graph $G(\mathcal{S})$ using Algorithm 1.10.

Our goal is to characterize all triples A, B, C with $1 \le A \le B < C$ for which $\mathcal{S}$ has 14 elements. This characterization is the content of Proposition 1.16. To establish this result we will have to apply one step of Algorithm 1.10. If $A = B$ it will turn out that already after one step we produce a reduced graph that has at least 17 vertices which entails that $\mathcal{S}$ has at least 16 vertices (since 0 is to be removed and since the sequence of graphs produced by the algorithm is nested). If $A \neq B$, according to Figure 8 the reduced contact graph has 15 vertices. Thus there will occur the following two cases. In the first case the first step of the algorithm will

Edge	Labels	Exists under condition
$000 \to 000$	$\{0\|0, 1\|1, \ldots, (C-1)\|(C-1)\}$	–
$000 \to 100$	$\{0\|1, 1\|2, \ldots, (C-2)\|(C-1)\}$	–
$010 \to 001$	$\{0\|0, 1\|1, \ldots, (C-1)\|(C-1)\}$	–
$100 \to A10$	$\{0\|A, 1\|(A+1), \ldots, (C-A-1)\|(C-1)\}$	–
$100 \to (A-1)10$	$\{0\|(A-1), 1\|A, \ldots, (C-A)\|(C-1)\}$	–
$BA1 \to \overline{1}00$	$0\|C-1$	–
$A10 \to BA1$	$\{0\|B, 1\|(B+1), \ldots, (C-B-1)\|(C-1)\}$	–
$A10 \to (B-1)A1$	$\{0\|(B-1), 1\|B, \ldots, (C-B)\|(C-1)\}$	–
$(B-1)A1 \to \overline{A}\ \overline{1}0$	$\{0\|(C-A), 1\|(C-A+1), \ldots, (A-1)\|(C-1)\}$	–
$(B-1)A1$ $\downarrow$ $\overline{A-1}\ \overline{1}0$	$\{0\|(C-A+1), 1\|(C-A+2), \ldots, (A-2)\|(C-1)\}$	$A \geq 2$
$(B-A)(A-1)1$ $\downarrow$ $\overline{B}\ \overline{A}\ \overline{1}$	$\{0\|(C-B), 1\|(C-B+1), \ldots, (B-1)\|(C-1)\}$	–
$(B-A)(A-1)1$ $\downarrow$ $\overline{B-1}\ \overline{A}\ \overline{1}$	$\{0\|(C-B+1), 1\|(C-B+2), \ldots, (B-2)\|(C-1)\}$	$B \geq 2$
$(A-1)10$ $\downarrow$ $(B-A)(A-1)1$	$\{0\|(B-A), 1\|(B-A+1), \ldots, (C-B+A-1)\|(C-1)\}$	$A \geq 1$
$(B-A+1)(A-1)1$ $\downarrow$ $\overline{B-A}\ \overline{A-1}\ \overline{1}$	$\{0\|(C-B+A), 1\|(C-B+A+1), \ldots, (B-A-1)\|(C-1)\}$	$A \neq B$
$(A-1)10$ $\downarrow$ $(B-A+1)(A-1)1$	$\{0\|(B-A+1), 1\|(B-A+2), \ldots, (C-B+A-2)\|(C-1)\}$	$A \neq B$ $A \geq 1$
$(B-A+1)(A-1)1$ $\downarrow$ $\overline{B-A+1}\ \overline{A-1}\ \overline{1}$	$\{0\|(C-B+A-1), 1\|(C-B+A), \ldots, (B-A-2)\|(C-1)\}$	$A \neq B$

TABLE 1. The contact graph $G(\mathcal{R})$. The triple abc stands for the node $(a, b, c)^t$ and $\overline{a} = -a$. The last column of the table contains the condition under which the respective edge exists. For each edge $\alpha \xrightarrow{d|d'} \alpha'$ in the table there exists the additional edge $-\alpha \xrightarrow{d'|d} -\alpha' \in G(\mathcal{R})$.

produce a reduced graph with more than 15 vertices. This entails that $\mathcal{S}$ has more than 14 elements. In the second case the first step of the algorithm will produce a reduced graph with exactly 15 vertices which has to be $G(\mathcal{R})$ again (since it has to

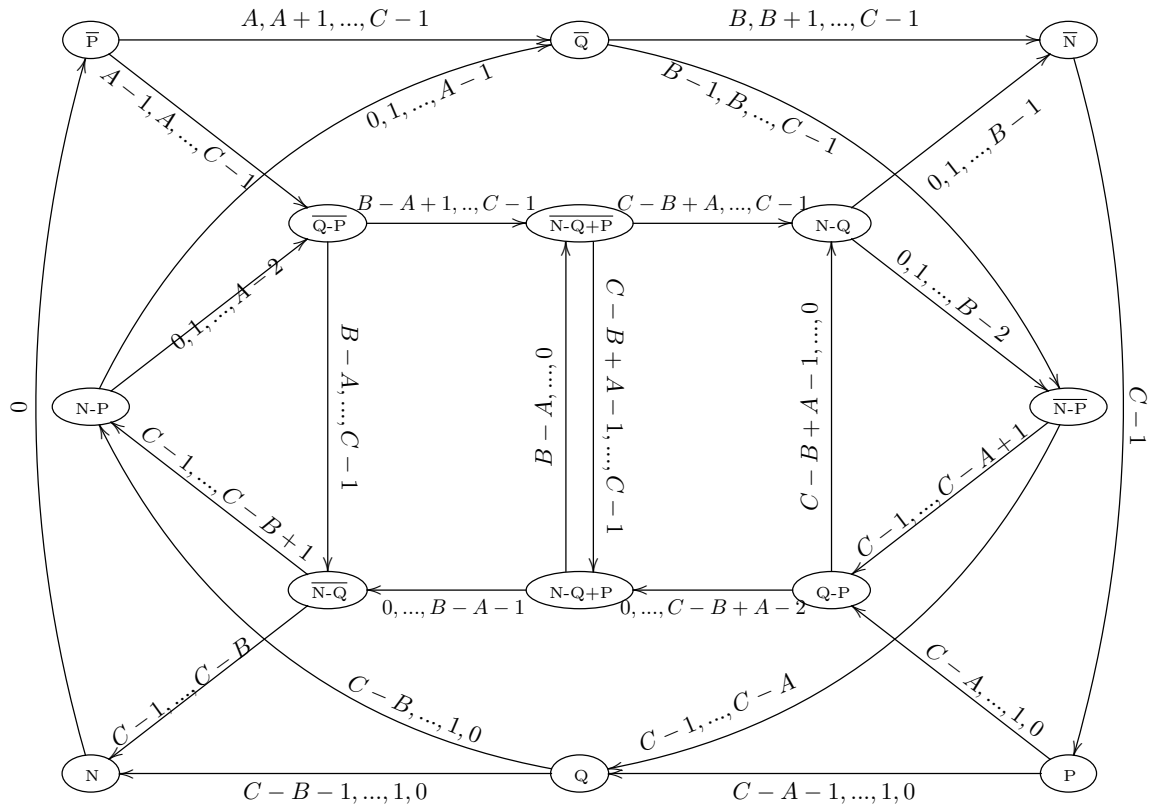

FIGURE 8. The reduced contact graph $\mathrm{Red}(G(\mathcal{R} \setminus \{0\}))$ under the condition $1 < A < B < C$. Here we set $P = (1, 0, 0)^t$, $Q = (A, 1, 0)^t$, $N = (B, A, 1)^t$. To obtain $\mathrm{Red}(G(\mathcal{R} \setminus \{0\}))$ under the condition $1 = A < B < C$ from the graph in the figure we just remove the edge from $N - P$ to $\overline{Q - P}$ and the edge from $\overline{N - P}$ to $Q - P$. If, in addition, the conditions of Proposition 1.16 are satisfied then this graph coincides with the neighbor graph $G(\mathcal{S})$. In this case each vertex α of the depicted graph corresponds to the nonempty 2-fold intersection $\boldsymbol{B}_\alpha = T \cap (T + \alpha)$.

contain $G(\mathcal{R})$). In this case the algorithm stops after the first step and we conclude that $\mathcal{R} \setminus \{0\} = \mathcal{S}$ has 14 elements.

Our characterization result reads as follows.

PROPOSITION 1.16. *Let T be an ABC-tile. Then T has 14 neighbors if and only if A, B, C satisfy one of the following conditions.*

(1) $1 \le A < B < C$, $B \ge 2A - 1$, *and* $C \ge 2(B - A) + 2$;
(2) $1 \le A < B < C$, $B < 2A - 1$, *and* $C \ge A + B - 2$.

In view of Section 1.2.2 Proposition 1.16 immediately implies Theorem 1.4.

LEMMA 1.17. *Let $G(\mathcal{R})$ be the contact graph of the ABC-tile $T = T(M, \mathcal{D})$. The product graph $G^{(2)} = G(\mathcal{R}) \otimes G(\mathcal{R})$ has 65 vertices and satisfies the symmetry property stated in Lemma 1.7 for all vertices. We classify the vertices of $G^{(2)}$ into 2×10 groups according to their second and third coordinates (and the symmetry).*

(1) $\mathbf{G1} := \{(x, 2A, 2)^t;\ 2B-2 \le x \le 2B\}$;
(2) $\mathbf{G2} := \{(x, A+1, 1)^t;\ A+B-2 \le x \le A+B\}$;
(3) $\mathbf{G3} := \{(x, 2A-1, 2)^t;\ 2B-A-1 \le x \le 2B-A+1\}$;
(4) $\mathbf{G4} := \{(x, 2A-2, 2)^t;\ 2B-2A \le x \le 2B-2A+2\}$;
(5) $\mathbf{G5} := \{(x, 2, 0)^t;\ 2A-2 \le x \le 2A\}$;
(6) $\mathbf{G6} := \{(x, A-2, 1)^t;\ B-2A \le x \le B-2A+2\}$;
(7) $\mathbf{G7} := \{(x, 0, 0)^t;\ 0 \le x \le 2\}$;
(8) $\mathbf{G8} := \{(x, A, 1)^t;\ B-2 \le x \le B+1\}$;
(9) $\mathbf{G9} := \{(x, 1, 0)^t;\ A-2 \le x \le A+1\}$;
(10) $\mathbf{G10} := \{(x, A-1, 1)^t;\ B-A-1 \le x \le B-A+2\}$.

Then the set of vertices of $G^{(2)}$ is the union of the 20 sets[2] $\pm\mathbf{G1}, \dots, \pm\mathbf{G10}$. *Moreover, the vertices of $G(\mathcal{R})$ are a subset of the union of the sets $\pm\mathbf{G7}, \dots, \pm\mathbf{G10}$.*

PROOF. This is an immediate consequence of the definition of the product "$\otimes$" (see Definition 1.9). The assertion about the vertices of $G(\mathcal{R})$ can be read off Table 1. □

We recall that $G(\mathcal{S}) \supset \mathrm{Red}(G^{(2)}) \setminus \{0\}$. In all what follows we suppose that $1 \le A \le B < C$. We first deal with the cases A, B, C that satisfy none of the conditions of Proposition 1.16. By taking the complement of the union of conditions (1) and (2) we conclude that we have to deal with the following four cases.

(i) $1 \le A = B < C$,
(ii) $1 \le A < B < C$, $B < 2A-1$, and $C < A+B-2$,
(iii) $1 \le A < B < C$, $C < 2(B-A)+2$, and $B \ge 2A-1$,
(iv) $1 \le A < B < C$, $C < 2(B-A)+2$, and $C < A+B-2$.

Indeed, for each of these cases we have to show that $\mathcal{S}$ has more than 14 elements. For (i) this is done in Lemma 1.18 and for (ii) it follows from Lemma 1.19. Since for $A \ge 2$ and $B < 2A-1$ we always have $2(B-A)+2 \le A+B-2$ the cases (iii) and (iv) are covered by Lemma 1.20. Thus the following three lemmas imply that $\mathcal{S}$ has more than 14 elements if none of the two conditions of Proposition 1.16 is satisfied.

LEMMA 1.18. *If $1 \le A = B < C$, then $\mathrm{Red}(G^{(2)})$ has at least 17 vertices.*

PROOF. Let $s_1 = (A+B-1, A+1, 1)^t = (2A-1, A+1, 1)^t$ and $s_2 = (-1, A-1, 1)^t$. We claim that $G^{(2)}$ contains the cycle

$$s_1 \xrightarrow{0|C-1} s_2 \xrightarrow{A-1|C-A} -s_1 \xrightarrow{C-1|0} -s_2 \xrightarrow{C-A|A-1} s_1. \tag{1.13}$$

The elements $\pm s_1, \pm s_2$ are vertices of $G^{(2)}$ by Lemma 1.17 (note that $B-A-1 = -1$ in our case). Moreover, the edges claimed in (1.13) exist because each label occurring in (1.13) is an element of $\mathcal{D}$ and

$$M \cdot s_1 + (C-1, 0, 0)^t = s_2, \quad M \cdot s_2 + (C-A, 0, 0)^t - (A-1, 0, 0)^t = -s_1.$$

Thus $\pm s_1, \pm s_2 \in \mathrm{Red}(G^{(2)})$. From Corollary 1.14 we know that $\mathrm{Red}(G(\mathcal{R}))$ has 13 vertices and $\pm s_1, \pm s_2 \notin \mathrm{Red}(G(\mathcal{R}))$. Since $\mathrm{Red}(G(\mathcal{R})) \subset \mathrm{Red}(G^{(2)})$ this implies that $\mathrm{Red}(G^{(2)})$ has at least 17 elements. □

[2]Note that $(0,0,0)^t$ occurs in **G7** and in $-\mathbf{G7}$.

LEMMA 1.19. *If* $1 \le A < B < C$, $B < 2A-1$, *and* $C < A+B-2$, *then* $\mathrm{Red}(G^{(2)})$ *has at least* 18 *vertices.*

PROOF. Denote $t_1 = (A+B-2, A+1, 1)^t$, $t_2 = (B-2A+1, A-2, 1)^t$, $t_3 = (-2B+A+1, 1-2A, -2)^t$. We claim that $G^{(2)}$ contains the cycle

$$t_1 \xrightarrow{2A-B-2|C-1} t_2 \xrightarrow{B-A-1|C-B} t_3 \xrightarrow{C-1|A+B-C-3} t_1. \tag{1.14}$$

From Lemma 1.17, we know that $t_1, t_2, t_3 \in G^{(2)}$. All the labels occurring in the cycle (1.14) are elements of $\mathcal{D}$ by the conditions of the lemma. The existence of the cycle now follows from verifying (1.8) for each edge occurring in (1.14). This implies the result as in the previous lemma because $\mathrm{Red}(G(\mathcal{R}))$ has 15 vertices by Corollary 1.14 and we exhibited 3 more vertices that belong to $\mathrm{Red}(G^{(2)})$. □

LEMMA 1.20. *If* $1 \le A < B < C$ *and* $C < 2(B-A)+2$, *then* $\mathrm{Red}(G^{(2)})$ *has at least* 17 *vertices.*

PROOF. Let $s = (2(B-A)+2, 2(A-1), 2)^t$. We claim that $G^{(2)}$ contains the cycle

$$s \xrightarrow{2(B-A)-C+1|C-1} -s \xrightarrow{C-1|2(B-A)-C+1} s.$$

The proof is done in the same way as the proof of Lemma 1.19. □

The following lemma deals with the case where condition (1) or (2) of Proposition 1.16 is satisfied.

LEMMA 1.21. *The elements of* $\pm\mathbf{G1}, \pm\mathbf{G2}, \pm\mathbf{G3}, \pm\mathbf{G4}, \pm\mathbf{G5}, \pm\mathbf{G6}$ *are not in* $\mathrm{Red}(G^{(2)})$ *if one of the following conditions holds.*

(1) $1 \le A < B < C$, $B \ge 2A-1$, *and* $C \ge 2(B-A)+2$.
(2) $1 \le A < B < C$, $B < 2A-1$, *and* $C \ge A+B-2$.

PROOF. We first prove the lemma for A, B, C satisfying condition (1). We split the set $\mathbf{G6}$ into $\mathbf{G6.1} = \{(B-2A, A-2, 1)^t\}$, $\mathbf{G6.2} = \{(B-2A+1, A-2, 1)^t\}$, and $\mathbf{G6.3} = \{(B-2A+2, A-2, 1)^t\}$. Now we look at the collection of eight sets of vertices given by

$$\mathcal{G} = \{\pm\mathbf{G1}, \pm\mathbf{G2}, \pm\mathbf{G3}, \pm\mathbf{G4}, \pm\mathbf{G5}, \pm\mathbf{G6.1}, \pm\mathbf{G6.2}, \pm\mathbf{G6.3}\}.$$

We prove the following claim. Suppose that γ is contained in some $X \in \mathcal{G}$. Then there exists an edge $\gamma \to \gamma' \in G^{(2)}$ only if γ' is contained in a set $Y \in \mathcal{G}$ such that there is an edge between the vertices X and Y in the graph depicted in Figure 9. Since this graph contains no cycles this claim will imply the result.

The case $\pm\mathbf{G1}$: The elements in $\mathbf{G1}$ have no successor in $G^{(2)}$ under condition (1). Indeed, let $s = (x, 2A, 2)^t \in \mathbf{G1}$, then $Ms = (-2C, x-2B, 0)^t$. Since $2B-2 \le x \le 2B$, the possible successors of s are of the form

$$s' \in Ms + \mathcal{D} - \mathcal{D} = \{(-2C+d, x-2B, 0)^t;\ d \in \mathcal{D}-\mathcal{D}\} \qquad (2B-2 \le x \le 2B).$$

According to its second and third coordinates, in the cases $x = 2B-1$ and $x = 2B$ the element $s' \in G^{(2)}$ can only belong to $-\mathbf{G9}$ and $\mathbf{G7}$, respectively. However, as the first coordinate of s' varies between $-3C+1$ and $-C-1$, this is impossible for both cases. Hence, for these choices of x the element s has no successor in $G^{(2)}$. For the case $x = 2B-2$ the element $s' \in G^{(2)}$ can only be an element of $-\mathbf{G5}$. However,

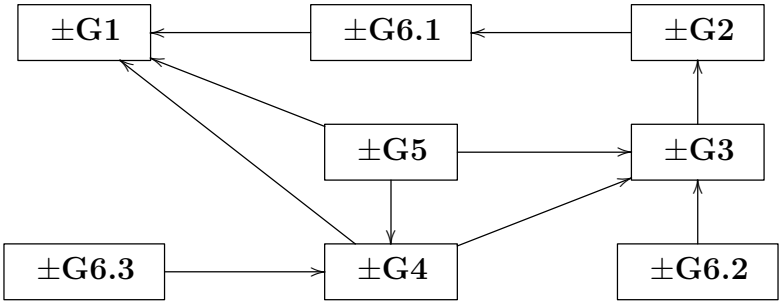

FIGURE 9. The possible edges leading away from the sets of vertices $\pm\mathbf{G1}$, $\pm\mathbf{G2}$, $\pm\mathbf{G3}$, $\pm\mathbf{G4}$, $\pm\mathbf{G5}$, $\pm\mathbf{G6.1}$, $\pm\mathbf{G6.2}$, and $\pm\mathbf{G6.3}$.

since $C > B \geq 2A - 1$, we have $-C - 1 < -2A$ this is impossible also in this case. Thus this case is done since by symmetry of $G^{(2)}$ also the elements in $-\mathbf{G1}$ have no successor in $G^{(2)}$ under condition (1).

The case $\pm\mathbf{G2}$: The elements in $\mathbf{G2}$ can only have successors contained in $\pm\mathbf{G6.1}$ under condition (1). To prove this let $s = (x, A+1, 1)^t$, then a possible successor of s is of the form

$$s' = Ms + \mathcal{D} - \mathcal{D} = \{(d - C, x - B, 1)^t;\ d \in \mathcal{D} - \mathcal{D}\} \qquad (A + B - 2 \leq x \leq A + B).$$

For the case $x = A + B - 2$, looking at the second and third coordinate, the successor s' can only be contained in $\mathbf{G6}$. The first coordinate $d - C$ of s' satisfies $1 - 2C \leq d - C \leq -1$. Since condition (1) is in force, $B - 2A \geq -1$, thus s' is in $\mathbf{G6}$ only if $B = 2A - 1$. In this case, $d - C = -1 = B - 2A$, hence, $s' \in \mathbf{G6.1}$. For $x = A + B - 1$, the successor s' can only fall into $\mathbf{G10}$. This would imply $-1 = B - A - 1$ and, hence, $A = B$ which contradicts condition (1). Thus in this case we have no successor. Finally, for $x = A + B$, the possible successor s' can only be contained in $\mathbf{G8}$ by its second and third coordinate. But by its first coordinate also this possibility is excluded. Again, this case is done by symmetry.

So far we proved the claim for the edges leading away from $\pm\mathbf{G1}$ and $\pm\mathbf{G2}$ in Figure 9. The remaining cases are routine calculations of the same kind and we omit them.

Condition (2) can be checked in the same way. In this case we have to subdivide the relevant vertices into nine sets. The corresponding graph, which is acyclic again, is depicted in Figure 10. □

We are now able to finish the proof of Proposition 1.16

PROOF OF PROPOSITION 1.16. To prove the "only if" part, we have to show that $|\mathcal{S}| > 14$ if none of the two conditions of the theorem are in force. Because $G(\mathcal{S}) \supset \mathrm{Red}(G^{(2)}) \setminus \{0\}$, this follows immediately from Lemmas 1.18, 1.19, and 1.20.

To prove the "if" part, we apply the Algorithm 1.10, and the first step is to calculate $\mathrm{Red}(G^{(2)})$ which is the reduced graph of the product graph $G(R) \otimes G(R)$. From Lemma 1.17, we already know that $G^{(2)}$ has 65 vertices. Since $\mathrm{Red}(G(\mathcal{R})) \setminus \{0\}$ has 14 vertices by Corollary 1.14 we have to show that $\mathrm{Red}(G^{(2)}) = \mathrm{Red}(G(\mathcal{R}))$. For this it suffices to prove that no vertex of $G^{(2)} \setminus G(\mathcal{R})$ is contained in $\mathrm{Red}(G^{(2)})$.

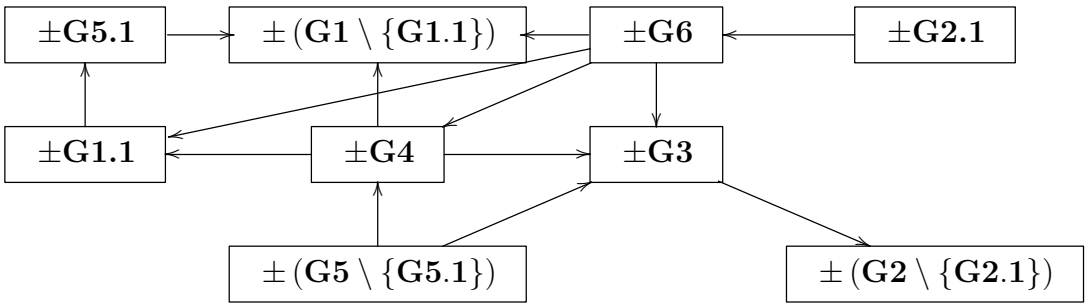

FIGURE 10. The graph corresponding to condition (2). Here we use the additional notations $\mathbf{G1.1} = \{(2B-2, 2A, 2)^t\}$, $\mathbf{G2.1} = \{(A+B-2, A+1, 1)^t\}$, $\mathbf{G5.1} = \{(2A, 2, 0)^t\}$.

By Lemma 1.21, none of the vertices contained in $\pm\mathbf{G1} \cup \cdots \cup \pm\mathbf{G6}$ is a vertex of $\mathrm{Red}(G^{(2)})$. Thus it remains to show that each vertex contained in $\pm(\mathbf{G7} \cup \mathbf{G8} \cup \mathbf{G9} \cup \mathbf{G10}) \setminus \mathcal{R}$ is not a vertex of $\mathrm{Red}(G^{(2)})$. By symmetry we can confine ourselves to proving the claim that $(\mathbf{G7} \cup \mathbf{G8} \cup \mathbf{G9} \cup \mathbf{G10}) \setminus \mathcal{R}$ does not contain a vertex of $\mathrm{Red}(G^{(2)})$.

Assume that condition (1) of the theorem is in force. For condition (2), we can prove the result in the same way.

We start with $\mathbf{G7} \setminus \mathcal{R} = \{(2, 0, 0)^t\}$. Let $s = (2, 0, 0)^t$. Then a possible successor s' of s in $G^{(2)}$ must sartisfy

$$s' \in Ms + \mathcal{D} - \mathcal{D} = \{(d, 2, 0)^t; d \in \mathcal{D} - \mathcal{D}\}.$$

By the second and third coordinate of $Ms + \mathcal{D} - \mathcal{D}$, we know that s' has to belong to $\mathbf{G5}$. So it cannot be in $\mathrm{Red}(G^{(2)})$ by Lemma 1.21.

For the elements $s \in \{(B-2, A, 1)^t, (B+1, A, 1)^t\} = \mathbf{G8} \setminus \mathcal{R}$ the successor has to be of the form

$$s' = Ms + \mathcal{D} - \mathcal{D} = \{(d - C, x - B, 0)^t;\ d \in \mathcal{D} - \mathcal{D}\} \quad (x \in \{B-2, B+1\}).$$

For $x = B - 2$, we have $s' \in -\mathbf{G5}$, so $(B-2, A, 1)^t \notin \mathrm{Red}(G^{(2)})$ by Lemma 1.21. For $x = B + 1$, the successor of s can only be contained in $\mathbf{G9}$. However, the first coordinate of the elements of $\mathbf{G9}$ varies between $A - 2$ and $A + 1$, thus s has no successors if $A \geq 2$ which is true by condition (1) of the theorem.

For the elements $s \in \{(A-2, 1, 0)^t, (A+1, 1, 0)^t\} = \mathbf{G9} \setminus \mathcal{R}$, the successor has to be of the form

$$s' \in Ms + \mathcal{D} - \mathcal{D} = \{(d, x, 1)^t;\ d \in \mathcal{D} - \mathcal{D}\} \quad (x \in \{A-2, A+1\}).$$

This implies that $s' \in \mathbf{G2} \cup \mathbf{G6}$ and, hence, $s \notin \mathrm{Red}(G^{(2)})$ by Lemma 1.21.

For the elements $s \in \{(B-A-1, A-1, 1)^t,\ (B-A+2, A-1, 1)^t\} = \mathbf{G10} \setminus \mathcal{R}$ the successor has to be of the form

$$s' \in Ms + \mathcal{D} - \mathcal{D} = \{(d - C, x - B, -1)^t;\ d \in \mathcal{D} - \mathcal{D}\} \qquad (x \in \{B-A-1, B-A+2\}).$$

This implies that $s' \in (-\mathbf{G6}) \cup (-\mathbf{G2})$ and, hence, $s \notin \mathrm{Red}(G^{(2)})$ by Lemma 1.21. Summing up, we proved the claim. □

REMARK 1.22. Figure 8 shows the neighbor graph $G(\mathcal{S})$ of an ABC-tile under the conditions of Proposition 1.16. We can see that each vertex except P and $\overline{P}$ has two predecessors. Precisely, let $\alpha \in \mathcal{S} \setminus \{P, \overline{P}\}$, and α_1, α_2 be the two predecessors of α. Let D_i denote the labels of edges from α_i to α for $i = 1, 2$. Then we know that D_1, D_2 are disjoint and they have the forms either $\{(0,0,0)^t, (1,0,0)^t, \dots, (d,0,0)^t\}$ or $\{(d+1,0,0)^t, \dots, (C-1,0,0)^t\}$ from Figure 8. Also, each vertex except N and $\overline{N}$ has two successors and the difference between the two successors is $\pm P$.

1.2.5. The directed graphs of multiple intersections. Let T be a $\mathbb{Z}^m$-tile and let $\mathcal{S}$ be the set of neighbors of T. For $\ell \geq 1$, the union of all $(\ell+1)$-*fold intersections with* T is then given by

$$\mathcal{I}_\ell = \bigcup_{\{\alpha_1,\dots,\alpha_\ell\} \subset \mathcal{S}} \boldsymbol{B}_{\alpha_1,\dots,\alpha_\ell}, \tag{1.15}$$

where the union is extended over all subsets of $\mathcal{S}$ containing ℓ pairwise disjoint elements. We can subdivide $\boldsymbol{B}_{\alpha_1,\dots,\alpha_\ell}$ by

(1.16)

$$\begin{aligned}
\boldsymbol{B}_{\alpha_1,\dots,\alpha_\ell} &= M^{-1}\Big((T+\mathcal{D}) \cap (T+\mathcal{D}+M\alpha_1) \cap \cdots \cap (T+\mathcal{D}+M\alpha_\ell)\Big) \\
&= M^{-1}\Big(\bigcup_{d,d_1,\dots,d_\ell \in \mathcal{D}} (T \cap (T+M\alpha_1+d_1-d) \cdots \cap (T+M\alpha_\ell+d_\ell-d)) + d\Big) \\
&= M^{-1}\Big(\bigcup_{\substack{d,d_1,\dots,d_\ell \in \mathcal{D} \\ \alpha_i' = M\alpha_i+d_i-d \\ i=1,2,\dots,\ell}} (\boldsymbol{B}_{\alpha_1',\alpha_2',\dots,\alpha_\ell'} + d)\Big)
\end{aligned}$$

and by Definition 1.6 we can rewrite this as

$$\boldsymbol{B}_{\alpha_1,\dots,\alpha_\ell} = \bigcup_{d \in \mathcal{D}} \bigcup_{d_1,\dots,d_\ell \in \mathcal{D}} \bigcup_{\substack{\alpha_i \xrightarrow{d \mid d_i} \alpha_i' \\ i=1,2,\dots,\ell}} M^{-1}(\boldsymbol{B}_{\alpha_1',\alpha_2',\dots,\alpha_\ell'} + d). \tag{1.17}$$

Of course, $\boldsymbol{B}_{\alpha_1,\dots,\alpha_\ell}$ can be nonempty only if $\{\alpha_1,\dots,\alpha_\ell\} \subset \mathcal{S}$. Thus the sets $\mathcal{I}_\ell$ can be determined by a certain graph which is a product of the neighbor graph $G(\mathcal{S})$ with itself which is defined in the following way.

DEFINITION 1.23. Let $G(\Gamma)$ with $\Gamma \subset \mathbb{Z}^m$ be a subgraph of $G(\mathbb{Z}^m)$. The ℓ-fold power $G_\ell(\Gamma) := \times_{j=1}^{\ell} G(\Gamma)$ is defined as the reduction $\mathrm{Red}(G'_\ell(\Gamma))$ of the following graph $G'_\ell(\Gamma)$:

- The states of $G'_\ell(\Gamma)$ are the sets $\{\alpha_1,\dots,\alpha_\ell\}$ consisting of ℓ (pairwise distinct) states α_i of $G(\Gamma)$.
- There exists an edge

$$\{\alpha_{11},\dots,\alpha_{1\ell}\} \xrightarrow{d} \{\alpha_{21},\dots,\alpha_{2\ell}\}$$

in $G'_\ell(\Gamma)$ if and only if there exist the edges

$$\alpha_{1i} \xrightarrow{d \mid d_i} \alpha_{2i} \quad (1 \leq i \leq \ell)$$

in $G(\Gamma)$ for certain $d_1, \dots, d_\ell \in \mathcal{D}$.

Using this definition we can write (1.17) as

$$\boldsymbol{B}_{\alpha_1,\dots,\alpha_\ell} = \bigcup_{\substack{d\in\mathcal{D},\,\{\alpha'_1,\dots,\alpha'_\ell\}\subset\mathcal{S}\\ \{\alpha_1,\dots,\alpha_\ell\}\xrightarrow{d}\{\alpha'_1,\dots,\alpha'_\ell\}\in\times_{j=1}^{\ell}G(\mathcal{S})}} M^{-1}(\boldsymbol{B}_{\alpha'_1,\alpha'_2,\dots,\alpha'_\ell}+d) \tag{1.18}$$

which can be regarded as the defining equation for the collection of nonempty compact sets $\{\boldsymbol{B}_{\boldsymbol{\alpha}};\, \boldsymbol{\alpha} \in \times_{j=1}^{\ell} G(\mathcal{S})\}$ as attractor of a graph-directed iterated function system (in the sense of Mauldin and Williams [**67**]) directed by the graph $\times_{j=1}^{\ell} G(\mathcal{S})$. We will often need the k-fold iteration of this set equation. To write this iteration in a convenient way we define the functions

$$f_d : \mathbb{R}^m \to \mathbb{R}^m \quad x \mapsto M^{-1}(x+d) \qquad (d \in \mathcal{D}),$$

which are contractions w.r.t. some suitable norm because M is an expanding matrix. Since we will often deal with compositions of these functions, we will use the abbreviation

$$f_{d_1 d_2 \dots d_k} = \begin{cases} f_{d_1} \circ \cdots \circ f_{d_k}, & k > 0, \\ \mathrm{id}, & k = 0 \end{cases}$$

for $d_1, \dots, d_k \in \mathcal{D}$. With this notation we get

$$\begin{aligned} \boldsymbol{B}_{\alpha_1,\dots,\alpha_\ell} &= \bigcup_{\{\alpha_1,\dots,\alpha_\ell\}\xrightarrow{d}\{\alpha'_1,\dots,\alpha'_\ell\}\in\times_{j=1}^{\ell}G(\mathcal{S})} f_d(\boldsymbol{B}_{\alpha'_1,\alpha'_2,\dots,\alpha'_\ell}) \\ &= \bigcup_{\{\alpha_1,\dots,\alpha_\ell\}\xrightarrow{d_1}\cdots\xrightarrow{d_k}\{\alpha_1^{(k)},\dots,\alpha_\ell^{(k)}\}\in\times_{j=1}^{\ell}G(\mathcal{S})} f_{d_1\dots d_k}(\boldsymbol{B}_{\alpha_1^{(k)},\dots,\alpha_\ell^{(k)}}), \end{aligned} \tag{1.19}$$

where the latter union is extended over all walks of length k in $\times_{j=1}^{\ell} G(\mathcal{S})$ starting at $\{\alpha_1, \dots, \alpha_\ell\}$. We can now characterize $\mathcal{I}_\ell$ as follows (see [**91**, Appendix] or [**81**, Proposition 6.2]).

PROPOSITION 1.24. *Let $\ell \geq 1$ and choose $\alpha_{01}, \dots, \alpha_{0\ell} \in \mathbb{Z}^m \setminus \{0\}$ pairwise different. Then the following three assertions are equivalent.*

(1)
$$x = \sum_{j\geq 1} M^{-j} d_j \in \boldsymbol{B}_{\alpha_{01},\dots,\alpha_{0\ell}}.$$

(2) *There exists an infinite walk*
$$\{\alpha_{01}, \dots, \alpha_{0\ell}\} \xrightarrow{d_1} \{\alpha_{11}, \dots, \alpha_{1\ell}\} \xrightarrow{d_2} \{\alpha_{21}, \dots, \alpha_{2\ell}\} \xrightarrow{d_3} \cdots$$
in $\times_{r=1}^{\ell} G(\mathcal{S})$.

(3) *There exist ℓ infinite walks*
$$\alpha_{0i} \xrightarrow{d_1} \alpha_{1i} \xrightarrow{d_2} \alpha_{2i} \xrightarrow{d_3} \cdots \quad (1 \leq i \leq \ell)$$
in $G(\mathcal{S})$.

The set equation (1.19) yields a sequence of collections of sets that cover $\boldsymbol{B}_{\alpha_1,\ldots,\alpha_\ell}$. Namely, for $\boldsymbol{\alpha}^{(0)} \in \times_{j=1}^{\ell} G(\mathcal{S})$ we define

$$\mathcal{C}_k(\boldsymbol{\alpha}^{(0)}) := \left\{ f_{d_1\ldots d_{k-1}}(\boldsymbol{B}_{\boldsymbol{\alpha}^{(k-1)}});\ \boldsymbol{\alpha}^{(0)} \xrightarrow{d_1} \cdots \xrightarrow{d_{k-1}} \boldsymbol{\alpha}^{(k-1)} \in \times_{j=1}^{\ell} G(\mathcal{S}) \right\} \tag{1.20}$$

and set

$$\mathcal{C}_k^{(\ell)} = \bigcup_{\boldsymbol{\alpha}\in\times_{j=1}^{\ell} G(\mathcal{S})} \mathcal{C}_k(\boldsymbol{\alpha}). \tag{1.21}$$

We will call $\mathcal{C}_k(\boldsymbol{\alpha})$ the *collection of* $(k-1)$*-th subdivisions* of $\boldsymbol{B}_{\boldsymbol{\alpha}}$. If $k = 2$ we will just call it the *collection of subdivisions* of $\boldsymbol{\alpha}$. The elements of these collections will be called *subtiles* of $\boldsymbol{B}_{\boldsymbol{\alpha}}$. The collection of subdivisions of $\boldsymbol{B}_{\boldsymbol{\alpha}} \cup \boldsymbol{B}_{\boldsymbol{\alpha}'}$ is the union of the collections of subdivisions of $\boldsymbol{B}_{\boldsymbol{\alpha}}$ and $\boldsymbol{B}_{\boldsymbol{\alpha}'}$. It should now be clear what we mean by the collections of $((k-1)$-th) subdivisions of a set $X = M^{-r}(\boldsymbol{B}_{\boldsymbol{\alpha}} + a)$ with $a \in \mathbb{Z}^m$ and $r \in \mathbb{N}$.

We will need the following lemma.

LEMMA 1.25.

(1) *For* $\boldsymbol{\alpha} \in \times_{j=1}^{\ell} G(\mathcal{S})$ *and* $k \geq 1$ *the collection* $\mathcal{C}_k(\boldsymbol{\alpha})$ *forms a covering of* $\boldsymbol{B}_{\boldsymbol{\alpha}}$.

(2) *Let* $k \geq 1$ *be given and let* $X_1, X_2 \in \mathcal{C}_k^{(\ell)}$ *be distinct. Then the intersection* $X_1 \cap X_2$ *is either empty or there exist* $\ell' > \ell$, $c \in \mathbb{Z}^m$, *and* $\boldsymbol{\alpha} \in \times_{j=1}^{\ell'} G(\mathcal{S})$ *with* $X_1 \cap X_2 = M^{-k+1}(\boldsymbol{B}_{\boldsymbol{\alpha}} + c)$.

PROOF. Assertion (1) follows immediately from (1.19) and the definition of $\mathcal{C}_k(\boldsymbol{\alpha})$.

To prove assertion (2) we conclude from (1.19) that $X_i = M^{-k+1}(T + \beta_{i0}) \cap \cdots \cap M^{-k+1}(T + \beta_{i\ell})$ holds with $\beta_{ij} \in \mathbb{Z}^m$ for $i \in \{1, 2\}$ and $j \in \{0, \ldots, \ell\}$. Here β_{ij} are pairwise distinct for fixed i and $j \in \{0, \ldots, \ell\}$. Since X_1 and X_2 are distinct elements of $\mathcal{C}_k^{(\ell)}$ there exists $\ell' > \ell$ and $\ell' + 1$ distinct elements

$$\gamma_0, \ldots, \gamma_{\ell'} \in \{\beta_{10}, \ldots \beta_{1\ell}, \beta_{20}, \ldots, \beta_{2\ell}\}$$

such that $X_1 \cap X_2 = M^{-k+1}(T + \gamma_0) \cap \cdots \cap M^{-k+1}(T + \gamma_{\ell'})$ and, hence, $X_1 \cap X_2$ is either empty or an element of $\mathcal{C}_k(\boldsymbol{\alpha})$ for some $\boldsymbol{\alpha} \in \times_{j=1}^{\ell'} G(\mathcal{S})$ as claimed. □

The following lemma is derived by direct calculation.

LEMMA 1.26. *Let* T *be an ABC-tile with neighbor graph* $G(\mathcal{S})$. *If* T *has* 14 *neighbors the following assertions hold.*

- *The* 3*-fold intersection graph* $G_2(\mathcal{S}) = \times_{j=1}^{2} G(\mathcal{S})$ *has* 36 *vertices and is given by*[3] *Table 2.*
- *The* 4*-fold intersection graph* $G_3(\mathcal{S}) = \times_{j=1}^{3} G(\mathcal{S})$ *has* 24 *vertices and is given by Figure 11.*
- *The* $(\ell + 1)$*-fold intersection graph* $G_\ell(\mathcal{S}) = \times_{j=1}^{\ell} G(\mathcal{S})$ *is empty for* $\ell \geq 4$.

By construction, all these graphs are symmetric in the sense that there exists an edge $\boldsymbol{\alpha} \xrightarrow{d} \boldsymbol{\alpha}'$ *if and only if* $-\boldsymbol{\alpha} \xrightarrow{C-1-d} -\boldsymbol{\alpha}'$.

[3]To save space, in this table and in what follows we will often write $\{{}^{X}_{Y}\}$ instead of $\{X, Y\}$.

Vertex	Successors	Label	Conditons
$\left\{\begin{smallmatrix} Q-P \\ N-P \end{smallmatrix}\right\}$	$\left\{\begin{smallmatrix} \overline{Q} \\ N-Q \end{smallmatrix}\right\}$	$\{0, 1, \ldots, A-1\}$	-
	$\left\{\begin{smallmatrix} \overline{Q-P} \\ N-Q \end{smallmatrix}\right\}$	$\{0, 1, \ldots, A-2\}$	$A \geq 2$
	$\left\{\begin{smallmatrix} \overline{Q-P} \\ N-Q+P \end{smallmatrix}\right\}$	$\{0, 1, \ldots, A-2\}$	$A \geq 2$
$\left\{\begin{smallmatrix} \overline{P} \\ Q-P \end{smallmatrix}\right\}$	$\left\{\begin{smallmatrix} \overline{Q} \\ N-Q \end{smallmatrix}\right\}$	$\{A, A+1, \ldots, C-B+A-1\}$	-
	$\left\{\begin{smallmatrix} \overline{Q-P} \\ N-Q \end{smallmatrix}\right\}$	$\{A-1, A, \ldots, C-B+A-1\}$	-
	$\left\{\begin{smallmatrix} \overline{Q-P} \\ N-Q+P \end{smallmatrix}\right\}$	$\{A-1, A, \ldots, C-B+A-2\}$	-
$\left\{\begin{smallmatrix} \overline{N-Q+P} \\ \overline{P} \end{smallmatrix}\right\}$	$\left\{\begin{smallmatrix} \overline{Q} \\ N-Q \end{smallmatrix}\right\}$	$\{C-B+A, \ldots, C-1\}$	-
	$\left\{\begin{smallmatrix} \overline{Q-P} \\ N-Q \end{smallmatrix}\right\}$	$\{C-B+A, \ldots, C-1\}$	-
	$\left\{\begin{smallmatrix} \overline{Q-P} \\ N-Q+P \end{smallmatrix}\right\}$	$\{C-B+A-1, \ldots, C-1\}$	-
$\left\{\begin{smallmatrix} P \\ Q \end{smallmatrix}\right\}$	$\left\{\begin{smallmatrix} Q-P \\ N-P \end{smallmatrix}\right\}$	$\{0, 1, \ldots, C-B\}$	-
	$\left\{\begin{smallmatrix} Q-P \\ N \end{smallmatrix}\right\}$	$\{0, 1, \ldots, C-B-1\}$	-
	$\left\{\begin{smallmatrix} Q \\ N \end{smallmatrix}\right\}$	$\{0, 1, \ldots, C-B-1\}$	-
$\left\{\begin{smallmatrix} \overline{N-Q} \\ P \end{smallmatrix}\right\}$	$\left\{\begin{smallmatrix} Q-P \\ N-P \end{smallmatrix}\right\}$	$\{C-B+1, \ldots, C-A\}$	-
	$\left\{\begin{smallmatrix} Q-P \\ N \end{smallmatrix}\right\}$	$\{C-B, \ldots, C-A\}$	-
	$\left\{\begin{smallmatrix} Q \\ N \end{smallmatrix}\right\}$	$\{C-B, \ldots, C-A-1\}$	-
$\left\{\begin{smallmatrix} \overline{N-P} \\ \overline{N-Q} \end{smallmatrix}\right\}$	$\left\{\begin{smallmatrix} Q-P \\ N-P \end{smallmatrix}\right\}$	$\{C-A+1, \ldots, C-1\}$	$A \geq 2$
	$\left\{\begin{smallmatrix} Q-P \\ N \end{smallmatrix}\right\}$	$\{C-A+1, \ldots, C-1\}$	$A \geq 2$
	$\left\{\begin{smallmatrix} Q \\ N \end{smallmatrix}\right\}$	$\{C-A, \ldots, C-1\}$	-
$\left\{\begin{smallmatrix} N-Q \\ N-Q+P \end{smallmatrix}\right\}$	$\left\{\begin{smallmatrix} \overline{N-Q+P} \\ \overline{N} \end{smallmatrix}\right\}$	$\{0, 1, \ldots, B-A\}$	-
	$\left\{\begin{smallmatrix} \overline{N-Q} \\ \overline{N} \end{smallmatrix}\right\}$	$\{0, 1, \ldots, B-A-1\}$	-
	$\left\{\begin{smallmatrix} \overline{N-Q} \\ \overline{N-P} \end{smallmatrix}\right\}$	$\{0, 1, \ldots, B-A-1\}$	-
$\left\{\begin{smallmatrix} \overline{Q-P} \\ N-Q \end{smallmatrix}\right\}$	$\left\{\begin{smallmatrix} \overline{N-Q+P} \\ \overline{N} \end{smallmatrix}\right\}$	$\{B-A+1, \ldots, B-1\}$	$A \geq 2$
	$\left\{\begin{smallmatrix} \overline{N-Q} \\ \overline{N} \end{smallmatrix}\right\}$	$\{B-A, \ldots, B-1\}$	-
	$\left\{\begin{smallmatrix} \overline{N-Q} \\ \overline{N-P} \end{smallmatrix}\right\}$	$\{B-A, \ldots, B-2\}$	$A \geq 2$
$\left\{\begin{smallmatrix} \overline{Q-P} \\ \overline{Q} \end{smallmatrix}\right\}$	$\left\{\begin{smallmatrix} \overline{N-Q+P} \\ \overline{N} \end{smallmatrix}\right\}$	$\{B, B+1, \ldots, C-1\}$	-
	$\left\{\begin{smallmatrix} \overline{N-Q} \\ \overline{N} \end{smallmatrix}\right\}$	$\{B, B+1, \ldots, C-1\}$	-
	$\left\{\begin{smallmatrix} \overline{N-P} \\ \overline{N-Q} \end{smallmatrix}\right\}$	$\{B-1, \ldots, C-1\}$	-
$\left\{\begin{smallmatrix} \overline{Q-P} \\ N-Q+P \end{smallmatrix}\right\}$	$\left\{\begin{smallmatrix} \overline{N-Q+P} \\ \overline{N-Q} \end{smallmatrix}\right\}$	$B-A$	-
$\left\{\begin{smallmatrix} \overline{Q} \\ N-Q \end{smallmatrix}\right\}$	$\left\{\begin{smallmatrix} \overline{N} \\ \overline{N-P} \end{smallmatrix}\right\}$	$B-1$	-
$\left\{\begin{smallmatrix} \overline{N} \\ N-P \end{smallmatrix}\right\}$	$\left\{\begin{smallmatrix} P \\ Q \end{smallmatrix}\right\}$	$C-1$	-
$\left\{\begin{smallmatrix} Q-P \\ N \end{smallmatrix}\right\}$	$\left\{\begin{smallmatrix} \overline{P} \\ N-Q \end{smallmatrix}\right\}$	0	-
$\left\{\begin{smallmatrix} Q \\ N \end{smallmatrix}\right\}$	$\left\{\begin{smallmatrix} \overline{P} \\ N-P \end{smallmatrix}\right\}$	0	-

Vertex	Successors	Label	Conditons
$\left\{\begin{smallmatrix}\overline{P}\\ N-P\end{smallmatrix}\right\}$	$\left\{\frac{\overline{Q}}{Q-P}\right\}$	$A-1$	-
$\left\{\frac{\overline{N}}{N-Q+P}\right\}$	$\left\{\begin{smallmatrix}P\\ N-Q+P\end{smallmatrix}\right\}$	$C-1$	-
$\left\{\frac{\overline{N}}{N-Q}\right\}$	$\left\{\begin{smallmatrix}P\\ N\end{smallmatrix}\right\}$	$C-1$	-
$\left\{\begin{smallmatrix}P\\ N\end{smallmatrix}\right\}$	$\left\{\frac{\overline{P}}{Q-P}\right\}$	0	-

TABLE 2. The graph $G_2(\mathcal{S})$ of triple intersections. To each edge $\boldsymbol{\alpha} \xrightarrow{d} \boldsymbol{\alpha}'$ in this table there exist another edge $-\boldsymbol{\alpha} \xrightarrow{C-1-d} -\boldsymbol{\alpha}' \in G_2(\mathcal{S})$. Here we set $P = (1,0,0)^t, Q = (A,1,0)^t, N = (B,A,1)^t$.

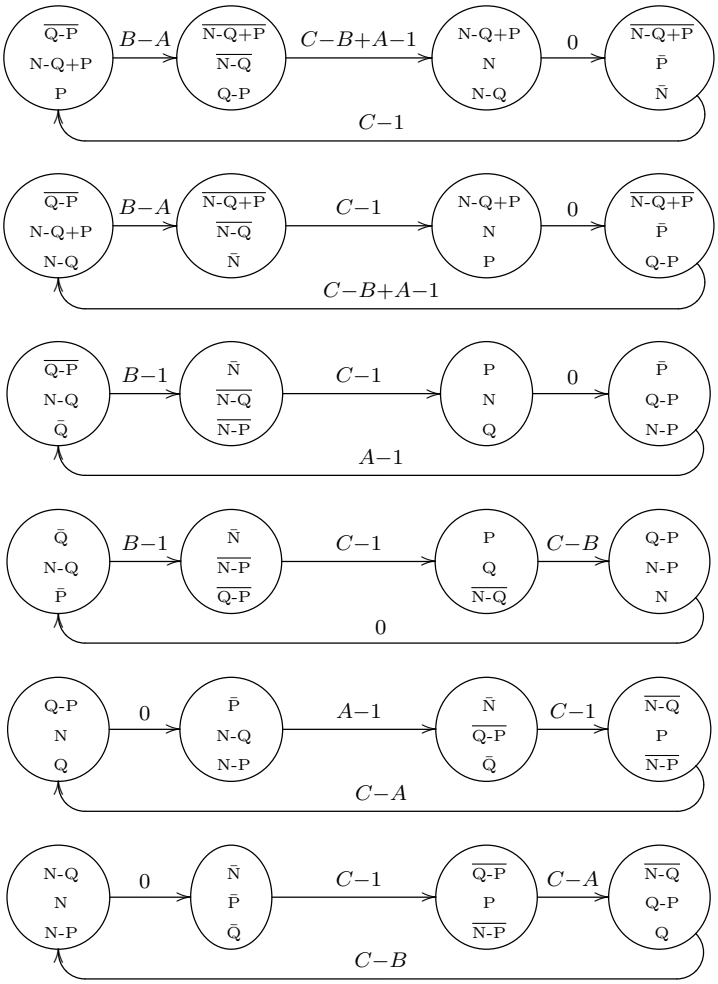

FIGURE 11. The graph $G_3(\mathcal{S})$ of 4-fold intersections of T under the conditions of Proposition 1.16. Here we set $P = (1,0,0)^t, Q = (A,1,0)^t, N = (B,A,1)^t$.

PROOF. By Proposition 1.16, we know that if $G(\mathcal{S})$ has 14 vertices then it is given by Figure 8. So the graphs $G_2(\mathcal{S})$ and $G_3(\mathcal{S})$ can be constructed from $G(\mathcal{S})$ by direct calculation using Definition 1.23. The fact that $G_4(\mathcal{S})$ (and, hence, $G_\ell(\mathcal{S})$ for $\ell \geq 5$) is empty can be seen easily from $G_3(\mathcal{S})$. The symmetry assertion is immediate from the construction of these graphs. □

1.3. Topological results

In this section we establish Theorem 1.1. Since each 3-dimensional self-affine tile with collinear digit set can be transformed to an ABC-tile in the way described in Section 1.2.2, it suffices to prove this theorem for ABC-tiles $T = T(M, \mathcal{D})$ with M and $\mathcal{D}$ given as in (1.11). Since the tiling assertion of Theorem 1.1 has already been established in Lemma 1.12, it remains to prove assertions (1) to (5) of Theorem 1.1 for ABC-tiles with 14 neighbors. We will prove (5) in Lemma 1.27, (4) in Lemma 1.28, (3) in Proposition 1.38, (1) in Proposition 1.51, and (2) in Proposition 1.52.

Throughout this section we assume that $T = T(M, \mathcal{D})$ is an ABC-tile with 14 neighbors.

1.3.1. Proof of the easy cases: Theorem 1.1 (4) and (5). We prove three simple lemmas. The first one concerns empty intersections.

LEMMA 1.27. *Let $T = T(M, \mathcal{D})$ be an ABC-tile with 14 neighbors. Assume that $\boldsymbol{\alpha} \subset \mathbb{Z}^3 \setminus \{0\}$ contains at least 4 elements. Then $\boldsymbol{B}_{\boldsymbol{\alpha}} = \emptyset$.*

PROOF. This follows immediately from Lemma 1.26 because the fact that $G_\ell(\mathcal{S})$ is empty for $\ell \geq 4$ implies in view of Proposition 1.24 that there are no points in which 5 or more tiles of the tiling $\{T + \beta;\, \beta \in \mathbb{Z}^3\}$ intersect. □

Lemma 1.27 establishes Theorem 1.1 (5) by the transformation described in Section 1.2.2. For the same reason, Theorem 1.1 (4) is a consequence of the following lemma.

LEMMA 1.28. *Let $T = T(M, \mathcal{D})$ be an ABC-tile with 14 neighbors. Assume that $\boldsymbol{\alpha} \subset \mathbb{Z}^3 \setminus \{0\}$ contains 3 elements. Then the 4-fold intersection $\boldsymbol{B}_{\boldsymbol{\alpha}}$ is homeomorphic to a single point if $\boldsymbol{\alpha} \in G_3(\mathcal{S})$. Otherwise, $\boldsymbol{B}_{\boldsymbol{\alpha}} = \emptyset$.*

PROOF. If $\boldsymbol{\alpha} \notin G_3(\mathcal{S})$, then $\boldsymbol{B}_{\boldsymbol{\alpha}} = \emptyset$ by Proposition 1.24. If $\boldsymbol{\alpha} \in G_3(\mathcal{S})$, then by Lemma 1.26 (see also Figure 11) there exists exactly one infinite walk in $G_3(\mathcal{S})$ starting from the vertex $\boldsymbol{\alpha}$. By Proposition 1.24, we know that $x = \sum_{j\geq 1} M^{-j} d_j \in \boldsymbol{B}_{\boldsymbol{\alpha}}$ if and only if there exists an infinite walk starting from vertex $\boldsymbol{\alpha} \in G_3(\mathcal{S})$ with labeling $d_1 d_2 \ldots$. Thus $\boldsymbol{B}_{\boldsymbol{\alpha}}$ is a singleton. □

Later we will need the following result on 4-fold intersections.

LEMMA 1.29. *Let T be an ABC-tile with 14 neighbors and let $\boldsymbol{\alpha} \in G_2(\mathcal{S})$. Then the 3-fold intersection $\boldsymbol{B}_{\boldsymbol{\alpha}}$ contains exactly two different points that are 4-fold intersections. If $\boldsymbol{\alpha}$ has more than one outgoing edge in $G_2(\mathcal{S})$ then these two points are located in two different subtiles of the first subdivision of $\boldsymbol{B}_{\boldsymbol{\alpha}}$.*

PROOF. First note that for each $\boldsymbol{\alpha} \in G_2(\mathcal{S})$ there are exactly two elements $\boldsymbol{\beta} \in G_3(\mathcal{S})$ with $\boldsymbol{\alpha} \subset \boldsymbol{\beta}$. Because $\boldsymbol{B}_{\boldsymbol{\beta}}$ is a single point for each $\boldsymbol{\beta} \in G_3(\mathcal{S})$ by Lemma 1.28, this proves the first assertion.

Let $\boldsymbol{\beta}_1, \boldsymbol{\beta}_2 \in G_3(\mathcal{S})$ be given with $\boldsymbol{\alpha} \subset \boldsymbol{\beta}_i$ for $i \in \{1, 2\}$. Then the edge leading away from $\boldsymbol{\beta}_1$ in $G_3(\mathcal{S})$ has a different labeling than the edge leading away from $\boldsymbol{\beta}_2$ in $G_3(\mathcal{S})$. Since there are no 5-fold intersections this means that the points $\boldsymbol{B}_{\boldsymbol{\beta}_1}$ and $\boldsymbol{B}_{\boldsymbol{\beta}_2}$ are located in two different subtiles of $\boldsymbol{B}_{\boldsymbol{\alpha}}$ and the second assertion is proved as well. □

1.3.2. Decreasing regular partitionings. Bing [**15**] developed a theory to characterize an m-sphere for $m \leq 3$ by using a sequence of "partitionings" $\mathcal{P}_k$ that become finer and finer in a way that the maximal diameter of an atom of $\mathcal{P}_k$ tends to zero for $k \to \infty$. For our purposes we will need Bing's characterizations of 1- and 2-spheres.

To be more precise, let $\mathcal{X}$ be a locally connected continuum. A *partitioning* of $\mathcal{X}$ is a collection of mutually disjoint open sets whose union is dense in $\mathcal{X}$. A sequence $\mathcal{P}_1, \mathcal{P}_2, \ldots$ of partitionings is called a *decreasing sequence of partitionings* if $\mathcal{P}_{k+1}$ is a refinement of $\mathcal{P}_k$ and the maximum of the diameters of the atoms of $\mathcal{P}_k$ tends to 0 as k tends to infinity. A partitioning is called *regular* if each of its atoms is the interior its closure.

In the sequel we will need two kinds of decreasing sequences of regular partitionings. One is for ∂T and another is one for

$$L_\alpha = \bigcup_{\substack{\beta \in \mathcal{S} \\ \{\alpha,\beta\} \in G_2(\mathcal{S})}} \boldsymbol{B}_{\alpha,\beta} \qquad (\alpha \in \mathcal{S}). \tag{1.22}$$

(We note already here that we will prove in Lemma 1.41 that $L_\alpha = \partial_{\partial T} \boldsymbol{B}_\alpha$.) For the construction of these sequences of partitionings the set equation of the self-affine ABC-tile T and its intersections given by (1.19) will be used.

1.3.3. Preparatory results on 3-fold intersections. In this subsection we show that each nonempty 3-fold intersection as well as each L_α, $\alpha \in \mathcal{S}$, is a Peano continuum. Moreover, we provide some combinatorial results on the subdivision structure of L_α. All this will be needed in order to prove Theorem 1.1 (3).

We start with a definition.

DEFINITION 1.30 (*cf. e.g.* [**84**, Definition 6.6]). Let $\mathcal{K} = \{X_1, \ldots, X_\nu\} \subset \mathbb{R}^m$ be a finite collection of sets.

- The collection $\mathcal{K}$ forms a *regular chain* if $|X_i \cap X_{i+1}| = 1$ for each $i \in \{1, \ldots, \nu - 1\}$ and $X_i \cap X_j = \emptyset$ if $|i - j| \geq 2$. (Here we use $|K|$ to denote the cardinality of a set K.)
- The collection $\mathcal{K}$ forms a *circular chain* if $|X_i \cap X_{i+1}| = 1$ for each $i \in \{1, \ldots, \nu - 1\}$, $|X_1 \cap X_\nu| = 1$, and $X_i \cap X_j = \emptyset$ if $2 \leq |i - j| \leq \nu - 2$.
- The *Hata graph* of $\mathcal{K}$ is an undirected graph. Its vertices are the elements of $\mathcal{K}$ and there is an edge between X_i and X_j if and only if $i \neq j$ and $X_i \cap X_j \neq \emptyset$.

We need the following result on connectedness of the attractor of a graph-directed iterated function system in the sense of Mauldin and Williams [**67**].

LEMMA 1.31 (*cf.* [**64**, Theorem 4.1]). *Let $\{S_1, \dots, S_q\}$ be the attractor of a graph-directed iterated function system with (directed) graph G with set of vertices $\{1, \dots, q\}$, set of edges E, and contractions F_e ($e \in E$) as edge labels,* i.e., *the nonempty compact sets $S_1, \dots, S_q$ are uniquely defined by*

$$S_i = \bigcup_{i \xrightarrow{e} j} F_e(S_j),$$

where the union is taken over all edges in G starting from i. Then S_i is a Peano continuum or a single point for each $i \in \{1, \dots, q\}$ if and only if for each $i \in \{1, \dots, q\}$ the successor collection

$$\big\{F_e(S_j);\ i \xrightarrow{e} j \text{ is an edge in } G \text{ starting from } i\big\}$$

of i has a connected Hata graph.

Let $\ell \geq 1$ and assume that each edge label $d \in \mathcal{D}$ of $G_\ell(\mathcal{S})$ is interpreted as the contraction f_d. Then by the set equation (1.19) the graph $G_\ell(\mathcal{S})$ defines a graph-directed iterated function system with attractor $\{B_{\boldsymbol{\alpha}};\ \boldsymbol{\alpha} \in G_\ell(\mathcal{S})\}$. The following lemma gives first topological information on the set of 3-fold intersections.

LEMMA 1.32.

(1) *For each vertex $\boldsymbol{\alpha} \in G_2(\mathcal{S})$, the set $\boldsymbol{B}_{\boldsymbol{\alpha}}$ is a Peano continuum.*
(2) *For each $\alpha \in \mathcal{S}$, the set L_α is a Peano continuum.*

PROOF. By the set equation (1.19) the collection $\{\boldsymbol{B}_{\boldsymbol{\alpha}};\ \boldsymbol{\alpha} \in G_2(\mathcal{S})\}$ is the attractor of the graph-directed iterated function system directed by the graph $G_2(\mathcal{S})$. To prove assertion (1), we want to apply Lemma 1.31. Thus we have to show that the Hata graph of the successor collection of each vertex $\boldsymbol{\alpha} \in G_2(\mathcal{S})$ is connected. We denote this Hata graph by $H(\boldsymbol{\alpha})$. (Note that $\boldsymbol{B}_{\boldsymbol{\alpha}}$ cannot be a singleton because each vertex of $G_2(\mathcal{S})$ is the starting point of infinitely many walks.) For convenience, we multiply each element of these successor collections by M. This has no effect on the Hata graph.

From Table 2 we see that $G_2(\mathcal{S})$ has 36 vertices. If $A \geq 2$, then 18 of them have only one outgoing edge, if $A = 1$ this is the case for 24 vertices. For these "trivial" vertices the graph $H(\boldsymbol{\alpha})$ is a single vertex and, hence, it is connected. Thus we have to deal with the remaining "nontrivial" vertices of $G_2(\mathcal{S})$ (18 for $A \geq 2$ and 12 for $A = 1$).

Let X_1, X_2 be two elements of a (multiplied by M) successor collection of a "nontrivial" vertex $\boldsymbol{\alpha} \in G_2(\mathcal{S})$. Then there are $a_1, a_2 \in \mathcal{D}$ and $\boldsymbol{\beta}_1, \boldsymbol{\beta}_2 \in G_2(\mathcal{S})$ such that $X_i = \boldsymbol{B}_{\boldsymbol{\beta}_i} + a_i$ for $i \in \{1, 2\}$. To check if there is an edge in $H(\boldsymbol{\alpha})$ connecting X_1 and X_2, we note that by the definition of $G_3(\mathcal{S})$ and the fact that $G_\ell(\mathcal{S}) = \emptyset$ for $\ell \geq 4$ we have

$$\begin{aligned} X_1 \cap X_2 \neq \emptyset \quad &\Longleftrightarrow \quad \boldsymbol{B}_{\boldsymbol{\beta}_1} \cap (\boldsymbol{B}_{\boldsymbol{\beta}_2} + a_2 - a_1) \neq \emptyset \\ &\Longleftrightarrow \quad (\boldsymbol{\beta}_1 \cup (\boldsymbol{\beta}_2 + a_2 - a_1) \cup \{a_2 - a_1\}) \setminus \{0\} \in G_3(\mathcal{S}). \end{aligned} \tag{1.23}$$

Thus the graph $H(\boldsymbol{\alpha})$ can be set up by checking the the graphs $G_2(\mathcal{S})$ and $G_3(\mathcal{S})$.

It turns out that the Hata graphs $H(\boldsymbol{\alpha})$ for the nontrivial vertices of $\boldsymbol{\alpha} \in G_2(\mathcal{S})$ all have the same structure. Indeed, let

(1.24)
$$\begin{array}{lllllllll} \boldsymbol{\zeta}_1 &=& \{\overline{Q}, N-Q\}, & \boldsymbol{\eta}_1 &=& \{\overline{Q-P}, N-Q\}, & \boldsymbol{\vartheta}_1 &=& \{\overline{Q-P}, N-Q+P\}, \\ \boldsymbol{\zeta}_2 &=& \{Q-P, N-P\}, & \boldsymbol{\eta}_2 &=& \{Q-P, N\}, & \boldsymbol{\vartheta}_2 &=& \{Q, N\}, \\ \boldsymbol{\zeta}_3 &=& \{\overline{N}, \overline{N-Q+P}\}, & \boldsymbol{\eta}_3 &=& \{\overline{N}, \overline{N-Q}\}, & \boldsymbol{\vartheta}_3 &=& \{\overline{N-P}, \overline{N-Q}\} \end{array}$$

be elements of $G_2(\mathcal{S})$ and set

$$V_i = \{\boldsymbol{\zeta}_i + d, \boldsymbol{\eta}_i + d, \boldsymbol{\vartheta}_i + d;\ d \in \mathcal{D}\} \qquad (1 \le i \le 3). \tag{1.25}$$

Then using (1.23) and inspecting the graph $G_3(\mathcal{S})$ we gain that

$$(\boldsymbol{B}_{\boldsymbol{\zeta}_i} + d) \cap (\boldsymbol{B}_{\boldsymbol{\eta}_i} + d),\ (\boldsymbol{B}_{\boldsymbol{\eta}_i} + d) \cap (\boldsymbol{B}_{\boldsymbol{\vartheta}_i} + d),\ (\boldsymbol{B}_{\boldsymbol{\vartheta}_i} + d) \cap \big(\boldsymbol{B}_{\boldsymbol{\zeta}_i} + (d+P)\big)$$

contain a single element for $(1 \le i \le 3,\ d \in \mathcal{D})$ and all the other intersections of the form $\boldsymbol{B}_{\boldsymbol{\gamma}} \cap \boldsymbol{B}_{\boldsymbol{\gamma}'}$ with $\boldsymbol{\gamma}, \boldsymbol{\gamma}' \in V_i$ are empty. Thus we conclude that V_i is a regular chain whose Hata graph is the *path graph* depicted in Figure 12.

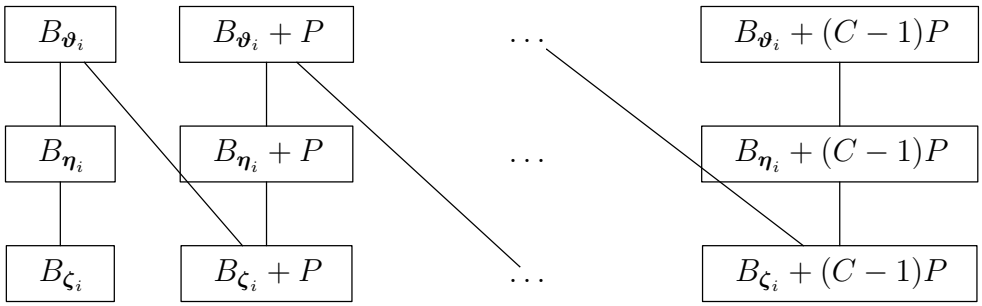

FIGURE 12. The Hata graph of the regular chain V_i $(1 \le i \le 3)$.

We can read off from the graph $G_2(\mathcal{S})$ in Table 2 that each nontrivial vertex $\boldsymbol{\alpha}$ has a Hata graph $H(\boldsymbol{\alpha})$ which is a path graph that is a subgraph of the Hata graph of V_i for some $i \in \{1, 2, 3\}$. Thus $H(\boldsymbol{\alpha})$ is a connected graph and the proof of (1) is finished.

To prove assertion (2), it suffices to show that it holds for $\alpha \in \{P,\ Q,\ N,\ Q-P,\ N-Q,\ N-P,\ N-Q+P\}$ by the symmetry mentioned in Lemma 1.26. From the definition of L_α we get

(1.26)
$$\begin{aligned} L_P &= \boldsymbol{B}_{\left\{{\overline{Q-P} \atop P}\right\}} \cup \boldsymbol{B}_{\left\{{P \atop N-Q+P}\right\}} \cup \boldsymbol{B}_{\left\{{P \atop N}\right\}} \cup \boldsymbol{B}_{\left\{{P \atop Q}\right\}} \cup \boldsymbol{B}_{\left\{{\overline{N-Q} \atop P}\right\}} \cup \boldsymbol{B}_{\left\{{\overline{N-P} \atop P}\right\}}, \\ L_Q &= \boldsymbol{B}_{\left\{{\overline{N-Q} \atop Q}\right\}} \cup \boldsymbol{B}_{\left\{{Q-P \atop Q}\right\}} \cup \boldsymbol{B}_{\left\{{Q \atop N}\right\}} \cup \boldsymbol{B}_{\left\{{P \atop Q}\right\}}, \\ L_N &= \boldsymbol{B}_{\left\{{N-P \atop N}\right\}} \cup \boldsymbol{B}_{\left\{{N-Q \atop N}\right\}} \cup \boldsymbol{B}_{\left\{{N-Q+P \atop N}\right\}} \cup \boldsymbol{B}_{\left\{{P \atop N}\right\}} \cup \boldsymbol{B}_{\left\{{Q \atop N}\right\}} \cup \boldsymbol{B}_{\left\{{Q-P \atop N}\right\}}, \\ L_{Q-P} &= \boldsymbol{B}_{\left\{{\overline{N-Q+P} \atop Q-P}\right\}} \cup \boldsymbol{B}_{\left\{{\overline{N-Q} \atop Q-P}\right\}} \cup \boldsymbol{B}_{\left\{{Q-P \atop Q}\right\}} \cup \boldsymbol{B}_{\left\{{Q-P \atop N-P}\right\}} \cup \boldsymbol{B}_{\left\{{Q-P \atop N-P}\right\}} \cup \boldsymbol{B}_{\left\{{\overline{P} \atop Q-P}\right\}}, \\ L_{N-Q} &= \boldsymbol{B}_{\left\{{\overline{Q-P} \atop N-Q}\right\}} \cup \boldsymbol{B}_{\left\{{\overline{Q} \atop N-Q}\right\}} \cup \boldsymbol{B}_{\left\{{\overline{P} \atop N-Q}\right\}} \cup \boldsymbol{B}_{\left\{{N-Q \atop N-P}\right\}} \cup \boldsymbol{B}_{\left\{{N-Q \atop N}\right\}} \cup \boldsymbol{B}_{\left\{{N-Q \atop N-Q+P}\right\}}, \\ L_{N-P} &= \boldsymbol{B}_{\left\{{Q-P \atop N-P}\right\}} \cup \boldsymbol{B}_{\left\{{\overline{P} \atop N-P}\right\}} \cup \boldsymbol{B}_{\left\{{N-Q \atop N-P}\right\}} \cup \boldsymbol{B}_{\left\{{N-P \atop N}\right\}}, \\ L_{N-Q+P} &= \boldsymbol{B}_{\left\{{P \atop N-Q+P}\right\}} \cup \boldsymbol{B}_{\left\{{N-Q+P \atop N}\right\}} \cup \boldsymbol{B}_{\left\{{N-Q \atop N-Q+P}\right\}} \cup \boldsymbol{B}_{\left\{{\overline{Q-P} \atop N-Q+P}\right\}}. \end{aligned}$$

Each union on the right hand side is ordered in a way that consecutive sets have nonempty intersection (indeed, by using (1.23) and the graph $G_3(\mathcal{S})$ we see that the collection of the elements of each union even forms a circular chain). Thus each of the sets L_α in (1.26) is a connected union of finitely many Peano continua and, hence, a Peano continuum. □

Next we prove a combinatorial result. The collection $\mathcal{L}_{\alpha,k}$ defined in the following lemma is the set of pieces of the $(k-1)$-th subdivision of the set L_α. Thus this result already hints at the fact that L_α is a simple closed curve. Recall that for $\boldsymbol{\alpha} \in \times_{j=1}^{\ell} G(\mathcal{S})$ the collection $\mathcal{C}_k(\boldsymbol{\alpha})$ is defined in (1.20).

LEMMA 1.33. *For each $\alpha \in \mathcal{S}$ the collection*

$$\mathcal{L}_{\alpha,k} = \bigcup_{\alpha' \colon \{\alpha,\alpha'\} \in G_2(\mathcal{S})} \mathcal{C}_k(\{\alpha, \alpha'\}) \tag{1.27}$$

forms a circular chain for each $k \geq 1$ (if the sets in this collection are ordered properly).

PROOF. Let $\alpha \in \mathcal{S}$ be arbitrary but fixed throughout this proof. Let $H(\mathcal{L}_{\alpha,k})$ be the Hata graph of $\mathcal{L}_{\alpha,k}$. Using induction on k we will prove first that $H(\mathcal{L}_{\alpha,k})$ consists of a single cycle. In the proof of Lemma 1.32 (2) we showed that this is true for $k = 1$. To perform the induction step we assume $H(\mathcal{L}_{\alpha,k})$ consists of a single cycle for some $k \in \mathbb{N}$. To prove that the same holds for $H(\mathcal{L}_{\alpha,k+1})$, we examine each edge of $H(\mathcal{L}_{\alpha,k})$ carefully. Let

$$X_1 — X_2 \tag{1.28}$$

be an arbitrary edge in $H(\mathcal{L}_{\alpha,k})$. This edge represents two sets $X_i = M^{-k+1}(\boldsymbol{B}_{\boldsymbol{\beta}_i} + a_i)$ with $a_1, a_2 \in \mathcal{D}$ and $\boldsymbol{\beta}_1, \boldsymbol{\beta}_2 \in G_2(\mathcal{S})$ that have nonempty intersection. When we pass from $H(\mathcal{L}_{\alpha,k})$ to $H(\mathcal{L}_{\alpha,k+1})$ each vertex X_i is replaced by a path $\bullet — \cdots — \bullet$ (possibly degenerated to a single vertex) whose vertices are the elements of the subdivision of X_i. Indeed, from the proof of Lemma 1.32 (1) we know that X_i is subdivided according to the graph $G_2(\mathcal{S})$ into a finite collection of sets that forms a regular chain. Thus passing from $H(\mathcal{L}_{\alpha,k})$ to $H(\mathcal{L}_{\alpha,k+1})$ the edge (1.28) is transformed to a subgraph consisting of two disjoint finite path graphs that are connected by at least one edge.

We claim that this subgraph is itself a path graph. If we multiply each vertex of $H(\mathcal{L}_{\alpha,k})$ by M^{k-1} and shift it by an appropriate vector in $\mathbb{Z}^3$ then the structure of the Hata graph as well as the way a given vertex subdivides into its subtiles is not changed. Thus we may assume w.l.o.g. that the edge (1.28) has the form

$$\boldsymbol{B}_{\alpha_1,\alpha_2} — \boldsymbol{B}_{\alpha_1,\alpha_3} \tag{1.29}$$

with $\{\alpha_1, \alpha_2, \alpha_3\} \in G_3(\mathcal{S})$. In order to prove the claim for each $\boldsymbol{\alpha} \in G_3(\mathcal{S})$ and each distinct $\boldsymbol{\beta}_1, \boldsymbol{\beta_2} \subset \boldsymbol{\alpha}$, we have to show that the subdivision of $\boldsymbol{B}_{\boldsymbol{\beta}_1} \cup \boldsymbol{B}_{\boldsymbol{\beta}_2}$ has a Hata graph which is a path graph. We will denote this Hata graph by $H(\boldsymbol{\beta}_1, \boldsymbol{\beta}_2)$. (Note that $\boldsymbol{\beta}_1, \boldsymbol{\beta}_2$ are always vertices of $G_2(\mathcal{S})$.)

Inspecting the graphs $G_2(\mathcal{S})$ and $G_3(\mathcal{S})$ we see that we have the following three cases to distinguish.

(i) Both, $\boldsymbol{\beta}_1$ and $\boldsymbol{\beta}_2$ have only one outgoing edge in $G_2(\mathcal{S})$.

(ii) Exactly one of the two vertices, $\boldsymbol{\beta}_1$ and $\boldsymbol{\beta}_2$ have only one outgoing edge in $G_2(\mathcal{S})$.

(iii) Both, $\boldsymbol{\beta}_1$ and $\boldsymbol{\beta}_2$ have more than one outgoing edge in $G_2(\mathcal{S})$.

We show that $H(\boldsymbol{\beta}_1, \boldsymbol{\beta}_2)$ is a path graph for each of these cases separately.

Case (i) is trivial because the subdivision of both, $\boldsymbol{B}_{\boldsymbol{\beta}_1}$ and $\boldsymbol{B}_{\boldsymbol{\beta}_2}$, consists of only one element. Thus $H(\boldsymbol{\beta}_1, \boldsymbol{\beta}_2)$ is of the form •—• and we are done.

Case (ii): Assume w.l.o.g. that $\boldsymbol{\beta}_1$ has more than one outgoing edge in $G_2(\mathcal{S})$ (we call it the nontrivial vertex). Then $\boldsymbol{\beta}_2$ has only one outgoing edge in $G_2(\mathcal{S})$ (we call it the trivial vertex). We know from the proof of Lemma 1.32 (1) that the subdivision of $\boldsymbol{B}_{\boldsymbol{\beta}_1}$ has a Hata graph $H(\boldsymbol{\beta}_1)$ which is a path graph $Y_1 \text{ — } \cdots \text{ — } Y_r$ for some $r \geq 2$. The Hata graph $H(\boldsymbol{\beta}_2)$ is a single vertex Z by assumption. We have to show that the Hata graph $H(\boldsymbol{\beta}_1, \boldsymbol{\beta}_2)$ of the subdivision of $\boldsymbol{B}_{\boldsymbol{\beta}_1} \cup \boldsymbol{B}_{\boldsymbol{\beta}_2}$ is a path graph. We know that $H(\boldsymbol{\beta}_1, \boldsymbol{\beta}_2)$ consists of the path $H(\boldsymbol{\beta}_1)$ and the vertex $H(\boldsymbol{\beta}_2)$ together with some edges connecting these two subgraphs. Thus we have to prove that the only connection between these two subgraphs is a single edge of the form $Y_{i_0} \text{ — } Z$ for $i_0 \in \{1, r\}$.

To do this, we have to show that $Y_j \cap Z = \emptyset$ for $j \neq i_0$ and $Y_{i_0} \cap Z \neq \emptyset$. Since all occurring vertices are triple intersections these intersections are nonempty if and only if they correspond to vertices of $G_3(\mathcal{S})$.

We illustrate this for an example. Assume that $A \geq 2$ and let $\boldsymbol{\beta}_1 = \{Q - P,\ N - P\}$ and $\boldsymbol{\beta}_2 = \{Q - P,\ N\}$. Then $H(\boldsymbol{\beta}_1)$ (multiplied by M) is the subpath of the graph in Figure 12 for the choice $i_0 = 1$ given by

$$Y_1 = \{\overline{Q},\ N - Q\} \text{ — } \cdots \text{ — } \{\overline{Q},\ N - Q + (A-1)P\} = Y_r.$$

The graph $H(\boldsymbol{\beta}_2)$ is the vertex $\{\overline{P},\ N - Q\}$. Since

$$B_{\{\overline{Q},\ N-Q\}} \cap B_{\{\overline{P},\ N-Q\}} = B_{\{\overline{P},\overline{Q},\ N-Q\}}$$

with $\{\overline{P}, \overline{Q},\ N - Q\} \in G_3(\mathcal{S})$, we see that $Y_1 \cap Z \neq \emptyset$ in this case. All the other intersections are easily seen to be not in $G_3(\mathcal{S})$; most of them would even correspond to 5-fold intersections which do not exist.

The calculation we have done corresponds to the first line of Table 3. (The constellations of Case (ii) in the proof of Lemma 1.33 where we deal with the subdivision of a pair $\{\boldsymbol{\beta}_1, \boldsymbol{\beta}_2\}$ of vertices exactly one of which, say $\boldsymbol{\beta}_1$, is nontrivial. This table contains all possible constellations of this type modulo symmetry (recall that $\boldsymbol{\alpha} \xrightarrow{d} \boldsymbol{\alpha}' \in G_2(\mathcal{S})$ if and only if $-\boldsymbol{\alpha} \xrightarrow{C-1-d} -\boldsymbol{\alpha}' \in G_2(\mathcal{S})$). The first column contains the possibilities for $\boldsymbol{\beta}_1$ that can occur in such a constellation. The second column contains the first and the last element the subdivision of $\boldsymbol{\beta}_1$. The third column contains $\boldsymbol{\beta}_2$, whose (trivial) subdivision is contained in the fourth column. The fifth column describes if the first or the last element of the subdivision of $\boldsymbol{\beta}_1$ intersects $\boldsymbol{\beta}_2$. Finally, the sixth column gives the condition under which a given constellation exists.) Each line in this table corresponds to a possible constellation. In the fifth column of this table we indicate if the single vertex $H(\boldsymbol{\beta}_2)$ has nonempty intersection with the first[4] vertex Y_1 or the last vertex Y_r of $H(\boldsymbol{\beta}_1)$. The last column

[4]Since the path graph $H(\boldsymbol{\beta}_1)$ is undirected, we are free which end of the path we regard as "first" and "last" vertex. The choice which one is the first and which one is the last is indicated in the second column of Table 3.

shows under which conditions on A the constellation of the respective path can occur. All this can easily be verified by checking the intersections occurring in $G_3(\mathcal{S})$ as we did above.

Nontrivial vertex	First and Last vertex of its subdivision	Trivial vertex	Its subdivision	First/ Last	Condition
$\left\{\begin{smallmatrix}Q-P\\N-P\end{smallmatrix}\right\}$	$\left\{\begin{smallmatrix}\overline{Q}\\N-Q\end{smallmatrix}\right\}$, $\left\{\begin{smallmatrix}\overline{Q}\\N-Q\end{smallmatrix}\right\}+x_1$	$\left\{\begin{smallmatrix}Q-P\\N\end{smallmatrix}\right\}$	$\left\{\begin{smallmatrix}\overline{P}\\N-Q\end{smallmatrix}\right\}$	first	$A\geq 2$
		$\left\{\begin{smallmatrix}\overline{P}\\N-P\end{smallmatrix}\right\}$	$\left\{\begin{smallmatrix}\overline{Q}\\\overline{Q-P}\end{smallmatrix}\right\}+x_1$	last	
		$\left\{\begin{smallmatrix}N-P\\N\end{smallmatrix}\right\}$	$\left\{\begin{smallmatrix}\overline{Q}\\\overline{P}\end{smallmatrix}\right\}$	first	
$\left\{\begin{smallmatrix}\overline{P}\\Q-P\end{smallmatrix}\right\}$	$\left\{\begin{smallmatrix}\overline{Q-P}\\N-Q\end{smallmatrix}\right\}+x_1$, $\left\{\begin{smallmatrix}\overline{Q-P}\\N-Q\end{smallmatrix}\right\}+x_2$	$\left\{\begin{smallmatrix}\overline{N-Q+P}\\Q-P\end{smallmatrix}\right\}$	$\left\{\begin{smallmatrix}N-Q\\N-Q+P\end{smallmatrix}\right\}+x_2$	last	$A\geq 1$
		$\left\{\begin{smallmatrix}\overline{P}\\N-P\end{smallmatrix}\right\}$	$\left\{\begin{smallmatrix}\overline{Q}\\\overline{Q-P}\end{smallmatrix}\right\}+x_1$	first	
$\left\{\begin{smallmatrix}\overline{N-Q+P}\\\overline{P}\end{smallmatrix}\right\}$	$\left\{\begin{smallmatrix}\overline{Q-P}\\N-Q+P\end{smallmatrix}\right\}+x_2$, $\left\{\begin{smallmatrix}\overline{Q-P}\\N-Q+P\end{smallmatrix}\right\}+x_7$	$\left\{\begin{smallmatrix}\overline{P}\\N\end{smallmatrix}\right\}$	$\left\{\begin{smallmatrix}\overline{Q-P}\\P\end{smallmatrix}\right\}+x_7$	last	$A\geq 1$
		$\left\{\begin{smallmatrix}\overline{N}\\\overline{N-Q+P}\end{smallmatrix}\right\}$	$\left\{\begin{smallmatrix}P\\N-Q+P\end{smallmatrix}\right\}+x_7$	last	
		$\left\{\begin{smallmatrix}\overline{N-Q+P}\\Q-P\end{smallmatrix}\right\}$	$\left\{\begin{smallmatrix}N-Q\\N-Q+P\end{smallmatrix}\right\}+x_2$	first	
$\left\{\begin{smallmatrix}P\\Q\end{smallmatrix}\right\}$	$\left\{\begin{smallmatrix}Q-P\\N-P\end{smallmatrix}\right\}$, $\left\{\begin{smallmatrix}Q-P\\N-P\end{smallmatrix}\right\}+x_3$	$\left\{\begin{smallmatrix}Q\\N\end{smallmatrix}\right\}$	$\left\{\begin{smallmatrix}\overline{P}\\N-P\end{smallmatrix}\right\}$	first	$A\geq 1$
		$\left\{\begin{smallmatrix}Q\\\overline{N-Q}\end{smallmatrix}\right\}$	$\left\{\begin{smallmatrix}N-P\\N\end{smallmatrix}\right\}+x_3$	last	
		$\left\{\begin{smallmatrix}P\\N\end{smallmatrix}\right\}$	$\left\{\begin{smallmatrix}\overline{P}\\Q-P\end{smallmatrix}\right\}$	first	
$\left\{\begin{smallmatrix}\overline{N-Q}\\P\end{smallmatrix}\right\}$	$\left\{\begin{smallmatrix}Q-P\\N\end{smallmatrix}\right\}+x_3$, $\left\{\begin{smallmatrix}Q-P\\N\end{smallmatrix}\right\}+x_4$	$\left\{\begin{smallmatrix}\overline{N-Q}\\Q\end{smallmatrix}\right\}$	$\left\{\begin{smallmatrix}N\\N-P\end{smallmatrix}\right\}+x_3$	first	$A\geq 1$
		$\left\{\begin{smallmatrix}P\\\overline{N-P}\end{smallmatrix}\right\}$	$\left\{\begin{smallmatrix}Q-P\\Q\end{smallmatrix}\right\}+x_4$	last	
$\left\{\begin{smallmatrix}\overline{N-Q}\\\overline{N-P}\end{smallmatrix}\right\}$	$\left\{\begin{smallmatrix}Q\\N\end{smallmatrix}\right\}+x_4$, $\left\{\begin{smallmatrix}Q\\N\end{smallmatrix}\right\}+x_7$	$\left\{\begin{smallmatrix}\overline{N}\\\overline{N-P}\end{smallmatrix}\right\}$	$\left\{\begin{smallmatrix}P\\Q\end{smallmatrix}\right\}+x_7$	last	$A\geq 2$
		$\left\{\begin{smallmatrix}\overline{N}\\\overline{N-Q}\end{smallmatrix}\right\}$	$\left\{\begin{smallmatrix}P\\N\end{smallmatrix}\right\}+x_7$	last	
		$\left\{\begin{smallmatrix}\overline{N-P}\\P\end{smallmatrix}\right\}$	$\left\{\begin{smallmatrix}Q-P\\Q\end{smallmatrix}\right\}+x_4$	first	
$\left\{\begin{smallmatrix}N-Q\\N-Q+P\end{smallmatrix}\right\}$	$\left\{\begin{smallmatrix}\overline{N}\\\overline{N-Q+P}\end{smallmatrix}\right\}$, $\left\{\begin{smallmatrix}\overline{N}\\\overline{N-Q+P}\end{smallmatrix}\right\}+x_5$	$\left\{\begin{smallmatrix}N-Q+P\\\overline{Q-P}\end{smallmatrix}\right\}$	$\left\{\begin{smallmatrix}\overline{N-Q+P}\\\overline{N-Q}\end{smallmatrix}\right\}+x_5$	last	$A\geq 1$
		$\left\{\begin{smallmatrix}N-Q\\N\end{smallmatrix}\right\}$	$\left\{\begin{smallmatrix}\overline{P}\\\overline{N}\end{smallmatrix}\right\}$	first	
		$\left\{\begin{smallmatrix}N-Q+P\\N\end{smallmatrix}\right\}$	$\left\{\begin{smallmatrix}\overline{N-Q+P}\\\overline{P}\end{smallmatrix}\right\}$	first	
$\left\{\begin{smallmatrix}N-Q\\\overline{Q-P}\end{smallmatrix}\right\}$	$\left\{\begin{smallmatrix}\overline{N}\\\overline{N-Q}\end{smallmatrix}\right\}+x_5$, $\left\{\begin{smallmatrix}\overline{N}\\\overline{N-Q}\end{smallmatrix}\right\}+x_6$	$\left\{\begin{smallmatrix}\overline{Q}\\N-Q\end{smallmatrix}\right\}$	$\left\{\begin{smallmatrix}\overline{N}\\\overline{N-P}\end{smallmatrix}\right\}+x_6$	last	$A\geq 2$
		$\left\{\begin{smallmatrix}N-Q+P\\\overline{Q-P}\end{smallmatrix}\right\}$	$\left\{\begin{smallmatrix}\overline{N-Q+P}\\\overline{N-Q}\end{smallmatrix}\right\}+x_5$	first	
$\left\{\begin{smallmatrix}\overline{Q}\\\overline{Q-P}\end{smallmatrix}\right\}$	$\left\{\begin{smallmatrix}\overline{N-P}\\\overline{N-Q}\end{smallmatrix}\right\}+x_6$, $\left\{\begin{smallmatrix}\overline{N-P}\\\overline{N-Q}\end{smallmatrix}\right\}+x_7$	$\left\{\begin{smallmatrix}\overline{Q}\\N-Q\end{smallmatrix}\right\}+x_6$	$\left\{\begin{smallmatrix}\overline{N}\\\overline{N-P}\end{smallmatrix}\right\}+x_6$	first	$A\geq 1$
		$\left\{\begin{smallmatrix}\overline{N}\\\overline{Q}\end{smallmatrix}\right\}$	$\left\{\begin{smallmatrix}\overline{N-P}\\P\end{smallmatrix}\right\}+x_7$	last	
		$\left\{\begin{smallmatrix}\overline{Q-P}\\\overline{N}\end{smallmatrix}\right\}$	$\left\{\begin{smallmatrix}\overline{N-Q}\\P\end{smallmatrix}\right\}+x_7$	last	

TABLE 3. For abbreviation we set $x_1=(A-1)P, x_2=(C-B+A-1)P, x_3=(C-B)P, x_4=(C-A)P, x_5=(B-A)P, x_6=(B-1)P, x_7=(C-1)P$.

Case (iii): By inspecting the graph $G_2(\mathcal{S})$ we see that in this case both vertices, $\boldsymbol{\beta}_1$ and $\boldsymbol{\beta}_2$, have the same three vertices as successors. These three vertices are of the

form given in (1.24) for some $i \in \{1,2,3\}$. Moreover, by inspecting the labels of the edges going out of $\boldsymbol{\beta}_1$ and $\boldsymbol{\beta}_2$ we see that the collection of successors of $\boldsymbol{B}_{\boldsymbol{\beta}_1} \cup \boldsymbol{B}_{\boldsymbol{\beta}_2}$ is a (consecutive) subcollection of $M^{-1}V_i$ with V_i as in (1.25). Hence, the Hata graph $H(\boldsymbol{\beta}_1, \boldsymbol{\beta}_2)$ is a path graph which is a subgraph of the graph depicted in Figure 12.

Summing up this finishes the proof of the claim.

We now show that $H(\mathcal{L}_{\alpha,k+1})$ is a cycle. To this end, let $\mathcal{L}_{\alpha,k} = \{Y_1, \dots, Y_p\}$ be the set of vertices of $H(\mathcal{L}_{\alpha,k})$ and Y_i — Y_{i+1} for $1 \le i \le p$ (whe always assume that $Y_0 := Y_p$ and $Y_{p+1} := Y_1$; note that $p \ge 4$ by (1.26)) its set of edges. Each vertex Y_i of $H(\mathcal{L}_{\alpha,k})$ becomes a path l_i in $H(\mathcal{L}_{\alpha,k+1})$. If l_i is a single vertex, then the above claim (see Case (i) and Case (ii)) implies that this vertex is connected with a terminating vertex of l_{i-1} and with a terminating vertex of l_{i+1}. If l_i is a (nondegenerate) path Z_1 — $\cdots$ — Z_2, then a terminating vertex of l_{i-1} is connected to Z_r for some $r \in \{1,2\}$ and a terminating vertex of l_{i+1} is connected to Z_s for some $s \in \{1,2\}$ (see Case (ii) and Case (iii)). We have to show that $r \neq s$. Indeed, suppose on the contrary that both paths are connected to the same vertex, say Z_1. Then the element Z_1 of the subdivision of Y_i contains two disjoint[5] 4-fold intersections (one with an element of Y_{i-1} and one with an element of Y_{i+1}) which would contradict Lemma 1.29. Thus the paths l_i $(1 \le i \le p)$ are arranged in a circular order and, hence, $H(\mathcal{L}_{\alpha,k+1})$ is a cycle.

Since the edges in $H(\mathcal{L}_{\alpha,k+1})$ correspond to nonempty 4-fold intersections they represent single points by Lemma 1.28. This implies that $\mathcal{L}_{\alpha,k+1}$ is a circular chain and the induction proof is finished. □

1.3.4. Topological characterization of 3-fold intersections. This section is devoted to the proof of Theorem 1.1 (3). Our first task is the construction of a sequence of collections of sets that will turn out to be the appropriate partitionings suitable to apply the theory of Bing [**15**] to it.

Fix $\alpha \in \mathcal{S}$. In order to construct the partitionings for L_α, for each $\boldsymbol{\beta}^{(0)} \in G_2(\mathcal{S})$ with $\alpha \in \boldsymbol{\beta}^{(0)}$ set

(1.30)

$$\mathcal{P}_{\alpha,k}(\boldsymbol{\beta}^{(0)}) = \{f_{d_1 d_2 \dots d_{k-1}}(\boldsymbol{B}_{\boldsymbol{\beta}^{(k-1)}})^\circ;\ \boldsymbol{\beta}^{(0)} \xrightarrow{d_1} \boldsymbol{\beta}^{(1)} \xrightarrow{d_2} \cdots \xrightarrow{d_{k-1}} \boldsymbol{\beta}^{(k-1)} \in G_2(\mathcal{S})\}\ (k \ge 1).$$

Here the interior K° of a set K is taken w.r.t. the subspace topology on L_α; this is why $\mathcal{P}_{\alpha,k}(\boldsymbol{\beta}^{(0)})$ depends on α. Now the sequence $(\mathcal{P}_{\alpha,k})_{k\ge1}$ is defined by

$$\mathcal{P}_{\alpha,k} = \bigcup_{\substack{\{\beta_1,\beta_2\}\in G_2(\mathcal{S})\\ \beta_1=\alpha}} \mathcal{P}_{\alpha,k}(\{\beta_1,\beta_2\}) \qquad (k \ge 1). \tag{1.31}$$

We want to prove that $(\mathcal{P}_{\alpha,k})_{k\ge1}$ is a decreasing sequence of regular partitionings of L_α for each $\alpha \in \mathcal{S}$. To this end we need a result on the boundary and the interior of a 3-fold intersection. Before we state it we emphasize that throughout the remaining part of the proof of Theorem 1.1 the ambient space will change and we always have to keep in mind with respect to which ambient space we will take boundaries or interiors. For this reason we will always make clear in which space we are working. As mentioned before, the boundary w.r.t. a given space X will

[5]Note that Y_{i-1} and Y_{i+1} are disjoint for any $i \in \{1,\dots,p\}$ because $p \ge 4$.

be denoted by ∂_X (for the closure and the interior we do not use any notation to emphasize on the space; this space should always be clear from the context or will be mentioned explicitly). In the following lemma recall the notations L_α and $\mathcal{L}_{\alpha,k}$ introduced in (1.22) and (1.27), respectively.

LEMMA 1.34. *Let $\alpha \in \mathcal{S}$ be given. For each vertex $\boldsymbol{\alpha} = \{\alpha, \alpha'\} \in G_2(\mathcal{S})$ we have $\overline{\boldsymbol{B}_{\boldsymbol{\alpha}}^\circ} = \boldsymbol{B}_{\boldsymbol{\alpha}}$, w.r.t. the subspace topology on L_α. More generally, we have $\overline{X^\circ} = X$ for each $X \in \mathcal{L}_{\alpha,k}$ and each $k \geq 1$.*

PROOF. The ambient space in this proof is L_α. First observe that (1.22) implies that the collection $\{\boldsymbol{B}_{\alpha,\gamma};\, \{\alpha,\gamma\} \in G_2(\mathcal{S})\}$ is a finite collection of compact sets which covers L_α. Thus for each $\boldsymbol{\alpha} = \{\alpha, \alpha'\} \in G_2(\mathcal{S})$ we have

$$\partial_{L_\alpha} \boldsymbol{B}_{\alpha,\alpha'} \subset \bigcup_{\substack{\gamma \notin \{\alpha,\alpha'\} \\ \{\alpha,\gamma\} \in G_2(\mathcal{S})}} \boldsymbol{B}_{\alpha,\gamma}$$

which implies that (since $\boldsymbol{B}_{\alpha,\alpha'}$ is closed in $\mathbb{R}^3$ and, hence, also closed in L_α)

$$\partial_{L_\alpha} \boldsymbol{B}_{\alpha,\alpha'} \subset \bigcup_{\substack{\gamma \in \mathcal{S} \\ \{\alpha,\alpha',\gamma\} \in G_3(\mathcal{S})}} \boldsymbol{B}_{\alpha,\alpha',\gamma}. \tag{1.32}$$

Thus, since the sets $\boldsymbol{B}_{\alpha,\alpha',\gamma}$ contain at most one point by Lemma 1.28, $\partial_{L_\alpha} \boldsymbol{B}_{\boldsymbol{\alpha}}$ is a finite set. Now choose $\varepsilon > 0$ and $x \in \boldsymbol{B}_{\boldsymbol{\alpha}}$ arbitrary. Subdivide $\boldsymbol{B}_{\boldsymbol{\alpha}}$ according to the set equation (1.19) for $r \in \mathbb{N}$ large enough to obtain a subtile $Z = M^{-r+1}(\boldsymbol{B}_{\boldsymbol{\beta}} + a) \in \mathcal{C}_r(\boldsymbol{\alpha})$ (with $\boldsymbol{\beta} \in G_2(\mathcal{S})$ and $a \in \mathbb{Z}^3$) of $\boldsymbol{B}_{\boldsymbol{\alpha}}$ with diameter less than ε with $x \in Z$. Since Z is a Peano continuum by Lemma 1.32 it contains infinitely many points and, hence, there is a point $y \in Z$ with $y \in \boldsymbol{B}_{\boldsymbol{\alpha}}^\circ$. Since ε was arbitrary, y can be chosen arbitrarily close to x. This proves the result for $\boldsymbol{B}_{\boldsymbol{\alpha}}$.

The assertion for the elements of the subdivisions $\mathcal{L}_{\alpha,k}$, $k \geq 1$, is proved in an analogous way. Indeed, the finite collection $\mathcal{L}_{\alpha,k}$ covers L_α which entails that for each $X \in \mathcal{L}_{\alpha,k}$ we have

$$\partial_{L_\alpha} X \subset \bigcup_{Y \in \mathcal{L}_{\alpha,k} \setminus \{X\}} (X \cap Y). \tag{1.33}$$

By Lemma 1.33 the sets $X \cap Y$ contain at most one element, hence, $\partial_{L_\alpha} X$ is a finite set. Since $X = M^{-k+1}(\boldsymbol{B}_{\boldsymbol{\beta}} + a)$ for some $\boldsymbol{\beta} \in G_2(\mathcal{S})$ and some $a \in \mathbb{Z}^3$ we may now subdivide $\boldsymbol{B}_{\boldsymbol{\beta}}$ according to the set equation (1.19) and argue as in the paragraph before. □

We are now in a position to prove that $(\mathcal{P}_{\alpha,k})_{k\geq 1}$ has the desired properties.

LEMMA 1.35. *The sequence $(\mathcal{P}_{\alpha,k})_{k\geq 1}$ in (1.31) is a decreasing sequence of regular partitionings of L_α for each $\alpha \in \mathcal{S}$.*

PROOF. The ambient space in this proof is L_α. We first claim that $\mathcal{P}_{\alpha,k}$ is a partitioning of L_α for each $k \geq 1$. To prove this we have to show that two distinct elements of $\mathcal{P}_{\alpha,k}$ are disjoint and

$$L_\alpha = \bigcup_{X \in \mathcal{P}_{\alpha,k}} \overline{X}. \tag{1.34}$$

For given distinct $X_1, X_2 \in \mathcal{P}_{\alpha,k}$ we have $\overline{X_1}, \overline{X_2} \in \mathcal{C}_k^{(2)}$ by Lemma 1.34. Lemma 1.25 thus implies that $\overline{X_1} \cap \overline{X_2}$ is either empty or an affine copy of $\boldsymbol{B}_{\boldsymbol{\beta}}$ for some $\boldsymbol{\beta} \in G_3(\mathcal{S})$ and, hence, by Lemma 1.28 the intersection $\overline{X_1} \cap \overline{X_2}$ contains at most one point p. Since $\overline{X_1}$ and $\overline{X_1}$ are Peano continua by Lemma 1.32 they do not contain isolated points which implies that the point p cannot be contained in the open set $X_1 \cap X_2$. Thus we conclude that $X_1 \cap X_2 = \emptyset$. Since (1.34) follows from the definition of $\mathcal{P}_{\alpha,k}$ together with Lemma 1.34 and the set equation (1.19) we proved the claim.

Now we will show that $(\mathcal{P}_{\alpha,k})_{k\geq 1}$ is a decreasing sequence of partitionings. First we prove that $\mathcal{P}_{\alpha,k+1}$ is a refinement of $\mathcal{P}_{\alpha,k}$ for each $k \geq 1$. Indeed, by the set equation (1.18) the closure $f_{d_1\cdots d_{k-1}d_k}(\boldsymbol{B}_{\boldsymbol{\beta}^{(k)}})$ of each element of $\mathcal{P}_{\alpha,k+1}$ is contained in the closure $f_{d_1\cdots d_{k-1}}(\boldsymbol{B}_{\boldsymbol{\beta}^{(k-1)}})$ of some element of $\mathcal{P}_{\alpha,k}$. Taking interiors we get the refinement assertion. The maximum of the diameters of the elements of $\mathcal{P}_{\alpha,k}$ approaches zero because f_d is a contraction for each $d \in \mathcal{D}$. Finally, $\mathcal{P}_{\alpha,k}$ is regular for each $k \in \mathbb{N}$ by Lemma 1.34. □

The basis of our proof of Theorem 1.1 (3) is given by the following characterization of a simple closed curve due to Bing [**15**].

Proposition 1.36 (*cf.* [**15**, Theorem 8]). *Let $\mathcal{X}$ be a locally connected continuum. A necessary and sufficient condition that $\mathcal{X}$ be a simple closed curve is that one of its decreasing sequences of regular partitionings $\mathcal{P}_1, \mathcal{P}_2, \ldots$ have the following properties:*

(1) *The boundary of each element of $\mathcal{P}_i$ is a pair of distinct points.*
(2) *No three elements of $\mathcal{P}_i$ have a boundary point in common.*

In our proof of Theorem 1.1 (3) we will need the fact that L_α is homeomorphic to a simple closed curve for every $\alpha \in G(\mathcal{S})$. To this end we have to show that $(\mathcal{P}_{\alpha,k})_{k\geq 1}$ satisfy (1) and (2) of Proposition 1.36. We start with the following lemma.

Lemma 1.37. *For $\alpha, \beta \in \mathcal{S}$ with $\{\alpha, \beta\} \in G_2(\mathcal{S})$ we have*

$$\partial_{L_\alpha} \boldsymbol{B}_{\alpha,\beta} = \bigcup_{\substack{\gamma\in\mathcal{S} \\ \{\alpha,\beta,\gamma\}\in G_3(\mathcal{S})}} \boldsymbol{B}_{\alpha,\beta,\gamma}. \tag{1.35}$$

More generally, for each $k \geq 1$ and each $X \in \mathcal{L}_{\alpha,k}$ (which is defined in (1.27)*) we have*

$$\partial_{L_\alpha} X = \bigcup_{Y\in\mathcal{L}_{\alpha,k}\setminus\{X\}} (X \cap Y). \tag{1.36}$$

Proof. The ambient space in this proof is L_α. Let $\mathcal{B}(x,\delta) = \{y \in L_\alpha;\, |x-y| < \delta\}$. The fact that the left hand side of (1.35) is contained in the right hand side follows from (1.32). To prove the reverse inclusion, suppose that for some $\gamma \in \mathcal{S}$ with $\{\alpha,\beta,\gamma\} \in G_3(\mathcal{S})$ there exists $x \in \boldsymbol{B}_{\alpha,\beta,\gamma} \setminus \partial_{L_\alpha} \boldsymbol{B}_{\alpha,\beta}$. Since $\boldsymbol{B}_{\alpha,\beta,\gamma} \subset \boldsymbol{B}_{\alpha,\beta}$, this implies that $x \in \boldsymbol{B}^\circ_{\alpha,\beta}$ and, hence, there exists $\delta > 0$ with $\mathcal{B}(x,\delta) \subset \boldsymbol{B}_{\alpha,\beta}$. Since $\boldsymbol{B}_{\alpha,\beta,\gamma} \subset \boldsymbol{B}_{\alpha,\gamma}$, we also have $x \in \boldsymbol{B}_{\alpha,\gamma}$ and by Lemma 1.34 there exists $y \in \boldsymbol{B}^\circ_{\alpha,\gamma} \cap \mathcal{B}(x,\delta)$. Thus there exists $\delta' > 0$ such that $\mathcal{B}(y,\delta') \subset \boldsymbol{B}_{\alpha,\gamma} \cap \mathcal{B}(x,\delta)$. This implies $\mathcal{B}(y,\delta') \subset \boldsymbol{B}_{\alpha,\beta} \cap \boldsymbol{B}_{\alpha,\gamma} = \boldsymbol{B}_{\alpha,\beta,\gamma}$. By Lemma 1.28, $\boldsymbol{B}_{\alpha,\beta,\gamma}$ is single point for each vertex $\{\alpha,\beta,\gamma\}$ in $G_3(\mathcal{S})$. However, a single point cannot contain a ball

in L_α because this set is a Peano continuum by Lemma 1.32. This contradiction finishes the proof for $\partial_{L_\alpha} \boldsymbol{B}_{\alpha,\beta}$.

The second assertion is proved along the same lines. Indeed, by (1.33) the left hand side of (1.36) is contained in the right hand side. For the reverse inclusion assume that for some $Y \in \mathcal{L}_{\alpha,k} \setminus \{X\}$ there exists $x \in (X \cap Y) \setminus \partial_{L_\alpha} X$. Thus $x \in X^\circ$ and, hence, there exists $\delta > 0$ with $\mathcal{B}(x,\delta) \subset X$. Since we also have $x \in Y$, by Lemma 1.34 there exists $y \in Y^\circ \cap \mathcal{B}(x,\delta)$. Thus there exists $\delta' > 0$ such that $\mathcal{B}(y,\delta') \subset Y \cap \mathcal{B}(x,\delta) \subset X \cap Y$. By Lemma 1.33, this set is a singleton which cannot contain a ball in the Peano continuum L_α, a contradiction. □

By the transformation described in Section 1.2.2 the following proposition implies Theorem 1.1 (3).

PROPOSITION 1.38. *Let $T = T(M,\mathcal{D})$ be an ABC-tile with 14 neighbors. Assume that $\boldsymbol{\alpha} \subset \mathbb{Z}^3 \setminus \{0\}$ contains 2 elements. Then the 3-fold intersection $\boldsymbol{B}_{\boldsymbol{\alpha}}$ is homeomorphic to an arc if $\boldsymbol{\alpha} \in G_2(\mathcal{S})$. Otherwise, $\boldsymbol{B}_{\boldsymbol{\alpha}} = \emptyset$.*

PROOF. In this proof we work in the ambient space L_α for an arbitrary but fixed $\alpha \in \mathcal{S}$. We first show that L_α is a simple closed curve. This is done with help of Proposition 1.36. To apply this result, let $(\mathcal{P}_{\alpha,k})_{k\geq 1}$ be the sequence given in (1.31). This sequence is a decreasing sequence of regular partitionings of L_α by Lemma 1.35. We now have to prove that (1.31) satisfies the two conditions of Proposition 1.36. First we claim that the boundary of each $X \in \mathcal{P}_{\alpha,k}$ is a pair of distinct points for each $k \in \mathbb{N}$. By Lemmas 1.34 and 1.33, we know that $\overline{X}$ intersects the elements in the union

$$\bigcup_{Y \in \mathcal{P}_{\alpha,k}\setminus\{X\}} (\overline{X} \cap \overline{Y}) = \bigcup_{Y \in \mathcal{L}_{\alpha,k}\setminus\{\overline{X}\}} (\overline{X} \cap Y)$$

in exactly two points. Thus (1.36) implies the claim and, hence, Proposition1.36(1). The fact that there are no three elements of $\mathcal{P}_{\alpha,k}$ having a common boundary point is an immediate consequence of Lemma 1.33 yielding Proposition 1.36 (2). Now we can apply Proposition 1.36 which yields that L_α is a simple closed curve for every $\alpha \in \mathcal{S}$.

Since for each $\{\alpha,\beta\} \in G_2(\mathcal{S})$, the set $\boldsymbol{B}_{\alpha,\beta}$ is a Peano continuum which is a proper subset of the simple closed curve L_α, it is an arc. As $\alpha \in \mathcal{S}$ was arbitrary, this implies that $\boldsymbol{B}_{\boldsymbol{\alpha}}$ is homeomorphic to an arc if $\boldsymbol{\alpha} \in G_2(\mathcal{S})$. If $\boldsymbol{\alpha} \notin G_2(\mathcal{S})$ then $\boldsymbol{B}_{\boldsymbol{\alpha}} = \emptyset$ by Proposition 1.24. □

In the sequel we need some results on dimension theory. A good reference for this topic is Kuratowski [**48**, §§25–28]. In particular, we will often need the following basic results.

LEMMA 1.39. *For a set $X \subset \mathbb{R}^3$, denote its topological dimension by* $\dim(X)$.

(1) *If $X \subset Y \subset \mathbb{R}^3$, then* $\dim(X) \leq \dim(Y)$.
(2) *Let $Y \subset \mathbb{R}^3$. If $X_1,\ldots,X_n$ are closed in Y with $Y = X_1 \cup \cdots \cup X_n$, then* $\dim(Y) \leq \max_{1\leq i\leq n} \dim(X_i)$.

PROOF. Assertion (1) is a special case of Kuratowski [**48**, §25, II, Theorem 1], while (2) follows from Kuratowski [**48**, §27, I, Corollary 2f]. □

LEMMA 1.40. *For each $\alpha \in \mathcal{S}$, we have $\overline{\boldsymbol{B}_\alpha^\circ} = \boldsymbol{B}_\alpha$ w.r.t. the subspace topology on ∂T. More generally, the same holds for each element of the subdivision $\mathcal{C}_k^{(1)}$ defined in* (1.21) *for $k \geq 1$.*

PROOF. The ambient space in this proof is ∂T. Recall first that by (1.6) the collection $\{\boldsymbol{B}_\gamma;\, \gamma \in \mathcal{S}\}$ is a finite collection of compact sets which covers ∂T. Thus for each $\alpha \in \mathcal{S}$ the boundary $\partial_{\partial T}\boldsymbol{B}_\alpha$ is covered by $\bigcup_{\gamma\neq\alpha} \boldsymbol{B}_\gamma$ which implies that

$$\partial_{\partial T}\boldsymbol{B}_\alpha \subset L_\alpha. \tag{1.37}$$

By Proposition 1.38, L_α is a finite union of arcs (having topological dimension 1). Thus Lemma 1.39 implies that $\dim(\partial_{\partial T}\boldsymbol{B}_\alpha) \leq 1$. On the other hand, since ∂T forms a cut of $\mathbb{R}^3$, we have $\dim(\partial T) \geq 2$ by [**49**, §59, II, Theorem 1]. Therefore, by Lemma 1.39 (2) there exists $\beta \in \mathcal{S}$ such that $\dim(\boldsymbol{B}_\beta) \geq 2$. Since $G(\mathcal{S})$ is strongly connected, the same is true for each $\beta \in \mathcal{S}$ by Lemma 1.39 (1). Now choose $\varepsilon > 0$ and $x \in \boldsymbol{B}_\alpha$ arbitrary. Subdivide $\boldsymbol{B}_\alpha$ according to the set equation (1.19) for k large enough to yield the existence of $X = M^{-k+1}(\boldsymbol{B}_\beta + a) \in \mathcal{C}_k(\alpha)$ with $\beta \in \mathcal{S}$ and $a \in \mathbb{Z}^3$ such that X is a subtile of $\boldsymbol{B}_\alpha$ with diameter less than ε and $x \in X$. As $X \subset \boldsymbol{B}_\alpha$ with $\dim(X) \geq 2$ and $\dim(\partial_{\partial T}\boldsymbol{B}_\alpha) \leq 1$ there is a point $y \in X$ with $y \in \boldsymbol{B}_\alpha^\circ$. Since ε was arbitrary, y can be chosen arbitrarily close to x. This proves the result for $\boldsymbol{B}_\alpha$.

The assertion for the elements of the subdivisions $\mathcal{C}_k(\alpha)$, $k \geq 1$, follows by the same argument. Just note that $\mathcal{C}_k^{(1)}$ is a finite collection of compact sets covering ∂T. Thus for each $X \in \mathcal{C}_k^{(1)}$ we have

$$\partial_{\partial T}X \subset \bigcup_{Y \in \mathcal{C}_k^{(1)}\setminus\{X\}} X \cap Y \tag{1.38}$$

and we may continue in the same way as in the special case. □

LEMMA 1.41. *For $\alpha \in \mathcal{S}$, we have $\partial_{\partial T}\boldsymbol{B}_\alpha = L_\alpha$.*

PROOF. The ambient space in this proof is ∂T. Let $\mathcal{B}(x,\delta) = \{y \in \partial T;\, |x-y| < \delta\}$. The fact that $\partial_{\partial T}\boldsymbol{B}_\alpha \subset L_\alpha$ follows from (1.37). To prove the reverse inclusion, suppose that for some $\beta \in \mathcal{S}$ with $\{\alpha,\beta\} \in G_2(\mathcal{S})$ there exists $x \in \boldsymbol{B}_{\alpha,\beta} \setminus \partial_{\partial T}\boldsymbol{B}_\alpha$. Since $\boldsymbol{B}_{\alpha,\beta} \subset \boldsymbol{B}_\alpha$ this implies that $x \in \boldsymbol{B}_\alpha^\circ$ and, hence, there exists $\delta > 0$ with $\mathcal{B}(x,\delta) \subset \boldsymbol{B}_\alpha$. Since $\boldsymbol{B}_{\alpha,\beta} \subset \boldsymbol{B}_\beta$, we also have $x \in \boldsymbol{B}_\beta$ and by Lemma 1.40 there exists $y \in \boldsymbol{B}_\beta^\circ \cap \mathcal{B}(x,\delta)$. Thus there exists $\delta' > 0$ such that $\mathcal{B}(y,\delta') \subset \boldsymbol{B}_\beta \cap \mathcal{B}(x,\delta)$. This implies $\mathcal{B}(y,\delta') \subset \boldsymbol{B}_\alpha \cap \boldsymbol{B}_\beta = \boldsymbol{B}_{\alpha,\beta}$. By Proposition 1.38, $\boldsymbol{B}_{\alpha,\beta}$ is a simple arc for each vertex $\{\alpha,\beta\}$ in $G_2(\mathcal{S})$ which cannot contain a ball in ∂T by a dimension theoretical argument analogous to the one in the proof of Lemma 1.40. This contradiction finishes the proof. □

Together with the proof of Proposition 1.38, Lemma 1.41 immediately yields the following result.

PROPOSITION 1.42. *Let $T = T(M,\mathcal{D})$ be an ABC-tile with* 14 *neighbors. For each $\alpha \in \mathcal{S}$ the boundary $\partial_{\partial T}\boldsymbol{B}_\alpha$ is a simple closed curve.*

1.3.5. Topological characterization of 2-fold intersections and of the boundary of T. We start with a sequence of partitionings for ∂T. To construct this sequence, for $\alpha^{(0)} \in G(\mathcal{S})$, let

(1.39)
$$\mathcal{Q}_k(\alpha^{(0)}) = \{f_{d_1 d_2 \dots d_{k-1}}(\boldsymbol{B}_{\alpha^{(k-1)}})^\circ;\ \alpha^{(0)} \xrightarrow{d_1} \alpha^{(1)} \xrightarrow{d_2} \cdots \xrightarrow{d_{k-1}} \alpha^{(k-1)} \in G(\mathcal{S})\} \quad (k \geq 1),$$

where the interior K° of a set K is taken w.r.t. the subspace topology on ∂T. Using (1.39) we define the sequence of collections $(\mathcal{Q}_k)_{k\geq 0}$ by

$$\begin{aligned} \mathcal{Q}_0 &= \{\partial T\}, \\ \mathcal{Q}_k &= \bigcup_{\alpha \in G(\mathcal{S})} \mathcal{Q}_k(\alpha) \quad (k \geq 1). \end{aligned} \tag{1.40}$$

LEMMA 1.43. *The sequence $(\mathcal{Q}_k)_{k\geq 1}$ in (1.40) is a decreasing sequence of regular partitionings of ∂T.*

PROOF. Throughout this proof ∂T is our ambient space. We claim that $\mathcal{Q}_k$ is a partitioning of ∂T for every $k \geq 1$. To prove this claim fix $k \geq 1$. Firstly, the closure of the union of all elements in $\mathcal{Q}_k$ is ∂T by Lemma 1.40, (1.6), and the set equation (1.18). Secondly, each element of $\mathcal{Q}_k$ has the form $f_{d_1 \dots d_{k-1}}(\boldsymbol{B}_{\alpha^{(k-1)}})^\circ$, and, hence, is open. Thirdly we have to show that the elements of $\mathcal{Q}_k$ are mutually disjoint. Suppose that this is wrong. Then there exist $f_{d_1 \dots d_{k-1}}(\boldsymbol{B}_{\alpha^{(k-1)}})$ and $f_{d'_1 \dots d'_{k-1}}(\boldsymbol{B}_{\alpha'^{(k-1)}})$ whose intersection X has nonempty interior. By arguing as in the proof of Lemma 1.40 this implies that $\dim(X) \geq 2$. However, by definition, X is a shrinked copy of an ℓ-fold intersection for some $\ell \geq 2$. More precisely, multiplying X by M^{k-1} and shifting it appropriately we see that X is homeomorphic to $\boldsymbol{B}_{\boldsymbol{\beta}}$ for some $\boldsymbol{\beta} \in G_\ell(\mathcal{S})$ with $\ell \geq 2$. Thus X is homeomorphic to an arc or to a point by Proposition 1.38 and Lemma 1.28 and, hence, $\dim(X) \leq 1$. This contradiction proves mutual disjointness of the elements of $\mathcal{Q}_k$. Summing up, the claim is established.

Next we will check that $(\mathcal{Q}_k)_{k\geq 1}$ is a decreasing sequence. First, we show that $\mathcal{Q}_{k+1}$ is a refinement of $\mathcal{Q}_k$ for each $k \geq 1$. Indeed, by the set equation (1.18) the closure $f_{d_1 \dots d_{k-1} d_k}(\boldsymbol{B}_{\alpha^{(k)}})$ of each element of $\mathcal{Q}_{k+1}$ is contained in the closure $f_{d_1 \dots d_{k-1}}(\boldsymbol{B}_{\alpha^{(k-1)}})$ of some element of $\mathcal{Q}_k$. Taking interiors we get the refinement assertion. The maximum of the diameters of the elements of $\mathcal{Q}_k$ approaches zero because f_d is a contraction for each $d \in \mathcal{D}$.

Finally, since the elements of $\mathcal{Q}_k$ are open sets, $\mathcal{Q}_k$ is regular for all $k \geq 1$ by Lemma 1.40. □

We now prove Theorem 1.1 (1) and (2). An important ingredient of this proof is the following characterization of a simple surface which is also due to Bing [**15**].

PROPOSITION 1.44 (see [**15**, Theorem 9]). *A necessary and sufficient condition that a locally connected continuum $\mathcal{X}$ be a 2-sphere is that one of its decreasing sequences of regular partitionings $\mathcal{Q}_1, \mathcal{Q}_2, \dots$ have the following properties:*

1. *The boundary of each element of $\mathcal{Q}_k$ is a simple closed curve.*
2. *The intersection of the boundaries of 3 elements of $\mathcal{Q}_k$ contains no arc.*
3. *If U is an element of $\mathcal{Q}_{k-1}$ (take $U = \mathcal{X}$ if $k = 1$) the elements of $\mathcal{Q}_k$ in U may be ordered as $U_1, U_2, \dots, U_n$ so that the boundary of U_j, which*

we denote by ∂U_j, intersects $\partial U \cup \partial U_1 \cup \cdots \cup \partial U_{j-1}$ in a nondegenerate connected set.

The following result shows that the boundary operator $\partial_{\partial T}$ commutes with certain affine maps.

LEMMA 1.45. *Let $f_{d_1 \dots d_{k-1}}(\boldsymbol{B}_\alpha)^\circ \in \mathcal{Q}_k$ for some $k \geq 1$. Then in the ambient space ∂T we have*

$$f_{d_1 \dots d_{k-1}}(\partial_{\partial T}(\boldsymbol{B}_\alpha)) = \partial_{\partial T}(f_{d_1 \dots d_{k-1}}(\boldsymbol{B}_\alpha)) = \partial_{\partial T}(f_{d_1 \dots d_{k-1}}(\boldsymbol{B}_\alpha)^\circ). \tag{1.41}$$

PROOF. Since different spaces play a role in this proof we will always emphasize w.r.t. which space closures, interiors, and boundaries will be taken.

In (1.41) closures and interiors are taken in ∂T. Thus the second identity in (1.41) is a consequence of Lemma 1.40.

To prove the first identity, let $f = f_{d_1 \dots d_{k-1}}$ and $Y = f(\boldsymbol{B}_\alpha)^\circ$ (interior is taken in ∂T) for convenience. As $Y \in \mathcal{Q}_k$, there is $\alpha' \in \mathcal{S}$ such that $Y \subset \boldsymbol{B}_{\alpha'} \subset \partial T$ (boundary is taken in $\mathbb{R}^3$). Thus there are $\beta, \beta' \in \mathbb{Z}^3$ such that $Y = (U \cap V)^\circ$ (interior is taken in ∂T) with $U := M^{-k+1}(T + \beta) \subset T$ and $V := M^{-k+1}(T + \beta') \subset \overline{\mathbb{R}^3 \setminus T}$ (closure is taken in $\mathbb{R}^3$). Then $U = f(T)$ and $Y \subset \partial U$ (boundary is taken in $\mathbb{R}^3$). Since f is a homeomorphism satisfying $f(\partial T) = \partial U$ (boundaries are taken in $\mathbb{R}^3$), we have $f(\partial_{\partial T}(\boldsymbol{B}_\alpha)) = \partial_{\partial U}(f(\boldsymbol{B}_\alpha)) = \partial_{\partial U}\overline{Y}$ (closure of Y is taken in ∂T). Thus it remains to prove

$$\partial_{\partial U}\overline{Y} = \partial_{\partial T}\overline{Y} \tag{1.42}$$

in order to establish the first identity in (1.41). Suppose first that $x \in \partial_{\partial U}\overline{Y}$.

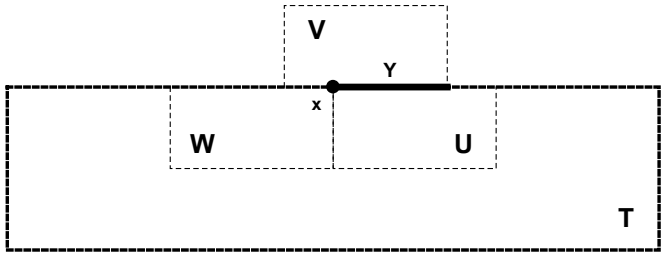

FIGURE 13. If we take a small neighborhood $\mathcal{N}$ of x we see that $\mathcal{N} \cap \partial T$ is different from $\mathcal{N} \cap \partial U$. This is what causes the difficulties in the proof. Note that T, U, V, W are 3-dimensional objects, Y is 2-dimensional and x is an arc. So this figure is just a schematic illustration of what is going on in a "slice" of T.

Then in each $\mathbb{R}^3$-neighborhood of x there is a point x' with $x' \in Y \subset \partial T$. On the other hand, by Lemma 1.41 (shifted by β and multiply by M^{-k+1}) there is $\gamma \in \mathbb{Z}^3 \setminus \{\beta, \beta'\}$ such that $x \in W := M^{-k+1}(T+\gamma)$ (see Figure 13 for an illustration). Summing up, we have $x \in U \cap V \cap W = M^{-k+1}(\boldsymbol{B}_{\beta'-\beta,\gamma-\beta} + \beta)$. Assume that $W = M^{-k+1}(T + \gamma) \subset T$ (the contrary case is treated in the same way), then $V \cap W = M^{-k+1}(\boldsymbol{B}_{\gamma-\beta'} + \beta') \subset \partial T$. Each element of any subdivision of $V \cap W$ has topological dimension at least 2 (see the proof of Lemma 1.40), while $U \cap V \cap W$ is an arc by Proposition 1.38 and, hence, has topological dimension 1. Thus we can

find an element $x'' \in V \cap W \setminus U \cap V \cap W = U \cap W \setminus U \cap V \subset \partial T \setminus \overline{Y}$ in each $\mathbb{R}^3$-neighborhood of x and, hence, $x \in \partial_{\partial T}\overline{Y}$.

Suppose now that $x \in \partial_{\partial T}\overline{Y}$. Then each $\mathbb{R}^3$-neighborhood of x there is a point x' with $x' \in Y \subset \partial U$. On the other hand, by (1.38) there is $\gamma \in \mathbb{Z}^3 \setminus \{\beta, \beta'\}$ such that $x \in U \cap V \cap W = M^{-k+1}(\boldsymbol{B}_{\beta'-\beta,\gamma-\beta} + \beta)$ with $W := M^{-k+1}(T + \gamma)$. Since $U \cap W = M^{-k+1}(\boldsymbol{B}_{\gamma-\beta} + \beta) \subset \partial U$ and each element of any subdivision of $U \cap W$ has topological dimension at least 2, while $U \cap V \cap W$ has topological dimension 1, as before we can find an element $x'' \in \partial U \setminus \overline{Y}$ in each $\mathbb{R}^3$-neighborhood of x. Thus $x \in \partial_{\partial U}\overline{Y}$.

Summing up we proved (1.42) and the result is established.

□

We can now establish the first two conditions of Proposition 1.44.

LEMMA 1.46.

(1) *The boundary $\partial_{\partial T}X$ is a simple closed curve for each $X \in \mathcal{Q}_k$ and each $k \geq 1$.*
(2) *The intersection of the boundary of three elements of $\mathcal{Q}_k$ contains no arc for each $k \geq 1$.*

PROOF. We start with proving assertion (1). Let $X \in \mathcal{Q}_k$. Then $\partial_{\partial T}X$ is an affine copy of $\partial_{\partial T}\boldsymbol{B}_\alpha$ for some $\alpha \in \mathcal{S}$ by Lemma 1.45. The assertion follows because $\partial_{\partial T}\boldsymbol{B}_\alpha$ is a simple closed curve by Proposition 1.42.

To prove assertion (2) we note that

$$\partial_{\partial T}\boldsymbol{B}^\circ_\alpha \cap \partial_{\partial T}\boldsymbol{B}^\circ_\beta \cap \partial_{\partial T}\boldsymbol{B}^\circ_\gamma \subset \boldsymbol{B}_\alpha \cap \boldsymbol{B}_\beta \cap \boldsymbol{B}_\gamma = \boldsymbol{B}_{\alpha,\beta,\gamma},$$

so the intersection of the boundary of three elements of $\mathcal{Q}_1$ is either a single point or the empty set since $\boldsymbol{B}_{\alpha,\beta,\gamma}$ contains at most one point. The same is true for $\mathcal{Q}_k$ because triple intersections of boundaries of elements in $\mathcal{Q}_k$ are just affine images of triple intersections of boundaries of elements in $\mathcal{Q}_1$. □

By the above lemma, we know that the sequence of partitionings $(\mathcal{Q}_k)_{k\geq 1}$ satisfies the first two conditions of Proposition 1.44. It remains to check the third condition.

For a fixed $\boldsymbol{B}_\alpha$, $\alpha \in \mathcal{S}$, it is easy to determine the *neighbors of $\boldsymbol{B}_\alpha$ in ∂T*, *i.e.*, the elements $\boldsymbol{B}_\beta$ with $\boldsymbol{B}_{\alpha,\beta} \neq \emptyset$. Indeed, in view of Lemma 1.41 we know the neighbors of $\boldsymbol{B}_\alpha$ in ∂T immediately from the right side of the identities in (1.26). This information allows to construct the Hata graph of $\{\boldsymbol{B}_\alpha;\ \alpha \in \mathcal{S}\}$ which we denote by $H(\mathcal{S})$. This graph is depicted in Figure 14. We give an order to the 2-fold intersections $\boldsymbol{B}_\alpha$ by setting $\boldsymbol{O}_i := \boldsymbol{B}_{\alpha_i}$ $(1 \leq i \leq 14)$ according to the right side of Figure 14. We have the following lemma.

LEMMA 1.47. *Let ∂T be our ambient space. Then*

$$\partial\boldsymbol{O}_i \cap (\partial\boldsymbol{O}_1 \cup \partial\boldsymbol{O}_2 \cup \cdots \cup \partial\boldsymbol{O}_{i-1})$$

is a nondegenerate connected set for each $i \in \{2, \ldots, 14\}$.

PROOF. Let $\boldsymbol{O}_{j,k} := \boldsymbol{O}_j \cap \boldsymbol{O}_k$ $(1 \leq j, k \leq 14)$. First, by Lemma 1.41 the set

$$\boldsymbol{A}_i := \partial\boldsymbol{O}_i \cap (\partial\boldsymbol{O}_1 \cup \partial\boldsymbol{O}_2 \cup \cdots \cup \partial\boldsymbol{O}_{i-1}) = \boldsymbol{O}_{i,1} \cup \boldsymbol{O}_{i,2} \cup \cdots \cup \boldsymbol{O}_{i,i-1}.$$

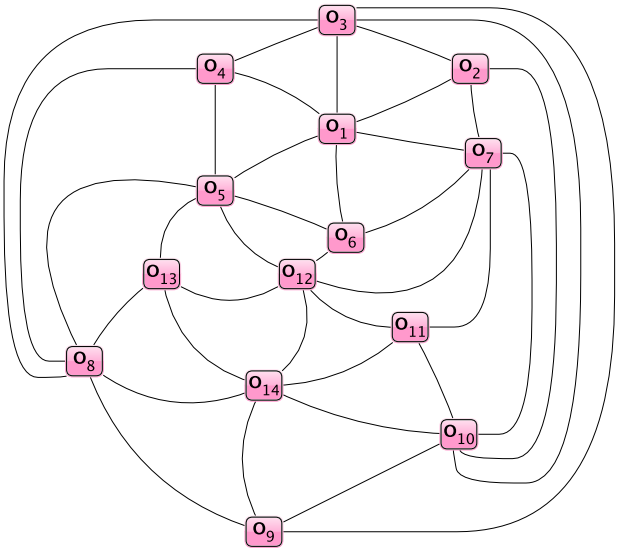

Vertex	Odered name
$\boldsymbol{B}_{\{\overline{Q-P}\}}$	$\boldsymbol{O}_1$
$\boldsymbol{B}_{\{N-Q+P\}}$	$\boldsymbol{O}_2$
$\boldsymbol{B}_{\{N-Q\}}$	$\boldsymbol{O}_3$
$\boldsymbol{B}_{\overline{Q}}$	$\boldsymbol{O}_4$
$\boldsymbol{B}_{\overline{N}}$	$\boldsymbol{O}_5$
$\boldsymbol{B}_{\{\overline{N-P}\}}$	$\boldsymbol{O}_6$
$\boldsymbol{B}_{P}$	$\boldsymbol{O}_7$
$\boldsymbol{B}_{\overline{P}}$	$\boldsymbol{O}_8$
$\boldsymbol{B}_{\{N-P\}}$	$\boldsymbol{O}_9$
$\boldsymbol{B}_{N}$	$\boldsymbol{O}_{10}$
$\boldsymbol{B}_{Q}$	$\boldsymbol{O}_{11}$
$\boldsymbol{B}_{\{\overline{N-Q}\}}$	$\boldsymbol{O}_{12}$
$\boldsymbol{B}_{\{\overline{N-Q+P}\}}$	$\boldsymbol{O}_{13}$
$\boldsymbol{B}_{\{Q-P\}}$	$\boldsymbol{O}_{14}$

FIGURE 14. The left hand side figure is the Hata graph $H(\mathcal{S})$ and the table on the right hand side lists the order of the vertices $\{\boldsymbol{B}_\alpha;\ \alpha \in \mathcal{S}\}$.

From the Hata graph $H(\mathcal{S})$, we can read off which of the sets $\boldsymbol{O}_{j,k}$ is nonempty. Together with the table in Figure 14 this information leads to the following identities.

$$
\begin{aligned}
\boldsymbol{A}_2 &= \boldsymbol{O}_{2,1} = \boldsymbol{B}_{\left\{\substack{\overline{Q-P}\\ N-Q+P}\right\}},\\
\boldsymbol{A}_3 &= \boldsymbol{O}_{3,1} \cup \boldsymbol{O}_{3,2} = \boldsymbol{B}_{\left\{\substack{\overline{Q-P}\\ N-Q}\right\}} \cup \boldsymbol{B}_{\left\{\substack{N-Q\\ N-Q+P}\right\}},\\
\boldsymbol{A}_4 &= \boldsymbol{O}_{4,1} \cup \boldsymbol{O}_{4,2} \cup \boldsymbol{O}_{4,3} = \boldsymbol{O}_{4,1} \cup \boldsymbol{O}_{4,3} = \boldsymbol{B}_{\left\{\substack{\overline{Q}\\ N-Q}\right\}} \cup \boldsymbol{B}_{\left\{\substack{\overline{Q}\\ \overline{Q-P}}\right\}},\\
\boldsymbol{A}_5 &= \boldsymbol{O}_{5,1} \cup \cdots \cup \boldsymbol{O}_{5,4} = \boldsymbol{O}_{5,4} \cup \boldsymbol{O}_{5,1} = \boldsymbol{B}_{\left\{\substack{\overline{N}\\ \overline{Q}}\right\}} \cup \boldsymbol{B}_{\left\{\substack{\overline{N}\\ \overline{Q-P}}\right\}},\\
\boldsymbol{A}_6 &= \boldsymbol{O}_{6,1} \cup \cdots \cup \boldsymbol{O}_{6,5} = \boldsymbol{O}_{6,1} \cup \boldsymbol{O}_{6,5} = \boldsymbol{B}_{\left\{\substack{\overline{N-P}\\ \overline{Q-P}}\right\}} \cup \boldsymbol{B}_{\left\{\substack{\overline{N}\\ \overline{N-P}}\right\}},\\
\boldsymbol{A}_7 &= \boldsymbol{O}_{7,1} \cup \cdots \cup \boldsymbol{O}_{7,6} = \boldsymbol{O}_{7,6} \cup \boldsymbol{O}_{7,1} \cup \boldsymbol{O}_{7,2} = \boldsymbol{B}_{\left\{\substack{\overline{N-P}\\ P}\right\}} \cup \boldsymbol{B}_{\left\{\substack{\overline{Q-P}\\ P}\right\}} \cup \boldsymbol{B}_{\left\{\substack{P\\ N-Q+P}\right\}},\\
\boldsymbol{A}_8 &= \boldsymbol{O}_{8,1} \cup \cdots \cup \boldsymbol{O}_{8,7} = \boldsymbol{O}_{8,3} \cup \boldsymbol{O}_{8,4} \cup \boldsymbol{O}_{8,5} = \boldsymbol{B}_{\left\{\substack{\overline{P}\\ N-Q}\right\}} \cup \boldsymbol{B}_{\left\{\substack{\overline{P}\\ \overline{Q}}\right\}} \cup \boldsymbol{B}_{\left\{\substack{\overline{P}\\ \overline{N}}\right\}},\\
\boldsymbol{A}_9 &= \boldsymbol{O}_{9,1} \cup \cdots \cup \boldsymbol{O}_{9,8} = \boldsymbol{O}_{9,3} \cup \boldsymbol{O}_{9,8} = \boldsymbol{B}_{\left\{\substack{N-P\\ N-Q}\right\}} \cup \boldsymbol{B}_{\left\{\substack{N-P\\ \overline{P}}\right\}},\\
\boldsymbol{A}_{10} &= \boldsymbol{O}_{10,1} \cup \cdots \cup \boldsymbol{O}_{10,9} = \boldsymbol{O}_{10,7} \cup \boldsymbol{O}_{10,2} \cup \boldsymbol{O}_{10,3} \cup \boldsymbol{O}_{10,9}\\
&= \boldsymbol{B}_{\left\{\substack{N\\ P}\right\}} \cup \boldsymbol{B}_{\left\{\substack{N\\ N-Q+P}\right\}} \cup \boldsymbol{B}_{\left\{\substack{N\\ N-Q}\right\}} \cup \boldsymbol{B}_{\left\{\substack{N\\ N-P}\right\}},\\
\boldsymbol{A}_{11} &= \boldsymbol{O}_{11,1} \cup \cdots \cup \boldsymbol{O}_{11,10} = \boldsymbol{O}_{11,7} \cup \boldsymbol{O}_{11,10} = \boldsymbol{B}_{\left\{\substack{Q\\ P}\right\}} \cup \boldsymbol{B}_{\left\{\substack{Q\\ N}\right\}},\\
\boldsymbol{A}_{12} &= \boldsymbol{O}_{12,1} \cup \cdots \cup \boldsymbol{O}_{12,11} = \boldsymbol{O}_{12,5} \cup \boldsymbol{O}_{12,6} \cup \boldsymbol{O}_{12,7} \cup \boldsymbol{O}_{12,11}\\
&= \boldsymbol{B}_{\left\{\substack{\overline{N-Q}\\ \overline{N}}\right\}} \cup \boldsymbol{B}_{\left\{\substack{\overline{N-Q}\\ \overline{N-P}}\right\}} \cup \boldsymbol{B}_{\left\{\substack{\overline{N-Q}\\ P}\right\}} \cup \boldsymbol{B}_{\left\{\substack{\overline{N-Q}\\ Q}\right\}},\\
\boldsymbol{A}_{13} &= \boldsymbol{O}_{13,1} \cup \cdots \cup \boldsymbol{O}_{13,12} = \boldsymbol{O}_{13,8} \cup \boldsymbol{O}_{13,5} \cup \boldsymbol{O}_{13,12}\\
&= \boldsymbol{B}_{\left\{\substack{\overline{N-Q+P}\\ \overline{P}}\right\}} \cup \boldsymbol{B}_{\left\{\substack{\overline{N-Q+P}\\ \overline{N}}\right\}} \cup \boldsymbol{B}_{\left\{\substack{\overline{N-Q+P}\\ \overline{N-Q}}\right\}},\\
\boldsymbol{A}_{14} &= \boldsymbol{O}_{14,1} \cup \cdots \cup \boldsymbol{O}_{14,13} = \partial \boldsymbol{O}_{14}.
\end{aligned}
$$

We can now read off the graph $G_3(\mathcal{S})$ that $\boldsymbol{A}_i$ is connected for each $2 \leq i \leq 14$. The fact that it is nondegenerate follows because each 3-fold intersection is an arc by Proposition 1.38. □

Note that $\partial_{\partial T}\boldsymbol{O}_j^\circ = \partial_{\partial T}\boldsymbol{O}_j$ for $j \in \{1, \ldots, 14\}$ by Lemma 1.40 and $\partial_{\partial T}\partial T = \emptyset$. Thus Lemma 1.47 implies that $(\mathcal{Q}_k)_{k\geq 1}$ satisfies condition (3) of Proposition 1.44 for the case $k = 1$ (by setting $\mathcal{Q}_0 = \partial T$).

To show that Proposition 1.44 (3) is true for $k \geq 2$, we need the following results on intersections.

LEMMA 1.48. *Let $\alpha \in \mathcal{S}$, $1 \leq j \leq C-1$, and $j \leq i \leq C-1$, then*

(1) $\big(\boldsymbol{B}_\alpha + (i-j)P\big) \cap \big(\boldsymbol{B}_\alpha + iP\big) = \emptyset$ *and*
(2) $\big(\boldsymbol{B}_\alpha + (i-j)P\big) \cap \big(\boldsymbol{B}_{\alpha+P} + iP\big) = \emptyset$.

PROOF. Shifting by $-(i-j)P$, we see that $\big(\boldsymbol{B}_\alpha + (i-j)P\big) \cap \big(\boldsymbol{B}_\alpha + iP\big)$ is homeomorphic to $\boldsymbol{B}_{\alpha,jP,jP+\alpha}$. Looking at Figure 11, we see that $\{\alpha, jP, jP+\alpha\}$ is not a vertex of $G_3(\mathcal{S})$. Thus Lemma 1.28 yields (1). The second assertion follows in a similar way. □

LEMMA 1.49. *If $\alpha \in \{Q,\ N,\ N-Q+P,\ \overline{N-Q},\ \overline{Q-P},\ \overline{N-P}\}$, then*

(1) $\boldsymbol{B}_\alpha \cap \big(\boldsymbol{B}_{\alpha-P} + P\big) \neq \emptyset$ *and*
(2) $\boldsymbol{B}_\alpha \cap \boldsymbol{B}_{\alpha-P} \neq \emptyset$.

PROOF. Since $\boldsymbol{B}_\alpha \cap \big(\boldsymbol{B}_{\alpha-P} + P\big) = \boldsymbol{B}_{\alpha,P}$ and $\{\alpha, P\}$ is a vertex of $G_2(\mathcal{S})$ for each $\alpha \in \{Q,\ N,\ N-Q+P,\ \overline{N-Q},\ \overline{Q-P},\ \overline{N-P}\}$ (see Table 2), assertion (1) follows from Proposition 1.38. Assertion (2) is proved in the same way. □

With help of these lemmas we can prove that the subdivisions of $\boldsymbol{B}_\alpha$ have a linear order.

COROLLARY 1.50. *Each 2-fold intersection $\boldsymbol{B}_\alpha$, $\alpha \in \mathcal{S}$, can be generated by the following ordered set equations (we only need to give the equations for the following 7 elements of $\mathcal{S}$ by symmetry).*

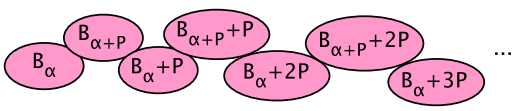

FIGURE 15. Order of the intersections on the right hand side of the identities in (1.43).

(1.43)

$$
\begin{aligned}
M\boldsymbol{B}_P &\triangleq \Big(\bigcup_{i=0}^{C-A-1} (\boldsymbol{B}_{Q-P} \cup \boldsymbol{B}_Q) + iP\Big) \cup \big(\boldsymbol{B}_{Q-P} + (C-A)P\big),\\
M\boldsymbol{B}_Q &\triangleq \Big(\bigcup_{i=0}^{C-B-1} (\boldsymbol{B}_{N-P} \cup \boldsymbol{B}_N) + iP\Big) \cup \big(\boldsymbol{B}_{N-P} + (C-B)P\big),\\
M\boldsymbol{B}_N &\triangleq \boldsymbol{B}_{\overline{P}},\\
M\boldsymbol{B}_{Q-P} &\triangleq \Big(\bigcup_{i=0}^{C-B+A-2} (\boldsymbol{B}_{N-Q} \cup \boldsymbol{B}_{N-Q+P}) + iP\Big) \cup (\boldsymbol{B}_{N-Q} + (C-B+A-1)P),\\
M\boldsymbol{B}_{N-Q+P} &\triangleq \Big(\bigcup_{i=0}^{B-A-1} (\boldsymbol{B}_{\overline{N-Q+P}} \cup \boldsymbol{B}_{\overline{N-Q}}) + iP\Big) \cup (\boldsymbol{B}_{\overline{N-Q+P}} + (B-A)P),\\
M\boldsymbol{B}_{N-P} &\triangleq \Big(\bigcup_{i=0}^{A-2} (\boldsymbol{B}_{\overline{Q}} \cup \boldsymbol{B}_{\overline{Q-P}}) + iP\Big) \cup (\boldsymbol{B}_{\overline{Q}} + (A-1)P),\\
M\boldsymbol{B}_{N-Q} &\triangleq \Big(\bigcup_{i=0}^{B-2} (\boldsymbol{B}_{\overline{N}} \cup B_{\overline{N-P}}) + iP\Big) \cup (\boldsymbol{B}_{\overline{N}} + (B-1)P).
\end{aligned}
$$

Here we use "$\triangleq$" to amphasize that the union on the right hand side is given by the order indicated in Figure 15 and that only the sets being adjacent in this order have nonempty intersection. Each of these intersections is an arc.

Proof. By Lemma 1.48 and Lemma 1.49, we conclude that the sets belonging to the union on the right hand side intersect if and only if they are adjacent in the order illustrated in Figure 15. □

Proposition 1.51. *Let $T = T(M, \mathcal{D})$ be an ABC-tile with 14 neighbors. The decreasing sequence of regular partitionings $(\mathcal{Q}_k)_{k\geq 1}$ of ∂T defined in (1.40) satisfies the conditions in Proposition 1.44. Hence, ∂T is a 2-sphere.*

Proof. Throughout this proof, ∂T is our ambient space. Conditions (1) and (2) of Proposition 1.44 are satisfied by Lemma 1.46. Lemma 1.47 and the remark after it shows that condition (3) of Proposition 1.44 is true for $k = 1$.

By Corollary 1.50, $\mathcal{Q}_k$ satisfies condition (3) of Proposition 1.44 for $k = 2$. Indeed, for each $\alpha \in \mathcal{S}$ we have $\boldsymbol{B}_\alpha^\circ \in \mathcal{Q}_1$ and $\boldsymbol{B}_\alpha$ is the union of $\{U_j\}_{j=1}^{\ell_\alpha}$, where MU_j is given by the right side of (1.43). By the linear ordering of the sets U_j proved in Corollary 1.50

$$
\partial U_j \cap (\partial \boldsymbol{B}_\alpha \cup \partial U_1 \cup \cdots \cup \partial U_{j-1}) = \begin{cases} \partial U_j \setminus (U_j \cap U_{j+1}), & j < \ell_\alpha, \\ \partial U_j, & j = \ell_\alpha. \end{cases}
$$

Since ∂U_j is a simple closed curve by Proposition 1.38 and $U_j \cap U_{j+1}$ is a subarc of this curve by Corollary 1.50, we conclude that $\partial U_j \cap (\partial \boldsymbol{B}_\alpha \cup \partial U_1 \cup \cdots \cup \partial U_{j-1})$ is an arc or a simple closed curve, and, hence, nondegenerate and connected.

By definition, each $U = (M^{-k+1}(\boldsymbol{B}_\alpha + a))^\circ \in \mathcal{Q}_k$ for $k \geq 2$ and $M^{-k+1}(\boldsymbol{B}_\alpha + a)$ is a contracted copy of $\boldsymbol{B}_\alpha$ for some $\alpha \in \mathcal{S}$ which is subdivided in the same way as $\boldsymbol{B}_\alpha$.

Moreover, the boundary each $(M^{-k+1}(\boldsymbol{B}_\alpha + a))^\circ \in \mathcal{Q}_k$ satisfies $\partial M^{-k+1}(\boldsymbol{B}_\alpha + a) = M^{-k+1}(\partial \boldsymbol{B}_\alpha + a)$ by Lemma 1.45.

Thus the subdivision of U also satisfies condition (3), because the subdivision of $\boldsymbol{B}_\alpha^\circ$ satisfies it. This implies that $\mathcal{Q}_k$ satisfies condition (3) of Proposition 1.44 for $k > 2$ as well. □

In view of the transformation introduced in Section 1.2.2, Proposition 1.51 proves Theorem 1.1 (1). Finally, Theorem 1.1 (2) is a consequence of the following proposition (again by Section 1.2.2).

PROPOSITION 1.52. *Let $T = T(M, \mathcal{D})$ be an ABC-tile with 14 neighbors. Assume that $\alpha \in \mathbb{Z}^3 \setminus \{0\}$. Then $\boldsymbol{B}_\alpha$ is homeomorphic to a closed disk if $\alpha \in \mathcal{S}$ and empty otherwise.*

PROOF. For $\alpha \in \mathcal{S}$, the intersection $\boldsymbol{B}_\alpha$ is a subset of the 2-sphere ∂T (by Proposition 1.51) whose boundary $\partial_{\partial T} \boldsymbol{B}_\alpha$ is homeomorphic to a simple closed curve (see Proposition 1.42). Thus $\boldsymbol{B}_\alpha$ is homeomorphic to a closed disk by the Schönflies Theorem. If $\alpha \notin \mathcal{S}$, then $\boldsymbol{B}_\alpha = \emptyset$ by the definition of $\mathcal{S}$ in (1.3). □

REMARK 1.53. The topological results of the present section go through as soon as the graphs $G_\ell(\mathcal{S})$ as well as some Hata graphs have certain properties. Verifying these properties for ABC-tiles was a nontrivial issue. However, all these properties can be checked for a given 3-dimensional self-affine tile $T = T(M, \mathcal{D})$ in finite time (regardless of the structure of the digit set). For instance, one has to check that the graphs $G_\ell(\mathcal{S})$ have 14, 36, and 24 vertices for $\ell = 1, 2, 3$, respectively, and that they are empty for $\ell \geq 4$. Moreover, the Hata graphs of the subdivision of 3-fold intersections should be path graphs and the Hata graphs of 2-fold intersections should have a structure that is suitable for applying Proposition 1.44. We will work this out in detail in a forthcoming paper.

1.4. Perspectives

We conclude the Chapter by mentioning some topics for further research. A first natural question is whether each self-affine tile satisfying the conditions of Theorem 1.1 is homeomorphic to a 3-ball. For a single example this can be checked by an algorithm given by Conner and Thuswaldner [**20**, Section 7]. However, we currently do not know how to do this for a whole class of tiles. Although Conner and Thuswaldner [**20**, Section 8.2] exhibited a self-affine tile whose boundary is a 2-sphere but which is itself not a 3-ball (a self-affine *Alexander horned sphere*), we conjecture the following to be true.

CONJECTURE 1.54. *A self-affine tile that satisfies the conditions of Theorem 1.1 is homeomorphic to a 3-ball.*

Besides that we think that using the results of Bing [**15**] and Kwun [**50**] one could prove more topological results for self-affine tiles (and attractors of iterated function systems in the sense of Hutchinson [**37**] in general). In particular, getting information on the topology of 3-dimensional Rauzy fractals (see *e.g.* [**28, 40, 84**]) would be interesting. Even topological results for higher dimensional self-affine tiles should be tractable by using modifications of our theory. However, particularly for

manifolds of dimension 4 and higher, according to Kwun's result, one has to deal with more complicated conditions which lead to new challenges.

Let T be a 2-dimensional self-affine tile. Recently, Akiyama and Loridant [**3**] provided Hölder continuous surjective mappings $h : \mathbb{S}^1 \to \partial T$ whose Hölder exponent, which is defined in terms of the Hausdorff dimension of ∂T, is optimal. This has been considered in a more general framework in Rao and Zhang [**76**]. We formulate the following problem for mappings from the 2-sphere to the boundary of a 3-dimensional self-affine tile.

PROBLEM 1.55. *For a* 3*-dimensional self-affine tile whose boundary is a* 2*-sphere find a homeomorphism* $h : \mathbb{S}^2 \to \partial T$ *which is Hölder continuous. What is the optimal Hölder exponent for such a homeomorphism?*

CHAPTER 2

Topology of a class of $p2$-crystallographic replication tiles

This chapter contains the article [**63**] with the same title. It is joint work with Benoit Loridant.

2.1. Introduction

A *crystallographic replication tile* with respect to a crystallographic group $\Gamma \subset \mathrm{Isom}(\mathbb{R}^n)$ is a nonempty compact set $T \subset \mathbb{R}^n$ that is the closure of its interior ($\overline{T^o} = T$) and satisfies the following properties.

(*i*) There is an expanding affine mapping $g : \mathbb{R}^n \to \mathbb{R}^n$ such that $g \circ \Gamma \circ g^{-1} \subset \Gamma$, and a finite collection $\mathcal{D} \subset \Gamma$ called *digit set* such that

$$g(T) = \bigcup_{\delta \in \mathcal{D}} \delta(T). \tag{2.1}$$

(*ii*) The family $\{\gamma(T); \gamma \in \Gamma\}$ is a *tiling* of $\mathbb{R}^n$. In other words, $\mathbb{R}^n = \bigcup_{\gamma\in\Gamma} \gamma(T)$ and $\gamma(T^o) \cap \gamma'(T^o) = \emptyset$ for distinct elements $\gamma, \gamma' \in \Gamma$.

There is a vast literature dealing with the lattice case, *i.e.*, when Γ is isomorphic to $\mathbb{Z}^n$: criteria exist to check basic properties, such as the tiling property [**52**], connectedness [**47**] or, in the planar case ($n = 2$), homeomorphy to a closed disk (*disk-likeness*). For instance, Bandt and Wang recognize disk-like self-affine lattice tiles by the number and location of the neighbors in the tiling [**12**], and Lau and Leung characterize all the disk-like tiles among the class of self-affine lattice tiles with collinear digit set [**55**]. A powerful tool in the study of topological properties is the *neighbor graph*: it gives a precise description of the boundary of the tile in terms of a *graph directed iterated function system* (*GIFS*). Akiyama and the first author elaborated a boundary parametrization method by making extensive use of the neighbor graph [**3**]. Algorithms allow to determine the neighbor graph for any given tile T [**80**], while it is usually difficult to deal with infinite classes of tiles. However, Akiyama and Thuswaldner computed the neighbor graph for an infinite class of planar self-affine lattice tiles associated with canonical number systems and used it to characterize the disk-like tiles among this class [**4**]. Methods relying on the neighbor graph were extended to crystallographic replication tiles in [**61, 62**].

If T is a crystallographic replication tile, the associated digit set $\mathcal{D}$ must be a complete set of right coset representatives of the subgroup $g \circ \Gamma \circ g^{-1}$. On the other hand, if $T \subset \mathbb{R}^n$ is a nonempty compact set satisfying (2.1) and $\mathcal{D}$ is a complete set of right coset representatives of the subgroup $g \circ \Gamma \circ g^{-1}$, Gelbrich proves that there is a subset $\Gamma' \subset \Gamma$ called *tiling set* such that the family $\{\gamma(T); \gamma \in \Gamma'\}$ is a tiling of $\mathbb{R}^n$. Under these conditions, it is not known in general whether the tiling set Γ' is a *subgroup* of the crystallographic group Γ, contrary to the lattice case

(see [**51**]). However, the first author defined in [**59**] the *crystallographic number systems*, in analogy to the canonical number systems from the lattice case (see *e.g.* [**42**]). This gives a way to produce classes of crystallographic replication tiles whose tiling set is the whole group Γ. An infinite class of examples given in [**59**] reads as follows. Let $p2$ be the planar crystallographic group generated by the translations $a(x,y) = (x+1,y)$, $b(x,y) = (x,y+1)$ and the π-rotation $c(x,y) = (-x,-y)$. Moreover, for $A, B \in \mathbb{Z}$ satisfying $|A| \leq B \geq 2$, let g be the expanding mapping defined on $\mathbb{R}^2$ by

$$g(x,y) = \begin{pmatrix} 0 & -B \\ 1 & -A \end{pmatrix} \begin{pmatrix} x \\ y \end{pmatrix} + \begin{pmatrix} \frac{B-1}{2} \\ 0 \end{pmatrix}. \tag{2.2}$$

Then the equation

$$g(T) = T \cup \left(T + \begin{pmatrix} 1 \\ 0 \end{pmatrix}\right) \cup \cdots \cup \left(T + \begin{pmatrix} B-2 \\ 0 \end{pmatrix}\right) \cup (-T) \tag{2.3}$$

defines a crystallographic replication tile whose tiling set is the whole group $p2$. This tiling property follows from the crystallographic number system property only for $A \geq -1$, as stated in [**59**], but we will deduce it for all values of A (see Proposition 2.6). Moreover, we will obtain topological information on T by comparing it with the self-affine lattice tile T^l defined by

$$\begin{pmatrix} 0 & -B \\ 1 & -A \end{pmatrix} T^\ell = T^\ell \cup \left(T^\ell + \begin{pmatrix} 1 \\ 0 \end{pmatrix}\right) \cup \cdots \cup \left(T^\ell + \begin{pmatrix} B-1 \\ 0 \end{pmatrix}\right). \tag{2.4}$$

In fact, for fixed A and B, the tile T^ℓ is a translation of $T \cup (-T)$, as shown in [**59**]. It follows from Leung and Lau's result [**55**] on self-affine tiles with collinear digit set that T^l is disk-like if and only if $2|A| - B < 3$. However, it was noticed in [**59**] that it can happen that T^ℓ is disk-like while T is not disk-like (see Figure 3 and Figure 24). The current paper will establish exactly for which parameters A, B this phenomenon occurs. For $2|A| - B < 3$, the associated lattice tile T^ℓ is disk-like and a result of Akiyama and Thuswaldner [**4**] on canonical number system tiles will allow us to estimate the set of neighbors of T. Finding out the disk-like tiles for parameters satisfying $2|A| - B < 3$ will then rely on the construction of the associated neighbor graphs for the whole class. For $2|A| - B \geq 3$, a purely topological argument will enable us to prove that the associated tiles are not disk-like.

Our results easily generalize to a broader class of crystallographic replication tiles, closely related to the class of self-affine tiles with consecutive collinear digit set as studied by Leung and Lau in [**55**]. Therefore, we are able to show the following classification theorem.

THEOREM 2.1. *Let $A, B \in \mathbb{Z}$ satisfying $|A| \leq B$ and $B \geq 2$, $M \in \mathbb{Z}^{2\times 2}$ a matrix with characteristic polynomial $x^2 + Ax + B$ and let $\mathbf{v} \in \mathbb{Z}^2$ such that $(\mathbf{v}, M\mathbf{v})$ are linearly independent. Let T be the crystallographic replication tile defined by*

$$MT + \frac{B-1}{2}\mathbf{v} = T \cup (T+\mathbf{v}) \cup (T+2\mathbf{v}) \cup \cdots \cup (T+(B-2)\mathbf{v}) \cup (-T). \tag{2.5}$$

Then T is disk-like if and only if $-2 \leq A \leq 1$ and $B \geq 2$ or $A = B = 2$.

This class is obtained from Leung and Lau's class by replacing the last translation digit $(B-1)\mathbf{v}$ by the π-rotation around the origin. In this way, the digit set remains

"almost consecutive" and the digit tiles $-T, T, T+\mathbf{v}, \ldots, T+(B-2)\mathbf{v}$ form a connected chain, so that T itself is still connected. The original expanding mapping $(x,y)^t \mapsto M(x,y)^t$ of Leung and Lau is adjusted by a translation vector $\frac{B-1}{2}\mathbf{v}$ in order for the digit set to be a complete set of right coset representatives of $g \circ p2 \circ g^{-1}$. Note that there might be other choices for the digit set, but they may not preserve the connectedness of the tiles (see [**56**]).

The result tells us that only a few tiles of the class are disk-like. For larger values of A, the tiles become thiner, so that adjacent neighbors from both sides of the tile happen to meet, creating cut points (local or global).

We will see in Lemma 2.4 that, to prove Theorem 2.1, it suffices to prove the result for T given by (2.3). Then the proof of the theorem will be completed by Theorem 2.18 and 2.21.

The paper is organized as follows. In Section 2.2, we give basic definitions on crystallographic groups and general properties of the class of crystallographic replication tiles under consideration. Sections 2.3 and 2.4 are devoted to the construction of the neighbor graphs for part of this class. They will be the main tool for our topological study. In Section 2.5 and Section 2.6, we characterize the disk-like tiles among our class for the range of parameters A, B satisfying $2|A| - B < 3$. In Section 2.7, we show that T is not disk-like for all parameters satisfying $2|A| - B \geq 3$. Finally, Section 2.8 illustrates the theorem by examples.

2.2. Preliminaries

2.2.1. Basic definitions. Let us recall some definitions and facts about planar tilings and crystallographic replication tiles (*crystiles* for short).

A tiling of $\mathbb{R}^2$ is a cover of the space by nonoverlapping sets, *i.e.*, such that the interiors of two distinct sets of the cover are disjoint. We consider tilings using a single tile T with $\overline{T^\circ} = T$ and a family Γ of isometries of $\mathbb{R}^2$ such that

$$\mathbb{R}^2 = \bigcup_{\gamma \in \Gamma} \gamma(T).$$

Assume that Γ contains id, the identity map of $\mathbb{R}^2$. Then $T = id(T)$ is called the *central tile* of the tiling. Given two isometries $\gamma, \gamma' \in \Gamma$ with $\gamma \neq \gamma'$, we say that $\gamma(T), \gamma'(T)$ (or simply γ, γ') are *neighbors* if $\gamma'(T) \cap \gamma(T) \neq \emptyset$. The neighbor set of T is the set of neighbors of id, *i.e.*,

$$\mathcal{S} = \{\gamma \in \Gamma \setminus \{id\}; \gamma(T) \cap T \neq \emptyset\}.$$

It is symmetric and it generates Γ. The tiles considered in this paper will be compact and the tilings locally finite, *i.e.*, every compact set intersects finitely many tiles of the tiling. Therefore, $\mathcal{S}$ will always be a finite set. The neighbor set of a tile $\gamma(T)$ ($\gamma \in \Gamma$) is equal to $\gamma\mathcal{S}$.

We will deal with families Γ of isometries that are *crystallographic groups* in dimension 2, *i.e.*, discrete cocompact subgroups Γ of the group $\mathrm{Isom}(\mathbb{R}^2)$ of all isometries on $\mathbb{R}^2$ with respect to some metric. By a theorem of Bieberbach (see [**18**]), a crystallographic group Γ in dimension 2 contains a group Λ of translations isomorphic to the lattice $\mathbb{Z}^2$, and the quotient group Γ/Λ, called *point group*, is

finite. There are 17 nonisomorphic such groups. However, in this paper, we will mainly consider the following crystallographic $p2$-groups.

DEFINITION 2.2. Let $a(x,y) = (x+1, y)$, $b(x,y) = (x, y+1)$, $c(x,y) = (-x,-y)$. Then a crystallographic *p2-group* is a group of isometries of $\mathbb{R}^2$ isomorphic to the subgroup of $\mathrm{Isom}(\mathbb{R}^2)$ generated by the translations a, b and the π-rotation c.

In particular, the standard $p2$-group Γ has the form

$$\Gamma = \{a^p b^q c^r; p, q \in \mathbb{Z}, r \in \{0,1\}\}. \tag{2.6}$$

We will call a tiling with respect to a $p2$-group a *p2-tiling*, and a tiling with respect to a lattice group (*i.e.*, for which the point group only contains the class of the identity map of $\mathbb{R}^2$) a *lattice tiling*.

We will be concerned with self-replicating tiles constructed in the following way. We refer the reader to [**30, 62**] for further information about these tiles.

DEFINITION 2.3. A planar *crystallographic replication tile* with respect to a crystallographic group Γ is a compact nonempty set $T \subset \mathbb{R}^2$ with the following properties:

- The family $\{\gamma(T); \gamma \in \Gamma\}$ is a tiling of $\mathbb{R}^2$.
- There is an expanding affine map $g : \mathbb{R}^2 \longrightarrow \mathbb{R}^2$ such that $g \circ \Gamma \circ g^{-1} \subset \Gamma$ and there exists a finite collection $\mathcal{D} \subset \Gamma$ called *digit set* such that (2.1) is satisfied.

2.2.2. Lattice tiling and $p2$-tiling. Let Γ be the standard $p2$-group defined in (2.6). We recall that an expanding affine map g in $\mathbb{R}^n$ has the form $g(x) = Mx+t$, where $t \in \mathbb{R}^n$ and M is an $n \times n$ expanding matrix, *i.e.*, all its eigenvalues have modulus greater than 1.

We consider a special class of $p2$-crystallographic replication tiles, closely related to the class of self-affine tiles with collinear digit set studied by Leung and Lau in [**55**]. For $A, B \in \mathbb{Z}$, $B \geq 2$, let $M \in \mathbb{Z}^{2\times 2}$ be a matrix with characteristic polynomial $x^2 + Ax + B$. Then M is expanding if and only if $|A| \leq B$. Moreover, let $\mathbf{v} \in \mathbb{Z}^2$ such that $(\mathbf{v}, M\mathbf{v})$ are linearly independent. The purpose of this paper is to study the topology of the crystallographic replication tiles defined by (2.5). A change of coordinate system will simplify the proof of Theorem 2.1, as stated in the following lemma.

LEMMA 2.4. *Let $A, B \in \mathbb{Z}$ with $|A| \leq B$ and $B \geq 2$. Then the crystallographic replication tile defined by* (2.5) *is homeomorphic to the tile defined by* (2.3).

PROOF. The expanding matrices used in (2.5) and (2.3) are similar via the transfer matrix $C = (\mathbf{v}, M\mathbf{v})$. It follows that the tiles defined by these equations only differ from the linear transformation associated with C. □

From now on, given $A, B \in \mathbb{Z}$ satisfying $|A| \leq B$ and $B \geq 2$, we denote by g the expanding affine map (2.2), by $\mathcal{D}$ the digit set

$$\mathcal{D} = \{id, a, \ldots, a^{B-2}, c\} \tag{2.7}$$

where a, c are defined in Definition 2.2, and by $T = T(A, B)$ the associated tile satisfying (2.3), *i.e.*, $g(T) = \bigcup_{\delta\in\mathcal{D}} \delta(T)$.

The relation to self-affine tiles with collinear digit set reads as follows. Let

$$\mathcal{N} = \left\{ \begin{pmatrix} 0 \\ 0 \end{pmatrix}, \begin{pmatrix} 1 \\ 0 \end{pmatrix}, \dots, \begin{pmatrix} B-1 \\ 0 \end{pmatrix} \right\} \quad \text{and} \quad M = \begin{pmatrix} 0 & -B \\ 1 & -A \end{pmatrix}. \tag{2.8}$$

We denote by $T^\ell(A,B) = T^\ell$ the associated lattice tile satisfying (2.4), *i.e*, $MT^\ell = \bigcup_{d\in\mathcal{N}}(T^\ell + d)$.

LEMMA 2.5 ([**59**]). *We have*

$$T^\ell = T \cup (-T) + (M - I_2)^{-1} \begin{pmatrix} \frac{B-1}{2} \\ 0 \end{pmatrix}, \tag{2.9}$$

where I_2 is the 2×2 identity matrix.

In the rest of the Chapter, we denote the crystallographic tile and lattice tile associated with the above data $(p2, g, \mathcal{D})$ and $(\mathbb{Z}^2, M, \mathcal{N})$ by T and T^ℓ, respectively.

PROPOSITION 2.6. *T is a $p2$-crystallographic replication tile.*

PROOF. By a result of Gelbrich [**30**], since $\mathcal{D}$ is a complete set of right coset representatives of $g \circ \Gamma \circ g^{-1}$, we know that T has nonempty interior and the family $\{\gamma(T); \gamma \in \Gamma\}$ is a cover of $\mathbb{R}^2$. Thus we only need to prove that this cover is in fact a tiling of $\mathbb{R}^2$. For $A \geq -1$, the family $\{T^\ell + z; z \in \mathbb{Z}^2\}$ is a tiling of $\mathbb{R}^2$, since the tile T^ℓ is associated to a quadratic canonical number system (see *e.g.* [**4**]). This also holds for the tiles T^ℓ with $A \leq 0$, as it is mentioned in [**2**] that changing A to $-A$, for a fixed B, results in an isometric transformation for the associated tiles T^ℓ (see Equation (2.16)). Therefore, by Lemma 2.5, we just need to show that T and $c(T) = -T$ do not overlap. This follows from the fact that T has nonempty interior and satisfies the set equation (2.3). Indeed, each of the B sets on the right side of this equation has two-dimensional Lebesgue measure α/B, where $\alpha > 0$ is the two-dimensional Lebesgue measure of T. The total measure of the right side being equal to α, the sets can not overlap. □

Note that for $-1 \leq A \leq B$, the above proposition is also a consequence of the crystallographic number system property [**59**].

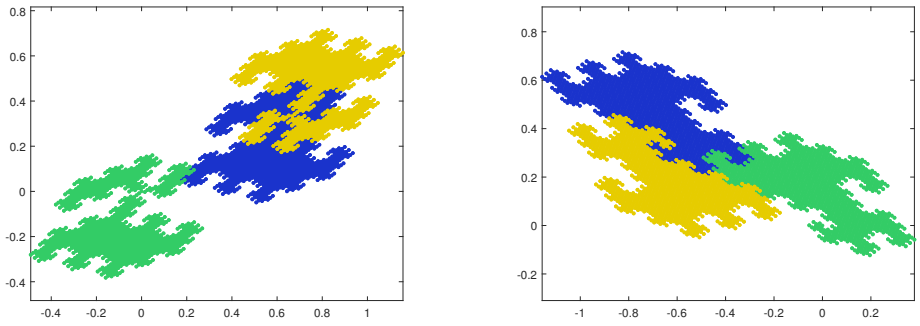

FIGURE 16. $B = 3$. For $A = 2$ on the left, T is not disk-like and for $A = -2$ on the right, T is disk-like

REMARK 2.7. In the above proof, we mentioned the simple relation (2.16) between the lattice tiles T^ℓ associated to A and $-A$. It turns out that no such easy relation can be found for the corresponding tiles T, and the topology may become different when changing A to $-A$ (see Figure 16, Section 2.6 for detail).

For the lattice data $(\mathbb{Z}^2, M, \mathcal{N})$, the following proposition is proved by Leung and Lau [**55**].

PROPOSITION 2.8. *Let A and B satisfy $|A| \leq B$ and $B \geq 2$. Then T^ℓ is homeomorphic to a closed disk if and only if $2|A| < B + 3$.*

2.2.3. Neighbor graph. Finally, we introduce an important tool for our study, namely, the neighbor graph.

DEFINITION 2.9. ([**62**]) For $\Omega \subset \Gamma$ we define the graph $G(\Omega)$ as follows. The states of $G(\Omega)$ are the elements of Ω, and there is an edge

$$\gamma \xrightarrow{\delta|\delta'} \gamma' \quad \text{iff } \delta^{-1} g \gamma g^{-1} \delta' = \gamma' \text{ with } \gamma, \gamma' \in \Omega \text{ and } \delta, \delta' \in \mathcal{D}.$$

The *neighbor graph* $G(\mathcal{S})$ is very important in the proof of the main result.

Recall that the neighbor set of T is defined by $\mathcal{S} = \{\gamma \in \Gamma \setminus \{id\};\ T \cap \gamma(T) \neq \emptyset\}$. Set $B_\gamma = T \cap \gamma(T)$ for $\gamma \in \Gamma$. The nonoverlapping property yields for the boundary of T that $\partial T = \bigcup_{\gamma \in \mathcal{S}} B_\gamma$. Moreover using the above notation, the sets B_γ satisfy the set equation ([**62**])

$$B_\gamma = \bigcup \Big\{ g^{-1}\delta(B_{\gamma'});\ \delta \in \mathcal{D}, \gamma' \in \mathcal{S}, \exists\ \delta' \in \mathcal{D}, \gamma \xrightarrow{\delta|\delta'} \gamma' \in G(\mathcal{S}) \Big\}.$$

The following characterization is from [**62**].

CHARACTERIZATION 2.10. Let t be a point in $\mathbb{R}^2$, $(\delta_j)_{j \in \mathbb{N}} \in \mathcal{D}^{\mathbb{N}}$ and $\gamma \in \mathcal{S}$. Then the following assertions are equivalent.

- $x = \lim_{n \to \infty} g^{-1}\delta_1 \dots g^{-1}\delta_n(t) \in B_\gamma$.
- There is an infinite walk in $G(\mathcal{S})$ of the shape

$$\gamma \xrightarrow{\delta_1|\delta_1'} \gamma_1 \xrightarrow{\delta_2|\delta_2'} \gamma_2 \xrightarrow{\delta_3|\delta_3'} \dots$$

  for some $\gamma_i \in \mathcal{S}$ and $\delta_i' \in \mathcal{D}$.

This means that for each $\gamma \in \mathcal{S}$, there is at least one infinite walk in $G(\mathcal{S})$ starting from the state γ. This will provide a method to construct the neighbor graph.

2.3. The neighbor set of T for $A \geq -1$ and $2A < B + 3$

For the sake of simplicity, in Sections 2.3, 2.4 and 2.5 we will restrict to the case $A \geq -1$ and $2A < B + 3$ and indicate in Section 2.6 the method to get the results for $A \leq -2$. Let T be the crystile and T^ℓ be the lattice tile defined by (2.3) and (2.4), and let $\mathcal{S}, \mathcal{S}^\ell$ be the neighbor sets of T, T^ℓ, respectively. $G(\mathcal{S})$ is the neighbor graph of T.

In this section, we will derive an "approximation" of the neighbor set $\mathcal{S}$ for $A \geq -1$, $2A < B + 3$ from the relationship between the neighbor set of T and the neighbor set of T^ℓ. Akiyama and Thuswaldner prove the following characterization of the neighbors of T^ℓ in [**4**].

PROPOSITION 2.11. *If $2A < B+3$ and $A \neq 0$, then $\sharp\mathcal{S}^\ell = 6$. In particular,*

(1) *If $A > 0$, then $\mathcal{S}^\ell = \{a^A b,\ a^{A-1}b,\ a,\ a^{-1},\ a^{-A}b^{-1},\ a^{-A+1}b^{-1}\}$;*
(2) *If $A = -1$, we have $\mathcal{S}^\ell = \{a^{-1}b,\ b,\ a,\ a^{-1},\ ab^{-1},\ b^{-1}\}$;*
(3) *If $A = 0$, we have $\mathcal{S}^\ell = \{a,\ a^{-1}, ab, a^{-1}b,\ ab^{-1}, a^{-1}b^{-1},\ b,\ b^{-1}\}$.*

The following lemma gives a first coarse estimate of the neighbor set of T in terms of the neighbor set of T^ℓ.

LEMMA 2.12. *$\mathcal{S}$ is a subset of $\mathcal{S}^\ell \cup \{c\} \cup \mathcal{S}^\ell c$, where $\mathcal{S}^\ell c = \{s \circ c;\ s \in \mathcal{S}^\ell\}$.*

PROOF. Using Lemma 2.5, we know that the lattice tile is a translation of the union $T \cup c(T)$. Then it is easy to see that all possible neighbors of T are included in the union of the neighbor set of T^ℓ, the π-rotation of the neighbor set of T^ℓ and the π-rotation itself. □

From the above lemma, we know an upper bound for the number of neighbors of the $p2$-tile T. We deduce from [**61**] a lower bound for this number.

LEMMA 2.13. *In a lattice tiling or a $p2$-tiling of the plane, each tile has at least six neighbors. This implies $\sharp\mathcal{S} \geq 6$ and $\sharp\mathcal{S}^\ell \geq 6$.*

We use Characterization 2.10 to refine the estimate of the neighbor set of T (compare with Lemma 2.12).

LEMMA 2.14. *Let $\mathcal{S}' = \mathcal{S}^\ell \cup \{c\} \cup \mathcal{S}^\ell c$. Then the following statements hold.*

(1) *For $A > 0$, $\mathcal{S} \subset \mathcal{S}' \setminus \{a^A b, a^{-A}b^{-1}, a^{-A}b^{-1}c\}$;*
(2) *For $A = -1$, $\mathcal{S} \subset \mathcal{S}' \setminus \{a^{-1}b,\ b,\ ab^{-1},\ b^{-1},\ ab^{-1}c,\ b^{-1}c\}$;*
(3) *For $A = 0$, $\mathcal{S} \subset \mathcal{S}' \setminus \{ab, a^{-1}b^{-1},\ ab^{-1}, a^{-1}b,\ b,\ b^{-1},\ a^{-1}b^{-1}c,\ ab^{-1}c,\ b^{-1}c\}$.*

In particular, $\mathcal{S}$ has at least 6 but not more than 10 elements.

PROOF. We know that $G(\mathcal{S})$ is a subgraph of $G(\mathcal{S}')$ by Lemma 2.12. The definition of the edges requires to calculate $g\mathcal{S}'g^{-1} = \{g\gamma g^{-1};\ \gamma \in \mathcal{S}'\}$ at first. Let p and q be arbitrary elements in $\mathbb{Z}$. Recall that g has the form (2.2). Then

$$ga^p b^q g^{-1}\begin{pmatrix} x \\ y \end{pmatrix} = \begin{pmatrix} x \\ y \end{pmatrix} + \begin{pmatrix} -qB \\ p - qA \end{pmatrix}, \tag{2.10}$$

$$ga^p b^q c g^{-1}\begin{pmatrix} x \\ y \end{pmatrix} = -\begin{pmatrix} x \\ y \end{pmatrix} + \begin{pmatrix} (1-q)B - 1 \\ p - qA \end{pmatrix}. \tag{2.11}$$

Thus the following relations hold:

$$ga^A b g^{-1} = a^{-B}, \quad ga^{-A}b^{-1}g^{-1} = a^B, \quad ga^{-A}b^{-1}cg^{-1} = a^{2B-1}c.$$

We claim that there are no edges starting from the states $a^A b,\ a^{-A}b^{-1}$, and $a^{-A}b^{-1}c$ for $A > 0$.

Indeed, for $\delta, \delta' \in \mathcal{D}$,

$$\delta^{-1}ga^A b g^{-1}\delta' = \delta^{-1}a^{-B}\delta' = \begin{cases} a^{-B}, & \delta = \delta' = id; \\ a^B, & \delta = \delta' = c; \\ a^{-B}c, & \delta = id,\ \delta' = c; \\ a^B c, & \delta = c,\ \delta' = id; \\ a^{B-p+q}, & \delta = a^p,\ \delta' = a^q,\ 1 \leq p, q \leq B-2. \end{cases}$$

Therefore, $\delta^{-1} g a^A b g^{-1} \delta'$ is not an element of $\mathcal{S}'$, which means that there is no edge starting from $a^A b$. The computation is similar for $a^{-A} b^{-1}$, $a^{-A} b^{-1} c$. Hence, we obtain that $a^A b$, $a^{-A} b^{-1}$, $a^{-A} b^{-1} c$ are not elements of $\mathcal{S}$ by Characterization 2.10, which proves Item (1).

For $A = -1$ and $A = 0$, similar computations as above show that there is no edge starting from the states removed from $\mathcal{S}'$ in Item (2) and Item (3).

Finally, by Lemma 2.13 and the above discussion, we obtain that the neighbor set of the crystile has at least 6 but not more than 10 elements because $\sharp\mathcal{S}' = 13$ by Lemma 2.12. □

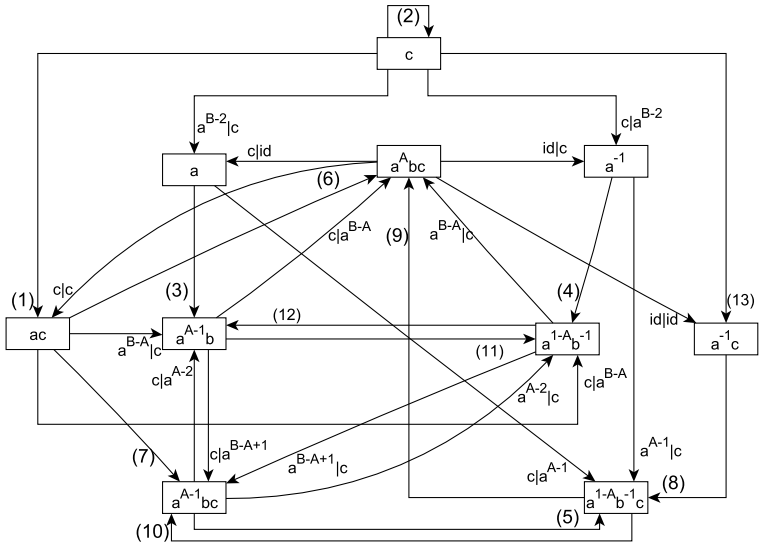

FIGURE 17. The graph $G(\mathcal{S}'')$ for $A \geq 3$ and $B \geq 5$ and $2A < B + 3$.

2.4. The neighbor graph of T for $A \geq -1$ and $2A < B + 3$

In this section, we explicitly construct the neighbor graph. Throughout the whole section, we restrict to the case $A \geq -1$ and $2A < B+3$. In Lemma 2.14, we denoted by $\mathcal{S}'$ the set $\mathcal{S}' = \mathcal{S}^\ell \cup \{c\} \cup \mathcal{S}^\ell c$. Now for $A > 0$, let $\mathcal{S}'' = \mathcal{S}' \setminus \{a^A b, a^{-A} b^{-1}, a^{-A} b^{-1} c\}$, that is,

$$\mathcal{S}'' = \{a^{A-1} b, a, a^{-1}, b^{-1}, a^{1-A} b^{-1}, c, a^A bc, a^{A-1} bc, ac, a^{-1} c, a^{1-A} b^{-1} c\}. \tag{2.12}$$

For $A = 0$, we set

$$\mathcal{S}'' = \{a, a^{-1}, c, ac, a^{-1} c, a^{-1} bc, bc, abc\}, \tag{2.13}$$

and for $A = -1$,

$$\mathcal{S}'' = \{a, a^{-1}, c, ac, a^{-1} c, a^{-1} bc, bc\}. \tag{2.14}$$

By Lemma 2.14, we know that $\mathcal{S} \subset \mathcal{S}''$. We call the graph $G(\mathcal{S}'')$ the *pseudo-neighbor graph*. Tables 1 and 2 show all information on $G(\mathcal{S}'')$. The last column indicates the parameters A, B for which these edges exist. Furthermore, the pseudo-neighbor

graphs for the cases $A \geq 3, B \geq 5$ are depicted in Figure 17. The edges named by $(1), \ldots, (13)$ are listed in Tables 1 and 2.

Edge	Labels $(\delta\|\delta')$	Name	Condition
$c \to ac$	$a^{B-2}\|id, a^{B-3}\|a, \ldots, id\|a^{B-2}$	(1)	$B \geq 2$ and $A \geq -1$
$c \to a^{-1}c$	$a^{B-2}\|a^2, a^{B-3}\|a^3, \ldots, a^2\|a^{B-2}$	(13)	$B \geq 4$ and $A \geq -1$
$c \to c$	$a^{B-2}\|a, a^{B-3}\|a^2, \ldots, a\|a^{B-2}$	(2)	$B \geq 3$ and $A \geq -1$
$c \to a^{-1}$	$c\|a^{B-2}$		$B \geq 2, A \geq -1$
$c \to a$	$a^{B-2}\|c$		$B \geq 2, A \geq -1$
$a \to a^{A-1}b$	$id\|a^{A-1}, a\|a^A, \ldots, a^{B-A-1}\|a^{B-2}$	(3)	$B \geq 2, A \geq 1$ and $(A, B) \neq (2, 2)$
$a^{-1} \to bc$	$c\|id$		$B \geq 3, \|A\| \leq 1$
$a \to a^{1-A}b^{-1}c$	$c\|a^{A-1}$		$B \geq 2, A \geq 1$ and $(A, B) \neq (2, 2)$
$a \to bc$	$id\|c$		$B \geq 2, \|A\| \leq 1$
$a^{A-1}bc \to abc$	$c\|c$		$B \geq 2, \|A\| \leq 1$
$a \to a^{-1}bc$	$a\|c$		$B \geq 3, A \in \{0, -1\}$
$a^{-1} \to a^{-1}bc$	$c\|a$		$B \geq 3, A \in \{0, -1\}$
$a^{-1} \to a^{1-A}b^{-1}$	$a^{A-1}\|id, a^A\|a, \ldots, a^{B-2}\|a^{B-A+1}$	(4)	$B \geq 2, A \geq 1$ and $(A, B) \neq (2, 2)$
$a^{-1} \to a^{1-A}b^{-1}c$	$a^{A-1}\|c$		$B \geq 2, A \geq 1$ and $(A, B) \neq (2, 2)$
$abc \to a^{-1}bc$	$id\|id$		$B \geq 2, A = 0$
$a^{A-1}bc \to a^{1-A}b^{-1}c$	$a^{A-2}\|id, a^{A-3}\|a, \ldots, id\|a^{A-2}$	(5)	$B \geq 2$ and $A \geq 2$
$a^{A-1}bc \to a^{A-1}b$	$c\|a^{A-2}$		$B \geq 2, A \geq 2$
$a^{A-1}bc \to a^{1-A}b^{-1}$	$a^{A-2}\|c$		$B \geq 2, A \geq 2$
$ac \to a^Abc$	$a^{B-A-1}\|id, a^{B-A-2}\|a, \ldots, id\|a^{B-A+1}$	(6)	$B \geq 2, A \geq 1$ and $(A, B) \neq (2, 2)$
$ac \to a^{-1}bc$	$a^{B-2}\|a^2, a^{B-3}\|a^3, \ldots, id\|a^{B-2}$	$(6)'$	$B \geq 4, A \in \{0, -1\}$
$ac \to abc$	$a^{B-2}\|id, a^{B-3}\|a, \ldots, id\|a^{B-2}$	(14)	$B \geq 2, A = 0$
$ac \to a^{A-1}bc$	$a^{B-A}\|id, a^{B-A-1}\|a, \ldots, id\|a^{B-A}$	(7)	$B \geq 2$ and $A \geq 2$

Table 1. Edges of $G(\mathcal{S}'')$ (Case $A \geq -1$ and $2A < B + 3$)

Edge	Labels $(\delta\|\delta')$	Name	Condition
$ac \to bc$	$a^{B-2}\|a, a^{B-3}\|a^2, \ldots, a\|a^{B-2}$	$(7)'$	$B \geq 3, \|A\| \leq 1$
$ac \to a^{A-1}b$	$a^{B-A}\|c$		$B \geq 2, A \geq 2$
$ac \to a^{1-A}b^{-1}$	$c\|a^{B-A}$		$B \geq 2, A \geq 2$
$a^Abc \to a^{-1}c$	$id\|id$		$B \geq 2, A \geq -1$
$a^Abc \to a$	$c\|id$		$B \geq 2, A \geq -1$
$a^Abc \to a^{-1}$	$id\|c$		$B \geq 2, A \geq -1$
$a^Abc \to ac$	$c\|c$		$B \geq 2, A \geq -1$
$bc \to a^{-1}bc$	$id\|id$		$B \geq 2, A = -1$
$a^{-1}c \to a^{1-A}b^{-1}c$	$a^{B-2}\|a^A, a^{B-3}\|a^{A+1}, \ldots, a^A\|a^{B-2}$	(8)	$B \geq A+2, A > 0$
$a^{-1}c \to a^{-1}bc$	$c\|c$		$B = 2,\ A = -1$
$a^{1-A}b^{-1}c \to a^Abc$	$a^{B-2}\|a^{B-A+1}, a^{B-3}\|a^{B-A+2}, \ldots, a^{B-A+1}\|a^{B-2}$	(9)	$B \geq 4$ and $A \geq 3$
$a^{1-A}b^{-1}c \to a^{A-1}bc$	$a^{B-2}\|a^{B-A+2}, a^{B-3}\|a^{B-A+3}, \ldots, a^{B-A+2}\|a^{B-2}$	(10)	$B \geq 6$ and $A \geq 4$
$a^{A-1}b \to a^{1-A}b^{-1}$	$id\|a^{B-A+1}, a\|a^{B-A+2}, \ldots, a^{A-3}\|a^{B-2}$	(11)	$B \geq 4$ and $A \geq 3$
$a^{A-1}b \to a^Abc$	$c\|a^{B-A}$		$B \geq 2$ and $A \geq 2$
$a^{A-1}b \to a^{A-1}bc$	$c\|a^{B-A+1}$		$B \geq 4$ and $A \geq 3$
$a^{1-A}b^{-1} \to a^{A-1}b$	$a^{B-A+1}\|id, a^{B-A+2}\|a, \ldots, a^{B-2}\|a^{A-3}$	(12)	$B \geq 4$ and $A \geq 3$
$a^{1-A}b^{-1} \to a^Abc$	$a^{B-A}\|c$		$B \geq 2$ and $A \geq 2$
$a^{1-A}b^{-1} \to a^{A-1}bc$	$a^{B-A+1}\|c$		$B \geq 4$ and $A \geq 3$

Table 2. Edges of $G(\mathcal{S}'')$ (Case $A \geq -1$ and $2A < B + 3$)

Since $\mathcal{S} \subset \mathcal{S}''$, it is clear that the neighbor graph $G(\mathcal{S})$ is a subgraph of the pseudo-neighbor graph. We will see that Characterization 2.10 will play an important role in the relationship between the neighbor graph $G(\mathcal{S})$ and the pseudo-neighbor graph $G(\mathcal{S}'')$.

THEOREM 2.15. *Let $\mathcal{S}$ be the neighbor set of T and $\mathcal{S}''$ be defined as in* (2.12), (2.13) *and* (2.14). *The following results hold for A, B satisfying $-1 \leq A \leq B$, $B \geq 2$ and $2A < B + 3$.*

(1) *For $A \geq 3$ and $B \geq 5$, $\mathcal{S} = \mathcal{S}''$.*
(2) *For $A = 3$ and $B = 4$, $\mathcal{S} = \mathcal{S}'' \setminus \{a^{-1}c\}$.*
(3) *For $A = 2$ and $B = 2$, $\mathcal{S} = \mathcal{S}'' \setminus \{a^{-1}c, a^{1-A}b^{-1}c, a, a^{-1}\}$.*
(4) *For $A = 2$ and $B \geq 3$, $\mathcal{S} = \mathcal{S}'' \setminus \{a^{-1}c, a^{1-A}b^{-1}c\}$.*

(5) *For* $A = 1$ *and* $B \geq 2$, $\mathcal{S} = \mathcal{S}'' \setminus \{a^{-1}c, a^{1-A}b^{-1}c, a^{A-1}b, a^{1-A}b^{-1}\}$.
(6) *For* $A = 0$ *and* $B \geq 2$, $\mathcal{S} = \{a,\ a^{-1},\ c,\ ac,\ a^{-1}bc,\ bc, abc\}$.
(7) *For* $A = -1$ *and* $B = 2$, $\mathcal{S} = \{a,\ a^{-1},\ c,\ a^{-1}c,\ a^{-1}bc,\ bc\}$;
For $A = -1$ *and* $B \geq 3$, $\mathcal{S} = \{a,\ a^{-1},\ c,\ ac,\ a^{-1}bc,\ bc\}$.

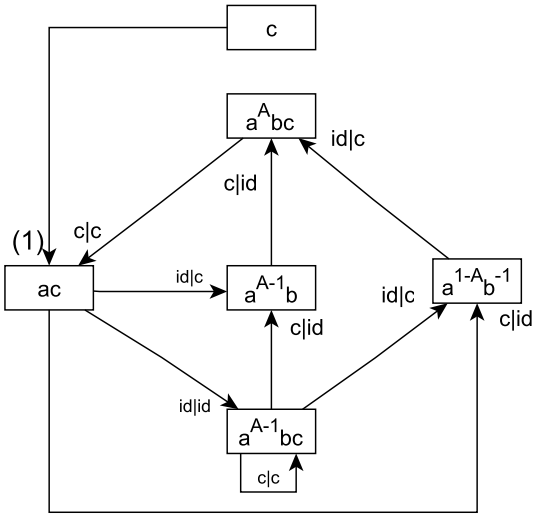

(a) Theorem 2.15, Case $A = 2, B = 2$

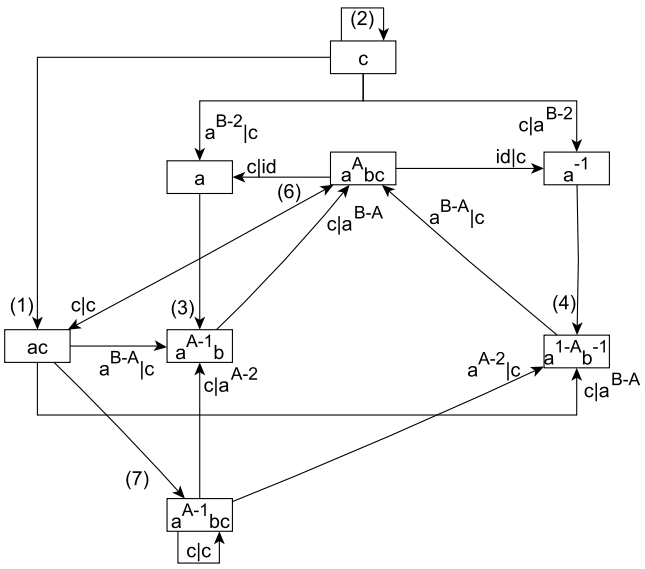

(b) Theorem 2.15, Case $A = 2, B \geq 3$

FIGURE 18. The neighbor graph $G(\mathcal{S})$ of T

PROOF. By Characterization 2.10, the neighbor graph $G(\mathcal{S})$ is obtained from the pseudo-neighbor graph $G(\mathcal{S}'')$ by deleting the states that are not the starting state of an infinite walk. For $A \geq 3, B \geq 5$, from Figure 17, it is clear that there

is an infinite walk starting from each state of $G(\mathcal{S}'')$. For $A = 3, B = 4$, from Table 1 and Table 2, we know that there is exactly one state $a^{-1}c$ from which there is no outgoing edge. For Item (3),(4),(5), and (6), see Figure 18(a), Figure 18(b), Figure 19 and Figure 21, respectively. For Item (7), it is easy to check that $a^{-1}c$ is the starting state of an infinite walk if and only if $B = 2$ and ac is the starting state of an infinite walk if and only if $B \geq 3$. Since the neighbor set has at least six elements by Lemma 2.13, we get the results of Item (7) (see Figure 20 for more details). □

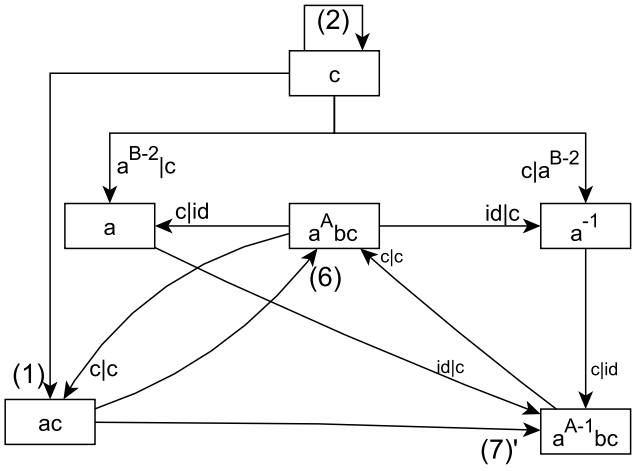

FIGURE 19. Theorem 2.15, Case $A = 1, B \geq 2$. We refer to Tables 1 and Table 2 for the conditions on the edges.

2.5. Characterization of the disk-like tiles for $A \geq -1$ and $2A < B + 3$

We are now in a position to study the topological properties of our family of $p2$-tiles under the conditions $A \geq -1$, $2A < B + 3$. We will characterize the disk-like tiles of the family under this condition. Loridant and Luo in [**61**] provided necessary and sufficient conditions for a $p2$-tile to be disk-like. Before stating the theorem, we need a definition.

DEFINITION 2.16. ([**61**]) If $\mathcal{P}$ and $\mathcal{F}$ are two sets of isometries in $\mathbb{R}^2$, we say that $\mathcal{P}$ is $\mathcal{F}$-connected iff for every disjoint pair (d, d') of elements in $\mathcal{P}$, there exist $n \geq 1$ and elements $d =: d_0, d_1, \ldots, d_{n-1}, d_n := d'$ of $\mathcal{P}$ such that $d_i^{-1} d_{i+1} \in \mathcal{F}$ for $i = 0, 1, \ldots, n-1$.

The following statement is from [**61**]. In fact, the necessary part is due to the classification of Grünbaum and Shephard [**33**].

PROPOSITION 2.17. *Let K be a crystile that tiles the plane by a $p2$-group. Let $\mathcal{F}$ be the corresponding digit set. Let a, b be translations, and c be a π-rotation.*

(1) *Suppose that the neighbor set $\mathcal{S}$ of K has six elements. Then K is disk-like iff $\mathcal{F}$ is $\mathcal{S}$-connected.*

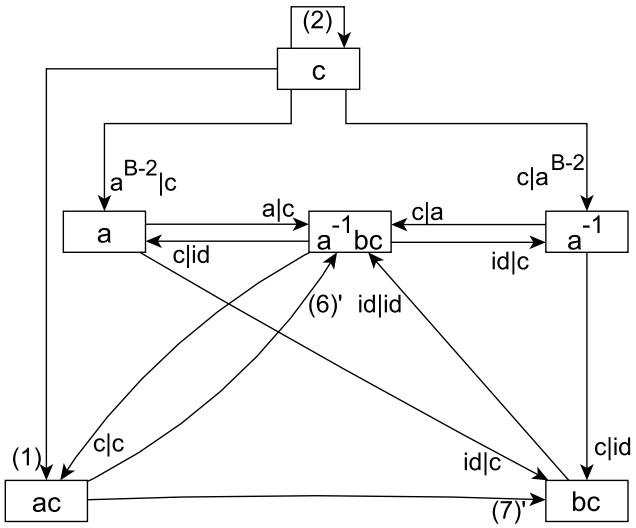

FIGURE 20. Theorem 2.15, case $A = -1, B \geq 3$. For the case $B = 2$, we only need to replace ac by $a^{-1}c$ and change the incoming and outgoing edges according to Tables 1 and Table 2.

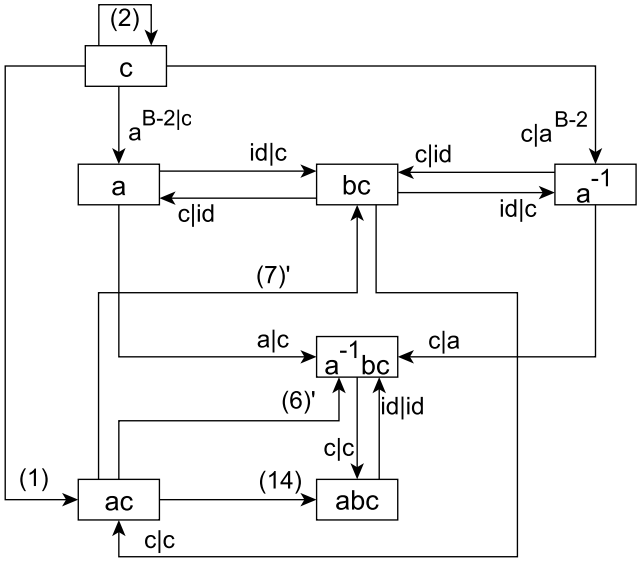

FIGURE 21. Theorem 2.15, the case $A = 0, B \geq 2$. We refer to Tables 1 and Table 2 for the conditions on the edges.

(2) *Suppose that the neighbor set $\mathcal{S}$ of K has seven elements*

$$\{b^{\pm 1}, c, bc, a^{-1}c, a^{-1}bc, a^{-1}b^{-1}c\}.$$

Then K is disk-like iff $\mathcal{F}$ is $\{b^{\pm 1}, c, bc, a^{-1}c\}$-connected.

(3) *Suppose that the neighbor set $\mathcal{S}$ of K has eight elements*

$$\{b^{\pm 1}, (a^{-1}b)^{\pm 1}, c, bc, ac, ab^{-1}c\}$$

$$(resp.\ \{b^{\pm 1}, c, bc, a^{-1}c, b^{-1}c, a^{-1}bc, a^{-1}b^{-1}c\}),$$

Then K is disk-like iff $\mathcal{F}$ is $\{c, bc, ac, ab^{-1}c\}$-(resp.$\{b^{\pm 1}, c, a^{-1}c\}-$) connected.

(4) *Suppose that the neighbor set $\mathcal{S}$ of K has twelve elements*

$$\{a^{\pm 1}, b^{\pm 1}, (ab)^{\pm 1}, c, a^{-1}c, bc, abc, a^{-1}bc, a^{-1}b^{-1}c\},$$

Then K is disk-like iff $\mathcal{F}$ is $\{c, a^{-1}c, bc\}$-connected.

Applying this result, we obtain the following theorem.

THEOREM 2.18. *Let $A, B \in \mathbb{Z}$ satisfy $-1 \leq A \leq B,\ B \geq 2$ and $2A < B+3$, and let T be the crystallographic replication tile defined by the data $(g, \mathcal{D})$ given in* (2.2) *and* (2.3)*. Then the following statements hold.*

(1) *If $A \in \{-1,\ 0,\ 1\}, B \geq 2$ or $A = 2,\ B = 2$, then T is disk-like.*
(2) *If $A \geq 2, B \geq 3$, then T is non-disk-like.*

PROOF. Let $\mathcal{S}$ be the neighbor set of T. By Theorem 2.15, we know that in the assumption of $A \in \{-1,\ 1\},\ B \geq 2$ and $A = 2, B = 2$, the neighbor sets of T all have six elements. Let us check the case $A = 1, B \geq 2$ by showing that $\mathcal{D}$ is $\mathcal{S}$-connected and applying Proposition 2.17 (1). Then $A = -1, B \geq 2$ and $A = 2, B = 2$ can be checked in the same way.

For $A = 1, B \geq 2$, the digit set is $\mathcal{D} = \{id, a, \ldots, a^{B-2}, c\}$ and the neighbor set is $\mathcal{S} = \{a, a^{-1}, c, abc, bc, ac\}$. It is easy to find that the disjoint pairs (d, d') in $\mathcal{D} \times \mathcal{D}$ are the following ones:

$$(id, a^{\ell}), (a^{\ell}, id), (id, c), (c, id), (a^k, a^{k'})(a^j, c), \text{or } (c, a^j), \tag{2.15}$$

where $\ell, k, k', j \in \{1, 2, \ldots, B-2\}$.

We will check the pair $(a^k, a^{k'})$ at first. If $k < k'$, then let $n = k' - k$, and

$$d_0 = a^k, d_1 = a^{k+1}, \ldots, d_{n-1} = a^{k'-1}, d_n = a^{k'}.$$

hence $d_i^{-1}d_{i+1} = a$ is in $\mathcal{S}$ for $0 \leq i \leq n-1$. If $k > k'$, $d_i^{-1}d_{i-1} = a^{-1}$ is also in $\mathcal{S}$ for $0 \leq i \leq n-1$. To check (id, a^{ℓ}) and (a^j, c), it suffices to check (id, a) and (a, c). It is clear for (id, a). For (a, c), let $n = 2$, and $d_0 = a,\ d_1 = id,\ d_2 = c$. Hence, we have proved that $\mathcal{D}$ is $\mathcal{S}$- connected. By Proposition 2.17 (1), T is disk-like.

For $A = 0$ and $B \geq 2$ and the neighbor set

$$\mathcal{S} = \{a, a^{-1}, c, a^{-1}bc, bc, ac, abc\}$$

has seven elements. By Proposition 2.17 (2), we need to prove that $\mathcal{D}$ is $\{a, a^{-1}, c, ac, bc\}$-connected. This is achieved in the same way as above.

We now prove Item (2). For $A = 2, B \geq 3$ and by Theorem 2.15, we know that

$$\mathcal{S} = \{a,\ a^{-1},\ ab,\ a^{-1}b^{-1},\ c,\ abc,\ a^2bc,\ ac\}.$$

Let $a' = a^2b, b' = ab$, then $\mathcal{S}$ has the form

$$\Upsilon := \{b',\ b'^{-1},\ a'^{-1}b',\ a'b'^{-1},\ c,\ b'c,\ a'c,\ a'b'^{-1}c\}$$

of Proposition 2.17 (3). However, it is easily checked that $\mathcal{D}$ is not $\{c, abc, ab^2c, ac\}$-connected. By Proposition 2.17 (3), T is not disk-like.

For $A \geq 3,\ B \geq 4$, we have $\sharp\mathcal{S} = 9$ if $A = 3, B = 4$, and $\sharp\mathcal{S} = 10$ if $A \geq 3, B \geq 5$ by Theorem 2.15. According to Grünbaum and Shephard's classification of isohedral

tillings (see [**33**, Sect. 6.2, p.285]), the cases in Proposition 2.17 are the only ones leading to disk-like $p2$-tiles in the plane. So T is non-disk-like for $A \ge 3, B \ge 4$. □

2.6. Characterization of the disk-like tiles for $A \le -2$ and $2|A| < B+3$

We now deal with the case $A \le -2$ and $2|A| < B+3$. Let us recall a statement in [**2**, Equation (2.11), p. 2177]. Let T^ℓ be the lattice tile associated with M and the digit set $\mathcal{N}$ (see (2.8)) and $\bar{T}^\ell$ the lattice tile associated with $\bar{M} = \begin{pmatrix} 0 & -B \\ 1 & A \end{pmatrix}$ and $\mathcal{N}$. Then we have

$$\bar{T}^\ell = \begin{pmatrix} -1 & 0 \\ 0 & 1 \end{pmatrix} T^\ell + \sum_{k=1}^{\infty} \bar{M}^{-2k} \begin{pmatrix} B-1 \\ 0 \end{pmatrix}. \tag{2.16}$$

It follows that T^ℓ and $\bar{T}^\ell$ have the same topology. It is remarkable that this does not hold for the associated crystiles T and $\bar{T}$, as is illustrated below.

By [**4**], we know all the information on the neighbor set of the lattice tile T^ℓ for $A \ge -1$, hence we can derive the neighbor set of $\bar{T}^\ell$ immediately.

LEMMA 2.19. *If $2A < B+3$ and $A > 0$, then the neighbor set of $\bar{T}^\ell$ is*

$$\{(-A,1),(-A+1,1),(-1,0),(1,0),(A,-1),(A-1,-1)\}, \tag{2.17}$$

or, using translation mappings rather than vectors,

$$\{a^{-A}b, a^{-A+1}b, a^{-1}, a, a^A b^{-1}, a^{A-1}b^{-1}\}. \tag{2.18}$$

PROOF. $\gamma = a^p b^q \in \Gamma$ $(p,q \in \mathbb{Z})$ is a neighbor of T^ℓ iff $T^\ell \cap \gamma(T^\ell) \ne \emptyset$. Let $\gamma' = a^{-p}b^q$, then this is equivalent to $\bar{T}^\ell \cap \gamma'(\bar{T}^\ell) \ne \emptyset$ by (2.16). Thus, using Proposition 2.11, we get the neighbor set (2.17) of $\bar{T}^\ell$. □

For $-1 \le A \le B \ge 2$, the data $(g, \mathcal{D}, p2)$ is a crystallographic number system, hence, the tiling group is the whole crystallographic group $p2$ [**59**]. It follows from Proposition 2.6 that this property still holds for $A \le -2$. Now, by Lemma 2.19, to obtain the neighbor set of $p2$-crystiles for $A \le -2$, we only need to repeat the methods in Section 2.3 and 2.4, dealing with similar estimates and computations. We come to the following theorem for $A \le -2$ (we do not reproduce the computations).

THEOREM 2.20. *Let $A, B \in \mathbb{Z}$ satisfy $2 \le -A \le B$ and $2|A| < B+3$, and let T be the crystallographic replication tile defined by the data $(g, \mathcal{D})$ given in* (2.2) *and* (2.3). *Then the following statements hold.*

(1) *For $A = -2$ and $B = 2$ or 3, the neighbor set of the crystile T is*
$$\mathcal{S} = \{a, a^{-1}, c, a^{-1}c, a^{-2}bc, a^{-1}bc\};$$

(2) *For $A = -2, B \ge 4$, the neighbor set of the crystile T is*
$$\mathcal{S} = \{a,\ a^{-1},\ c,\ ac,\ a^{-2}bc,\ a^{-1}bc\}.$$

(3) *For $A = -3, B = 4$, the neighbor set of the crystile T is*
$$\mathcal{S} = \{a,\ a^{-1},\ a^{-2}b,\ a^2b^{-1},\ c,\ a^{-1}c,\ a^{-2}bc,\ a^{-3}bc\}.$$

(4) *For $A = -3, B \ge 5$, the neighbor set of the crystile T is*
$$\mathcal{S} = \{a,\ a^{-1},\ a^{A+1}b,\ a^{-1-A}b^{-1},\ c,\ ac,\ a^{A+1}bc,\ a^Abc,\ a^{-1}c\}.$$

(5) *For $A \leq -4, B \geq 6$, the neighbor set of the crystile T is*

$$\mathcal{S} = \{a,\ a^{-1},\ a^{A+1}b,\ a^{-1-A}b^{-1},\ c,\ a^{-1}c,\ ac,\ a^{A+1}bc,\ a^{A}\ bc,\ a^{-A-1}b^{-1}c\}.$$

Consequently, we can infer from Lemma 2.17 the following theorem.

THEOREM 2.21. *Let $A, B \in \mathbb{Z}$ satisfy $2 \leq -A \leq B$ and $2|A| < B+3$, and let T be the crystallographic replication tile defined by the data $(g, \mathcal{D})$ given by* (2.2) *and* (2.3) *. Then the following statements hold.*

(1) *If $A = -2, B \geq 2$, then T is disk-like.*
(2) *If $A \leq -3, B \geq 4$, then T is not disk-like.*

PROOF. For Item (1), we know from Theorem 2.20 that the neighbor set of T has six neighbors. Thus, by Proposition 2.17 Item (1), T is disk-like.

For $A = -3, B = 4$, the neighbor set is

$$\mathcal{S} = \{a,\ a^{-1},\ a^{-2}b,\ a^{2}b^{-1},\ c,\ a^{-2}bc,\ a^{-3}bc,\ a^{-1}c\}.$$

Let $a' = a^{-3}b, b' = a^{-1}$, then $\mathcal{S}$ has the form

$$\Upsilon := \{b',\ b'^{-1},\ a'^{-1}b',\ a'b'^{-1},\ c,\ b'c,\ a'c,\ a'b'^{-1}c\}$$

of Proposition 2.17 (3). However, it is easily checked that $\mathcal{D}$ is not $\{c,\ a^{-2}bc,\ ab^{-3}c,\ a^{-1}c\}$-connected. By Proposition 2.17 Item (3), T is not disk-like.

For the cases $A = -3,\ B \geq 5$ and $A \leq -4,\ B \geq 6$, T has 9 and 10 neighbours, respectively. Thus T is not disk-like as we have discussed in Theorem 2.18. □

2.7. Non-disk-likeness of tiles for $2|A| \geq B+3$

So far, we have dealt with the case $2|A| < B+3$ and characterized the disk-like $p2$-tiles in Theorem 2.18 and Theorem 2.21. If $2|A| \geq B+3$, it was proved in [**55**] that the lattice tiles T^{ℓ} are not disk-like. We prove that this also holds for the corresponding $p2$-tiles T.

Recall that the $p2$-tile T satisfies the equation

$$T = \bigcup_{i=1}^{B} f_i(T), \tag{2.19}$$

where

$$f_1 = g^{-1} \circ id,\ f_i = g^{-1} \circ a^{i-1}\ (2 \leq i \leq B-1),\ f_B = g^{-1} \circ c,$$

g is the expanding map given by (2.2) , and $\mathcal{D}$ is the digit set defined as (2.7). We denote the fixed point of a mapping f by $\mathrm{Fix}(f)$ and the linear part of g by M. Then we have the following facts:

$$\mathrm{Fix}(f_i) = (M - I_2)^{-1} \begin{pmatrix} i - 1 - \frac{B-1}{2} \\ 0 \end{pmatrix} \text{ for } 1 \leq i \leq B-1, \tag{2.20}$$

$$\mathrm{Fix}(f_B) = (M + I_2)^{-1} \begin{pmatrix} \frac{B-1}{2} \\ 0 \end{pmatrix}. \tag{2.21}$$

By (2.19), the fixed points given by (2.20) and (2.21) all belong to T. First of all, we give a key lemma for the main result.

LEMMA 2.22. *Let $A, B \in \mathbb{Z}$ satisfying $|A| \leq B$ and $2|A| \geq B+3$, and let T be the p2-crystile defined by the data $(g, \mathcal{D})$ given in (2.2) and (2.3) and $c(T)$ be the π-rotation of T. Then $\sharp\big(T \cap c(T)\big) \geq 2$.*

PROOF. By (2.20), we notice that for $2 \leq p, q \leq B-2$

$$\mathrm{Fix}(f_p) = -\mathrm{Fix}(f_q) \text{ if } p+q = B-1.$$

This means that $\mathrm{Fix}(f_p)$ and $\mathrm{Fix}(f_q)$ are both in T and $c(T)$. If $B > 3$, these points are different and we are done. If $B \leq 3$, we only need to consider the case $|A| = 3, B = 3$ since we assume that $2|A| \geq B+3$. Since $B = 3$, by (2.20), $\mathrm{Fix}(f_2) = \begin{pmatrix} 0 \\ 0 \end{pmatrix}$ which is in $T \cap c(T)$. And for the case $A = 3, B = 3$, there exists an eventually periodic sequence of edges (see Figure 22).

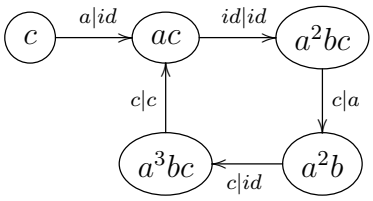

FIGURE 22. An eventually periodic sequence of edges for $A = 3, B = 3$.

The edges of this figure are defined in the same way as in Definition 2.9 and it follows that

$$x_0 = \lim_{n\to\infty} g^{-1}a \circ (g^{-1} \circ g^{-1}c \circ g^{-1}c \circ g^{-1}c)^n(t) \in T \cap c(T,)$$

(see also Characterization 2.10). Here, $t \in \mathbb{R}^2$ is arbitrary. Note that

$$x_0 = g^{-1}a\Big(\mathrm{Fix}(g^{-1} \circ g^{-1}c \circ g^{-1}c \circ g^{-1}c)\Big),$$

and it is easy to compute that $x_0 = \begin{pmatrix} -\frac{13}{73} \\ \frac{16}{219} \end{pmatrix} \neq \begin{pmatrix} 0 \\ 0 \end{pmatrix}$.

For the case $A = -3, B = 3$, we find the eventually periodic sequence of edges

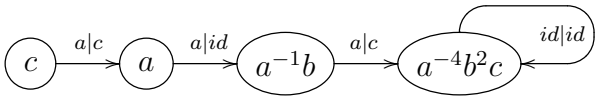

So we have

$$x_0' = \lim_{n\to\infty} g^{-1}a \circ g^{-1}a \circ g^{-1}a \circ (g^{-1})^n(t) \in T \cap c(T),$$

and it is easy to verify that $x_0' = \begin{pmatrix} 0 \\ 1 \end{pmatrix} \neq \begin{pmatrix} 0 \\ 0 \end{pmatrix}$. □

THEOREM 2.23. *Let $A, B \in \mathbb{Z}$ satisfying $|A| \leq B$ and $2|A| \geq B+3$, and let T be the crystallographic replication tile defined by the data $(g, \mathcal{D})$ given in (2.2) and (2.3). Then T is not disk-like.*

PROOF. By a result of [**55**], we know that if $2|A| \geq B + 3$, then T^ℓ is not disk-like. Suppose that T is disk-like. By Lemma 2.22, we have $\sharp(T \cap c(T)) \geq 2$. By [**62**, Proposition 4.1 item (2), p. 127], this implies that $T \cap c(T)$ is a simple arc. Therefore $T \cup c(T)$ is disk-like, as the union of two topological disks whose intersection is a simple arc is again a topological disk. However, by Lemma 2.5, T^ℓ is a translation of $T \cup c(T)$, therefore T^ℓ must be disk-like. This contradicts the assumption $2|A| \geq B + 3$. □

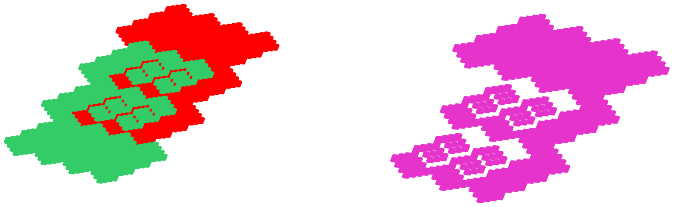

(a) The lattice tile (b) The crystallographic tile

FIGURE 23. $A = 1, B = 4$.

(a) The lattice tile $T^\ell \simeq T \cup c(T)$ (b) The crystallographic tile T

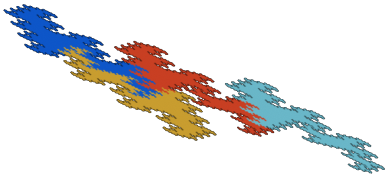

(c) The crystallographic tile $T = g^{-1}(T) \cup g^{-1} \circ a(T) \cup g^{-1} \circ a^2(T) \cup g^{-1} \circ c(T)$

FIGURE 24. Lattice tile and Crystile for $A = -3, B = 4$.

2.8. Examples

Now we provide some examples. For fixed A and B, even though the lattice tile T^ℓ is a translate of $T \cup (-T)$, T and T^ℓ may have completely different topological

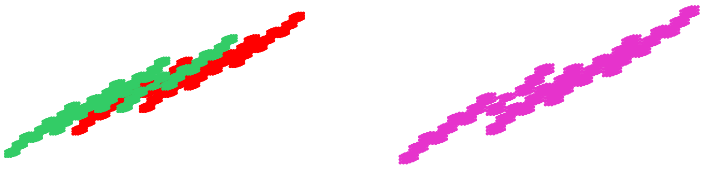

(a) The lattice tile $T^\ell \simeq T \cup c(T)$ (b) The crystallographic tile T

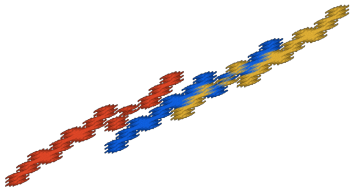

(c) The crystallographic tile $T = g^{-1}(T) \cup g^{-1} \circ a(T) \cup g^{-1} \circ c(T)$

FIGURE 25. Lattice tile and Crystile for $A = 3, B = 3$.

behaviour. We give the following examples to illustrate this phenomenon. In Figure 23, $A = 1, B = 4$, T and T^ℓ are both disk-like. For Figure 3 and Figure 24, T^ℓ is disk-like while T is not. In Figure 25, T and T^ℓ are both not disk-like. To see that T of Figures 24 (b) and 25 (b) are not disk-like, we depicted $T = \cup_{\delta \in \mathcal{D}} g^{-1} \circ \delta(T)$ in Figures 24 (c) and 25 (c) with a better resolution, using the IFStile package of [**38**].

CHAPTER 3

Space-filling curves of self-affine sets and Rauzy fractal

This chapter contains the preprint [**98**] with the title "Optimal parametrizations of a class of self-affine sets". It is also based on the articles [**22**] which is joint work with Xin-Rong Dai and Hui Rao and [**76**] which is the joint work with Hui Rao.

3.1. Introduction

The topic of space-filling curves (SFCs) has a very long history. Recently, Rao and Zhang [**76**] as well as Dai, Rao, and Zhang [**22**] found a systematic method to construct space-filling curves for connected self-similar sets satisfying the open set condition. This method generalizes almost all known results in this field. To generalize their result to self-affine sets, we first need to show that [**76**, Theorem 1.1] is also true if we change the similitudes associated with edges to the affine contractions. Due to the different contraction ratios in different directions, the related invariant sets have more complex structures than in the self-similar case.

3.1.1. Single-matrix GIFS. Let (V,Γ) be a directed graph with vertex set V and edge set Γ. Let

$$\mathcal{G}=\{S_e:\mathbb{R}^d\to\mathbb{R}^d;\ e\in\Gamma\}$$

be a collection of contractions. The triple $(V,\Gamma,\mathcal{G})$, or simply $\mathcal{G}$, is called *a graph-directed iterated function system* (GIFS). Usually, we set $V=\{1,2,\ldots,N\}$ and denote Γ_{ij} to be the set of edges from vertex i to j. Then there exist unique non-empty compact sets $\{E_i\}_{i=1}^N$ satisfying

$$E_i=\bigcup_{j=1}^{N}\bigcup_{e\in\Gamma_{ij}} S_e(E_j),\qquad 1\le i\le N. \tag{3.1}$$

The family $\{E_i\}_{i=1}^N$ is called the *invariant sets* of the GIFS (cf. [**67**]). By [**41**], $\mathcal{G}$ is called a *single-matrix GIFS* if there is a $d\times d$ expanding matrix M such that all functions related to $e\in\Gamma$ have the form

$$S_e(x)=M^{-1}(x+d_e), \tag{3.2}$$

where $d_e\in\mathbb{R}^d$. We say that the system $\mathcal{G}$ satisfies the *open set condition* (OSC) if there exist non-empty open sets $U_1,\ldots,U_N$ such that

$$U_i\subset\bigcup_{j=1}^{N}\bigcup_{e\in\Gamma_{ij}} S_e(U_j),\qquad 1\le i\le N,$$

and the right hand sets union are disjoint (see [**37, 67**]). In addition, if $U_i\cap E_i\neq\emptyset$ for all $1\le i\le N$, then we say the GIFS satisfies the strong open set condition

(SOSC) ([**82**]). When the graph (V, Γ) has only one vertex with self-edges, then the GIFS will degenerate into an iterated function system (IFS). In this case the invariant set is called *self-affine set*, and it is called *self-similar set* when $\mathcal{G}$ is a collection of similitudes.

Denote $A = (m_{ij})_{1\le i,j\le N}$ the *associated matrix* of the directed graph $(\mathcal{A}, \Gamma)$, that is, $m_{ij} = \sharp\Gamma_{ji}$ counts the number of edges from j to i. We say a directed graph (V, Γ) is *primitive*, if the associated matrix is primitive, i.e., A^n is a positive matrix for some n. (See [**67, 29**].) Through the whole chapter, we always assume that (V, Γ) is primitive.

3.1.2. Optimal parametrization. Let $E \subset \mathbb{R}^d$ be a compact set and $\mathcal{H}^s(E)$ denote the Hausdorff measure with respect to Euclidean norm of E. Basically, if $\psi : [0, 1] \to E$ is a continuous onto mapping, then ψ is a *parametrization* of E. If E is a self-similar set satisfying the open set condition, then $0 < \mathcal{H}^s(E) < \infty$, where s is the Hausdorff dimension of E. In this case, we may expect that E has a better parametrization. The following concept is first given by Dai and Wang [**23**]:

Definition 3.1 ([**23**]). A surjective mapping $\psi : [0, 1] \to E$ is called an *optimal parametrization* of E if the following conditions are fulfilled.

(*i*) ψ is a *measure isomorphism* between $([0, 1], \mathcal{B}([0, 1]), \mathcal{L})$ and $(E, \mathcal{B}(E), \mathcal{H}^s)$, that is, there exist $E' \subset E$ and $I' \subset [0, 1]$ with full measure such that $\psi : I' \to E'$ is a bijection and it is measure-preserving in the sense that

$$\mathcal{H}^s(\psi(F)) = c\mathcal{L}(F) \text{ and } \mathcal{L}(\psi^{-1}(B)) = c^{-1}\mathcal{H}^s(B),$$

for any Borel set $F \subset [0, 1]$ and any Borel set $B \subset E$, where $c = \mathcal{H}^s(E)$. (See for instance, Walters [**95**].)

(*ii*) ψ is $1/s$-*Hölder continuous*, that is, there is a constant $c' > 0$ such that

$$\|\psi(x) - \psi(y)\| \le c'\|x - y\|^{\frac{1}{s}} \quad \text{for all } x, y \in [0, 1].$$

We call $1/s$ the *Hölder exponent*.

For a self-affine set K, the Hausdorff measure may be 0 or ∞, and hence we cannot require an optimal parametrization satisfying (i) of the above. Also, the $1/s$-Hölder continuity may fail. So we are forced to define the optimal parametrization in some other way.

To this end, we choose a pseudo-norm $\|\cdot\|_\omega$ instead of the Euclidean norm on K. This pseudo-norm was first introduced by Lemarié-Rieusset [**54**] to deal with problems in the theory of wavelets. Then He and Lau [**35**] developed the Hausdorff dimension (denoted by $\dim_\omega$) and Hausdorff measure (denoted by $\mathcal{H}^s_\omega$) with respect to pseudo-norm (see Section 3.2.2 for details). The advantage of the pseudo-norm is that we can regard the expanding matrix M as a 'similitude'. By replacing the norm, dimension and measure by their counterpart w.r.t. the pseudo-norm, we can define an optimal parametrization similar to Definition 3.1; details will be given in Theorem 3.5.

The following idea of linear GIFS was designed for self-simiar set to construct the SFC by Rao and Zhang [**76**].

3.1.2.1. **Linear GIFS.** Let $(V, \Gamma, \mathcal{G})$ be a GIFS with vertex set V, edge set Γ and mapping set $\mathcal{G}$. Let $\Gamma_i = \Gamma_i^1$ be the set of outgoing edges from the state i. For $i \in V$, let

$$\Gamma_i^k \text{ and } \Gamma_i^\infty$$

be the set of all walks of length k and the set of all infinite walks, starting at state i, respectively. If there exists a partial order $\prec$ on Γ such that

(*i*) $\prec$ is a linear order when restricted on Γ_j for every $j \in V$,

(*ii*) elements in Γ_i and Γ_j are not comparable if $i \neq j$,

we call $(V, \Gamma, \mathcal{G}, \prec)$ an *ordered GIFS*. (See [**76**] for detail.)

The order $\prec$ induces a lexicographical order on each Γ_i^k. Observe that $(\Gamma_i^k, \prec)$ is a linear order; two paths $\boldsymbol{\gamma}, \boldsymbol{\omega} \in \Gamma_i^k$ are said to be *adjacent* if there is no walk between them with respect to the order $\prec$.

Definition 3.2. (see [**76**]) An ordered GIFS $(V, \Gamma, \mathcal{G}, \prec)$ with invariant sets $\{E_i\}_{i=1}^N$ is called a *linear* GIFS, if for all $i \in V$ and $k \geq 1$,

$$E_{\boldsymbol{\gamma}} \cap E_{\boldsymbol{\omega}} \neq \emptyset$$

for adjacent walks $\boldsymbol{\gamma}, \boldsymbol{\omega}$ in Γ_i^k .

For $i \in V$, a walk $\boldsymbol{\omega} \in \Gamma_i^\infty$ is called the *lowest* walk, if $\boldsymbol{\omega}|_n$ is the lowest walk in Γ_i^n for all n; in this case, we call $a = \pi_i(\boldsymbol{\omega})$ the *head* of E_i. Similarly, we define the highest walk $\boldsymbol{\omega}'$ of Γ_i^∞, and we call $b = \pi_i(\boldsymbol{\omega}')$ the the *tail* of E_i.

Definition 3.3. (see [**76**, Definition 4.1])An ordered GIFS is said to satisfy the *chain condition*, if for any $i \in V$, and any two adjacent edges $\omega, \gamma \in \Gamma_i$ with $\omega \prec \gamma$,

$$g_\omega(\text{tail of } E_{t(\omega)}) = g_\gamma(\text{ head of } E_{t(\gamma)}).$$

Lemma 3.4. *An ordered GIFS is a linear GIFS if and only if it satisfies the chain condition.*

Remark. Definition 3.2, Definition 3.3 and Lemma 3.4 still make sense when $\mathcal{G}$ is a family of contractions.

3.1.3. Main result. Rao and Zhang [**76**] proved that as soon as we find a linear GIFS structure of a self-similar set, then a space-filling curve can be constructed accordingly. Dai, Rao, and Zhang [**22**] develop a very general method to explore linear GIFS structures of a given self-similar set. To obtain the optimal parametrizations for self-affine sets, we have the following statement.

Theorem 3.5. *Let $(V, \Gamma, \mathcal{G}, \prec)$ be a linear single-matrix GIFS with expanding matrix M satisfying the open set condition and assume that the associated matrix A of the graph is primitive. Then there exists a parametrization ψ_j of the invariant E_j for all $j \in V$ such that*

(*i*) *ψ_j is a* measure isomorphism *between*

$$([0,1], \mathcal{B}([0,1]), \mathcal{L}) \text{ and } (E_j, \mathcal{B}(E_j), \mathcal{H}_\omega^s).$$

(*ii*) *There is a constant $c > 0$ such that*

$$\|\psi_j(x) - \psi_j(y)\|_\omega \leq c\|x - y\|^{\frac{1}{\alpha}} \quad \text{for all } x, y \in [0,1],$$

where $\alpha = \dim_\omega E_j$.

To prove the above theorem, we will not go in detail and only show the crucial difference with the proof of [**76**, Theorem 1.1].(see Section 3.2.3.)

According to the relation between Euclidean norm and pseudo-norm (See Proposition 3.11), we have the following result for the Hölder continuity of the parametrization ψ_j obtained by the above theorem.

COROLLARY 3.6. *Let λ_M be the maximal eigenvalue of M. Let λ_{max} and λ_{min} be the maximal modulus and minimal modulus of the eigenvalues of A, respectively. For any $0 < \epsilon < \lambda_{min} - 1$,*

- *ψ_j is $\frac{\ln(\lambda_{\max}+\epsilon)}{\ln \lambda_M}$-Hölder continuous if $\|\psi_j(x) - \psi_j(y)\| \geq 1$;*
- *ψ_j is $\frac{\ln(\lambda_{\min}-\epsilon)}{\ln \lambda_M}$-Hölder continuous if $\|\psi_j(x) - \psi_j(y)\| \leq 1$.*

The matrices M and A have the same meaning as in the above theorem.

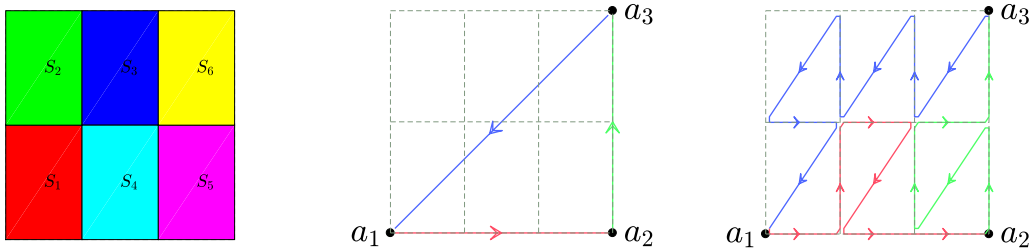

(a) Unit square $Q = \cup_{i=1}^{6} S_i(Q)$. (b) Initial cycle. (c) First generation.

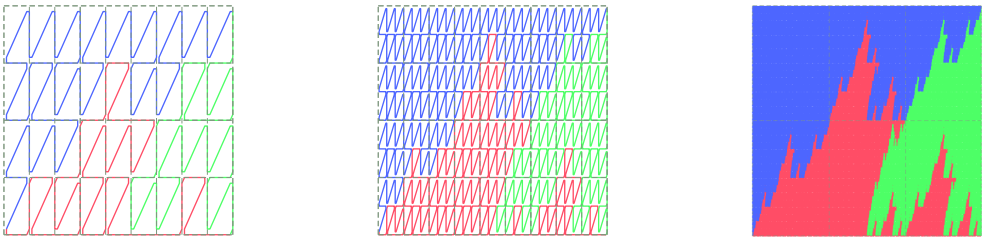

(d) Second generation. (e) Third generation. (f) Parametrized square.

FIGURE 26. The space-filling curve of unit square given by IFS $\{S_i\}_{i=1}^{6}$.

Inspired by [**22**], we shall do some further study on construting SFCs of self-affine sets, such as McMullen sets, self-affine tiles and Rauzy fractals. To this matter, we try to find a suitable method as we did for self-similar sets. Here we want to emphasis that to do the parametrization of a Rauzy fractal is based on invariant sets of a graph-directed iterated system, that is to say, we construct a linear GIFS from a given GIFS. ([**22**] focused on constructing a linear GIFS from a given IFS.) Thus here we need a modified definition for the skeleton for the GIFS which is first prepared for self-similar sets by [**23, 77**].

3.1.4. Skeleton of a GIFS. Recall that $\{E_i\}_{i\in V}$ are the invariant sets of the GIFS $(V, \Gamma, \mathcal{G})$ given by the set equation (3.1). The vertex set is $V = \{1, 2, \ldots, N\}$ and Γ_{ij} is the set of edges from vertex i to j.

For fixed $i \in V$, let A_i be a subset of E_i, we define a graph $H(A_i)$ as follows.

- The vertex set is $\{S_e; e \in \Gamma_{ij}, j \in V\}$.
- There is an edge between two vertices S_ω and S_γ if and only if $S_\omega(A_{t(\omega)}) \cap S_\gamma(A_{t(\gamma)}) \neq \emptyset$ where $t(e)$ denotes the terminate state of the edge $e \in \Gamma$.

We call $H(A_i)$ the *Hata graph* induced by A_i.

We say a graph is connected if any two vertices in the graph can be reached by a path.

REMARK 3.7. For V is a single point set, the GIFS degenerates to an IFS and Hata [**34**] intoduced the above graph $H(E)$ ($E = E_1 = \cdots = E_N$) to study the connectedness of self-similar set. It proved that a self-similar set E is connected if and only if the graph $H(E)$ is connected.

Later, Luo, Akiyama and Thuswaldner [**64**] generalized this result and proved the connectedness for GIFS by the following statement.

LEMMA 3.8 ([**64**]). *Let $\{E\}_{j\in V}$ be the invariant set of the GIFS $(V, \Gamma, \mathcal{G})$ given by* (3.1)*. Then E_j is connected for all $j \in V$ iff $H(E_j)$ is connected.*

DEFINITION 3.9. Let $\{E_j\}_{j\in V}$ be the invariant sets of the GIFS $(V, \Gamma, \mathcal{G})$, and let A_j be a finite subset of E_j. We call $\{A_j\}_{j\in V}$ a *skeleton* of the GIFS $\mathcal{G}$ (or $\{E_j\}_{j\in V}$), if $\{A_j\}_{j\in V}$ satisfies the following two conditions.

- A_j is stable under iteration, *i.e.*

$$A_j \subset \bigcup_{i\in V} \bigcup_{e\in\Gamma_{ji}} S_e(A_i).$$

- The Hata graph $H(A_j)$ are connected for all $j \in V$.

To continue our construction, we need the substitution rule as we did for self-similar sets. The *edge-to-trail substitution* is introduced by [**22**] for self-similar IFS case. Here we general this concept for the GIFS.

3.1.5. Edge-to-trail substitution. When we have a skeleton $A_i = \{a_{i1}, a_{i2}, \ldots, a_{im_i}\}$ of the GIFS $\mathcal{G}$, we denote the cycle passing $a_{i1}, \ldots, a_{im_i}$ one by one by Λ_i. Let G_i be the union of the affine images of Λ_j under S_e for $e \in \Gamma_{ij}$, that is

$$G_i = \bigcup_{j=1}^{N} \bigcup_{e\in\Gamma_{ij}} S_e(\Lambda_j).$$

which we call *refined graph*.

For $i \in V$, let τ_i be the mapping from Λ_i to trails of G_i; We call τ_i an *edge-to-trail substitution* , if for all $u \in \Lambda_i$, $\tau_i(u)$ has the same origin and terminus as u. (See more details in Section 3.3.)

After we have an edge-to-trail substitution rule, we will show in Section 3.3.3 that we can construct an ordered GIFS according. Then we show that this ordered GIFS is actually linear (See Theorem 3.17). To apply Theorem 3.5, we have to check this linear GIFS satisfying more conditions.

Instead of discussing these conditions, we will do more efforts on the examples of constructing SFCs for different sets. In Section 3.4, we will show the examples

for constructing SFCs for unit square for Dekking's plane filling curve and for a McMullen set. Section 3.5 will contribute to create the SFCs for a class of self-affine disk-like tiles. And in the last Section, the SFC for the classical Rauzy fractal will be presented.

3.2. Pseudo norm and Proof of Theorem 3.5

3.2.1. The symbolic space related to a graph G. First, we recall some terminologies of graph theory, see for instance, [**8**]. Let $G = (V, \Gamma)$ be a directed graph. A sequence of edges in G, denoted by $\boldsymbol{\omega} = \omega_1 + \omega_2 + \cdots + \omega_n$, is called a *walk*, if the terminal state of ω_i coincides with the initial state of ω_{i+1} for $1 \le i \le n-1$. The walk is *closed* if the origin of ω_1 and the terminus of ω_n coincide. A walk is called a *trail*, if all the edges appearing in the walk are distinct. A trail is called a *path* if all the vertices are distinct. A closed path is called a *cycle*. A subgraph H of G is called *spanning*, if H contains all the vertices of G. An *Euler trail* in G is a spanning trail in G that contains all the edges of G. An *Euler tour* of G is a closed Euler trail of G.

For $i \in V$, let Γ_i^* be the set all walks of finite length starting at state i. Note that $\Gamma_i^* = \bigcup_{k\ge 1} \Gamma_i^k$.

For $\boldsymbol{\omega} = (\omega_k)_{k=1}^{\infty}$, define by $\boldsymbol{\omega}|_n = \omega_1 + \omega_2 + \cdots + \omega_n$ the prefix of $\boldsymbol{\omega}$ of length n. Moreover, call $[\omega_1 \ldots \omega_n] := \{\boldsymbol{\gamma} \in \Gamma_i^{\infty};\ \boldsymbol{\gamma}|_n = \omega_1 + \cdots + \omega_n\}$ the *cylinder* associated with a walk $\omega_1 + \cdots + \omega_n$.

For a walk $\boldsymbol{\gamma} = \gamma_1 + \cdots + \gamma_n \in \Gamma_i^n$, set $g_{\boldsymbol{\gamma}} := g_{\gamma_1} \circ g_{\gamma_2} \cdots \circ g_{\gamma_n}$, then we denote

$$E_{\boldsymbol{\gamma}} := g_{\boldsymbol{\gamma}}(E_{t(\boldsymbol{\gamma})}),$$

where $t(\boldsymbol{\gamma})$ denotes the terminal state of the path $\boldsymbol{\gamma}$ (which equalsγ_n here). Iterating (3.1) k-times, we obtain

$$E_i = \bigcup_{\boldsymbol{\gamma}\in\Gamma_i^k} E_{\boldsymbol{\gamma}}. \tag{3.3}$$

We define the projection $\pi : \Gamma_1^{\infty} \times \cdots \times \Gamma_N^{\infty} \to \mathbb{R}^d \times \cdots \times \mathbb{R}^d$, where $\pi_i := \pi|_{\Gamma_i^{\infty}} : \Gamma_i^{\infty} \to \mathbb{R}^d$ is given by

$$\{\pi_i(\boldsymbol{\omega})\} := \bigcap_{n\ge 1} E_{\boldsymbol{\omega}|_{\boldsymbol{n}}}. \tag{3.4}$$

For $x \in E_i$, we call $\boldsymbol{\omega}$ a *coding* of x if $\pi_i(\boldsymbol{\omega}) = x$. It is easy to see that $\pi_i(\Gamma_i^{\infty}) = E_i$.

3.2.2. Pseudo-norm and Hausdorff measure in pseudo-norm. The notion of pseudo-norm was first introduced by [**54**]. And He and Lau [**35**] use this concept to study the dimension and the separation properties of the invariant sets of single-matrix IFS's.

Denote by $B(x, r)$ the open ball with center x and radius r. Recall that A is the expanding matrix with $|\det A| = q$, then $V = A(B(0,1)) \setminus B(0,1)$ is homeomorphic to an annulus. For $\delta \in (0, \frac{1}{2})$, choose a positive $\mathbb{C}^{\infty}$-function $\phi_\delta(x)$ with support in $B(0,\delta)$ such that $\phi_\delta(x) = \phi_\delta(-x)$ and $\int \phi_\delta(x)dx = 1$, and then define a pseudo-norm

$\|\cdot\|_\omega$ in $\mathbb{R}^d$ by

$$\|x\|_\omega = \sum_{n\in\mathbb{Z}} q^{-n/d} h(A^n x),$$

where $h(x) = \chi_V * \phi_\delta(x) = \int_{\mathbb{R}^d} \chi_V(x-y)\cdot\phi_\delta(y)dy$.

We list some basic properties of $\|\cdot\|_\omega$.

PROPOSITION 3.10. *(See* [**35**, Proposition 2.1]*) The function $\|\cdot\|_\omega$ has the properties as follows.*

(i) $\|x\|_\omega \geq 0$; $\|x\|_\omega = 0$ if and only if $x = 0$.

(ii) $\|x\|_\omega = \|-x\|_\omega$;

(iii) $\|Ax\|_\omega = q^{1/d}\|x\|_\omega \geq \|x\|_\omega$ for all $x \in \mathbb{R}^d$.

(iv) There exists a constant $\beta > 0$ such that $\|x+y\|_\omega \leq \beta\max\{\|x\|_\omega, \|y\|_\omega\}$ for any $x, y \in \mathbb{R}^d$.

The pseudo-norm $\|\cdot\|_\omega$ is comparable with the Euclidean norm $\|x\|$.

PROPOSITION 3.11. *(See* [**35**, Proposition 2.4]*) Let $\lambda_{\max}$ and $\lambda_{\min}$ be the maximal modulus and minimal modulus of the eigenvalues of A, respectively. For any $0 < \varepsilon < \lambda_{\min} - 1$, there exists $C > 0$(depends on ε) such that*

$$C^{-1}\|x\|^{\ln q/d\ln(\lambda_{\max}+\varepsilon)} \leq \|x\|_\omega \leq C\|x\|^{\ln q/d\ln(\lambda_{\min}-\varepsilon)}, \qquad \text{if } \|x\| > 1;$$

$$C^{-1}\|x\|^{\ln q/d\ln(\lambda_{\min}-\varepsilon)} \leq \|x\|_\omega \leq C\|x\|^{\ln q/d\ln(\lambda_{\max}+\varepsilon)}, \qquad \text{if } \|x\| \leq 1.$$

The Hausdorff measure with respect to the pseudo-norm $\|\cdot\|_\omega$ was given by He and Lau [**35**] as follows. For $E \subset \mathbb{R}^d$, set $\operatorname{diam}_\omega E = \sup\{\|x-y\|_\omega;\ x, y \in E\}$ to be the ω-diameter of E. For $s \geq 0, \delta > 0$, set

$$\mathcal{H}^s_{\omega,\delta}(E) = \inf\Big\{\sum_{i=1}^{\infty}(\operatorname{diam}_\omega E_i)^s;\ E \subset \bigcup_i E_i,\ \operatorname{diam}_\omega E_i \leq \delta\Big\},$$

$$\mathcal{H}^s_\omega(E) = \lim_{\delta\to 0}\mathcal{H}^s_{\omega,\delta}(E).$$

$\mathcal{H}^s_\omega$ has the translation invariance property and the scaling property [**35**], that is,

$$\mathcal{H}^s_\omega(E+x) = \mathcal{H}^s_\omega(E) \text{ and } \mathcal{H}^s_\omega(A^{-1}E) = q^{-s/d}\mathcal{H}^s_\omega(E).$$

Thus the Hausdorff dimension with respect to $\|\cdot\|_\omega$ can be defined by

$$\dim_\omega E = \inf\{s;\ \mathcal{H}^s_\omega(E) = 0\} = \sup\{s;\ \mathcal{H}^s_\omega(E) = \infty\}.$$

3.2.3. Proof of Theorem 3.5. In this section, we prove Theorem 3.5 by constructing an auxiliary GIFS (which we call measuring-recording GIFS), which is very similar to the proof in [**76**]. However, the theorem related to the open set condition of Mauldin and Williams [**67**] does not hold when A is not a similitude. So we need to use the result of Luo and Yang [**41**] to modify the proof.

3.2.3.1. **Markov measure induced by GIFS.** Let $(V,\Gamma,\mathcal{G})$ be single-matrix GIFS with expanding matrix M and $\{E_i\}_{i=1}^N$ be the invariant sets. Denote $q = |\det(M)|$. And $A = (m_{ij})_{1\le i,\ j\le N}$ is the associated matrix of the directed graph (V,Γ). Due to the following lemma from [**41**], we can construct the Markov measure.

LEMMA 3.12. *([**41**, Theorem 1.2]) For a single matrix GIFS $(V,\Gamma,\mathcal{G})$, let λ be the maximal eigenvalue of A. If A is primitive and the OSC holds, then for any $1\le i\le N$,*

(i) $\alpha = \dim_\omega E_i = d\frac{\log\lambda}{\log q}$;

(ii) $0<\mathcal{H}^\alpha_\omega(E_i)<\infty$.

(iii) The right hand side of (3.1) *is a disjoint union in sense of the measure of* $\mathcal{H}^\alpha_\omega$.

Remark (1)**.** By item (*iii*) of the above lemma, we immediately have

$$\mathcal{H}^\alpha_\omega(E_{\boldsymbol{\omega}}\cap E_{\boldsymbol{\gamma}})=0$$

for any incomparable $\boldsymbol{\omega},\boldsymbol{\gamma}\in\Gamma_i^*$. (Two walks are said to be *comparable* if one of them is a prefix of the other.)

Remark (2)**.** Since $E_i=\bigcup_{j=1}^N\bigcup_{e\in\Gamma_{ij}}S_e(E_j)$, using Remark (1), we get

$$\mathcal{H}^\alpha_\omega(E_i)=\sum_{j=1}^N\sum_{e\in\Gamma_{ij}}\mathcal{H}^\alpha_\omega(S_e(E_j))=\lambda^{-1}\sum_{j=1}^N\sharp\Gamma_{ij}\mathcal{H}^\alpha_\omega(E_j).$$

This shows that $(\mathcal{H}^\alpha_\omega(E_1),\dots,\mathcal{H}^\alpha_\omega(E_N))$ is an eigenvector with respect to λ of A.

In the rest of the section, we will always assume that $\mathcal{G}$ satisfies the conditions of Lemma 3.12. Then $0<\mathcal{H}^\alpha_\omega(E_i)<\infty$ for all $1\le i\le N$. Now, we define Markov measures on the symbolic spaces Γ_i^∞, $i\in V$. For arbitrary edge $e\in\Gamma$ such that $e\in\Gamma_{ij}$, set

$$p_e=\frac{\mathcal{H}^\alpha_\omega(E_j)}{\mathcal{H}^\alpha_\omega(E_i)}\lambda^{-1}. \tag{3.5}$$

Using Remark (2) of Lemma 3.12, it is easy to verify that $(p_e)_{e\in\Gamma}$ satisfies

$$\sum_{j\in V}\sum_{e\in\Gamma_{ij}}p_e=1,\ \text{for all } i\in V. \tag{3.6}$$

We call $(p_e)_{e\in\Gamma}$ a *probability weight vector*. Let $\mathbb{P}_i$ be a Borel measure on Γ_i^∞ satisfying the relations

$$\mathbb{P}_i([\omega_1\dots\omega_n])=\mathcal{H}^\alpha_\omega(E_i)p_{\omega_1}\dots p_{\omega_n} \tag{3.7}$$

for all cylinder $[\omega_1\dots\omega_n]$. The existence of such measures is guaranteed by (3.6). We call $\{\mathbb{P}_i\}_{i=1}^N$ the *Markov measures* induced by the GIFS $\mathcal{G}$.

Denote the restriction of $\mathcal{H}^\alpha_\omega$ on E_i by $\mu_i=\mathcal{H}^\alpha_\omega|_{E_i}$, for $i=1,\dots,N$. The following Lemma gives the relation between the Markov measure and the restricted Hausdorff measure.

LEMMA 3.13. *(see* [**67, 41**]*) Suppose the single-matrix graph IFS $(V,\Gamma,\mathcal{G}_)$ satisfies the OSC and the associated matrix M is primitive. Let $\pi_i:\Gamma_i^\infty\to E_i$ be the projections defined by* (3.4)*. Then*

$$\mu_i=\mathbb{P}_i\circ\pi_i^{-1}.$$

3.2.3.2. **The construction of measure-recording GIFS.** Let $(V, \Gamma, \mathcal{G}, \prec)$ be a linear GIFS such that the open set condition is fulfilled and the associated matrix is primitive, then $0 < \mathcal{H}^\alpha_\omega(E_i) < \infty$ for all i, where $\alpha = d\frac{\log \lambda}{\log q}$ by Lemma 3.12.

For $i \in V$, we list the edges in Γ_i in the ascendent order with respect to $\prec$, i.e.,

$$\gamma_1 \prec \gamma_2 \prec \cdots \prec \gamma_{\ell_i}.$$

Recall that $t(\gamma)$ denotes the terminate vertex of an edge γ. Then by (3.1), we can rewrite E_i as

$$E_i \triangleq g_{\gamma_1}(E_{t(\gamma_1)}) \cup \cdots \cup g_{\gamma_{\ell_i}}(E_{t(\gamma_{\ell_i})}).$$

Here we use '$\triangleq$' to emphasize the order of the union of the right side.

Denote by $F_i = [0, \mathcal{H}^\alpha_\omega(E_i)]$ an interval on $\mathbb{R}$, then by equation (3.6), we have

$$F_i = \Big[0,\ \mathcal{H}^\alpha_\omega(g_{\gamma_1}(E_{t(\gamma_1)}))\Big] \cup \cdots \cup \Big[\sum_{j=1}^{\ell_i - 1} \mathcal{H}^\alpha_\omega(g_{\gamma_j}(E_{t(\gamma_j)})),\ \sum_{j=1}^{\ell_i} \mathcal{H}^\alpha_\omega(g_{\gamma_j}(E_{t(\gamma_j)}))\Big]. \tag{3.8}$$

We define the mappings,

$$f_{\gamma_k}(x) = q^{-\alpha/d}x + b_k :\ \mathbb{R} \longrightarrow \mathbb{R}, \quad 1 \le k \le \ell_i,$$

where $b_k = \sum_{j=1}^{k-1} \mathcal{H}^\alpha_\omega(E_{t(\gamma_j)}) q^{-\alpha/d}$. Then F_i satisfies the following equation by (3.8)

$$F_i \triangleq f_{\gamma_1}(F_{t(\gamma_1)}) \cup \cdots \cup f_{\gamma_{\ell_i}}(F_{t(\gamma_{\ell_i})}). \tag{3.9}$$

Repeating these procedures for all $i \in V$, equation (3.9) gives us an ordered GIFS on $\mathbb{R}$. Set $\mathcal{F} = \{f_\gamma : \mathbb{R} \longrightarrow \mathbb{R};\ \gamma \in \Gamma\}$, and denote this GIFS by

$$(V, \Gamma, \mathcal{F}, \prec),$$

and call it the *measure-recording GIFS* of $(V, \Gamma, \mathcal{G}, \prec)$. And the invariant sets of the measure-recording GIFS are $\{F_i\}_{i=1}^N$. (See [**76**].)

Obviously, the measure-recording GIFS has the same graph and the same order as the original GIFS; also keeps the Hausdorff measure information of the original GIFS. And it is easy to check $\mathcal{F}$ satisfies the open set condition. In fact, the open intervals $\{U_i = (0, \mathcal{H}^\alpha_\omega(E_i))\}_{i=1}^N$ are the according open sets.

For an edge $e \in \Gamma$, the contraction ratio of f_e is $q^{-\alpha/d} = \lambda^{-1}$, then it is easy to check $(\mathcal{L}(F_1), \ldots, \mathcal{L}(F_N))$ is an eigenvector of A with respect the eigenvalue λ^{-1}. Thus the Markov measure induced by the measure-recording GIFS coincides with $\{\mathbb{P}_i\}_{i=1}^N$ induced by the original GIFS.

Let

$$\pi_i : \Gamma_i^\infty \to E_i \text{ and } \rho_i : \Gamma_i^\infty \to F_i, \quad i = 1, \ldots, N,$$

be projections w.r.t. the GIFS $(\mathcal{G})$ and $(\mathcal{F})$, respectively, (see (3.4)). Define

$$\psi_i := \pi_i \circ \rho_i^{-1}. \tag{3.10}$$

In [**76**], it is shown that ψ_i is a well-defined mapping from F_i to E_i since we consider a linear GIFS.

Now, we prove Theorem 3.5 by showing that the mapping ψ_i is an optimal parametrization of E_i.

PROOF. We use the same notations as before, let $\mathcal{F}$ be the measure-recording GIFS of $\mathcal{G}$. Through the discussion before, we denote the common Markov measure induced by $\mathcal{G}$ and $\mathcal{F}$ by $\mathbb{P}_i$. $\psi_i = \pi_i \circ \rho_i^{-1}$ is the well-defined mapping from F_i to E_i. Let $\nu_i = \mathcal{L}|_{F_i}$ be the restriction of the Lebesgue measure on F_i and $\mu_i = \mathcal{H}^\alpha_\omega|_{E_i}$ be the restriction of the weak Hausdorff measure on E_i, then $\nu_i = \mathbb{P}_i \circ \rho_i^{-1}$, $\mu_i = \mathbb{P}_i \circ \pi_i^{-1}$ by Lemma 3.13.

The fact that ψ_i is almost one to one and measure preserving follows by the same arguments as in the self-similar case and we refer to the proof of [**76**, Theorem 1.1].

We have to prove the $1/\alpha$-Hölder continuity of ψ_i. From the previous construction, we know that $F_i = [0, \mathcal{H}^\alpha_\omega(E_i)]$. Now we choose two different points x_1, x_2 from F_i which are determined by $\boldsymbol{\omega} = (\omega_i)_{i=1}^\infty$ and $\boldsymbol{\gamma} = (\gamma_i)_{i=1}^\infty$, respectively, that is, $x_1 = \rho_i(\boldsymbol{\omega}), x_2 = \rho_i(\boldsymbol{\gamma})$. Then there is a smallest integer which we denote by k such that x_1, x_2 belongs to two different cylinders. Set $\boldsymbol{\omega}|_k = \omega_1 + \cdots + \omega_k$, we know that $\boldsymbol{\gamma}|_k$ is only different from $\boldsymbol{\omega}|_k$ at last edge, i.e., $\boldsymbol{\gamma}|_k = \omega_1 + \cdots + \omega_{k-1} + \gamma_k$. According to whether $\boldsymbol{\omega}|_k$ and $\boldsymbol{\gamma}|_k$ are adjacent or not, we consider two cases. First, we consider that ω_k and γ_k are not adjacent. (See Figure 27.) Then there is a cylinder

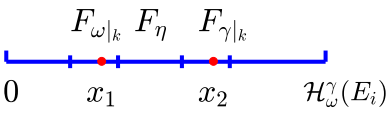

FIGURE 27. $\boldsymbol{\omega}$ and $\boldsymbol{\gamma}$ are not adjacent.

$\boldsymbol{\eta} = \omega_1 + \cdots + \omega_{k-1} + \eta_k$ between $\boldsymbol{\omega}|_k$ and $\boldsymbol{\gamma}|_k$, so

$$\|x_1 - x_2\| \geq \operatorname{diam} F_{\boldsymbol{\eta}} \geq h \cdot (q^{-\alpha/d})^k,$$

where $h = \min\{\mathcal{H}^\alpha_\omega(E_i);\ i = 1, \ldots, N\}$. Since x_1 and x_2 belong to $\rho([\omega_1\omega_2 \ldots \omega_{k-1}])$ and denote $\boldsymbol{\omega}_* = \omega_1 + \cdots + \omega_{k-1}$, the images of x_1 and x_2 under $\pi_i \circ \rho_i^{-1}$, which denote by y_1 and y_2, respectively, belong to $\pi_i([\boldsymbol{\omega}_*]) = E_{\boldsymbol{\omega}_*}$. Then we have

$$\begin{aligned} \|y_1 - y_2\|_\omega &\leq \operatorname{diam}_\omega E_{\boldsymbol{\omega}^*} \leq \left(\max_{1\leq m\leq N} \operatorname{diam}_\omega E_i\right) \cdot q^{-\frac{k-1}{d}} \\ &= D \cdot q^{1/d} \cdot (q^{-1/d})^k \leq D \cdot q^{1/d} \cdot (1/h)^{\frac{d}{\alpha}} \|x_1 - x_2\|^{\frac{1}{\alpha}}, \end{aligned} \tag{3.11}$$

where $D = \max_{1\leq i\leq N} \operatorname{diam}_\omega E_i$.

Now, we consider the case that $\boldsymbol{\omega}_k$ and $\boldsymbol{\gamma}_k$ are adjacent. (See Figure 28 (left).) Let x_3 be the intersection of $F_{\boldsymbol{\omega}|_k}$ and $F_{\boldsymbol{\gamma}|_k}$. Let k' be the smallest integer such that x_1 and x_3 belong to different cylinders of rank k', say, $x_1 \in \rho_i([\boldsymbol{\omega}'])$ and $x_3 \in \rho_i([\boldsymbol{\omega}''])$ (see Figure 28 (right)), then $\|x_1 - x_3\| \geq \operatorname{diam} F_{\boldsymbol{\omega}''}$ since x_3 is an endpoint. Let $y_3 = \psi_i(x_3)$. Similar to Case 1, we have

$$\|y_1 - y_3\|_\omega \leq D \cdot q^{1/d} \cdot (1/h)^{\frac{d}{\alpha}} \|x_1 - x_3\|^{\frac{1}{\alpha}}.$$

By the same argument, we have

$$\|y_2 - y_3\|_\omega \leq D \cdot q^{1/d} \cdot (1/h)^{\frac{d}{\alpha}} \|x_2 - x_3\|^{\frac{1}{\alpha}}.$$

FIGURE 28. $\boldsymbol{\omega}$ and $\boldsymbol{\gamma}$ are adjacent.

Hence, by the fact x_3 is located between x_1 and x_2,

$$\begin{aligned} \|y_1 - y_2\|_\omega &\le \beta \cdot \max\{\|y_1 - y_3\|_\omega, \|y_3 - y_2\|_\omega\} \\ &\le \beta \cdot D \cdot q^{1/d} \cdot (1/h)^{\frac{d}{\alpha}} \cdot \max\{\|x_1 - x_3\|^{\frac{1}{\alpha}}, \|x_2 - x_3\|^{\frac{1}{s}}\} \\ &\le \beta \cdot D \cdot q^{1/d} \cdot (1/h)^{\frac{d}{\alpha}} \cdot \|x_1 - x_2\|^{\frac{1}{\alpha}}, \end{aligned} \tag{3.12}$$

where the first inequality is from Proposition 3.10 (iv).

Therefore, (3.11) and (3.12) verify the $1/\alpha$- Hölder continuity of ψ_i. □

3.3. From skeleton to linear GIFS

Let $(V, \Gamma, \mathcal{G})$ be an GIFS possessing a skeleton $\{A_i\}_{i\in V}$ with invariant sets $\{E_i\}_{i\in V}$ and satisfying the OSC. Denote the vertex set $V = \{1, 2, \ldots, N\}$ for simplicity. And we denote the skeleton by

$$A_i = \{a_{i1}, a_{i2}, \ldots, a_{im_i}\},$$

where m_i is greater than 2 and $i \in V$.

Define

$$\Lambda_i = \Lambda_{A_i} := \overrightarrow{a_{i1}a_{i2}} + \cdots + \overrightarrow{a_{im_i-1}a_{im_i}} + \overrightarrow{a_{im_i}a_{i1}} \tag{3.13}$$

to be the cycle passing $a_{i1}, \ldots, a_{im_i}$ in turn. We denote the edge set of Λ_i by

$$V_i^+ = \{\overrightarrow{a_{i1}a_{i2}}, \ldots, \overrightarrow{a_{im_i-1}a_{im_i}}, \overrightarrow{a_{im_i}a_{i1}}\}.$$

We call Λ_i the *initial graph*. We note that the edges $\overrightarrow{a_{ik}a_{i(k+1)}}$ are abstract edges rather than oriented line segments.

To continue our construction, we need to define the *affine copy* of a directed graph which you can also find in [**22**].

DEFINITION 3.14. [**22**] Let G be a directed graph with edge set Γ such that the vertex set $\mathcal{A} \subset \mathbb{R}^d$. Let $S : \mathbb{R}^d \to \mathbb{R}^d$ be a affine mapping. We define a directed graph $G_S = (S(\mathcal{A}), \Gamma_S)$ as follows: there is an edge in Γ_S from $S(x)$ to $S(y)$, if and only if there is an edge $e \in \Gamma$ from vertex x to y. Moreover, we denote this edge by (e, S). For simplicity, we shall denote G_S, Γ_S, and (e, S) by $S(G), S(\Gamma)$ and $S(e)$, respectively.

REMARK 3.15. (i) If $(\mathcal{A}_1, \Gamma_1)$ and $(\mathcal{A}_2, \Gamma_2)$ are two graphs without common edges, then we define their union to be the graph $(\mathcal{A}_1 \cup \mathcal{A}_2, \Gamma_1 \cup \Gamma_2)$.

(ii) Even if $S_j(e_k)$ coincides with $S_{j'}(e_{k'})$ as oriented line segment, they should regarded as different edges, since $(e_k, S_j) \neq (e_{k'}, S_{j'})$.

3.3.1. Refined graph and edge-to-trail substitution. Let G_i be the union of affine images of Λ_j under S_e for $e \in \Gamma_{ij}$, that is,

$$G_i = \bigcup_{j=1}^{N} \bigcup_{e\in\Gamma_{ij}} S_e(\Lambda_j), \tag{3.14}$$

and we call it the *refined graph induced by* $\{\Lambda_i\}_{i=1}^N$.

For $1 \le i \le N$, let τ_i be a mapping from Λ_i to trails of G_i; we shall denote $\tau_i(u)$ by P_u^i to emphasize that $\tau_i(u)$ is a trail in G_i. We call τ_i an *edge-to-trail substitution*, if for all $u \in \Lambda_i$, P_u^i has the same origin and terminus as u.

An edge-to-trail substitution τ_i can be thought as replacing each big edge u by a trail P_u^i consisting of small edges. Our goal is to show that the edge-to-trail substitution can produce a linear GIFS.

LEMMA 3.16. *The refine graph G_i admits Euler tours for all $1 \le i \le N$.*

PROOF. The Lemma can be proved in the same way as [**22**, Lemma 5.1]. In fact, we apply the idea for each i. □

3.3.2. Iteration of edge-to-trail substitutions. We use the following two rules to iterate τ_i:

(i) For $I \in \Gamma_i^*$ and $u \in \Lambda_i$, if $\tau_i(u) = \gamma_1 + \cdots + \gamma_\ell$, we set

$$\tau_i(S_I(u)) = S_I(\gamma_1) + \cdots + S_I(\gamma_\ell); \tag{3.15}$$

(ii) Let

$$L = T_1(\gamma_1) + T_2(\gamma_2) \cdots + T_k(\gamma_k)$$

be a trail in G_i where $T_j \in \mathcal{G}, \gamma_j \in \bigcup_{i=1}^N \Lambda_i$. We define $\tau_i(L)$ to be the trail

$$\tau_i(L) = T_1(\tau_{h(\gamma_1)}(\gamma_1)) + T_2(\tau_{h(\gamma_2)}(\gamma_2)) + \cdots + T_k(\tau_{h(\gamma_k)}(\gamma_k)),$$

where $h(\gamma)$ denotes the initial vertex of an edge γ.

Hence, we can define $\tau_i^n(u)$ recurrently, which is a trail consisting of small edges. Geometrically, we can explain $\tau_i^n(u)$ as an oriented broken line which provides an approximation of the corresponding SFC of E_i.

3.3.3. The edge-to-trail substitution induces linear GIFS. In this part, we will define the induced GIFS from the edge-to-trail substitution and we shall prove that this is a linear GIFS. Actually, the method using here is the same as we did for constructing SFC for self-similar sets [**22**]. Here we repeat the procedure for each refined graph G_i, that is to say, for each i, we can find a partition

$$G_i = P_1^i + \cdots + P_{m_i}^i$$

such that P_j^i is a trail from a_{ij} to $a_{i(j+1)}$. (Here we consider G_i as a union of all edges in G_i.)

For $i \in V$, let $\tau_i : u \mapsto P_u^i, u \in \Lambda_i$ be an edge-to-trail substitution defined in Section 3.3.1. By the construction, the trail P_u^i can be written as

$$P_u^i = S_{u,1}(v_{u,1}) + \cdots + S_{u,\ell_u}(v_{u,\ell_u}), \tag{3.16}$$

where $S_{u,j} \in \{S_e;\ e \in \Gamma_i\}$ and $v_{u,j} \in \{\Lambda_{t(e)}; e \in \Gamma_i\}$ for $j = 1, \ldots, \ell_u$.

According to τ_i we can construct an ordered GIFS as follows. Replacing P_u^i by E_u on the left hand side, and replacing v by E_v on the right hand side of (3.16), we obtain an ordered GIFS:

$$E_u \mathrel{\mathring{=}} S_{u,1}(E_{v_{u,1}}) + \cdots + S_{u,\ell_u}(E_{v_{u,\ell_u}}), \quad u \in \Lambda_i, \tag{3.17}$$

which we call the *induced GIFS* of τ_i. In an ordered GIFS, we use " $+$ " to replace the "$\cup$" in the set equation to emphasis the order structure. And $\mathring{=}$ is to show the order of the right hand side.

For $i \in V$, we use a new notation

$$(\Lambda_i, \mathcal{E}_i, \mathcal{G}_i, \prec) \tag{3.18}$$

to denote the ordered GIFS given by equation (3.17). Here we use Λ_i to denote the state set which is the edges of the initial graph and the edge set $\mathcal{E}_i$ consists of quadruples (u, S_e, v, k), *i.e.* , if $S_e(v)$ is the k-th edge in the trail P_u^i, then it is an edge of $\mathcal{E}_i$ and we mark this edge by

$$(u, S_e, v, k) \in \mathcal{E}_i. \tag{3.19}$$

The contraction associated with this edge is S_e.

THEOREM 3.17. *The induced GIFS* (3.17) *is a linear GIFS for every* i.

PROOF. Let $u \in \Lambda_i$. We denote by a_u and b_u the origin and the terminus of u as an edge in the initial graph Λ_i. We claim that the lowest and highest elements in Γ_u^∞ are codings of a_u and b_u, respectively.

Let $S(v)$ be the first edge in P_u^i, then $\omega = (u, S, v, 1)$ is the lowest edge emanating from u in Γ_u. It follows that

$$a_u = S(a_v). \tag{3.20}$$

Therefore, if $(\omega_n)_{n=1}^\infty$ is a coding of a_v, then

$$\omega(\omega_n)_{n-1}^\infty$$

is a coding of a_u. Applying the same argument to v, we obtain a coding of a_u, such that the first two edges of this coding is the lowest walk in Γ_u^2. Continuing this argument, we conclude the lowest element in Γ_u^∞ is a coding of a_u.

Similarly, the highest element in Γ_u^∞ is a coding of b_u.

Now, let $\omega = (u, S, v, k)$ and $\gamma = (u, T, v', k+1)$ be two consecutive edges in Γ_u. This means that $S(v)$ and $T(v')$ are two adjacent edges in P_u^i, so $S(b_v) = T(a_{v'})$.

On the other hand, since $\omega(\omega_n)_{n\geq 1}$ is highest coding in Γ_u^∞ , $(\omega_n)_{n\geq 1}$ is the highest coding in Γ_v. So $\pi_v((\omega_n)_{n\geq 1}) = b_v$ by the claim above, and

$$\pi_u(\omega(\omega_n)_{n\geq 1}) = S \circ \pi_v((\omega_n)_{n\geq 1}) = S(b_v).$$

Similarly, we have $\pi_u(\gamma(\gamma_n)_{n\geq 1}) = T(a_{v'})$ if $\gamma(\gamma_n)_{n\geq 1}$ is the lowest coding of Γ_u^∞. This verifies the chain condition. Therefore, the ordered GIFS in consideration is linear. □

REMARK 3.18. The construction in this Section is designed for a GIFS, but we can apply the theory for a self-affine set if we regard an IFS as a GIFS with only one vertex and several self-edges. Later in Section 3.4, we will apply the construction for the unit square and the McMullen set.

3.4. Some simple examples for constructing SFCs

In this part, we will start to construct some examples to show how the theoretical parts introduced previous sections come true. In the following examples, we always use $\mathbf{e}_1, \mathbf{e}_2$ to denote the standard basis of $\mathbb{R}^2$. Denote the maximal eigenvalue of the associated matrix A by λ_A. And denote by the Hölder exponent (in the sense of Corollary 3.6)with respect to Euclidean norm $\text{Hölder}_{\mathcal{E}}$.

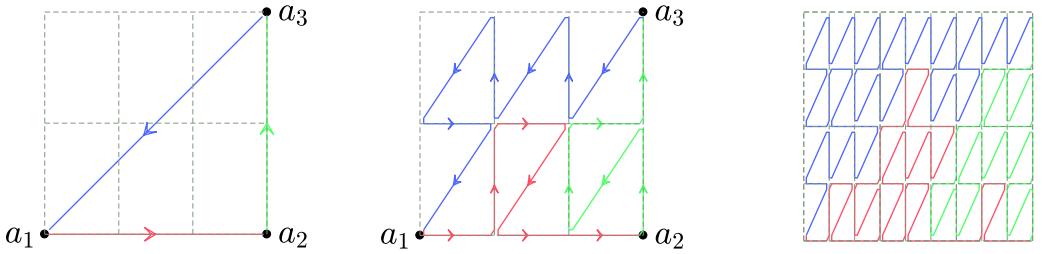

(a) Initial cycle. (b) First generation. (c) Second generation.

FIGURE 29. The edge-to-trail substitution for unit square.

EXAMPLE 1 (**A unit square**). Let Q be the unit square generated by the IFS $S_i(x) = M^{-1}(x + d_i)$, $d_i \in \mathcal{D}$, where $\mathcal{D} = \{0, \mathbf{e}_2, \mathbf{e}_1 + \mathbf{e}_2, \mathbf{e}_1, 2\mathbf{e}_1, 2\mathbf{e}_1 + \mathbf{e}_2\}$, and the expanding matrix is $M = \begin{pmatrix} 3 & 0 \\ 0 & 2 \end{pmatrix}$, (see Figure 26 (a)). Let a_1, a_2, a_3 be the three vertice of the unit square, then it is easy to check that $A = \{a_1, a_2, a_3\}$ is a skeleton of Q. Let Λ be the cycle passing by a_1, a_2, a_3 in turn (see Figure 29(a)). Denote by v_i the edge from a_i to $a_{i+1}, i = 1, 2, 3$ (assume $a_4 = a_1$). We have the refined graph $G = S_1(\Lambda) \cup \cdots \cup S_6(\Lambda)$. Clearly, we can find an Euler tour P with a partition $P = P_1 + P_2 + P_3$ in G such that P_i has the same origin and terminus as v_i for $i = 1, 2, 3$ (see Figure 29(b)). Then we have the following edge-to-trial substitution τ.

$$
\begin{aligned}
v_1 &\longrightarrow S_1(v_1) + S_1(v_2) + S_3(v_1) + S_4(v_3) + S_4(v_1) + S_5(v_1), \\
v_2 &\longrightarrow S_5(v_2) + S_5(v_3) + S_4(v_2) + S_6(v_1) + S_6(v_2), \\
v_3 &\longrightarrow S_6(v_3) + S_3(v_2) + S_3(v_3) + S_2(v_2) + S_2(v_3) + S_2(v_1) + S_1(v_3),
\end{aligned} \tag{3.21}
$$

where we use the symbol $'+'$ to connect the consecutive edges or sub-trails. Then the induced GIFS obtained the above substitution can be showed in the following set equation form.

$$
\begin{aligned}
E_1 &\triangleq S_1(E_1) + S_1(E_2) + S_3(E_1) + S_4(E_3) + S_4(E_1) + S_5(E_1), \\
E_2 &\triangleq S_5(E_2) + S_5(E_3) + S_4(E_2) + S_6(E_1) + S_6(E_2), \\
E_3 &\triangleq S_6(E_3) + S_3(E_2) + S_3(E_3) + S_2(E_2) + S_2(E_3) + S_2(E_1) + S_1(E_3).
\end{aligned}
$$

By Theorem 3.17, the above induced GIFS is a linear GIFS, or we can check it by Lemma 3.3 directly. Figure 30 shows us the induced GIFS with three vertice $\{v_1, v_2, v_3\}$ and the edges.

The associated matrix of the substitution which is defined as the associated matrix of the directed graph G obtained by the substitution is

$$A = \begin{pmatrix} 4 & 1 & 1 \\ 1 & 3 & 2 \\ 1 & 1 & 4 \end{pmatrix}, \quad \lambda_A = 6, \quad \text{Hölder}_{\mathcal{E}} = \log_6 2.$$

Compared with the unit square parametrized using the method as Hilbert or Peano which have the Hölder exponent $\frac{1}{2}$, the parametrization obtained here doesn't have a better smoothness.

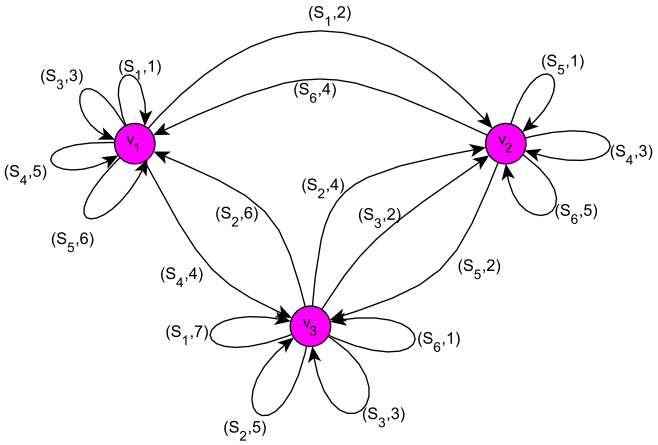

FIGURE 30. The directed graph G with vertex set $\{v_1, v_2, v_3\}$ and labelled edges obtained by the substitution rule (3.21). The label (S, i) with $S \in \{S_i\}_{i=1}^6$ and $i \in \mathbb{N}$ means that S is the contraction for the i-th edge starting from this vertex. The graph here determins a GIFS.

EXAMPLE 2 (**Dekking's plane filling curve** [**24**]). It is induced by the following substitution:

$$\sigma: \quad a \mapsto abadadab; \quad b \mapsto cbcbadab; \quad c \mapsto cbcbcdadcbcd; \quad d \mapsto adcd.$$

Denote $M = \begin{pmatrix} 4 & 0 \\ 0 & 2 \end{pmatrix}$ to be an expanding matrix. Through the substitution σ, we obtain an ordered GIFS by the set equation as follows.

$$\begin{aligned}
ME_a &\triangleq E_a + (E_b + \mathbf{e}_1) + (E_a + \mathbf{e}_1 + \mathbf{e}_2) \cup (E_d + 2\mathbf{e}_1 + \mathbf{e}_2) + (E_a + 2\mathbf{e}_1) + \\
&\quad (E_d + 3\mathbf{e}_1) + (E_a + 3\mathbf{e}_1 - \mathbf{e}_2) + (E_b + 4\mathbf{e}_1 - \mathbf{e}_2), \\
ME_b &\triangleq E_c + (E_b - \mathbf{e}_1) + (E_c - \mathbf{e}_1 + \mathbf{e}_2) + (E_b - 2\mathbf{e}_1 + \mathbf{e}_2) + (E_a - 2\mathbf{e}_1 + 2\mathbf{e}_2) + \\
&\quad (E_d - \mathbf{e}_1 + 2\mathbf{e}_2) + (E_a - \mathbf{e}_1 + \mathbf{e}_2) + (E_b + \mathbf{e}_2), \\
ME_c &\triangleq E_c + (E_b - \mathbf{e}_1) + (E_c - \mathbf{e}_1 + \mathbf{e}_2) + (E_b - 2\mathbf{e}_1 + \mathbf{e}_2) + (E_c - 2\mathbf{e}_1 + 2\mathbf{e}_2) + \\
&\quad (E_d - 3\mathbf{e}_1 + 2\mathbf{e}_2) + (E_a - 3\mathbf{e}_1 + \mathbf{e}_2) + (E_d - 2\mathbf{e}_1 + \mathbf{e}_2) + (E_c - 2\mathbf{e}_1) + \\
&\quad (E_b - 3\mathbf{e}_1) + (E_c - 3\mathbf{e}_1 + \mathbf{e}_2) + (E_d - 4\mathbf{e}_1 + \mathbf{e}_2), \\
ME_d &\triangleq E_a + (E_d + \mathbf{e}_1) + (E_c + \mathbf{e}_1 - \mathbf{e}_2) + (E_d - \mathbf{e}_2).
\end{aligned}$$

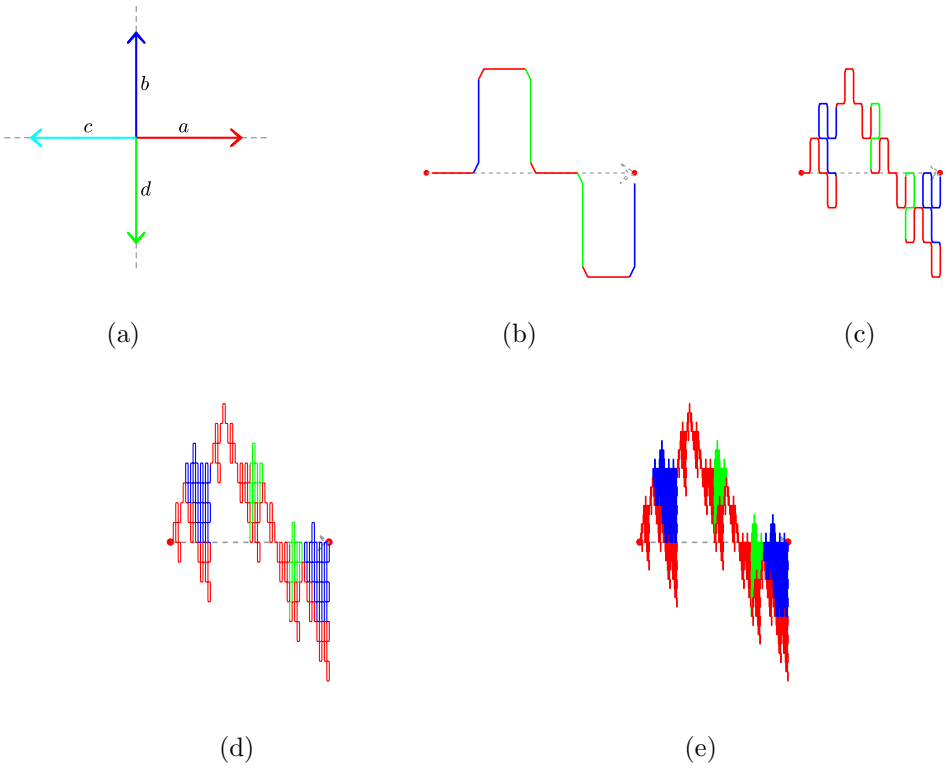

FIGURE 31. The figures (b), (c),(d),(e) show the first four approximation of E_a.

Moreover, the associated matrix of the substitution is

$$A = \begin{pmatrix} 4 & 2 & 1 & 1 \\ 2 & 3 & 3 & 0 \\ 0 & 2 & 5 & 1 \\ 2 & 1 & 3 & 2 \end{pmatrix}, \quad \lambda_A = 8, \quad \text{Hölder}_{\mathcal{E}} = \frac{1}{3}.$$

Then we can check that $\text{Hölder}_{\mathcal{E}}$ is between the two Hölder exponents obtained by Corollary 3.6.

We can check the ordered GIFS induced by the substitution σ is linear by the chain condition. To check the chain condition, we need to calculate the heads and tails of E_a, E_b, E_c, E_d. We denote the head of a set K by $h(E)$ and tail of a set $t(E)$. Then we have

$$h(E_a) = 0,\ t(E_a) = \mathbf{e}_1,\ h(E_b) = 0,\ t(E_b) = \mathbf{e}_2,$$
$$h(E_c) = 0,\ t(E_c) = -\mathbf{e}_1,\ h(E_d) = 0,\ t(E_d) = -\mathbf{e}_2.$$

Thus it is easy to check that it satisfies the chain condition. Figure 31 shows the proceeding of filling curve of E_a.

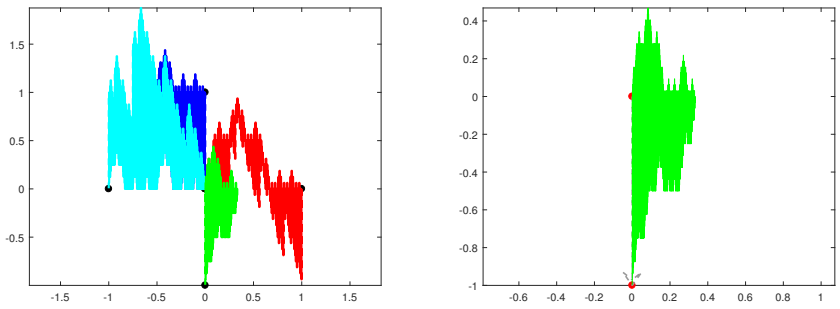

FIGURE 32. The left figure is $E = E_a \cup E_b \cup E_c \cup E_d$, and the right one is E_d. Example 2.

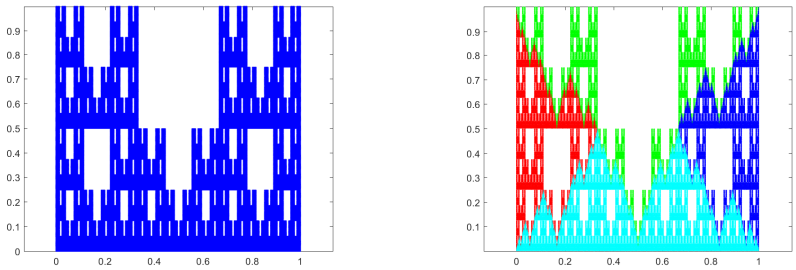

FIGURE 33. The left is Mcmullen set T and the right is $\cup_{i=1}^{5} E_i$.

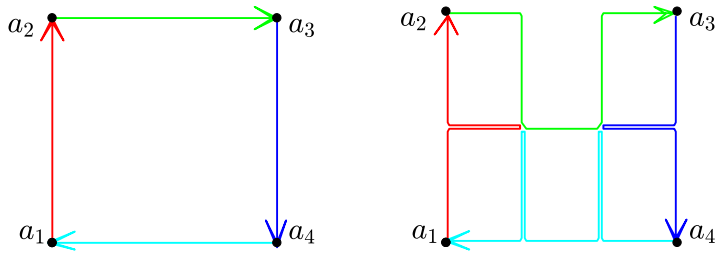

(a) (b)

FIGURE 34. Substitution rule of the Mcmullen set

EXAMPLE 3 (**A McMullen set [68]**). Denote $M = \begin{pmatrix} 3 & 0 \\ 0 & 2 \end{pmatrix}$ to be the expanding matrix. The McMullen set T (see Figure 33, left) is given by $T = \bigcup_{i=1}^{5} S_i(T)$ with

$$\left\{ S_i(x) = M^{-1}(x + d_i) \right\}_{i=1}^{5}, \quad d_1 = 0, d_2 = \mathbf{e}_1, d_3 = 2\mathbf{e}_1, d_4 = \mathbf{e}_2, d_5 = \mathbf{e}_1 + \mathbf{e}_2.$$

Denote the four vertices of the unit square by a_1, a_2, a_3, a_4. Then $A = \{a_1, \ldots, a_4\}$ is a skeleton of T. Let Λ be a cycle passing by $a_1, \ldots, a_4$ one by one (Figure 34 (a)). Denote $v_i = \overrightarrow{a_i a_{i+1}}, i = 1, 2, 3, 4$ (assume $a_5 = a_1$). Then we have the refined graph $G = S_1(\Lambda) \cup S_2(\Lambda) \cup S_3(\Lambda) \cup S_4(\Lambda)$, and an Euler tour $P = P_1 + P_2 + P_3 + P_4$ of G

and P_i is the trial sharing the same origin and terminus with v_i (see Figure 34 (b)). Then we have the following edge-to-trail substitution τ.

$$\begin{aligned}
v_1 &\longrightarrow S_1(v_1) + S_1(v_2) + S_4(v_4) + S_4(v_1),\\
v_2 &\longrightarrow S_4(v_2) + S_4(v_3) + S_2(v_2) + S_5(v_1) + S_5(v_2),\\
v_3 &\longrightarrow S_5(v_3) + S_5(v_4) + S_3(v_2) + S_3(v_3),\\
v_4 &\longrightarrow S_3(v_4) + S_3(v_1) + S_2(v_3) + S_2(v_4) + S_2(v_1) + S_1(v_3) + S_1(v_4).
\end{aligned}$$

Then we obtain the following set equation form of an ordered GIFS.

$$\begin{aligned}
E_1 &\triangleq S_1(E_1) + S_1(E_2) + S_4(E_4) + S_4(E_1),\\
E_2 &\triangleq S_4(E_2) + S_4(E_3) + S_2(E_2) + S_5(E_1) + S_5(E_2),\\
E_3 &\triangleq S_5(E_3) + S_5(E_4) + S_3(E_2) + S_3(E_3),\\
E_4 &\triangleq S_3(E_4) + S_3(E_1) + S_2(E_3) + S_2(E_4) + S_2(E_1) + S_1(E_3) + S_1(E_4).
\end{aligned}$$

In the same way as Example 2, we check that the above GIFS satisfied the chain condition. Then it is a linear GIFS and clearly the open set condition is satisfied. Actually the union of the invariant sets $\bigcup_{i=1}^{4} E_i$ is the McMullen set T.

Moreover, the associated matrix of the substitution τ is

$$A = \begin{pmatrix} 2 & 1 & 0 & 2\\ 1 & 3 & 1 & 0\\ 0 & 1 & 2 & 2\\ 1 & 0 & 1 & 3 \end{pmatrix}, \quad \lambda_A = 5, \quad \text{Hölder}_{\mathcal{E}} = \log_5 2.$$

Figure 35 shows the visualization of the filling curve of the Mcmullen set T. To give a self-avoiding visualization, we round off the corners of the approximating curves.

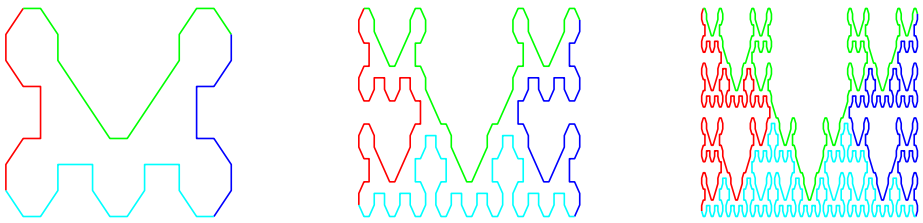

FIGURE 35. The first three approximations to the filling curve of Mcmullen set.

3.5. Construct SFCs for a class of self-affine tiles

In this section, we are interested in playing with the construction of the SFC for a class of self-affine tiles. There is a lot of work in the literature concentrated on tilings of $\mathbb{R}^n$ whose tiles are given by a finite collection of contractions. Among these, the self-affine tile is one of the most prevalent example. (For instance, the famous work by Thurston [**92**], Kenyon [**44**], Lagarias and Wang [**52, 51, 53**]. *etc.*, and reference therein.)

Assume that M is a 2×2 integer matrix which is expanding, *i.e.*, all of the eigenvalues are greater than 1 in modulus. Let $\mathcal{D} \in \mathbb{Z}^2$ be a set of cardinality

$|\det M|$ which is called digit set. By a result of Hutchinson [**37**], there is a unique nonempty compact subset $T = T(M, \mathcal{D})$ of $\mathbb{R}^2$ such that

$$MT = T + D.$$

If T has positive Lebesgue measure we call it a *self-affine tile*.

In this part, we focus on a class of self-affine tiles on $\mathbb{R}^2$ which we fix the expanding matrix M and digit set $\mathcal{D}$ as follows. For $0 < A \le B$ and $B \ge 2$, let

$$M = \begin{pmatrix} 0 & -B \\ 1 & -A \end{pmatrix} \text{ and } \mathcal{D} = \{0, e, 2e, \dots, (B-1)e\}, \tag{3.22}$$

where v is the vector $e = (1, 0)^t$. Then $T = T(M, D)$ is a self-affine tile (see [**55, 4**]) and tiles $\mathbb{R}^2$ by $\mathbb{Z}^2$, *i.e.*,

$$T + \mathbb{Z}^2 = \mathbb{R}^2 \text{ and } (T + \gamma)^\circ \cap (T + \omega)^\circ = \emptyset \text{ for } \gamma, \omega \in \mathbb{Z}^2.$$

We call it the *AB-tile*.

For the AB-tile, [**55**] also proved that the AB-tile is disklike if $2A < B + 3$; Moreover, [**4**] showed that for $2A < B + 3$ there exists exactly six points where T coincides with two other tiles. We will show later that these six points will play a crucial role in constructing the SFCs for the disklike AB-tiles. Actually, we will prove that the six points consist the skeleton of the AB-tile.

To continue our discussion, we shall introduce some new notations. Let $S_i(x) = M^{-1}(x + d_i)$ with $d_i = (i - 1, 0)^t \in \mathcal{D}$ be the contractions. Then the AB-tile can be written by

$$T = \bigcup_{i=1}^{B} S_i(T).$$

3.5.1. Neighbor of a self-affine tile. Let $T = T(M, \mathcal{D})$ be an AB-tile given by (3.22) and define the set of *neighbors* of T by

$$\mathcal{S} = \{\alpha \in \mathbb{Z}^2 \setminus \{0\};\ T \cap (T + \alpha) \neq \emptyset\}.$$

By a result of [**4**], we know that $\sharp\mathcal{S} = 6$ if $2A < B + 3$; precisely,

$$\mathcal{S} = \{(A, 1)^t, (A - 1, 1)^t, (-1, 0)^t, (1, 0)^t, (-A, -1)^t, (1 - A, -1)^t\}.$$

Furthermore, it also introduced the notion 2-*vertex* (or simply vertex) of T. A point $v \in T$ is called a vertex if v is contained in at least 2 other disjoint tiles differ from T. Precisely, the 2-vertex set of T is then defined by

$$V_2 = \bigcup_{s_1 \neq s_2 \in \mathcal{S}} \{v;\ v \in T \cap (T + s_1) \cap (T + s_2)\}.$$

Then it shows the following statement.

LEMMA 3.19. [**4**, Theorem 6.6] *Let T be an AB-tile with $2A < B+3$, then vertex set V_2 consists of exactly six points. Moreover, let*

$$\begin{aligned} \omega_1 &= (1AB)^\infty, \quad \omega_2 = ((B - A + 1)1B)^\infty, \\ \omega_3 &= (B1A)^\infty, \quad \omega_4 = (B(B - A + 1)1)^\infty, \\ \omega_5 &= (AB1)^\infty, \quad \omega_6 = (1B(B - A + 1))^\infty, \end{aligned} \tag{3.23}$$

be the infinite words in $\{1, 2, \ldots, B\}^\infty$*, then*

$$V_2 = \{\pi(\omega_1), \pi(\omega_2), \pi(\omega_3), \pi(\omega_4), \pi(\omega_5), \pi(\omega_6)\},$$

where π *is the projection from* $\{1, 2, \ldots, B\}^\infty$ *to* T *given by* (3.4)*.*

So far, we have given a simple description of neighbor and vertex of an AB-tile. Then we will show that the vertex set V_2 will build a bridge from the boundary to the curves filling an AB-tile. It is known that the concept skeleton plays an important role in constructing SFCs. Here we recommend [**77**] for the definition of the skeleton which is specially designed for a self-similar set; also, if we regard the AB-tile as an invariant set induced by a special GIFS with the directed graph having only one vertex, then the definition of skeleton is referenced to Section 3.1.4, Definition 3.9.

THEOREM 3.20. *Let* T *be an* AB*-tile with* $2A < B + 3$*. Then* V_2 *is a skeleton of* T*.*

PROOF. By the definition of V_2, it is clear that V_2 is a finite subset of T when A, B satisfy $2A < B + 3$. And by Lemma 3.19, we know that

$$V_2 \subset \bigcup_{i=1}^{B} S_i(V_2).$$

Indeed, it can be explained by the following relations.

$$S_B(\pi(\omega_1)) = \pi(B(\omega_1)) = \pi(\omega_3), \quad S_B(\pi(\omega_2)) = \pi(B(\omega_2)) = \pi(\omega_4),$$
$$S_A(\pi(\omega_3)) = \pi(A(\omega_3)) = \pi(\omega_5), \quad S_1(\pi(\omega_4)) = \pi(1(\omega_4)) = \pi(\omega_6),$$
$$S_1(\pi(\omega_5)) = \pi(1(\omega_5)) = \pi(\omega_1), \quad S_{B-A+1}(\pi(\omega_6)) = \pi((B - A + 1)(\omega_6)) = \omega_2.$$

The connectedness of the Hata graph $H(V_2)$ can be done by

$$S_i(V_2) \cap S_{i+1}(V_2) \neq \emptyset \text{ for } i = 1, 2, \ldots, B - 1.$$

□

3.5.2. Constructions of SFCs for AB-tiles. Recall that V_2 is the vertex set and by Theorem 3.20 and Lemma 3.19 we know that V_2 has six element and is a skeleton of the AB-tile. In this part, we will construct the SFC using the skeleton V_2 by edeg-to-trail substitution in Section 3.3. To illustrate the the procedure, we will start with an example.

EXAMPLE 4 (**The SFC of AB-tile with $A = 1, B = 3$**). In this example we consider the case for $A = 1, B = 3$. And we denote the vertex set by $V_2 = \{a_1, a_2, \ldots, a_6\}$ (see Figure 36 (a)). Let $v_i = \overrightarrow{a_i a_{i+1}}$, $i = 1, \ldots 6$ (assume $a_7 = a_1$). Then the initial graph is

$$\Lambda = \{v_1, \ldots, v_6\},$$

which is the cycle passing the $a_1, \ldots, a_6$ one by one. (See Figure 36 (a)). Thus the union of affine copy of Λ which we call refined graph is

$$G = \bigcup_{i=1}^{3} S_i(\Lambda).$$

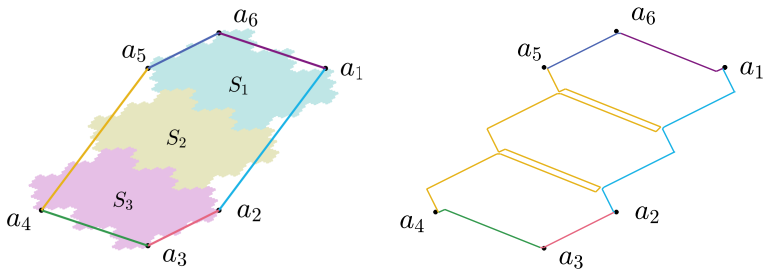

(a) Skeleton A and the initial graph Λ

(b) Refined graph and the partition

FIGURE 36. The AB-tile with $A = 1, B = 3$.

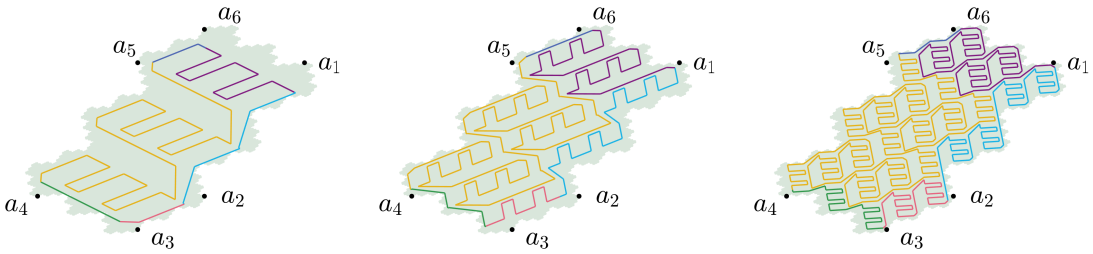

FIGURE 37. The approximating curves of AB-tile with $A = 1, B = 3$.

(See Figure 36 (b)). In Figure 36 (b) we use different color for the trails. Comparing the initial graph and the refined graph in Figure 36 (a) and (b), we get the edge-to-trail substitution

$$\begin{aligned}
v_1 &\longrightarrow S_1(v_5) + S_1(v_6) + S_2(v_5) + S_2(v_6) + S_3(v_5),\\
v_2 &\longrightarrow S_3(v_6),\\
v_3 &\longrightarrow S_3(v_1),\\
v_4 &\longrightarrow S_3(v_2) + S_3(v_3) + S_3(v_4) + S_2(v_1) + S_2(v_2) + S_2(v_3) + S_2(v_4) +\\
&\qquad S_1(v_1) + S_1(v_2),\\
v_5 &\longrightarrow S_1(v_3),\\
v_6 &\longrightarrow S_1(v_4).
\end{aligned} \tag{3.24}$$

Through the edge-to-trail substitution, we get the following induced GIFS.

$$\begin{aligned}
E_1 &\doteq S_1(E_5) + S_1(E_6) + S_2(E_5) + S_2(E_6) + S_3(E_5),\\
E_2 &\doteq S_3(E_6),\\
E_3 &\doteq S_3(E_1),\\
E_4 &\doteq S_3(E_2) + S_3(E_3) + S_3(E_4) + S_2(E_1) + S_2(E_2) + S_2(E_3)\\
&\qquad + S_2(E_4) + S_1(E_1) + S_1(E_2),\\
E_5 &\doteq S_1(E_3),\\
E_6 &\doteq S_1(E_4).
\end{aligned} \tag{3.25}$$

We can check that the ordered GIFS above is a linear GIFS by Lemma 3.4 checking the chain condition. In fact, by the set equation, we only need to calculate the heads and the trails of E_1 and E_4 and others can be obtained accordingly. Then by Theorem 3.5 the AB-tile admits an optimal parametrizaition. See Figure 37 for the approximating curves of it.

3.5.3. The general case. Our aim is to construct the SFCs of AB-tiles for all parameters A, B satisfying $2A < B + 3$. We know that every AB-tile in the family has a skeleton V_2 which we denote by $V_2 = \{a_1, a_2, \ldots, a_6\}$. Let Λ be the cycle passing $a_1, \ldots, a_6$ in turn. Let $G = \bigcup_{i=1}^{B} S_i(\Lambda)$ be the refined graph. We observe that there always exists an Euler tour P with a partition $P = P_1 + P_2 + \cdots + P_6$ of the refined graph G as follows.

$$
\begin{cases}
P_1 = \displaystyle\sum_{i=1}^{B-A} \Big(S_i(v_5) + S_i(v_6) \Big) + S_{B-A+1}(v_5), \\
P_2 = S_{B-A+1}(v_6) + \displaystyle\sum_{i=2}^{A} \Big(S_{B-A+i}(v_5) + S_{B-A+i}(v_6) \Big), \\
P_3 = S_B(v_1), \\
P_4 = \displaystyle\sum_{i=1}^{B-A} \Big(S_{B+1-i}(v_2) + S_{B+1-i}(v_3) + S_{B+1-i}(v_4) + S_{B-i}(v_1) \Big) + S_A(v_2), \\
P_5 = S_A(v_3) + \displaystyle\sum_{i=1}^{A-1} \Big(S_{A-i+1}(v_4) + S_{A-i+1}(v_1) + S_{A-i+1}(v_2) + S_{A-i}(v_3) \Big), \\
P_6 = S_1(v_4).
\end{cases} \tag{3.26}
$$

It is clear that the above equation is determined by A, B. Then we have the related edge-to-trail substitution

$$
\tau : v_i \longrightarrow P_i \text{ for } i = 1, 2, \ldots, 6. \tag{3.27}
$$

Thus we can obtain the following induced ordered GIFS.

$$
\begin{aligned}
E_1 &\triangleq \sum_{i=1}^{B-A} \Big(S_i(E_5) + S_i(E_6) \Big) + S_{B-A+1}(E_5), \\
E_2 &\triangleq S_{B-A+1}(E_6) + \sum_{i=2}^{A} \Big(S_{B-A+i}(E_5) + S_{B-A+i}(E_6) \Big), \\
E_3 &\triangleq S_B(E_1), \\
E_4 &\triangleq \sum_{i=1}^{B-A} \Big(S_{B+1-i}(E_2) + S_{B+1-i}(E_3) + S_{B+1-i}(E_4) + S_{B-i}(E_1) \Big) + S_A(E_2), \\
E_5 &\triangleq S_A(E_3) + \sum_{i=1}^{A-1} \Big(S_{A-i+1}(E_4) + S_{A-i+1}(E_1) + S_{A-i+1}(E_2) + S_{A-i}(E_3) \Big), \\
E_6 &\triangleq S_1(E_4).
\end{aligned} \tag{3.28}
$$

And it is easy to check that the ordered GIFS above is a linear GIFS. Indeed, the head and the trail of E_i are as follows.

$$
\begin{aligned}
&h(E_1) = \mathrm{Fix}(S_1 \circ S_A \circ S_B), && t(E_1) = \mathrm{Fix}(S_{B-A+1} \circ S_1 \circ S_B),\\
&h(E_2) = \mathrm{Fix}(S_{B-A+1} \circ S_1 \circ S_B), && t(E_2) = \mathrm{Fix}(S_B \circ S_1 \circ S_A),\\
&h(E_3) = \mathrm{Fix}(S_B \circ S_1 \circ S_A), && t(E_3) = \mathrm{Fix}(S_B \circ S_{B-A+1} \circ S_1),\\
&h(E_4) = \mathrm{Fix}(S_B \circ S_{B-A+1} \circ S_1), && t(E_4) = \mathrm{Fix}(S_A \circ S_B \circ S_1),\\
&h(E_5) = \mathrm{Fix}(S_A \circ S_B \circ S_1), && t(E_5) = \mathrm{Fix}(S_1 \circ S_B \circ S_{B-A+1}),\\
&h(E_6) = \mathrm{Fix}(S_1 \circ S_B \circ S_{B-A+1}), && t(E_6) = \mathrm{Fix}(S_1 \circ S_A \circ S_B).
\end{aligned}
\tag{3.29}
$$

Apparently, it satisfies the chain condition.

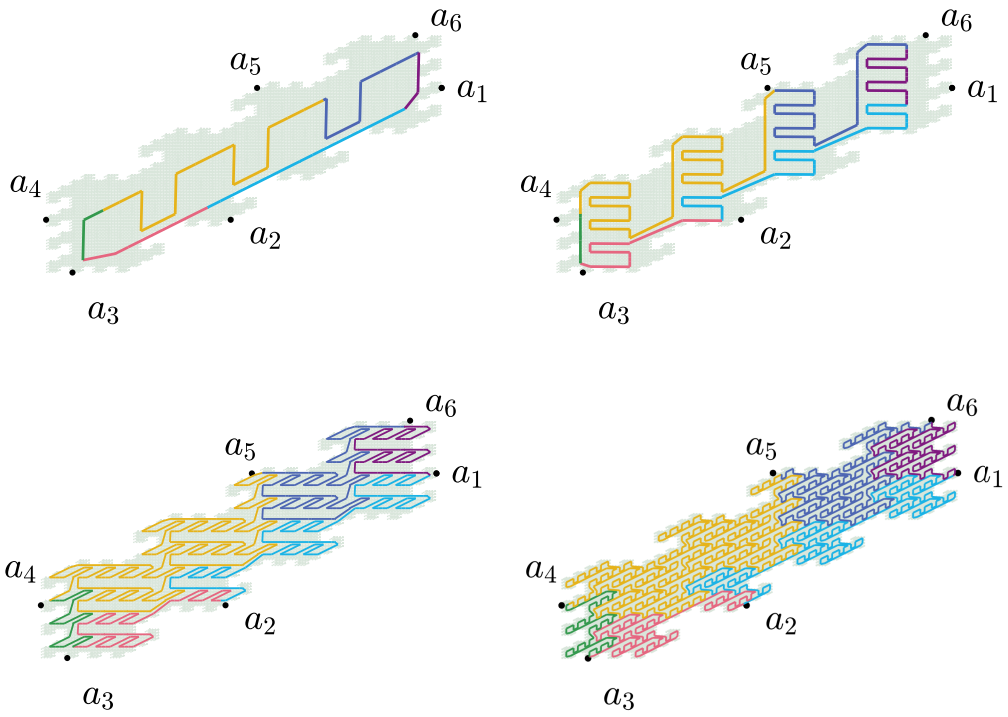

FIGURE 38. The approximating curves of AB tile with $A = 2, B = 4$.

From the induced GIFS (3.28), we have

$$T = \cup_{i=1}^{6} E_i,$$

by the uniqueness of $T = \cup_{i=1}^{B} S_i(T)$, and the right hand side is disjoint union. Moreover, it is easy to check the associated matrix of the induced GIFS is primitive.

According the partition (3.26) of the refined graph and the edge-to-trail substitution (3.27) we can construct the approximating curves of AB-tiles. To get a beautiful visualization and construct self-avoiding curves we can always choose suitable initial pattern. There are many example to show. Here we list some of them. See Figure 37, Figure 4, Figure 38 and Figure 39.

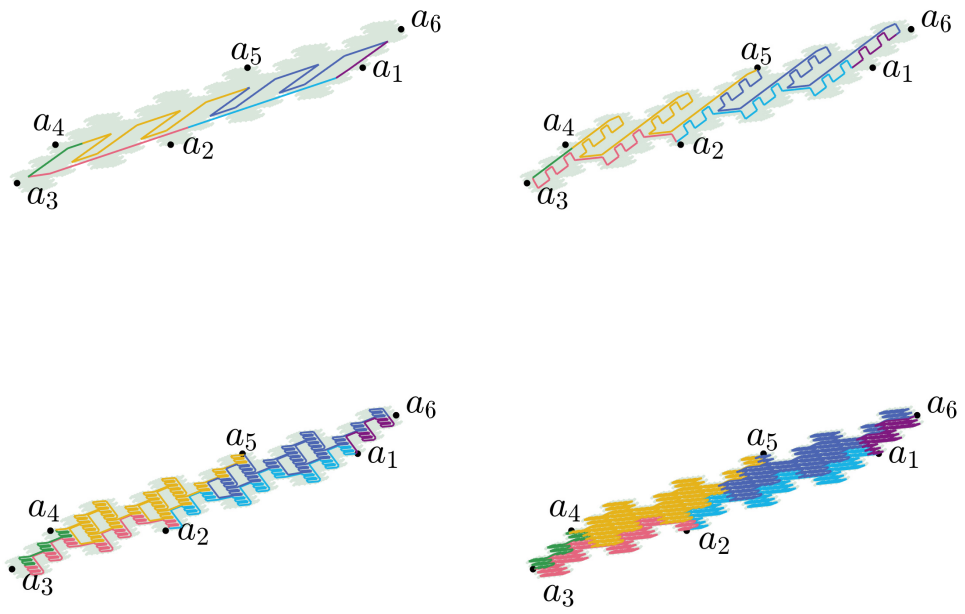

FIGURE 39. The approximating curves of AB tile with $A = 3, B = 5$.

3.6. Construct SFCs for a Rauzy fractal

Rauzy fractals play a major role in many branches of mathematics including number theory, dynamical systems, combinatorics and the theory of quasicrystals (See for instance[**78, 92, 36, 6**]). In this section, we will focus us on constructing the SFCs of the Rauzy fractal with an example.

By the study of Rauzy fractal, for instance [**84, 74, 75**], we know that the Rauzy fractal can be generated by a graph-directed GIFS. Then we can use the method which we introduce in Section 3.3 to construct the SFCs. To do this, the most important task is to find the skeleton of the Rauzy fractal and then we construct an edge-to-trail substitution producing a linear GIFS. In the rest of the Section, we will focus on the following example.

3.6.1. The classical Rauzy fractal. The classical example of Rauzy fractal is given by the so-called Tribonacci substitution defined as

$$\sigma_1 : \begin{array}{l} 1 \longrightarrow 12 \\ 2 \longrightarrow 13 \\ 3 \longrightarrow 1, \end{array} \qquad \text{associated matrix: } M_{\sigma_1} = \begin{pmatrix} 1 & 1 & 1 \\ 1 & 0 & 0 \\ 0 & 1 & 0 \end{pmatrix},$$

which is first studied by Rauzy [**78**]. After that there are many generalizations of the construction such as [**7, 88, 14, 75**]. The characteristic polynomial of M_{σ_1} is $x^3 - x^2 - x - 1$. Let β be the Pisot number satisfying $\beta^3 = \beta^2 + \beta + 1$. And denote the algebraic conjugates of β by $\beta', \bar{\beta}'$, where $\bar{a}$ is the conjugate of a complex number

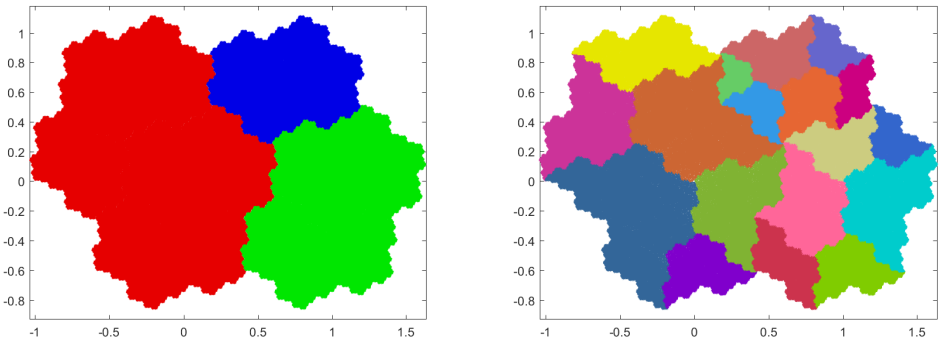

FIGURE 40. Classical Rauzy fractal (left) and the parametrized Rauzy fractal (right).

a. Denote

$$B = \begin{pmatrix} \text{Re } \beta' & -\text{Im } \beta' \\ \text{Im } \beta' & \text{Re } \beta' \end{pmatrix}.$$

By the idea of [**75**], Rauzy fracatal can be regard as the invariant sets of the following GIFS

$$\begin{aligned} X_1 =& BX_1 \cup BX_2 \cup BX_3, \\ X_2 =& BX_1 + e_1, \\ X_3 =& BX_2 + e_1, \end{aligned} \tag{3.30}$$

where $e_1 = (1, 0)^t$.

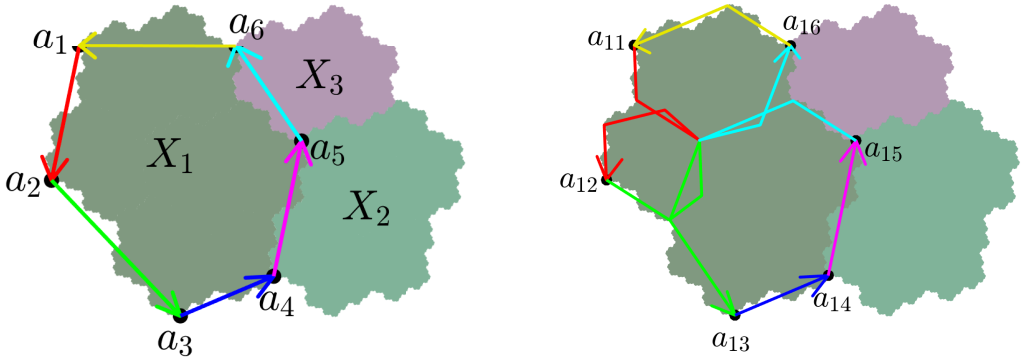

(a) (b)

FIGURE 41. (*a*): we only show part of the skeleton $\{a_{11}, \ldots, a_{16}\}$ of X_1. (*b*): show the edge-to-trail substitution σ_1 for X_1. It obtains by replacing the line segment by the same color broken lines. For X_2 and X_3, we can do in the same way.

3.6.1.1. **Skeleton**. To find a skeleton of a self-similar set, Rao and Zhang [**77**] introduce an algorithm which use the neighbor graph of self-similar sets satisfying the *finite type condition* to get the skeleton. For a graph-directed IFS, it is rather difficult to give such an algorithm. We will only focus on this example and give a set of points which can be proved being a skeleton.

For simplicity, we set

$$f_{11}(x) = f_{12}(x) = f_{13}(x) = Bx, \qquad f_{21}(x) = f_{32}(x) = Bx + e_1.$$

Then the set equation (3.30) has the following form.

$$\begin{aligned} X_1 =& f_{11}(X_1) \cup f_{12}(X_2) \cup f_{13}(X_3), \\ X_2 =& f_{21}(X_1), \\ X_3 =& f_{32}(X_2), \end{aligned} \tag{3.31}$$

Denote

$$\begin{aligned} &a_{11} = (I - B^3)^{-1} \cdot (Be_1), \quad a_{12} = (I - B^3)^{-1} \cdot (B^2e_1 + Be_1), \\ &a_{13} = (I - B^3)^{-1} \cdot (B^2e_1), \quad a_{14} = (I - B^3)^{-1} \cdot (B^3e_1 + B^2e_1), \\ &a_{15} = (I - B^3)^{-1} \cdot (B^3e_1), \quad a_{16} = (I - B^3)^{-1} \cdot (B^3e_1 + Be_1 - B^4e_1), \end{aligned}$$

where we use I for the 2×2 identity matrix, and P^{-1} is the inverse of the matrix P. Let

$$A_1 = \{a_{11}, a_{12}, a_{13}, a_{14}, a_{15}, a_{16}\}, A_2 = f_{21}(A_1) \text{ and } A_3 = f_{32}(A_2). \tag{3.32}$$

Then we will check that A_1, A_2, A_3 is a skeleton of the invariant X_1, X_2, X_3. First we show that $A_i \in X_i$ for $i \in \{1, 2, 3\}$. It is easy to check that A_1 is in X_1 since

$$\begin{aligned} &a_{11} = \mathrm{Fix}(f_{12} \circ f_{21} \circ f_{11}), \quad a_{12} = \mathrm{Fix}(f_{13} \circ f_{32} \circ f_{21}), \\ &a_{13} = f_{11}(a_{11}), \qquad\qquad a_{14} = f_{11}(a_{12}), \\ &a_{15} = f_{11}(a_{13}), \qquad\qquad a_{16} = f_{12} \circ f_{21}(a_{11}), \end{aligned} \tag{3.33}$$

where we use $\mathrm{Fix}(f)$ to denote the fixed point of contractible mapping f. Then we have a_{11}, a_{12} as well as a_{13}, a_{14}, a_{15} and a_{16} are elements of X_1. Second, we check that

$$A_1 \subset f_{11}(A_1) \cup f_{12}(A_2) \cup f_{13}(A_3).$$

This follows from

$$a_{11} \in f_{12}(A_2),\ a_{12} \in f_{13}(A_3),\ a_{13}, a_{14}, a_{15} \in f_{11}(A_1) \text{ and } a_{16} \in\ f_{12}(A_2).$$

Finally, we should check the connectedness of the Hata graph $H(A_j)$. Actually, $f_{11}(A_1), f_{12}(A_2)$ and $f_{13}(A_3)$ have a comment point (see Figure 41 (b)). Then it is clear that $H(A_1)$ is connected. The Hata graphs $H(A_i)$ for $i = 2, 3$ share the same connected property with $H(A_1)$.

Remark 3.21. From the skeleton obtained here, we know that it belongs to the boundary of the subdivision $X_1, X_2,$ and X_3.

3.6.1.2. **Edge-to-trail substitution and linear GIFS**. In this part, we will construct the edge-to-trail substitution from the skeleton which we obtain in the previous subsection.

Let A_1, A_2, A_3 be the skeleton of X_1, X_2, X_3 which we get from (3.32). We denote by

$$A_1 := \{a_{11}, a_{12}, \dots, a_{16}\}, A_2 := \{a_{21}, a_{22}, \dots, a_{26}\}, A_3 := \{a_{31}, a_{32}, \dots, a_{36}\}.$$

For $i \in \{1, 2, 3\}$, let Λ_i be the cycle passing $a_{i1}, a_{i2}, \dots, a_{i6}$ one by one. Denote the edge from a_{ij} to a_{ij+1} by $u_{ij} = \overrightarrow{a_{ij}a_{ij+1}}$ for $j \in \{1, 2, \dots 6\}$. Here $a_{i7} = a_{i1}$. Then we construct the refined graph G_i induced by (3.31). Here we only need to consider the case for $i = 1$. By (3.14), we have

$$G_1 = f_{11}(\Lambda_1) \cup f_{12}(\Lambda_2) \cup f_{13}(\Lambda_3).$$

Hence there exists an Euler tour P_1 of G_1 with a partition $P_1 = P_1^1 + P_2^1 + \cdots + P_6^1$ such that P_i^1 has the same origin and terminus as u_{1i}. (See Figure 41 (b).) Then we obtain the following edge-to-trail substitution τ_1.

$$\begin{aligned}
u_{11} &\longrightarrow f_{12}(u_{23}) + f_{12}(u_{24}) + f_{13}(u_{35}) + f_{13}(u_{36}) + f_{13}(u_{31}),\\
u_{12} &\longrightarrow f_{13}(u_{32}) + f_{13}(u_{33}) + f_{13}(u_{34}) + f_{11}(u_{15}) + f_{11}(u_{16}),\\
u_{13} &\longrightarrow f_{11}(u_{11}),\\
u_{14} &\longrightarrow f_{11}(u_{12}),\\
u_{15} &\longrightarrow f_{11}(u_{13}) + f_{11}(u_{14}) + f_{12}(u_{25}) + f_{12}(u_{26}),\\
u_{16} &\longrightarrow f_{12}(u_{21}) + f_{12}(u_{22}).
\end{aligned} \tag{3.34}$$

The ordered GIFS given by the substitution τ_1 is

$$\begin{aligned}
E_{u_{11}} &= f_{12}(E_{u_{23}}) + f_{12}(E_{u_{24}}) + f_{13}(E_{u_{35}}) + f_{13}(E_{u_{36}}) + f_{13}(E_{u_{31}}),\\
E_{u_{12}} &= f_{13}(E_{u_{32}}) + f_{13}(E_{u_{33}}) + f_{13}(E_{u_{34}}) + f_{11}(E_{u_{15}}) + f_{11}(E_{u_{16}}),\\
E_{u_{13}} &= f_{11}(E_{u_{11}}),\\
E_{u_{14}} &= f_{11}(E_{u_{12}}),\\
E_{u_{15}} &= f_{11}(E_{u_{13}}) + f_{11}(E_{u_{14}}) + f_{12}(E_{u_{25}}) + f_{12}(E_{u_{26}}),\\
E_{u_{16}} &= f_{12}(E_{u_{21}}) + f_{12}(E_{u_{22}}).
\end{aligned} \tag{3.35}$$

Then we can use the Lemma 3.3 to check that the ordered GIFS (3.35) is actually a linear GIFS. Moreover, by the construction and the uniqueness of the solution of (3.31), we have

$$X_1 = \cup_{i=1}^{6} E_{u_{1i}}$$

and the right hand union is disjoint.

REMARK 3.22. For the constructions of linear GIFS on X_i $(i = 2, 3)$, it is clear from the construction of X_1 by the relations $X_2 = f_{21}(X_1)$ and $X_3 = f_{32}(X_2)$.

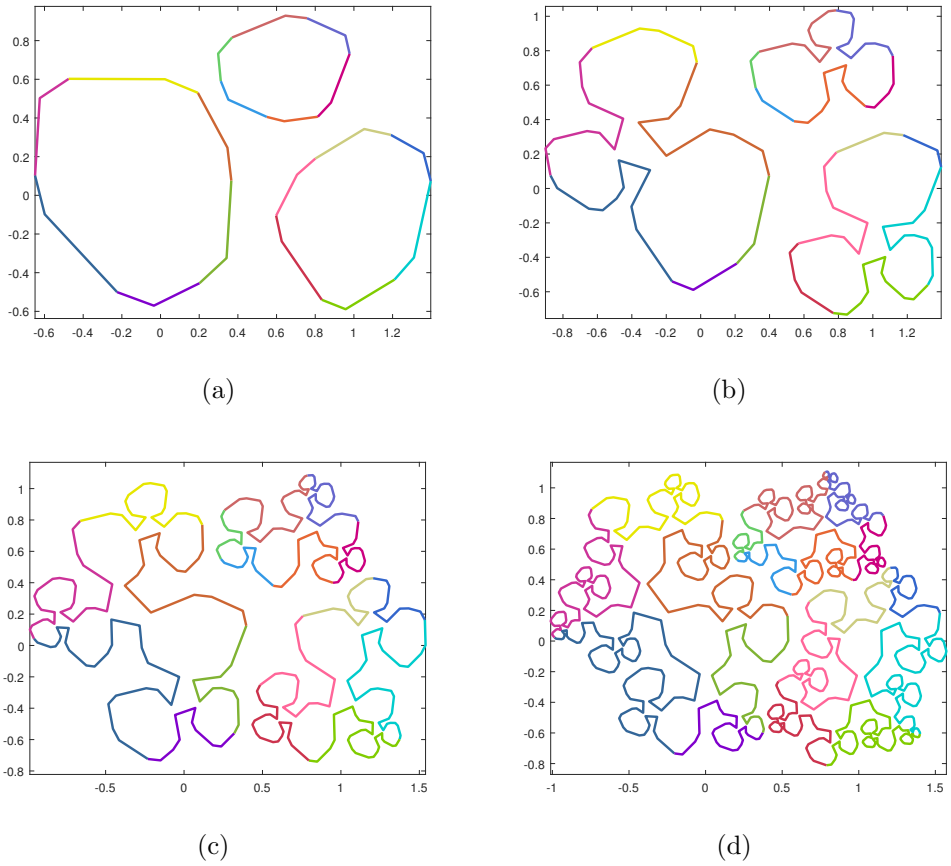

(a) (b)

(c) (d)

FIGURE 42. The first four approximations to the filling curve of classical Rauzy fractal of Example 3.6.1.

3.6.1.3. *Visualization.* The concept of visualization of space-filling curves is introduced by Rao and Zhang [**76**]. According to Theorem 3.5 we can construct the optimal parametrization ψ_i of $X_i (i = 1, 2, 3)$. To visualize the limit curve ψ_i, we choose an initial pattern which can be any curves, but a suitable choice will make the visualization beautiful (What we mean beautiful is a self-avoiding curve. But we can not always get the self-avoiding curves.). For the example of Rauzy fractal X_1, X_2, X_3, we choose a initial pattern as it shows in Figure 42 (a). Then $(b), (c), (d)$ show the approximating curves.

EXAMPLE 5. **The example of self-affine Rauzy fractal**. Figure 43 shows another example of the approximating curves of Rauzy fractal obtained by the substitution

$$\begin{aligned} \sigma_2 : 1 &\longrightarrow 12321 \\ 2 &\longrightarrow 321 \\ 3 &\longrightarrow 2. \end{aligned}$$

To get the optimal parametrizaition of this example, it follows the same idea of the classical Rauzy fractal case. We will not repeat the procedure and only give the figures we need here.

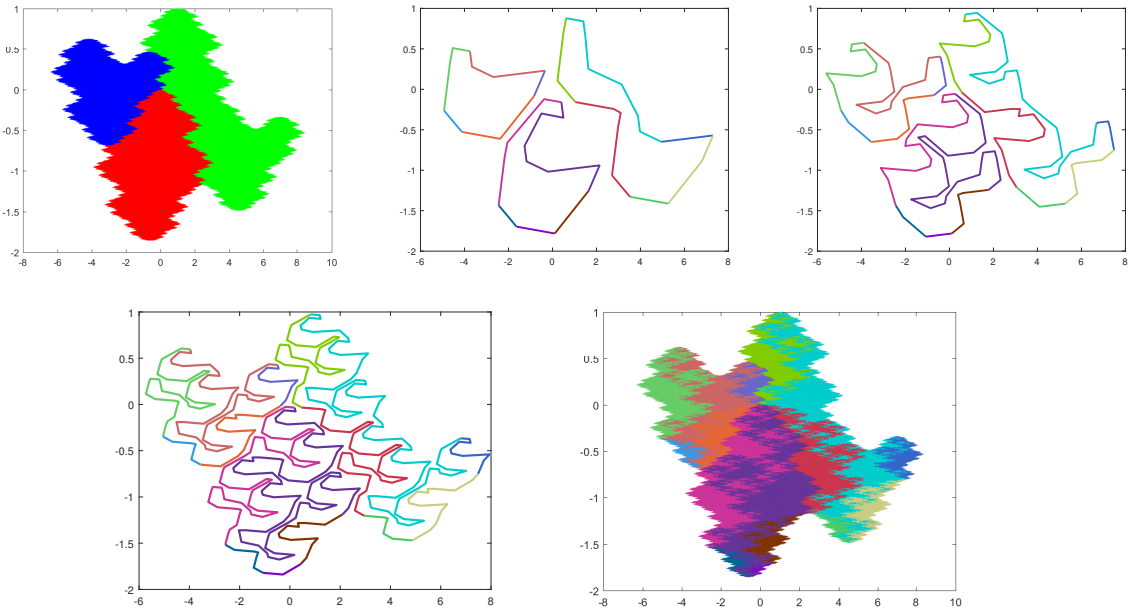

FIGURE 43. The first figure is the Rauzy fractal given by the substition σ_2. The following three Figures show the first three approximations of the filling curve of this Rauzy fractal.

Appendix: The open set condition

To apply Theorem 3.5, we also need the constructed linear GIFS satisfying the open set condition. In this supplement, we try to give the associated statements of the OSC. Recall that $(V, \Gamma, \mathcal{G})$ is a GIFS with

$$\mathcal{G}_{=}\{f_e : \mathbb{R}^d \longrightarrow \mathbb{R}^d;\ f_e \text{ is a contraction}, e \in \Gamma\}.$$

If the directed graph (V, Γ) has only one vertex with more than 2 self-edges and f_e is a similitude contraction mapping in $\mathbb{R}^d$ with similitude ratio $0 < r_i < 1$. Denote the invariant set by K and it satisfies $K = \cup_{e\in\Gamma} f_e(K)$. Let s be the similarity dimension, i.e., s satisfies $\sum_{e\in\Gamma} r_e^s = 1$. A. Schief [**82**] has proved the following chain of implications

$$SOSC \Longleftrightarrow OSC \Longleftrightarrow 0 < \mathcal{H}^s(K) < \infty.$$

Then, Li, W. X. [**57**] generalized this to the GIFS case with $\mathcal{G}$ being a family of similitudes. Denote the vertex set by $V = \{1, 2, \ldots, N\}$. Let E_i be the invariant sets of the GIFS $\mathcal{G}$. Assume that s is the similarity dimension, that is, s is the value such that the spectral radius of matrix $(\sum_{e\in\Gamma_{ij}} r_{ij}^s)_{N\times N}$ is 1. Then by [**57**] we have the following equivalent relation.

$$OSC \Longleftrightarrow SOSC \Longleftrightarrow 0 < \mathcal{H}^s(E_i) < \infty \text{ for some i.}$$

We investigate the single-matrix GIFS $\mathcal{G} = \{f_e;\ e \in \Gamma\}$ with the form

$$f_e(x) = M^{-1}(x + d_e), \tag{3.36}$$

where M is a $d \times d$ expanding matrix and $d_j \in \mathbb{R}^d$. We want to study whether we have the similar results with [**82, 57**] when M is not a similitude.

Motivated by the study of A. Schief [**82**] and using the result of Luo, J. and Yang, Y. M. [**41**], we give a positive answer. To state the questions, we introduce some notations at first.

Denote by Γ_{ij}^n the paths from vertex i to j with length n. For $I = i_1 \dots i_n \in \Gamma_{ij}^n$, set $f_I := f_{i_1} \circ f_{i_2} \circ \cdots \circ f_{i_n}(x)$ and define

$$d_I = M^{n-1}d_{i_1} + M^{n-2}d_{i_2} + \cdots + Md_{i_{n-1}} + d_{i_n},$$

then $f_I(x)$ has the form: $f_I(x) = M^{-n}(x + d_I)$. Set

$$\mathcal{D}_{ij}^n := \{d_I;\ I \in \Gamma_{ij}^n\}.$$

We say a set G is r-uniformly discrete if $|x - y| > r$ for any $x, y \in G$. [**41**] has proved the following theorem.

THEOREM 3.23. *For the single-matrix GIFS* (3.36)*, the following are equivalent:*

(1) *OSC.*
(2) $\sharp\, \mathcal{D}_{ij}^n = \sharp\, \Gamma_{ij}^n$ *and there is an* $r > 0$ *such that* $\mathcal{D}_{ij}^n$ *is* r*-uniformly discrete for all* $1 \le i, j \le N$ *and* $n \ge 1$.
(3) *SOSC.*

In [**41**], they use the pseudo norm $\omega(x)$ which was first defined in [**35**] to study the Hausdorff measure and the Hausdorff dimension. Denote A by the associated matrix of the directed graph (V, Γ). Let $\alpha = d \log \lambda / \log q$, where λ is the maximal eigenvalue of A and $q = |\det M|$. We call a set $E \subset \mathbb{R}^d$ is an α-set, if $0 < \mathcal{H}_\omega^\alpha(E) < \infty$. The open set condition satisfied means that

(i) $\dim_\omega E_i = \alpha$;
(ii) E_i is α-set for all i;
(iii) The right-hand side of (3.1) is a disjoint union in the sense of the measure $\mathcal{H}_\omega^\alpha$.

On the other hand, we want to show

$$E_i \text{ is } \alpha\text{-set for some } 1 \le i \le N \Longrightarrow \text{OSC}. \tag{3.37}$$

Then Theorem 3.23 together with (3.37) imply the following chain of implications:

$$OSC \Longleftrightarrow SOSC \Longleftrightarrow E_i \text{ is } \alpha\text{-set for some } i.$$

LEMMA 3.24. *Let* $P = (m_{ij})_{N\times N}$ *be a nonnegative primitive matrix. Let* $\rho(P)$ *denote the maximal eigenvalue of* P*. If there exists* $\mathbf{x} > \mathbf{0}$ *satisfies* $P\mathbf{x} \ge \rho(P)\mathbf{x}$*, then* $P\mathbf{x} = \rho(P)\mathbf{x}$*.*

LEMMA 3.25. *If* E_i *is an* α*-set for some* $1 \le i \le N$*, then all* E_i *are* α*-set, and*

$$(m_{ij})_{N\times N} \begin{pmatrix} \mathcal{H}_\omega^\alpha(E_1) \\ \vdots \\ \mathcal{H}_\omega^\alpha(E_N) \end{pmatrix} = \lambda \begin{pmatrix} \mathcal{H}_\omega^\alpha(E_1) \\ \vdots \\ \mathcal{H}_\omega^\alpha(E_N) \end{pmatrix}$$

PROOF. Suppose $0 < \mathcal{H}^\alpha_\omega(E_{i_0}) < \infty$. Since $(m_{ij})_{N\times N}$ is primitive, $\forall\ 1 \le i \le N$, $\exists\ n(i)$ such that $\sharp\ \Gamma^{n(i)}_{ii_0} > 0$. Using

$$E_i = \bigcup_{j=1}^{N} \bigcup_{I\in\Gamma^{n(i)}_{ij}} f_I(E_j),$$

we have

$$\mathcal{H}^\alpha_\omega(E_i) \ge \mathcal{H}^\alpha_\omega(f_I(E_{i_0})) = (\frac{1}{q})^{\alpha\cdot n(i)/d}\ \mathcal{H}^\alpha_\omega(E_{i_0}) > 0.$$

And we also have

$$\mathcal{H}^\alpha_\omega(E_i) = \mathcal{H}^\alpha_\omega\big(\bigcup_{j=1}^{N}\bigcup_{e\in\Gamma_{ij}} f_e(E_j)\big) \le \sum_{j=1}^{N}\sum_{e\in\Gamma_{ij}} (\frac{1}{q})^{\alpha/d}\ \mathcal{H}^\alpha_\omega(E_j)$$

$$i.e.\quad \lambda\mathcal{H}^\alpha_\omega(E_i) \le \sum_{j=1}^{N} m_{ij}\mathcal{H}^\alpha_\omega(E_j)$$

Then by the Lemma 3.24, the lemma is completed. □

Before giving the main result, we give some notations at first. For $I = i_1 i_2 \dots i_n \in \Gamma^n_{ij}$, denote $E_I = f_I(E_j)$.

Let E be a compact subset in $\mathbb{R}^d$. We set $E_{\omega,\varepsilon} = \{x \in \mathbb{R}^d;\ \omega(x-y) \le \varepsilon \text{ for some } y \in E\}$. Let $E,\ F$ be two compact sets in $\mathbb{R}^d$, we define the Hausdorff metric by

$$d_\omega(E,F) = \inf\{\varepsilon;\ E \subset F_{\omega,\varepsilon},\ F \subset E_{\omega,\varepsilon}\}.$$

We remark that if M is an expanding $d\times d$ matrix with $|\det M| = q$, we have

$$d_\omega(ME, MF) = q^{\frac{1}{d}} d_\omega(E,F). \tag{3.38}$$

Here $ME = \{Mx;\ x \in E\}$.

THEOREM 3.26. *If E_i is α-set for some $1 \le i \le N$, then the open set condition is fulfilled.*

PROOF. By the Lemma 3.25, we know all the E_i are α-set. For any fixed $1 \le i \le N$, by the definition of the Hausdorff dimension, we have $\forall\ 0 < \varepsilon < 1$, there exists open cover $\{U^{(i)}_j\}_{j\in\Lambda}$ (Λ is a infinity index set) such that

$$\sum_{j\in\Lambda} (\text{diam }{}_\omega U^{(i)}_j)^\alpha \le (1+\varepsilon)\mathcal{H}^\alpha_{\omega,\delta}(E_i),$$

Since E_i is compact, there exist $n(i)$ such that

$$E_i \subset \bigcup_{j=1}^{n(i)} U_j.$$

Denote $U(i) = \bigcup_{j=1}^{n(i)} U^{(i)}_j$. Hence, we have

$$\sum_{j=1}^{n(i)} (\text{diam}_\omega U^{(i)}_j)^\alpha \le (1+\varepsilon)\mathcal{H}^\alpha_\omega(E_i).$$

Let $\delta_i = D_\omega(E_i, U(i)^C) := \inf\{\omega(x-y);\ x \in E_i,\ y \in U(i)^C\}$. We prove that

$$\forall 1 \le p \le N,\ k \ge 1,\ I, J \in \Gamma_{ip}^k, \quad d_\omega(E_I, E_J) \ge \delta_p(\frac{1}{q})^{\frac{k}{d}}.$$

Otherwise, there exist $p, k,$ and $I, J \in \Gamma_{ip}^k$, such that $d_\omega(E_I, E_J) \le \delta_p(\frac{1}{q})^{\frac{k}{d}}$.

Denote $\zeta = \delta_p(\frac{1}{q})^{\frac{k}{d}}$. Since $E_I \subset f_I(U(p))$ and $D_\omega(E_I, f_I(U(p))^C) = \zeta$, we have $(E_I)_{\omega,\zeta} \subset f_I(U(p))$. Hence $E_J \subset (E_I)_{\omega,\zeta} \subset f_I(U(p))$. So $E_I \cup E_J \subset f_I(U(p))$. Since $\alpha = d\log\lambda/\log q$ and $E_I = f_I(E_p)$, we have

$$\mathcal{H}_\omega^\alpha(E_I) = (\frac{1}{q})^{\frac{k\alpha}{d}}\mathcal{H}_\omega^\alpha(E_p) = (\frac{1}{\lambda})^k\mathcal{H}_\omega^\alpha(E_p).$$

These implies

$$\begin{aligned}\mathcal{H}_\omega^\alpha(E_p)\frac{1}{\lambda^k}(1+\varepsilon) &< \mathcal{H}_\omega^\alpha(E_p)(\frac{1}{\lambda^k}+\frac{1}{\lambda^k}) = \mathcal{H}_\omega^\alpha(E_I)+\mathcal{H}_\omega^\alpha(E_J)\\ &= \mathcal{H}_\omega^\alpha(E_I\cup E_J) \le \sum_{j=1}^{n(p)}(\mathrm{diam}_\omega f_I(U_j^p))^\alpha\\ &= \sum_{j=1}^{n(p)}\frac{1}{\lambda^k}(\mathrm{diam}_\omega f_I(U_j^p))^\alpha \le \frac{1}{\lambda^k}(1+\varepsilon)\mathcal{H}_\omega^\alpha(E_p),\end{aligned}$$

which is a contradiction. The second equality follows from Lemma 3.25. We have the following equality

$$\mathcal{H}_\omega^\alpha(E_i) = \sum_{j=1}^N\sum_{\mathbf{e}\in\Gamma_{ij}^k}\mathcal{H}_\omega^\alpha(f_{\mathbf{e}}(E_j))$$

implies that the intersection of two of these atoms is an $\mathcal{H}_\omega^\alpha$-null set.

Let $\delta = \min_{1\le i\le N}\delta_i$, then we have

$$d_\omega(E_I, E_J) \ge \delta(\frac{1}{q})^{\frac{k}{d}}, \quad \forall\ I, J \in \Gamma_{ip}^k,\ \forall\ 1 \le i,\ p \le N, k \ge 1.$$

Besides, $E_I = M^{-k}(E_j + d_I)$, these mean that $d_I \ne d_J$. That is, $\sharp\mathcal{D}_{ip}^k = \sharp\Gamma_{ip}^k$.

Next, we can obtain the following equation from (3.38)

$$d_\omega(E_I, E_J) = (\frac{1}{q})^{\frac{k}{d}}d_\omega(E_j+d_I, E_j+d_J).$$

Then we have $(\frac{1}{q})^{\frac{k}{d}}\omega(d_I - d_J) \ge \delta(\frac{1}{q})^{\frac{k}{d}}$. Hence $\omega(d_I - d_J) \ge \delta$. So by the Proposition 3.11, we have $\|d_I - d_J\| \ge \delta'$, δ' is with respect to the expanding matrix M. Thus by the Theorem 3.23, we obtain the open set condition.

□

Bibliography

[**1**] S. Akiyama and N. Gjini, *On the connectedness of self-affine attractors*, Arch. Math. (Basel), 82 (2004), pp. 153–163.

[**2**] S. Akiyama and B. Loridant, *Boundary parametrization of planar self-affine tiles with collinear digit set*, Sci. China Math., 53 (2010), pp. 2173–2194.

[**3**] ——, *Boundary parametrization of self-affine tiles*, J. Math. Soc. Japan, 63 (2011), pp. 525–579.

[**4**] S. Akiyama and J. M. Thuswaldner, *The topological structure of fractal tilings generated by quadratic number systems*, Comput. Math. Appl., 49 (2005), pp. 1439–1485.

[**5**] L.-X. An and K.-S. Lau, *Characterization of a class of planar self-affine tile digit sets*, Trans. Amer. Math. Soc., (2018).

[**6**] P. Arnoux, V. Berthé, and S. Ito, *Discrete planes, $\mathbb{Z}^2$-actions, Jacobi-Perron algorithm and substitutions*, Ann. Inst. Fourier (Grenoble), 52 (2002), pp. 305–349.

[**7**] P. Arnoux and S. Ito, *Pisot substitutions and Rauzy fractals*, Bull. Belg. Math. Soc. Simon Stevin, 8 (2001), pp. 181–207. Journées Montoises d'Informatique Théorique (Marne-la-Vallée, 2000).

[**8**] R. Balakrishnan and K. Ranganathan, *A textbook of graph theory*, Universitext, Springer-Verlag, New York, 2000.

[**9**] C. Bandt, *Self-similar sets. V. Integer matrices and fractal tilings of $\mathbf{R}^n$*, Proc. Amer. Math. Soc., 112 (1991), pp. 549–562.

[**10**] ——, *Combinatorial topology of three-dimensional self-affine tiles*. Preprint, 2010.

[**11**] C. Bandt and G. Gelbrich, *Classification of self-affine lattice tilings*, J. London Math. Soc. (2), 50 (1994), pp. 581–593.

[**12**] C. Bandt and Y. Wang, *Disk-like self-affine tiles in $\mathbb{R}^2$*, Discrete Comput. Geom., 26 (2001), pp. 591–601.

[**13**] G. Barat, V. Berthé, P. Liardet, and J. Thuswaldner, *Dynamical directions in numeration*, Ann. Inst. Fourier (Grenoble), 56 (2006), pp. 1987–2092. Numération, pavages, substitutions.

[**14**] M. Barge and J. Kwapisz, *Geometric theory of unimodular Pisot substitutions*, Amer. J. Math., 128 (2006), pp. 1219–1282.

[**15**] R. H. Bing, *A characterization of* 3*-space by partitionings*, Trans. Amer. Math. Soc., 70 (1951), pp. 15–27.

[**16**] E. Bombieri and J. E. Taylor, *Quasicrystals, tilings, and algebraic number theory: some preliminary connections*, in The legacy of Sonya Kovalevskaya (Cambridge, Mass., and Amherst, Mass., 1985), vol. 64 of Contemp. Math., Amer. Math. Soc., Providence, RI, 1987, pp. 241–264.

[**17**] R. Bowen, *Markov partitions are not smooth*, Proc. Amer. Math. Soc., 71 (1978), pp. 130–132.

[**18**] J. J. Burckhardt, *Die Bewegungsgruppen der Kristallographie*, vol. 13 of Lehrbücher und Monographien aus dem Gebiete der exakten Wissenschaften, Verlag Birkhäuser, Basel, 1947.

[**19**] J. W. Cannon, ULC *properties in neighbourhoods of embedded surfaces and curves in* E^3, Canad. J. Math., 25 (1973), pp. 31–73.

[**20**] G. R. Conner and J. M. Thuswaldner, *Self-affine manifolds*, Adv. Math., 289 (2016), pp. 725–783.

[**21**] E. Curry, *Radix representations, self-affine tiles, and multivariable wavelets*, Proc. Amer. Math. Soc., 134 (2006), pp. 2411–2418 (electronic).

[**22**] X.-r. Dai, H. Rao, and S.-q. Zhang, *Space-filling curves of self-similar sets (II): Edge-to-trail substitution rule*, Nonlinearity, 32 (2019), pp. 1772–1809.

[**23**] X.-r. Dai and Y. Wang, *Peano curves on connected self-similar sets*, Unpublished note, (2010).

[**24**] M. Dekking, *Recurrent sets*, Adv. in Math., 44 (1982), pp. 78–104.

[**25**] ——, *Replicating superfigures and endomorphisms of free groups*, J. Combin. Theory Ser. A, 32 (1982), pp. 315–320.

[**26**] G. t. Deng, C. t. Liu, and S.-M. Ngai, *Topological properties of a class of self-affine tiles in* $\mathbb{R}^3$, Trans. Amer. Math. Soc., 370 (2018), pp. 1321–1350.

[**27**] P. Duvall, J. Keesling, and A. Vince, *The Hausdorff dimension of the boundary of a self-similar tile*, J. London Math. Soc. (2), 61 (2000), pp. 748–760.

[**28**] H. Ei, S. Ito, and H. Rao, *Atomic surfaces, tilings and coincidences. II. Reducible case*, Ann. Inst. Fourier (Grenoble), 56 (2006), pp. 2285–2313. Numération, pavages, substitutions.

[**29**] K. Falconer, *Fractal geometry,Mathematical Foundations and Applications*, John Wiley, New York, 1990.

[**30**] G. Gelbrich, *Crystallographic reptiles*, Geom. Dedicata, 51 (1994), pp. 235–256.

[**31**] K. Gröchenig and A. Haas, *Self-similar lattice tilings*, J. Fourier Anal. Appl., 1 (1994), pp. 131–170.

[**32**] K. Gröchenig and W. R. Madych, *Multiresolution analysis, Haar bases, and self-similar tilings of* $\mathbf{R}^n$, IEEE Trans. Inform. Theory, 38 (1992), pp. 556–568.

[**33**] B. Grünbaum and G. C. Shephard, *Tilings and patterns*, A Series of Books in the Mathematical Sciences, W. H. Freeman and Company, New York, 1989. An introduction.

[**34**] M. Hata, *On the structure of self-similar sets*, Japan J. Appl. Math., 2 (1985), pp. 381–414.

[**35**] X.-G. He and K.-S. Lau, *On a generalized dimension of self-affine fractals*, Math. Nachr., 281 (2008), pp. 1142–1158.

[**36**] P. Hubert and A. Messaoudi, *Best simultaneous Diophantine approximations of Pisot numbers and Rauzy fractals*, Acta Arith., 124 (2006), pp. 1–15.

[**37**] J. E. Hutchinson, *Fractals and self-similarity*, Indiana Univ. Math. J., 30 (1981), pp. 713–747.

[**38**] IFStile, *Main page — ifstile,*, 2017. [Online; accessed 25-April-2017].

[**39**] K.-H. Indlekofer, I. Kátai, and P. Racskó, *Some remarks on generalized number systems*, Acta Sci. Math. (Szeged), 57 (1993), pp. 543–553.

[**40**] S. Ito and H. Rao, *Atomic surfaces, tilings and coincidence. I. Irreducible case*, Israel J. Math., 153 (2006), pp. 129–155.

[**41**] L. Jun and Y.-M. Yang, *On single-matrix graph-directed iterated function systems*, J. Math. Anal. Appl., 372 (2010), pp. 8–18.

[**42**] I. Kátai, *Number systems and fractal geometry*, University of Pécs, (1995).

[**43**] I. Kátai and I. Környei, *On number systems in algebraic number fields*, Publ. Math. Debrecen, 41 (1992), pp. 289–294.

[**44**] R. Kenyon, *Self-replicating tilings*, in Symbolic dynamics and its applications (New Haven, CT, 1991), vol. 135 of Contemp. Math., Amer. Math. Soc., Providence, RI, 1992, pp. 239–263.

[**45**] ——, *The construction of self-similar tilings*, Geom. Funct. Anal., 6 (1996), pp. 471–488.

[**46**] R. Kenyon and A. Vershik, *Arithmetic construction of sofic partitions of hyperbolic toral automorphisms*, Ergodic Theory Dynam. Systems, 18 (1998), pp. 357–372.

[**47**] I. Kirat and K.-S. Lau, *On the connectedness of self-affine tiles*, J. London Math. Soc. (2), 62 (2000), pp. 291–304.

[**48**] K. Kuratowski, *Topology. Vol. I*, New edition, revised and augmented. Translated from the French by J. Jaworowski, Academic Press, New York, 1966.

[**49**] ——, *Topology. Vol. II*, New edition, revised and augmented. Translated from the French by A. Kirkor, Academic Press, New York, 1968.

[**50**] K. W. Kwun, *A characterization of the n-sphere*, Trans. Amer. Math. Soc., 101 (1961), pp. 377–383.

[**51**] J. C. Lagarias and Y. Wang, *Integral self-affine tiles in* $\mathbb{R}^n$*. I. Standard and nonstandard digit sets*, J. London Math. Soc. (2), 54 (1996), pp. 161–179.

[**52**] ——, *Self-affine tiles in* $\mathbf{R}^n$, Adv. Math., 121 (1996), pp. 21–49.

[**53**] ——, *Integral self-affine tiles in* $\mathbf{R}^n$*. II. Lattice tilings*, J. Fourier Anal. Appl., 3 (1997), pp. 83–102.

[**54**] P.-G. Lemarié-Rieusset, *Projecteurs invariants, matrices de dilatation, ondelettes et analyses multi-résolutions*, Rev. Mat. Iberoamericana, 10 (1994), pp. 283–347.

[**55**] K.-S. Leung and K.-S. Lau, *Disklikeness of planar self-affine tiles*, Trans. Amer. Math. Soc., 359 (2007), pp. 3337–3355.

[**56**] K.-S. Leung and J. J. Luo, *Connectedness of planar self-affine sets associated with non-consecutive collinear digit sets*, J. Math. Anal. Appl., 395 (2012), pp. 208–217.

[**57**] W. X. Li, *Separation properties for MW-fractals*, Acta Math. Sinica (Chin. Ser.), 41 (1998), pp. 721–726.

[**58**] A. Lindenmayer, *Mathematical models for cellular interacton in development, parts i and ii*, Journal of Theoretical Bilology, 30 (1968), pp. 280–315.

[**59**] B. Loridant, *Crystallographic number systems*, Monatsh Math, 167 (2012), pp. 511–529.

[**60**] ——, *Topological properties of a class of cubic Rauzy fractals*, Osaka J. Math., 53 (2016), pp. 161–219.

[**61**] B. Loridant and J. Luo, *On a theorem of Bandt and Wang and its extension to p2-tiles*, Discrete Comput. Geom., 41 (2009), pp. 616–642.

[**62**] B. Loridant, J. Luo, and J. M. Thuswaldner, *Topology of crystallographic tiles*, Geom. Dedicata, 128 (2007), pp. 113–144.

[**63**] B. Loridant and S.-Q. Zhang, *Topology of a class of p2-crystallographic replication tiles*, Indag. Math. (N.S.), 28 (2017), pp. 805–823.

[**64**] J. Luo, S. Akiyama, and J. M. Thuswaldner, *On the boundary connectedness of connected tiles*, Math. Proc. Cambridge Philos. Soc., 137 (2004), pp. 397–410.

[**65**] J. Luo, H. Rao, and B. Tan, *Topological structure of self-similar sets*, Fractals, 10 (2002), pp. 223–227.

[**66**] D. W. Matula, *Basic digit sets for radix representation*, J. Assoc. Comput. Mach., 29 (1982), pp. 1131–1143.

[**67**] R. D. Mauldin and S. C. Williams, *Hausdorff dimension in graph directed constructions*, Trans. Amer. Math. Soc., 309 (1988), pp. 811–829.

[**68**] C. McMullen, *The Hausdorff dimension of general Sierpiński carpets*, Nagoya Math. J., 96 (1984), pp. 1–9.

[**69**] Mekhontsev, D., *IFStile*, 2018. Available under ifstile.com.

[**70**] S.-M. Ngai and T.-M. Tang, *Topology of connected self-similar tiles in the plane with disconnected interiors*, Topology Appl., 150 (2005), pp. 139–155.

[**71**] A. M. Odlyzko, *Nonnegative digit sets in positional number systems*, Proc. London Math. Soc. (3), 37 (1978), pp. 213–229.

[**72**] G. Peano, *Sur une courbe qui remplit toute une aire plane*, Math. Ann., 36 (1890), pp. 157–160.

[**73**] B. Praggastis, *Numeration systems and Markov partitions from self-similar tilings*, Trans. Amer. Math. Soc., 351 (1999), pp. 3315–3349.

[**74**] H. Rao, *Dual systems of algebraic iterated functions systems, Rauzy fractals and β-tilings*, in Numeration and substitution 2012, RIMS Kôkyûroku Bessatsu, B46, Res. Inst. Math. Sci. (RIMS), Kyoto, 2014, pp. 125–147.

[**75**] H. Rao, Z.-Y. Wen, and Y.-M. Yang, *Dual systems of algebraic iterated function systems*, Adv. Math., 253 (2014), pp. 63–85.

[**76**] H. Rao and S.-Q. Zhang, *Space-filling curves of self-similar sets (I): iterated function systems with order structures*, Nonlinearity, 29 (2016), pp. 2112–2132.

[**77**] H. Rao and S.-Q. Zhang, *Space-filling curves of self-similar sets (III): Skeletons*, ArXiv e-prints, (2018).

[**78**] G. Rauzy, *Nombres algébriques et substitutions*, Bull. Soc. Math. France, 110 (1982), pp. 147–178.

[**79**] H. Sagan, *Space-filling curves*, Universitext, Springer-Verlag, New York, 1994.

[**80**] K. Scheicher and J. M. Thuswaldner, *Canonical number systems, counting automata and fractals*, Math. Proc. Cambridge Philos. Soc., 133 (2002), pp. 163–182.

[**81**] ——, *Neighbours of self-affine tiles in lattice tilings*, in Fractals in Graz 2001, Trends Math., Birkhäuser, Basel, 2003, pp. 241–262.

[**82**] A. Schief, *Separation properties for self-similar sets*, Proc. Amer. Math. Soc., 122 (1994), pp. 111–115.

[**83**] I. Schur, *Über Potenzreihen, die im Innern des Einheitskreises beschränkt sind. II*, J. reine und angew. Math, 148 (1918), pp. 122–145.

[**84**] A. Siegel and J. M. Thuswaldner, *Topological properties of Rauzy fractals*, Mém. Soc. Math. Fr. (N.S.), 118 (2009), p. 140.

[**85**] J. G. Sinaĭ, *Markov partitions and U-diffeomorphisms*, Funkcional. Anal. i Priložen, 2 (1968), pp. 64–89.

[**86**] V. c. F. Sirvent, *Space filling curves and geodesic laminations*, Geom. Dedicata, 135 (2008), pp. 1–14.

[**87**] ——, *Space-filling curves and geodesic laminations. II: Symmetries*, Monatsh. Math., 166 (2012), pp. 543–558.

[**88**] V. F. Sirvent and Y. Wang, *Self-affine tiling via substitution dynamical systems and Rauzy fractals*, Pacific J. Math., 206 (2002), pp. 465–485.

[**89**] B. Solomyak, *Dynamics of self-similar tilings*, Ergodic Theory Dynam. Systems, 17 (1997), pp. 695–738.

[**90**] R. S. Strichartz, *Wavelets and self-affine tilings*, Constr. Approx., 9 (1993), pp. 327–346.

[**91**] R. S. Strichartz and Y. Wang, *Geometry of self-affine tiles. I*, Indiana Univ. Math. J., 48 (1999), pp. 1–23.

[**92**] W. Thurston, *Groups, tilings, and finite state automata*. AMS Colloquium lecture notes, 1989.

[**93**] J. Thuswaldner and S.-Q. Zhang, *On self-affine tiles whose boundary is a sphere*, ArXiv e-prints, (2018).

[**94**] A. Vince, *Digit tiling of Euclidean space*, in Directions in mathematical quasicrystals, vol. 13 of CRM Monogr. Ser., Amer. Math. Soc., Providence, RI, 2000, pp. 329–370.

[**95**] P. Walters, *An introduction to ergodic theory*, vol. 79 of Graduate Texts in Mathematics, Springer-Verlag, New York-Berlin, 1982.

[**96**] Y. Wang, *Self-affine tiles*, in Advances in wavelets (Hong Kong, 1997), Springer, Singapore, 1999, pp. 261–282.

[**97**] ——, *Wavelets, tiling, and spectral sets*, Duke Math. J., 114 (2002), pp. 43–57.

[**98**] S.-Q. Zhang, *Optimal parametrizations of a class of self-affine sets*, ArXiv e-prints, (2018).